Pharmacological regulation of melanocortin-3 and -4 receptors by melanocortin-2 receptor accessory protein 1 or 2

by

Ren-Lei Ji

A dissertation submitted to the Graduate Faculty of
Auburn University
in partial fulfillment of the
requirements for the Degree of
Doctor of Philosophy

Auburn, Alabama
August 6, 2022

Keywords: G protein-coupled receptor, Melanocortin-3 receptor, Melanocortin-4 receptor, Energy homeostasis, melanocortin-2 receptor accessory protein, isoform

Approved by

Ya-Xiong Tao, Chair, Anatomy, Physiology and Pharmacology
Robert L. Judd, Professor of Anatomy, Physiology and Pharmacology
Muralikrishnan Dhanasekaran, Professor of Drug Discovery and Development
Satyanarayana R. Pondugula, Associate Professor of Anatomy, Physiology and Pharmacology
Chen-Che Jeff Huang, Assistant Professor of Anatomy, Physiology and Pharmacology

Abstract

The neural melanocortin receptors (MCRs), melanocortin-3 and -4 receptors (MC3R and MC4R), play essential non-redundant roles in the regulation of energy homeostasis. Melanocortin-2 receptor accessory proteins (MRAPs, MRAP1 and MRAP2) were shown to regulate neural MCRs. To gain a better understanding of the regulation of neural MCRs by MRAPs, we identified *MRAP2* splice variants from humans and canine, and investigated effects of isoforms of MRAPs on human and canine MC3R/MC4R pharmacology. We also conducted experiments to explore modulation of fish Mc3r/Mc4r by two isoforms of Mrap2.

We identified two new human (h) *MRAP2* splice variants, *MRAP2b* (465 bp open reading frame) and *MRAP2c* (381 bp open reading frame). Human MRAP2s are different in C-termini. We investigated effects of five isoforms of MRAPs, hMRAP1a, hMRAP1b, hMRAP2a, hMRAP2b, and hMRAP2c, on MC3R and MC4R pharmacology. At the hMC3R, hMRAP1a and hMRAP2c increased and hMRAP1b decreased the cell surface expression. hMRAP1a increased affinity to ACTH. Four MRAPs (hMRAP1a, hMRAP1b, hMRAP2a, and hMRAP2c) decreased the maximal responses in response to α-MSH and ACTH. For hMC4R, hMRAP1a, hMRAP2a, and hMRAP2c increased the cell surface expression of hMC4R. Human MRAP1b significantly increased affinity to ACTH while MRAP2a decreased affinity to ACTH. Human MRAP1a increased ACTH potency. MRAPs also affected hMC4R basal activities, with hMRAP1s increasing and hMRAP2s decreasing the basal activities. In summary, the newly identified splicing variants, hMRAP2b and hMRAP2c, could regulate MC3R and MC4R pharmacology. The two MRAP1s and three MRAP2s had differential effects on MC3R and MC4R trafficking, binding, and signaling.

The effect of MRAP1 and MRAP2 on canine neural MCRs are not understood. Herein, we cloned canine (c) *mc3r* and identified an canine *MRAP2* splice variant, *MRAP2b,* with extension at N-terminus of cMRAP2a. Canine MC3R showed higher B_{max} and R_{max}s to five agonists than that of hMC3R. We further investigated modulation of cMRAP1, cMRAP2a, and cMRAP2b, on cMC3R and cMC4R pharmacology. All MRAPs had no effect on cMC3R trafficking. Canine MRAP1 significantly decreased the B_{max}, whereas cMRAP2a and cMRAP2b increased B_{max} of cMC3R. Both MRAP1 and MRAP2a decreased R_{max}s in response to α-MSH and ACTH; MRAP2b only decreased α-MSH-stimulated cAMP generation cAMP production of cMC3R. At cMC4R, MRAP1 and MRAP2a increased cell surface expression of cMC4R. MRAP1 and MRAP2a increased B_{max}s of cMC4R. All MRAPs increased affinities to α-MSH and ACTH. MRAP2a increased ACTH-induced cAMP levels of cMC4R, whereas MRAP2b decreased α-MSH- and ACTH-stimulated cAMP production of cMC4R. All MRAPs decreased the basal activities of cMC4R.

Considering the crucial importance of energy metabolism, understanding the endocrine modulation of energy homeostasis is important for economically important fishes and may potentially lead to novel approaches to manipulate fish growth, feed efficiency, and final product quality in cultured fish. Hence, it is not surprising that Mc3r/Mc4r has also attracted some attention in fish. Topmouth culter (*Culter alburnus*) is an economically important freshwater fish in China. In this study, we cloned culter *mc3r*, *mrap2a*, and *mrap2b*. All agonists could bind and stimulate caMc3r to increase dose-dependently intracellular cAMP accumulation. Compared to hMC3R, culter Mc3r showed higher constitutive activity, higher efficacies and R_{max} to α-MSH, des-α-MSH, and ACTH. Both caMrap2a and caMrap2b markedly decreased caMc3r basal cAMP production. However, only caMrap2a significantly decreased cell surface expression, B_{max}

and R_{max} of caMc3r. These data indicated that the cloned caMc3r was a functional receptor. Mrap2a and Mrap2a had different effects on expression and signaling of caMc3r.

We also cloned culter *mc4r*, consisting of a 981 bp open reading frame encoding a protein of 326 amino acids. Culter Mc4r could bind to four peptide agonists and increase intracellular cAMP production dose dependently. Culter Mc4r could be constitutively active in both cAMP and Erk1/2 pathways, which differentially regulated by caMrap2a and caMrap2b. Culter Mrap2a significantly increased B_{max} and decreased agonist-stimulated cAMP, while Mrap2b increased cell surface and total expression but did not affect B_{max} and agonist-stimulated cAMP. These results will aid investigate the diverse physiological processes of Mc4r in topmouth culter.

In summary, we systemically investigated the modulation of MRAP1 and MRAP2 on MC3R/MC4R in humans, canine, and fish, and found that the effect of MRAPs on MC3R/MC4R is in species-dependent manner. We also studied functionality of Mc3r/Mc4r in an economically important fish, laying the foundation for further physiological studies of fish Mc3r or Mc4r that might provide new strategies for promoting growth and culture.

Acknowledgments

First and foremost, I would like to express my sincere appreciation to my mentor Dr. Ya-Xiong Tao, who has provided me with the opportunity to study abroad as a PhD student in his lab, for his unwavering help in my graduate study and ongoing support of my academic career. It is really an honor for both of me and my family. Without his insightful advice, valued trust, and persistent support, I would never have been able to finish my dissertation. I'm also indebted to my advisory committee, Drs. Robert Judd, Muralikrishnan Dhanasekaran, Satyanarayana R. Pondugula, and Chen-Che Jeff Huang for sharing their wisdom and experience and devoting their valuable time to instruct my study. I warmly thank my university reader, Ramesh Jeganathan, for his careful review and valuable guidance of my dissertation.

I would like to thank my lab colleagues and alumni, Chuan-ling Xu, Shan-shan Jiang, Yin Wang, Drs. Ting Liu, Zhi-Shuai Hou, Li-Kun Yang, Li-Qin Ji, Zheng-Rui Zhang, Yin-zhu Rao, Hong-Tao Nie, Qian Wang, and Fan Yu, for their valuable contributions, inspiring discussions, and helpful support to my work. My sincere thanks go to our collaborator: Dr. Min Tao, Hunan Normal University, China, and her students, for her contribution in gene cloning and gene synthesis of Chapter 4 and 5. I would like to thank other colleagues and many other friends for their friendship and help. I would like to thank all the faculty members and students in the Department of Anatomy, Physiology and Pharmacology for their kind support. Specifically, I would like to acknowledge China Scholarship Council of the People's Republic of China for the financial support throughout four years.

Finally, I am whole-heartedly grateful to my loved parents, older sister, and my brother, for their unconditional and unselfish love, encouragement, and unwavering support. I would like to thank my fiancée, Jing-Hua Cao, for her love, support, and encouragement all the time.

Table of Contents

List of Tables

List of Figures

List of Abbreviations

AC: Adenylyl cyclase

ACTH: adrenocorticotropic hormone

AgRP: Agouti-related peptide

ARC, arcuate nucleus

AMPK: 5'-AMP-activated protein kinase

BSA: Bovine serum albumin

cAMP: 3’,5’-cyclic adenosine monophosphate

CNS: central nervous system

EC_{50}: half maximal effective concentration

ECL: extracellular loop

ER: endoplasmic reticulum

ERK1/2: extracellular signal-regulated kinases 1/2

GPCR: G protein-coupled receptor

HEK 293T: human embryonic kidney 293T

IC_{50}: half maximal inhibitory concentration

ICL: intracellular loop

JNK: c-Jun N-terminal kinases

Kir7.1 channel: inward-rectifier potassium channel

MCR: melanocortin receptor

MSH: melanocyte-stimulating hormone

MRAP1: melanocortin-2 receptor accessory protein1

MRAP2: melanocortin-2 receptor accessory protein2

NDP-MSH: [Nle4, D-Phe7]-α-MSH

NPY: neuropeptide Y

ORF: open reading frame

PI3K: phosphatidylinositol 3-kinase

PKA/C: protein kinase A/C

PKB: protein kinase B

POMC: proopiomelanocortin

PVN: paraventricular nucleus

VMN: ventromedial nucleus

TMD: transmembrane domain

WT: wild-type

Chapter 1: Literature review

1.1. Introduction

The superfamily of G protein-coupled receptors (GPCRs) consists of the largest member of membrane proteins and about 800 GPCRs were reported in humans [1-3]. GPCRs transduce signals of numerous physicochemical stimulating, including neurotransmitters, hormones, as well as taste signals, vision, pheromone, and olfaction [3, 4]. The GPCRs in humans can be divided into five main groups (GRAFS), including glutamate (Class C), rhodopsin (Class A), adhesion, frizzled/taste2 (Class F), and secretin (Class B) [1]. GPCRs have regulatory functions in diverse physiological processes in almost all organ systems and dysfunctions of GPCR signaling has been implicated in the pathogenesis of in diverse human diseases [5-13]. GPCRs have been considered as the most popular drug targets, accounting for about 35% of all approved drugs (~700 approved drugs target ~130 GPCRs) and over 50% of total pharmacotherapies in the market today [14-16].

Melanocortin receptors (MCRs), MC1R to MC5R, are members of rhodopsin-like Family A G-protein-coupled receptors (GPCRs) activated by melanocortin peptides, including α-, β-, and γ--melanocyte-stimulating hormone (α-, β-, and γ-MSH) and adrenocorticotropic hormone (ACTH) [17, 18]. MC3R and MC4R (neural MCRs) are primarily expressed in the central nervous system [19-22] and play pivotal roles in regulating energy homeostasis [23, 24]. Neural MCRs show distinct non-redundant mechanisms in regulating energy homeostasis [25-29]. Mutations in *MC3R* and *MC4R* have been shown to be closely associated with monogenic human obesity [13, 30-33]. Additionally, MC3R/MC4R have been shown to regulate various other

physiological processes, such as cardiovascular function, reproduction and sexual function, anti-inflammation, and other functions [13, 32, 34-42].

MCRs have been shown to interact with small single transmembrane proteins-melanocortin-2 receptor accessory proteins (MRAPs, including MRAP1 and MRAP2). MRAP1, first identified as low molecular weight protein from fat tissue [43], was the first MC2R accessory protein identified, as the specific molecular chaperone for MC2R in regulating receptor expression, ligand binding, and signaling [3, 44-46]. There are two alternatively spliced isoforms of human (h) MRAP1, *hMRAP1a* and *hMRAP1b*, with similar effects on MC2R trafficking and signaling [44, 45]. *MRAP1a* and *MRAP1b* are widely expressed, but their distribution patterns are distinct [44, 220], indicating that it might possess multiple functions beyond regulating MC2R (primarily expressed in adrenal gland) [44]. Indeed, MRAP1 has been shown to regulate all five hMCRs in distinct ways [47-49].

Subsequent studied showed that there is a paralogue of MRAP1 in vertebrate genomes, termed MRAP2 [47, 48]. MRAP2 shares 40% homology with MRAP1 and has different functions from MRAP1. MRAP2 with high expression in brain is essential for modulation of energy homeostasis. *Mrap2* knockout mice display early-onset severe obesity [50, 51]. *MRAP2* mutations are associated with severe obesity in humans [50, 52-54]. MRAP2 regulates MC3R or MC4R signaling in mammals and other species [47, 50, 55-61]. In teleosts, there are two copies of *mrap2* (*mrap2a* and *mrap2b*) in zebrafish and topmouth culter with various modulatory roles of Mcrs in these fishes [55, 59, 60].

This chapter provides an overview of the central melanocortin system, including ligands and receptors. The physiological functions and intracellular signaling pathways of neural MCRs are discussed. Additionally, regulation of MC3R/MC4R by MRAP1 or MRAP2 is highlighted.

1.2. Melanocortin system

1.2.1 Endogenous ligands

The melanocortin system is comprised of six major known endogenous ligands (four agonists and two antagonists) and five receptors, named MC1R-MC5R based on the order of their cloning. Four agonists consist of α-, β-, γ-MSH, and ACTH, derived from tissue-specific post-translational processing of proopiomelanocortin (POMC) [17, 18]. Only MSHs are produced in the central nervous system (CNS) [62]. α-MSH, a major endogenous agonist in CNS, stimulates neural MCRs to induce a negative energy balance [63]. The melanocortin system is unique in that four agonists and two endogenous antagonists, Agouti and Agouti-related peptide (AgRP), exist.

These endogenous ligands show variable degrees of specificity for MCRs. α-MSH and β-MSH act as agonists for MC1R, MC3R, MC4R and MC5R. γ-MSH has modest selectivity for MC3R, while MC2R only binds to ACTH [64]. For two antagonists, Agouti functions specifically on MC1R and MC4R [65, 66], whereas AgRP acts a selective antagonist on MC3R and MC4R [67, 68]. AgRP antagonizes α-MSH binding to neural MCRs and stimulates a long-lasting increase in food intake, leading to a positive energy balance [63, 69]. However, mice lacking neuronal MSH show delayed and long-lasting effects of AgRP on appetite control,

indicating that AgRP regulates food intake in melanocortin-signaling independent manner [70, 71]. Subsequent studies suggest that AgRP decreases the basal activity of MC3R and MC4R [72-74]. These findings suggest that AgRP could act as an inverse agonist for MC3R/MC4R.

Among the five MCRs, MC3R and MC4R are primarily expressed in the CNS and have important role in regulating body weight and metabolic activity. The central melanocortin system maintains energy balance primarily via the leptin-melanocortin circuit to interconnect neuronal circuits affecting satiety and metabolism with signals of metabolic state.

1.2.2 Melanocortin-3 receptor

The *MC3R* was first cloned by Gantz and coworkers, encoding a 360 amino acid protein as a single exon gene located on 20q13.2 [20]. Subsequent studies suggest the translational starting site of human *MC3R* is at the evolutionarily conserved second ATG codon instead of the originally assumed nonconserved first ATG, resulting in losing 37 amino acids [75, 76]. Studies also found that human *MC3R* with an additional upstream exon can use the second ATG codon as the translational start site [76].

Human *MC3R* has high expression in the hypothalamus [21] especially in the ventromedial nucleus (VMN), the arcuate nucleus (ARC), and the posterior hypothalamic region [77]. According to the Human Protein Atlas database, human *MC3R* is mainly expressed in the brain, including thalamus, hypothalamus, amygdala, midbrain, pons, medulla oblongata, hippocampal formation, basal ganglia, and cerebral cortex (**Figure 1.1A**). Furthermore, *MC3R* has the wide expression in several peripheral tissues, including the intestine, kidney, placenta, gut, heart, and macrophages [20, 38, 39, 78, 79].

MC3R plays a key role in energy homeostasis [13, 80]. *Mc3r*$^{-/-}$ mice have a moderate obesity phenotype with increased fat mass and decreased lean mass [27, 28]. MC3R regulates feed efficiency probably due to the subtle imbalance between fat intake and oxidation, with markedly reduced fatty acid oxidation observed in *Mc3r* $^{-/-}$ mice. Moreover, during fasting, *Mc3r*$^{-/-}$ mice are defective in fasting-induced white adipose tissue lipolysis, liver triglyceride accumulation, refeeding response, and regulation of the adipostatic and hypothalamic-pituitary-adrenal axes [81]. MC3R might be a crucial modulator of boundary controls on melanocortin signaling in rheostatic control of energy storage [82]. MC3R is involved in the regulation of inputs of feeding-related signals into systems expressing rhythms of food anticipatory activity. Under restricted feeding, *Mc3r*$^{-/-}$ mice show decreased wakefulness before food presentation, suggesting impaired behavioral adaptation [83, 84]. MC3R might act as an inhibitory autoreceptor on POMC neurons, in that peripheral and central administration of selective MC3R agonist increase feeding in rats [85, 86].

Human genetic studies show a positive association between obesity and the chromosomal region 20q13 that harbors *MC3R*, making the *MC3R* a plausible candidate gene for human obesity and type 2 diabetes [87-91]. T6K and V81I *MC3R* were the first two variants identified, which are polymorphic variants in complete linkage disequilibrium [92, 93]. Since then, 27 naturally occurring mutations of *MC3R* have been identified in nonobese and obese individuals (for reviews, see Refs. [31, 33, 94]. I183N and I335S were identified only from obese individuals and show defects in pharmacological properties [95-100], and are regarded as potential pathogenic mutations or at least predisposing genetic factors conferring susceptibility to excessive weight gain since the cosegregation of these two mutations with obesity in family has been identified [97, 100-102]. Recently, over 200 mutations in *MC3R* are reported in gnomAD

v2.1.1 database (https://gnomad.broadinstitute.org/) based on Ref. [13, 103], These findings provide further evidence for its role in the regulation of energy homeostasis.

The MC3R has been shown to be involved in the mediation of inflammatory responses among multiple organs and tissues, including rheumatoid [104], lung inflammation [38, 105], arthritis [106], and periodontal disease [39]. *MC3R* is also expressed in macrophages of rodent and human, indicating an important modulatory role in host inflammatory responses [107, 108]. MC3R activation leads to the inhibition of pro-inflammatory cytokines, chemokine or nitric oxide and the enhancement of anti-inflammatory mediators [39, 109-111], whereas the anti-inflammatory effects are absent in $Mc3r^{-/-}$ mice [109]. Additionally, SHU9119, a mixed MC3/4R antagonist, prevents the inhibitory actions induced by either D-Trp^8-γ-MSH or γ2-MSH (MC3R selective agonists), whereas HS024, a selective MC4R antagonist, does not affect, indicating the pivotal and independent role of MC3R in inflammatory regulation.

Owing to the wide expression of *MC3R* in several peripheral tissues, MC3R might have other potential physiological functions in the periphery, including involvement in modulating natriuresis [41], cardiovascular function [34, 35], and timing of sexual maturation [42] **(Figure 1.2).**

1.2.3 Melanocortin-4 receptor

The human *MC4R* was first cloned in 1990s, encoding 332 amino acids by an intronless gene located at chromosome 18q21.3 [19, 22]. Human *MC4R* is primarily expressed in brain, including the thalamus, cortex, brain stem, hippocampus, hypothalamus, and spinal cord areas [19, 22]. In addition to its central expression, human *MC4R* is also detected in several peripheral

tissues, including heart, kidney, muscle, lung, and testis [112]. According to the Human Protein Atlas database, the *MC4R* is also highly expressed in the fallopian tube and retina (even higher than the brain) and lowly expressed in epididymis, salivary gland, thymus, tonsil, breast, adrenal gland, and spleen (**Figure 1.1B**). The potential physiological roles of the MC4R in these tissues have not been investigated yet. In non-mammalian species, such as fish, *mc4r* is also abundantly expressed in brain and peripheral tissues [59, 61, 113-118].

The crucial role of MC4R in modulation of energy balance has been established by numerous studies. The MC4R selective agonists and antagonists have been developed and results in animal studies using these selective ligands provide the indisputable role of MC4R in modulating energy homeostasis [119-123]. Mice lacking *Mc4r* show morbid obesity with decreased energy expenditure and increased food intake [25, 26]. Mutations in *MC4R* causing early-onset morbid obesity demonstrate the critical role of MC4R in regulating human energy homeostasis. Since the first *MC4R* frameshift mutations were reported [124, 125], numerous *MC4R* mutations have been identified. The obese *MC4R* mutation carriers are characterized by hyperphagia, hyperinsulinemia, and increased bone mineral density [126-130]. Three articles summarized the *MC4R* mutations identified then and functional studies on these mutations [13, 30, 131].

In addition to regulating energy homeostasis, MC4R is also involved in multiple physiological functions including glucose and lipid metabolism, pain modulation, reproduction, cardiovascular functions, brain inflammation, and bone metabolism (**Figure 1.2**) [13, 32].

Mc4r has been shown to act as a regulator of energy balance in fish. Mc4r agonists decrease food intake and antagonists increase food intake in goldfish and rainbow trout [132-134]. In zebrafish, knockout of *mc4r* or genetic deletion of α-Msh leads to hyperphagia and increased body weight [135, 136]; Mc4r agonists can ameliorates these phenotypes in fish lacking α-Msh [136]. Importantly, loss-of function mutations in Mexican cavefish *mc4r* are the likely cause of hyperphagia and obesity phenotype, similar results in human *MC4R* mutations [137].

In fish, *mc4r* is widely expressed including in the gonads [138]. Dimorphic expression has also been reported [59, 117]. Therefore, Mc4r might have a potential role in modulation of fish reproduction [116, 117, 139]. The roles of Mc4r in sexual behavior and reproductive function have been reported in several studies [139-145].

A unique property is observed in fish Mc4rs, for example, dramatically high constitutive activities compared to hMC4R. The hMC4R has modest constitutive activity in cAMP signaling, and the loss of constitutive activity in *MC4R* mutations is considered as one cause of obesity [9, 146]. The higher constitutive activity of hMC4R is pivotal in regulating energy homeostasis [147], and increased basal activity of MC4R might protect against obesity. Compared to hMC4R, teleost Mc4rs have much higher constitutive activity in cAMP signaling [59, 61, 115-118, 148, 149]. Mrap2- and Agrp-suppressed the basal activity of Mc4r is essential for promoting zebrafish growth [55, 141]. Constitutive activation of Erk1/2 signaling in some fish but not others has also been observed [59, 149]. Similar phenomenon is also observed in fish Mc3rs, in which high constitutive activities in cAMP signaling are reported in zebrafish, channel catfish, and topmouth culter [57, 60, 150]. However, hMC3R has little or no basal activity in cAMP pathway [74, 98].

Thus, high basal activity of Mc3r/Mc4r might provide new strategies to reduce basal signaling by antagonist or Mrap2 for growth promotion in aquaculture. The potential relevance and physiological functions of constitutive activity in teleost Mc3r/Mc4r need further study.

1.2.4 Multiple signaling pathways of neural MCRs

The canonical signaling pathway for the neural MCRs is to couple to the stimulatory heterotrimeric G protein (G). Neural MCR activation leads to stimulation of adenylyl cyclase (AC) activity, which will increase the intracellular level of the second messenger cyclic adenosine monophosphate (cAMP) and subsequently activate protein kinase A (PKA) to trigger downstream signaling. Gs-protein mediated signaling is the conventional intracellular and the most investigated signaling for MC3R/MC4R.

In addition to Gs, MC4R also couples to Gq (activates phospholipase C/protein kinase C (PLC/PKC) to increase intracellular calcium) and Gi protein (inhibits AC activity to decrease cAMP levels). MC4R activation results in increase of intracellular calcium via Gq/phospholipase C-dependent signaling pathway in GT1-1 cells, a murine hypothalamic cell line endogenously expressing MC4R [151]. This signaling is also confirmed in transfecting cells expressing MC4R [152]. In contrast, in GT1-7 cells, MC4R cannot stimulate intracellular calcium signaling [153]. Recently, several studies have confirmed that MC4R could couple to Gi and Gq [154, 155]. MC4R also binds to $G_{12/13}$ [156].

MC4R also carries out functions in G protein independent signaling pathway. In *vitro* and in *vivo* studies indicate that MC4R is involved in stimulating extracellular signal-regulated kinases 1/2 (ERK1/2) pathway [157-160]. The underlying mechanism of MC4R-ERK1/2

signaling depends on the cell types and ligand used. In GT1-7 cells, upon α-MSH, MC4R-activated ERK1/2 signaling is PKA-dependent [161]. Melanotan II (MTII), a MCR agonist, induces activated ERK 1/2 signaling via PKA-dependent way in in rat solitary nucleus neurons (expressing MC4R) [159]. [Nle4, D-Phe7]-α-MSH (NDP-MSH) stimulates ERK1/2 signaling via Ca^{2+}/PKC in GT1-1, through Gi protein in HEK293 cells expressing MC4R [160], and by phosphatidylinositol 3-kinase (PI3K) in CHO cells expressing hMC4R [158]. Gain-of-function MC4R variants exhibit signaling bias toward β-arrestin recruitment and increased ERK1/2 signaling [162]. MC4R also is involved in other signaling pathways, including 5'-AMP-activated protein kinase (AMPK), c-Jun N-terminal kinases (JNK), protein kinase B (PKB or AKT), potassium channel Kir7.1, and β-arrestin [163-167].

MC3R-induced intracellular signaling, compared to that of MC4R, is less extensively studied. In addition to the Gs signaling, MC3R can couple to Gi and Gq proteins [168, 169]. MC3R modulates intracellular Ca^{2+} mobilization by the IP3-dependent manner, indicating that MC3R can activate the Gq signaling [168]. MC3R also induces Gi signaling [169]. Furthermore, MC3R regulates ERK1/2 signaling via Gi rather than rather than PKA, PKC, and Ca^{2+} signaling in MC3R-transfected HEK293 cells upon NDP-MSH stimulation [169]. However, AgRP, an inverse agonist of MC3R, stimulates ERK1/2 signaling in a PKA- or PI3K-independent way [166]. MC3R was also demonstrated to regulate AKT [166, 170], and further increases intracellular Ca^{2+} concentration in IP3-dependent or independent manner [168, 171] and PKC pathway [172], and inhibits AMPK activity [166].

1.3. Melanocortin-2 receptor accessory proteins

1.3.1 MRAP1

1.3.1.1 MRAP1 discovery, tissue distribution, and structure

MC2R is expressed primarily in the adrenal cortex, and activation MC2R by ACTH stimulates intracellular cAMP generation and further results in adrenal glucocorticoid production. Loss-of-function mutations in *MC2R* cause the rare autosomal recessive disorder familial glucocorticoid deficiency (FGD) [173]. Mutations in *MC2R* cause about 25% of FGD syndrome cases, suggesting that other genetic causes the same clinical phenotype [174]. In addition, MC2R only is expressed in cells derived from an adrenal lineage and cannot reach the cell surface in heterologous cell lines, such as HEK293, CHO, or COS-7 cells [175], indicating the presence of an adrenal specific accessory protein for MC2R. Subsequent genetic studies on FGD patients with normal MC2R identified mutations in another gene, as another cause for this disease, accounting for ~20% of FGD cases [44, 176]. This gene that previously was identified from adipocytes and named fat tissue-specific low molecular weight protein [43] encodes a small single transmembrane protein of unknown functions. This gene has been shown to be necessary for functional MC2R expression, re-named melanocortin 2 receptor accessory protein (*MRAP*), as the specific molecular chaperone for MC2R in regulating receptor expression, ligand binding, and signaling [3, 44-46].

Human *MRAP1* is a six-exon gene on chromosome 21q22.11 [43]. *MRAP1* has two functional *MRAP* splice variants: *MRAP1a* derived from exon 1-5, encoding a protein with 172 amino acids (19 kDa), and *MRAP1b* derived from exon 1-4 and 6, encoding a protein with 102 Amino acids (14.1 kDa). These two splice variants have identical N-termini and transmembrane

domains (TMD) but differ at the C-terminus. Both *MRAP1a* and *MRAP1b* are present in adrenal, breast, testis, fat, skin, ovary, and jejunum tissues. *MRAP1a* is also present in heart, lymph node, liver, stomach, ileum, and *MRAP1b* alone is detected in brain [44]. These results suggest that hMRAP1a and hMRAP1b might possess multiple functions beyond regulating MC2R (primarily expressed in adrenal gland and pituitary) [44]. According to the Human Protein Atlas database, *MC2R* has high expression in adrenal gland and low expression in pituitary, testis, and epididymis, whereas *MRAP1* is present at high level in adrenal gland, breast, and adipose tissue, and low expression in 46 human tissues of 55 tested (**Figure 1.1C**).

MRAP1 forms a unique antiparallel homodimer (**Figure 1.3**). MRAPs were originally predicted to show a type II topology (N_{in}/C_{out}) [44]. Both biochemical and imaging approaches have found that MRAPs have a dual topology in the cell membrane in both N_{out}/C_{in} and N_{in}/C_{out} orientations [46, 177-179]. Utilizing antibodies specifically against the N- or C-terminus of MRAP1, both ends of the endogenous proteins are detected on the extracellular side of membrane in Y1 cells expressing endogenous MRAP1 [46]. After that, using bi-molecular fluorescence complementation, two complementary fragments of YFP fused on the N- and C-terminus of MRAP1 (YFP1-MRAP and MRAP-YFP2), individually, show that fluorescent is observed in ER, indicating that the anti-parallel dimer of MRAP1 is present in the ER early after translation [177, 180]. Existing research has indicated that MRAPs form stable anti-parallel oligomers; nevertheless, the mechanisms responsible for the development of this unusual structure and its stoichiometry have yet to be determined.

The N-terminal and TMD of MRAP1 are highly conserved, whereas the C-terminal region is very variable in evolution. Three conserved motifs are observed in the N-terminus by

site-specific deletions and mutagenesis (**Figure 1.3**). Amino acids 31-37 (LKANKHS) preceding the TMD deletion lead to almost exclusively in the N_{out}/C_{in} orientation of MRAP1, indicating that this motif is required for the dual topology of MRAP1 (topology motif); LDYI motif (18-21 amino acids) is necessary for ACTH binding to MC2R (activation motif), but not required for MC2R trafficking, and deletion or mutations of those four amino acids result in normal MC2R surface expression without binding to ACTH and signaling [177]. YEYY motif of MRAP1 is apparent in nearly every vertebrate examined [181], and plays an important role for MC2R activation [182], in which mutations of those amino acids result in diminished ACTH-induced signaling with normal MC2R expression [182]. TMD is essential for MC2R trafficking and not required for the dual topology of MRAP1, in which a chimeric protein, replacing the TMD of MRAP1 with the TMD of the receptor activity modifying protein 3 (RAMP3) or CD8, shows normal dual topology and leads to reduced MC2R cell face expression and ACTH-induced signaling [182, 183].

Additionally, the N-terminal region of MRAP1 on the outside of the cell is important for functional MC2R, in which mutating or deleting topology and activation motifs in the N_{in}/C_{out} MRAP1 with normal N_{out}/C_{in} has no effect on MC2R signaling, whereas mutation either motif in the N_{out}/C_{in} protomer results in no ACTH-induced signaling [182]. C-terminal of MRAP is not very conserved across species and plays less important for MC2R trafficking and signaling. MRAP constructs with deletion of the entire C-terminus appear to be able to function normally [46, 184]. Two MRAP1 spliced variants, MRAP1a and MRAP1b, differ only in their C-terminal tail, and show similar effects on MC2R trafficking and signaling [45].

1.3.1.2 Physiological roles of the MRAP1

MRAP1 is essential for MC2R trafficking and signaling. Mutations in either *MC2R* or *MRAP1* cause FDG, the manifestation of the adrenal disease (**Figure 1.4A**). *Mrap1* deficiency mice cannot not survive after birth without administration of corticosterone to pregnant dams and impairs adrenal gland development [185]. *MRAP* has wide expression beyond *MC2R*, indicating other physiological functions of MRAP1, especially breast and adipose tissue with high expression of *MRAP1*. The potential physiological roles of the MRAP1 in these tissues have not been investigated yet. Recently, studies have been done to document the potential role of MRAP1 in adipose tissue [186]. *In vitro*, overexpression or knockdown of *Mrap1* in 3T3-L1 cells increases or decreases ACTH-stimulated lipolysis, respectively [186]. *In vivo*, adipose overexpression of *Mrap1* enhances lipolysis mediated by ACTH-MC2R signaling in transgenic mice [186]. Furthermore, *Mrap1* overexpression in adipose tissue increases overall energy expenditure and thermogenesis and does not affect food intake in transgenic mice. Transgenic mice with *Mrap1* overexpression show leaner phenotype with reduced adipocyte size and less fat in adipose tissue than that of WT mice on an HFD, but with similar body weight on the chow diet. Adipose overexpression of *Mrap1* improves insulin sensitivity and hyperlipidemia in HFD-fed mice [186]. These findings indicate MRAP1 plays a critical role in the regulation adipose lipolysis and whole-body energy balance.

1.3.1.3 MRAP1 interactions with melanocortin receptors

In addition to regulating MC2R, MRAP1 was shown to interact with other melanocortin receptors [47]. Until now, there are only three studies focusing on the interaction of MRAP1 and MC1R [47, 187, 188]. Human MRAP1 does not alter MC1R trafficking and decreases NDP-MSH-induced cAMP signaling [47]. In rainbow trout, Mrap1 does not affect signaling of two

Mc1r variants [187]. In Xenopus tropicalis, MRAP1 increases cell surface expression of MC1R, basal and α-MSH- and ACTH-stimulated signaling [188].

At MC3R, human MRAP1a does not alter [47] or decreases cell surface expression of hMC3R [189]. MRAP1 decreases NDP-MSH-induced [47] or increases α-MSH-stimulated [49, 189] cAMP production of hMC3R. In other species, frog MRAP1 increases and chicken MRAP1 does not alter the surface expression of MC3Rs [56, 190]. Xenopus MRAP1 increases α-MSH and ACTH-induced cAMP signaling, and chicken MRAP1 does not modulate agonist-induced signaling of MC3Rs [56, 190].

At MC4R, hMRAP1a decreases the cell surface expression of hMC4R [47, 189], and inhibits α-MSH- and NDP-MSH-induced or does not affect α-MSH- and ACTH-stimulated hMC4R signaling [47, 49]. Chicken MRAP1 was shown to decrease α-MSH-stimulated and has no effect on ACTH-induced signaling of MC4R [56]. MRAP1 increases α-MSH- and ACTH-stimulated signaling of Xenopus MC4R [190]. Additionally, Human MRAP1 was shown to increase [49, 191, 192] or does not affect the basal activities of hMC4R [47, 48].

For MC5R, hMRAP1 decreases cell surface expression of hMC5R and diminishes NDP-induced signaling [47] or does not affect the α-MSH- and ACTH-induced signaling of hMC5R [49]. MRAP1a also is reported to disrupt dimerization and surface localization of MC5R [180].

1.3.1.4 MRAP1 interactions with non-melanocortin receptors

MRAP1 is not required for other MCR (except MC2R) trafficking, but it alters receptor signaling, implying that MRAP1 might interact with other receptors. Most recently, MRAP1 was

shown to interact with somatostatin receptors [193]. RAMPs were originally identified as chaperones that increases the cell surface expression of the calcitonin-like receptor (CLR), a member of Class B GPCR [194]. So far, RAMPs have been found to interact with over 11 different GPCRs from families A, B, and C, altering their trafficking, signaling, and pharmacology [195]. The newly identified and characterized GPCR interacted with RAMPs keeps growing continuously [196]. This experience shows that MRAP will eventually be found to encompass a wider range of activities than we presently understand.

1.3.2 MRAP2

1.3.2.1 MRAP2 discovery, tissue distribution, and structure

MRAP2, a paralogue of MRAP1, was identified in subsequent studied [47]. Human *MRAP2* gene is located at 6q14.3 and encodes a protein with 205 amino acids. MRAP2 shares approximately 40% identity with MRAP1a. Evolutionarily, the MRAP2 might be an ancient subtype, identified in sea lamprey, and MRAP1 separated from MRAP2 at a later stage [197]. In vertebrate evolution, MRAP2 undergoes a process of duplication, resulting in one copy became MRAP1 before the emergence of ray-finned fishes [197]. MRAP1 gene is absent in the most teleost fishes, and only is identified in rainbow trout and zebrafish [198, 199]. MRAP2 are found in almost vertebrate species. In some fishes, *mrap2* gene has two duplicated copies (termed *mrap2a* and *mrap2b*), including zebrafish and topmouth culter [55, 59]. Furthermore, the two forms of Mrap2 in zebrafish and culter, show different effects on Mc3r/Mc4r pharmacology [55, 59].

Similar to MRAP1, MRAP2 also forms the dual topology and several conserved motifs, including LKAHKY (topology motif), YEYY motif, and very conserved TMD (**Figure 1.3**) Interestingly, MRAP2 has been shown to form a heterodimer with the MRAP1 [183]. However, activation motif (LDYI) is absent in MRAP2. Indeed, unlike MRAP1, MRAP2 facilitates MC2R trafficking to cell membrane and subsequent signaling [47]. However, the dosage of ACTH necessary to activate the receptor is 1000 times higher than that of MRAP1 [183, 200]. This might be due to the absence of LDYI motif in MRAP2. Additionally, *Mrap2* mRNA level is significantly lower than *Mrap1* in rat adrenal gland, and *Mrap2* is expressed throughout the adult adrenal cortex, whereas *Mrap1* is mainly expressed in the zona fasciculata [200]. No adrenal phenotype has yet been described in *Mrap2*-deficient mice [55, 200].

According to the Human Protein Atlas database, *MC2R* has wide expression pattern in 55 human tissues tested, with high expression in the CNS (**Figure 1.1D**).

1.3.2.2 Physiological roles of the MRAP2

MRAP2 is abundantly expressed in the CNS, in which are associated with appetite control. MC4R is also expressed in the hypothalamus, especially in the paraventricular nucleus (PVN) where it controls food intake and energy expenditure. Mice lacking *Mc4r* display morbid obesity [25, 26]. Both global *Mrap2*$^{-/-}$ and brain targeted *Mrap2*$^{-/-}$ mice show morbidly obese, and *Mrap2* deficiency mice do not show hyperphagia or reduced energy consumption [50]. Although, both *Mc4r* KO mice and *Mrap2* KO mice show severe obesity, significant differences are observed between the two animal models, in which *Mc4r* KO mice show very early onset of obesity due to hyperphaegia, decreased energy expenditure, increased food intake [25, 26], and

Mrap2 KO mice develop a later onset of obesity without impairment in food intake or in energy expenditure [50]. The central injection of MC4R agonist MTII results in a normal anorexigenic response in *Mrap2* KO mice, indicating functional MC4R. Also, the double *Mc4r*$^{-/-}$ and *Mrap2*$^{-/-}$ mice show obesity phenotype, however, they have low weigh than *Mc4r*$^{-/-}$ mice [50]. *In vitro* studies also confirmed that MRAP2 interacts and regulates MC4R [47]. The important role of MRAP2-regulated-MC4R signaling also is confirmed by overexpression of *Mrap2* in adult paraventricular MC4R neurons [201]. Collectively MRAP2 might modulate energy homeostasis through MC4R-independent and MC4R-mediated manners.

There are two isoforms of Mrap2, Mrap2a and Mrap2b, in Zebrafish. Two Mrap2s have different expression patterns at different stages, with *Mrap2a* expressed from embryos to adults, stimulating growth by blocking Mc4r action in larvae, and *Mrap2b* mainly expressed in adults, enhancing Mc4r response [55]. *In vitro*, Mrap2a decreases the Mc4r affinity for α-MSH, but Mrap2b increases ligand sensitivity of zebrafish Mc4r [55]. Deletion of *mrap2a* caused a significant growth delay but *mrap2b* not [55]. This also demonstrates in-vivo that MRAP2 is an important regulator of the MC4R [55].

In addition to MC4R-mediated signaling, MRAP2 also can regulate the ghrelin receptor (GHSR1a) [202, 203], orexin receptors (OX1R and OX2R)[204], and prokineticin receptor 1 (PKR1) [204, 205]. MRAP2 potentiates ghrelin-stimulated signaling both *in vitro* and *in vivo*, and in the absence of MRAP2, fasting cannot activate AgRP neurons and the orexigenic effect of ghrelin is lost in mice lacking *Mrap2* [202]; MRAP2 was shown to significantly inhibit the anorexigenic signal mediated by blocking PKR1 signaling *in vivo* [205].

MRAP2 mutations are associated with severe obesity in humans [50, 52-54]. Several infrequent *MRAP2* variants are reported from severe obese human patients. Loss-of-function *MRAP2* variants are pathogenic for hyperglycemia, monogenic hyperphagic obesity, and hypertension [53]. About 100 mutations in MRAP2 have been identified (**Figure 1.4B**). Some *MRAP2* variants significantly impair MC4R or MC3R signaling [53, 189]. These findings also support the important roles of MRAP2 in energy balance.

1.3.2.3 MRAP2 interactions with melanocortin receptors

The effects of MRAP1 on MC4R are extensively studied. Human MRAP2 decreases the cell surface expression of hMC4R [47, 189]. Conflicting results were reported previously on and hMRAP2-regulated signaling of hMC4R, in which MRAP2 has no effect [206], or increases [189, 191] α-MSH-stimulated, decreases NDP-MSH-induced [47], and does not affect ACTH-induced [206] signaling of hMC4R. The reason for the discrepancy is not clear. In addition, MRAP2 interaction with MC4R converted the MC4R into an ACTH receptor are observed in fish, avian, and human MC4Rs, increasing the MC4R sensitivity to ACTH [56, 206, 207].

There are also several studies on Mrap2 effect of fish Mc4r pharmacology. Sea lamprey Mrap2 interacts with both Mca and Mcb, inhibits the cell surface expression of the receptors and improves α-MSH-stimulated signaling [208]. Mrap2 inhibits both basal and agonist-induced cAMP signaling of orange-spotted grouper Mc4r, whereas increases basal and decreases agonist-stimulated Erk1/2 signaling [117]. In Nile tilapia, Mrap2 was shown to decrease the cell surface expression and α-MSH-induced cAMP signaling at Mc4r [209]. In snakehead, Mrap2 does not

alter Mc4r trafficking, whereas decreases basal and agonist-induced cAMP signaling [61]. In zebrafish, Mrap2a and Mrap2b show different effect on Mc4r signaling [55].

In other species, MRAP2 enhances agonist-stimulated cAMP signaling of feline MC4R, including increased maximal response and decreased potency [210]. In amphibian species, MRAP2 has been reported to increase the cell surface expression of Xenopus MC4R, basal and ligand-induced signaling [190]; Axolotl Neural MRAP2 decrease the cell surface expression and basal activity at MC4R [211]. In avian, chicken MRAP2 does not alter MC4R trafficking and basal activity, but increases ACTH-stimulated and decreases a-MSH-induced signaling [56].

At the MC3R, MRAP2 decreases cell surface expression of hMC3R [47, 189], but increases α-MSH-stimulated [49, 189] and decreases NDP-MSH-induced [47] cAMP production of hMC3R. In amphibian species, MRAP2 decreases the cell surface expression of Xenopus MC3R, increases basal and ligand-induced signaling [190]; Axolotl Neural MRAP2 does not affect the cell surface expression but decreases basal activity at MC3R [211]. Chicken MRAP2 has no effect on cell surface expression of MC3R, decreases basal activity, increases ACTH-induced signaling but does not alter α-MSH-stimulated cAMP levels [56]. Zebrafish Mrap2s do not affect agonist-induced signaling of Mc3r [55]. In channel catfish, Mrap2 decreases basal and agonist-induced cAMP signaling of Mc3r, but does not affect the basal and agonist-induced Erk1/2 signaling [57].

The effect of MRAP2 on MC1R and MC5R pharmacology is less studied. At the hMC1R, MRAP2 has no effect on cell surface expression but decrease NDP-MSH-stimulated cAMP signaling [47]. MRAP2 interacts with zebrafish Mc1r but does not alter the

pharmacological properties [212]. In the orange-sotted grouper, Mrap2 decreases Mc1r trafficking to cell membrane and agonist-induced cAMP signaling, increases basal but does not change α-MSH-induced Erk1/2 signaling [213].

At the MC5R, When MRAP2 is co-expressed, the MC5R is retained intracellularly [47]. In ricefield eel, Mrap2 does not alter cell surface expression of Mc5r, and decreases agonist-induced cAMP signaling [214]. Elephant shark Mrap2 increases sensitivity to ACTH but not to Des-acetyl-α-MSH of stingray Mc5r [215], but has no effect on ligand sensitivity at elephant shark Mc5r [216].

1.3.2.4 MRAP2 interactions with non-melanocortin receptors

Recently, MRAP2 has been shown to interact with GPCRs beyond the MCRs, including ghrelin receptor (GHSR1a) [202, 203], orexin receptors (OX1R and OX2R) [204], and prokineticin receptor 1 (PKR1) [204, 205]. MRAP2 was shown to decrease the trafficking and signaling of OX1R and PKR1 and inhibits OX2R cell surface expression without affecting signaling [204, 205]. At the ghrelin receptor, MRAP2 has no effect or decreases cell surface expression of ghrelin receptor [202, 203], affects GHSR1a signaling by blocking constitutive activity, the recruitment and signaling of β-arrestin, and improving G protein-dependent signaling (Gs and Gq) [202, 203]. Additionally, MRAP2 regulated Gq and β-arrestin of GHSR1a are independent and involved in different domains of MRAP2 [203]. MRAP2 blocks β-arrestin recruitment to the ghrelin receptor via preventing GHSR1a phosphorylation [217].

Most recently, MRAP2 is reported to interact with glucagon like peptide 1 receptor (GLP1R) and melanin concentrating hormone receptor 1 (MCHR1), resulting in impaired

trafficking and signaling [218]. Wide expression of MRAP2 indicates that MRAP2 might regulate multiple GPCRs in different tissues.

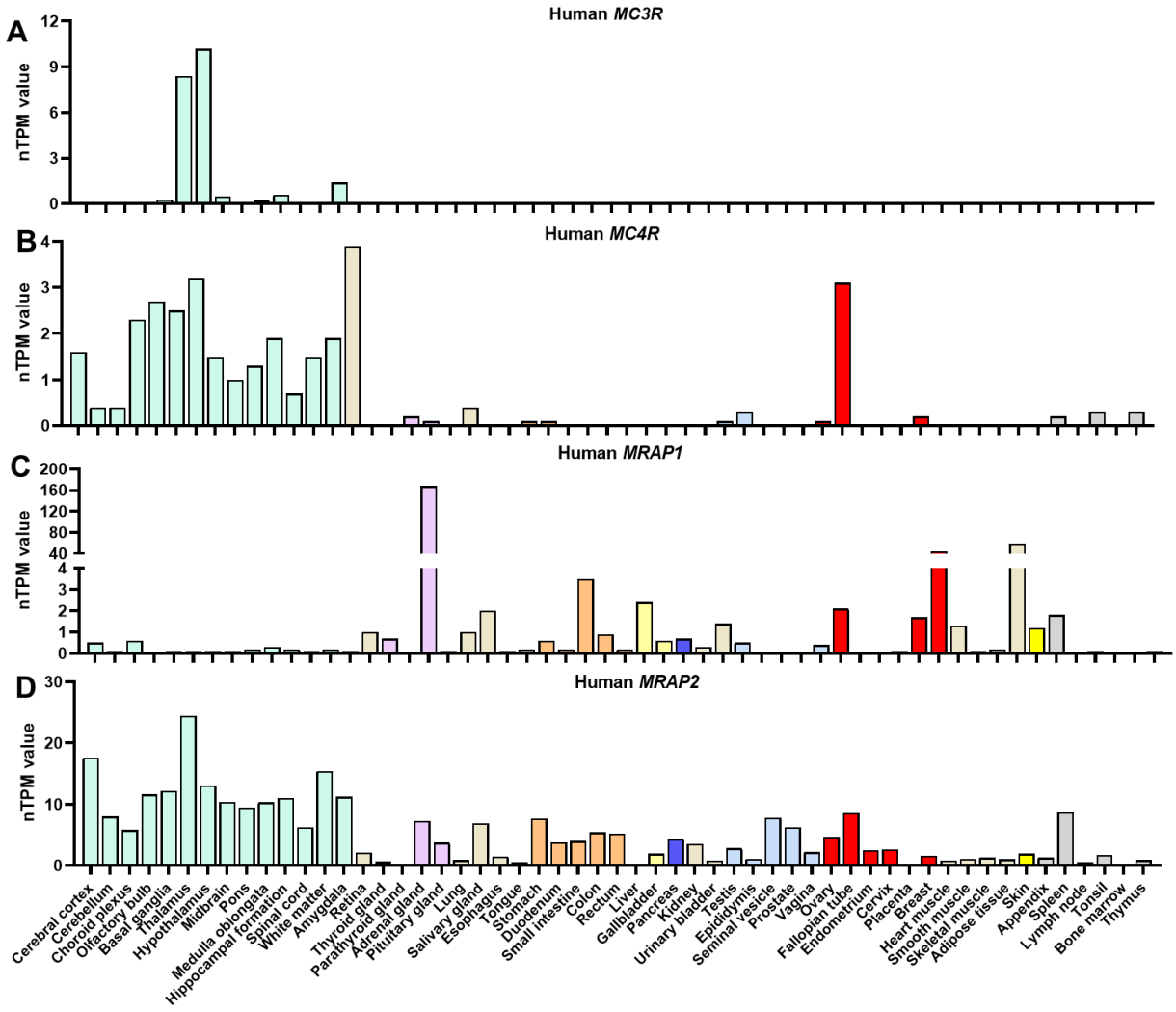

Figure 1.1 Gene expression. *MC3R* (A), *MC4R* (B), *MRAP1* (C), and *MRAP2* (D). Tissue based on https://www. proteinatlas.org/ [219]. nTPM indicates normalized protein-coding transcripts per million. Color-coding is based on tissue groups with functional features in common.

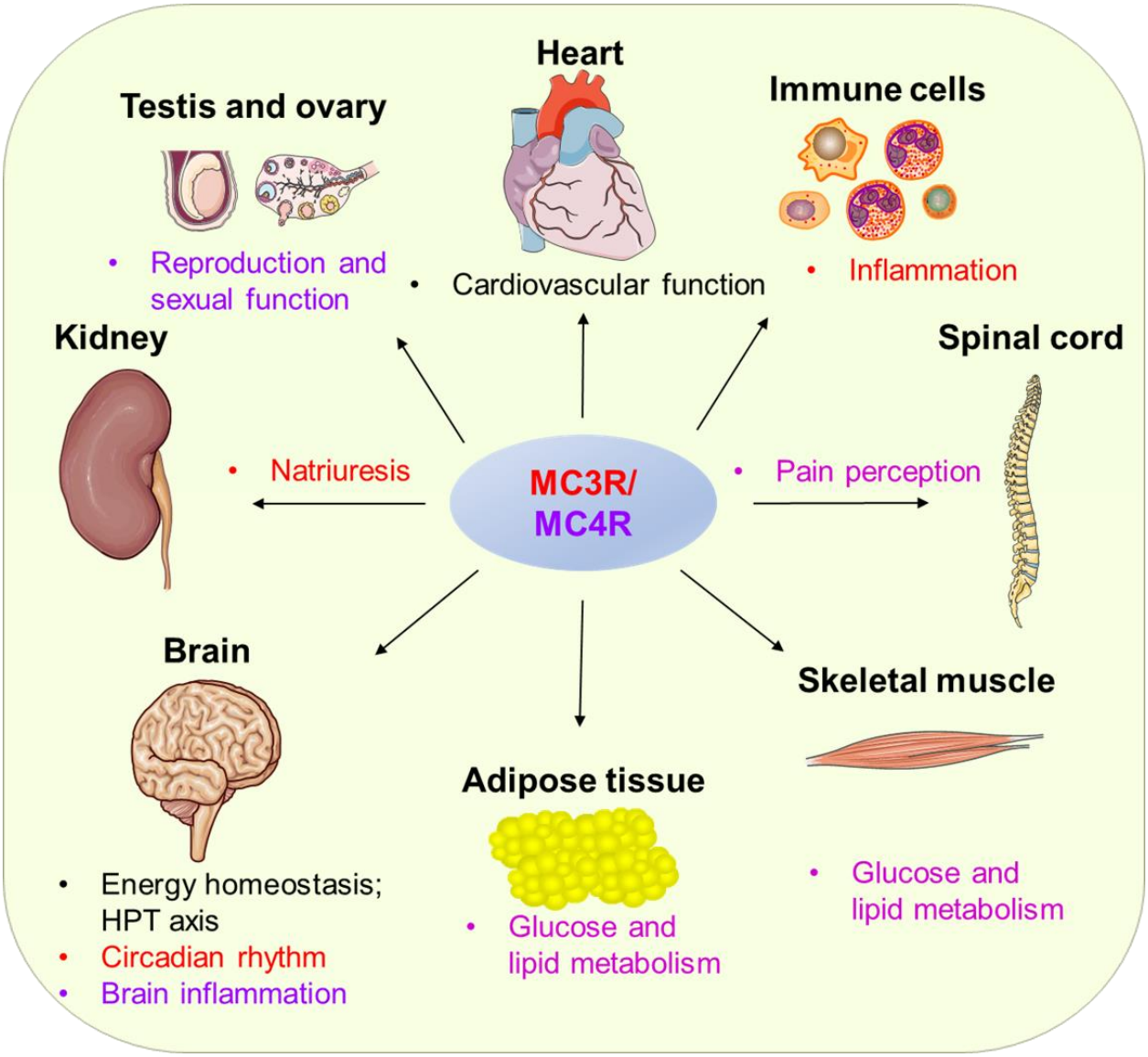

Figure 1.2 Pleiotropic functions of MC3R and MC4R. The red font representedMC3R function, and the purple font represented theMC4R function. The black font represented functions for both MC3R and MC4R. HPT: hypothalamus-pituitary-thyroid. Figure modified based on Liu T, Ji R L, and Tao Y X. Naturally occurring mutations in G protein-coupled receptors associated with obesity and type 2 diabetes mellitus[J]. Pharmacology & therapeutics, 2022: 108044. Copyright 2022 Elsevier.

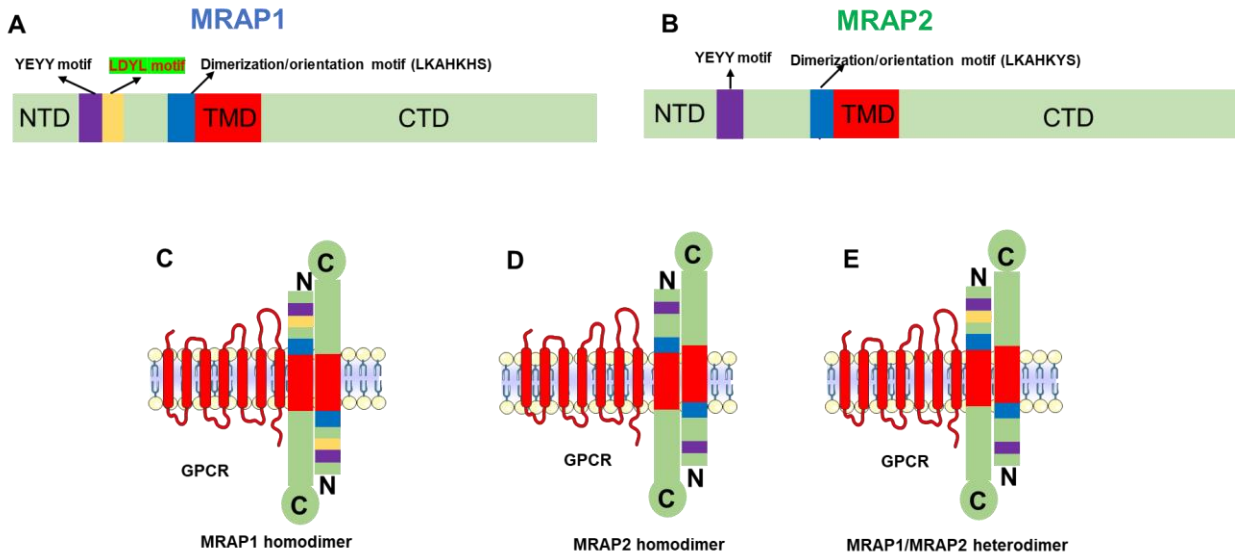

Figure 1.3 Structure and dual topology of MRAP1 and MRAP2. Structure of MRAP1 (A) and MRAP2 (B), MRAP1 homodimer (C), MRAP2 homodimer (D), MRAP1/MRAP2 heterodimer (E). NTD: N-terminus domain; TMD: transmembrane domain; CTD: C-terminus domain.

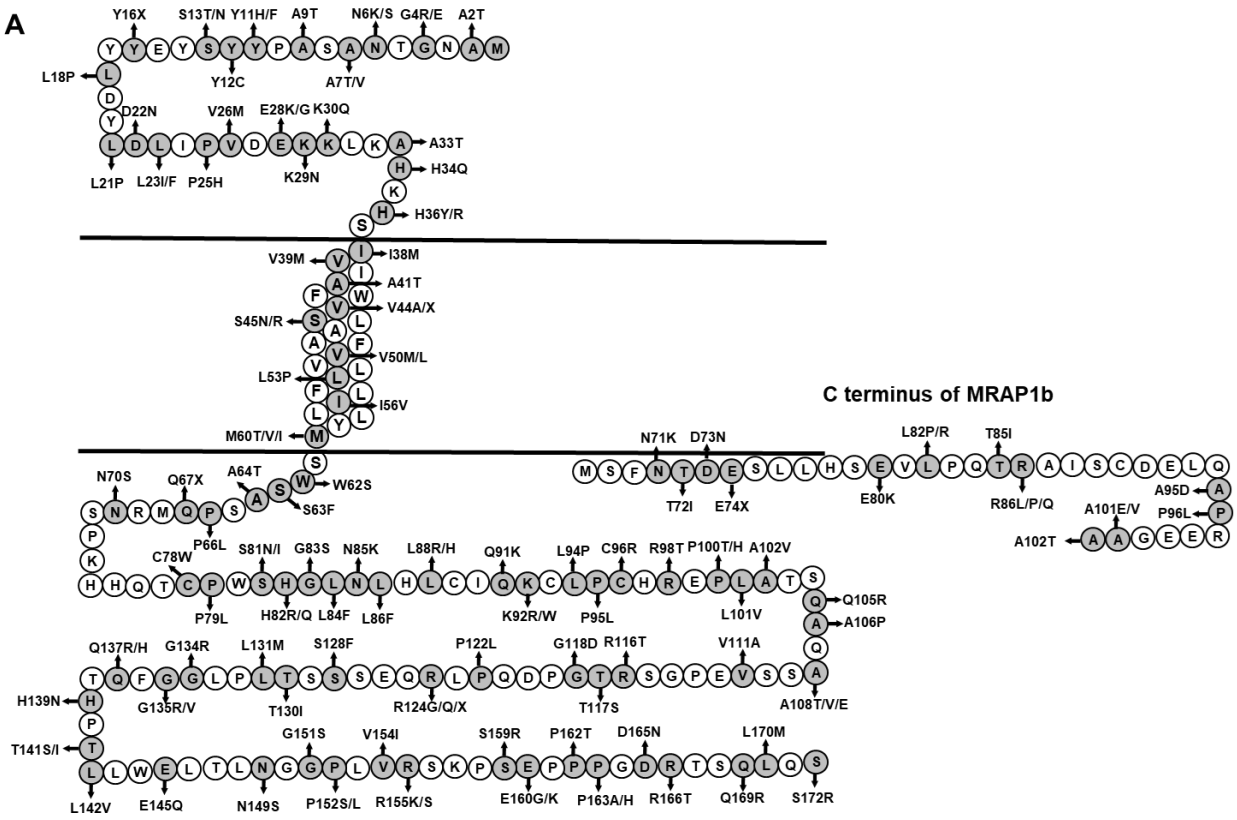
A
C terminus of MRAP1b

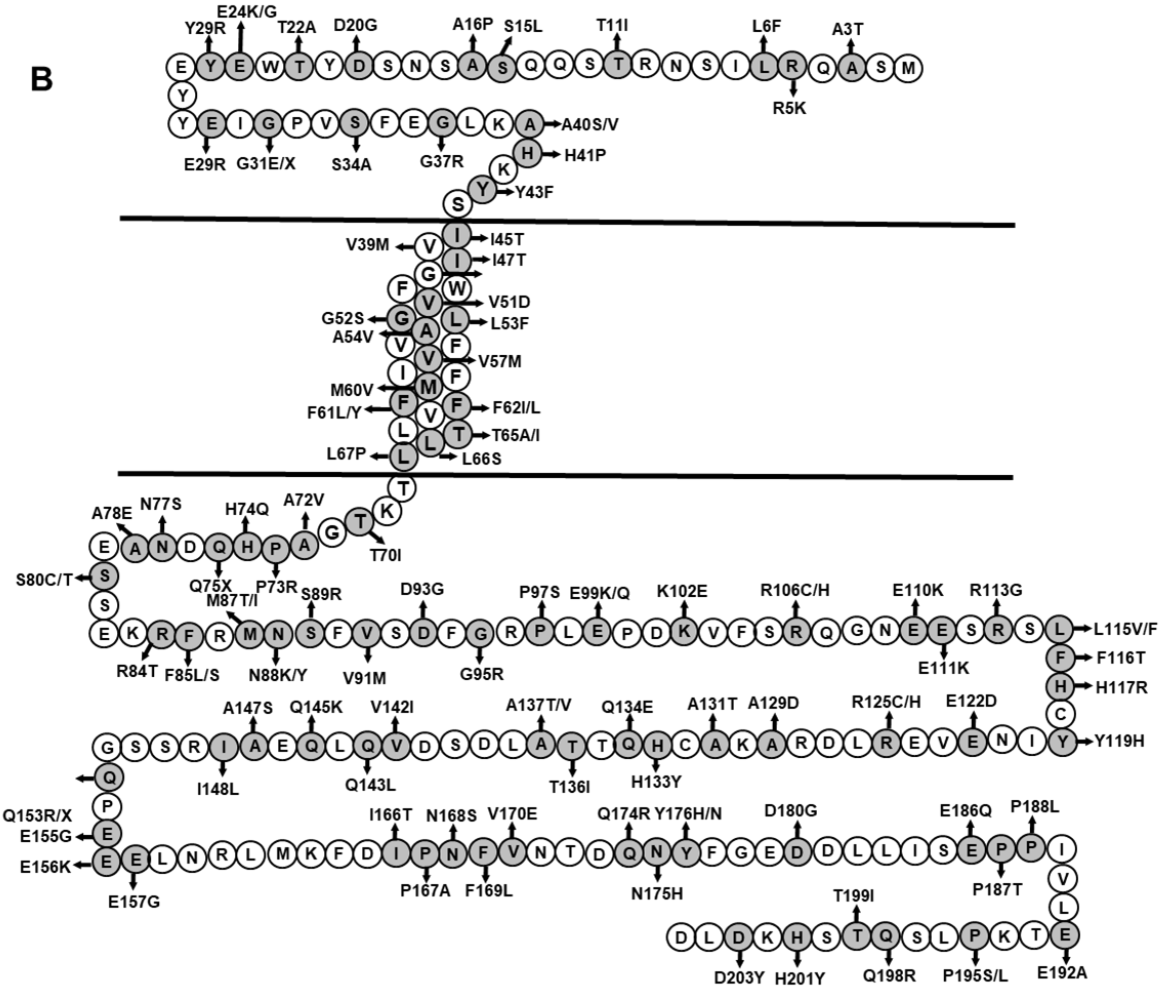

Figure 1.4 Naturally occurring mutations at human *MRAP1*(A) and *MRAP2* (B). The data was registered in gnome database v2.1.1. The circles filled with color were missense and nonsense mutations/polymorphisms. Frameshift mutations were not included in the figure.

Chapter 2: Regulation of melanocortin-3 and -4 receptors by isoforms of melanocortin-2 receptor accessory protein 1 and 2

2. 1 Introduction

Melanocortin receptors (MCRs), MC1R to MC5R, are members of rhodopsin-like Family A G-protein-coupled receptors (GPCRs) activated by melanocortin peptides including (α-, β-, and γ-melanocyte-stimulating hormone (α-, β-, and γ-MSH) and adrenocorticotropic hormone (ACTH) [17, 18]. MC3R and MC4R (neural MCRs) are primarily expressed in the central nervous system [19-22] and play pivotal roles in regulating energy homeostasis [23, 24]. Mice lacking *Mc4r* display morbid obesity with decreased energy expenditure and increased food intake [25, 26]. *Mc3r* knockout mice have moderate obesity phenotype with normal food intake and metabolism, increased fat mass, and decreased lean mass [27-29]. These results indicate distinct non-redundant mechanisms between MC3R and MC4R in regulating energy homeostasis. Furthermore, variants in *MC3R* and *MC4R* have been shown to be closely associated with monogenic human obesity [13, 30-33]. In addition, MC4R is also involved in sexual function and reproduction [13, 32]. MC3R is also expressed in the periphery and may have potential physiological functions in regulating cardiovascular function [34, 35], immune response [36-40], natriuresis [41], and timing of sexual maturation [42].

Melanocortin-2 receptor accessory protein 1 (MRAP1), first identified as low molecular weight protein from fat tissue [43], was the first MC2R accessory protein identified, as the specific molecular chaperone for MC2R in regulating receptor expression, ligand binding, and signaling [3, 44-46]. *MRAP1* mutations account for ~20% of familial glucocorticoid deficiency

cases [44, 176]. There are two alternatively spliced isoforms of human (h) MRAP1, hMRAP1a and hMRAP1b, with similar effects on MC2R trafficking and signaling [44, 45]. *MRAP1a* and *MRAP1b* are widely expressed, but their distribution patterns are distinct [44, 220]. These results suggest that hMRAP1a and hMRAP1b might possess multiple functions beyond regulating MC2R (primarily expressed in adrenal gland) [44]. Indeed, hMRAP1a has been shown to regulate all five hMCRs in distinct ways [47-49]. However, almost all of the investigations focus on MRAP1a and its regulation on MC3R/MC4R, and there are few studies on MRAP1b.

MRAP2 (a paralog of MRAP1) shares 40% homology with MRAP1 and has different functions from MRAP1s. MRAP2 with high expression in brain is essential for modulation of energy homeostasis. *Mrap2* knockout mice display early-onset severe obesity [50, 51]. *MRAP2* mutations are associated with severe obesity in humans [50, 52-54]. MRAP2 regulates MC3R or MC4R signaling in mammals and other species [47, 50, 55-61]. It has been reported that hMRAP2a either decreases NDP-MSH-stimulated [47] or increases α-MSH-stimulated [189] cAMP generation of hMC3R and hMC4R. In addition, hMRAP2a increases ACTH potency of hMC4R [206]. In teleosts, there are two copies of *mrap2* (*mrap2a* and *mrap2b*) in zebrafish and topmouth culter with various modulatory roles of MCRs in these fishes [55, 59, 60].

Recently, we identified two new human *MRAP2* splice variants, *MRAP2b* and *MRAP2c*. Human MRAP2b and MRAP2c share the same amino acid sequences in N-termini and transmembrane domains (TMD) with hMRAP2a. However, whether MRAP2b and MRAP2c are involved in MC3R/MC4R regulation was unknown. Additionally, the regulation of MC3R/MC4R by MRAP1b is not clear. Hence, the potential effects of all five isoforms of hMRAPs, hMRAP1a, hMRAP1b, hMRAP2a, hMRAP2b, and hMRAP2c, on hMC3R and hMC4R pharmacology were systematically investigated in this study.

2.2 Materials and Methods

2.2.1 Ligands and plasmids

NDP-MSH was obtained from Peptides International (now Vivitide, Louisville, KY, USA). α-MSH was purchased from Pi Proteomics (Huntsville, AL, USA). Human ACTH (1-24) was purchased from Phoenix Pharmaceuticals (Burlingame, CA, USA). [^{125}I]-NDP-MSH and [^{125}I]-cAMP were iodinated using chloramine T method [221, 222]. The N-terminal myc-tagged human MC4R (hMC4R) subcloned into pcDNA3.1 vector was generated as previously described [223]. N-terminal myc-tagged hMC3R and N-terminal Flag-tagged hMRAP1a, hMRAP1b, hMRAP2a, hMRAP2b, and hMRAP2c were commercially synthesized by Synbio Technologies (Monmouth Junction, NJ, USA) to generate the plasmids used for transfection.

2.2.2 Cell culture and transfection

Human embryonic kidney (HEK) 293T cells were obtained from the American Type Culture Collection (Manassas, VA, USA) and were cultured at 37 °C in a 5% CO_2-humidified atmosphere in Dulbecco's Modified Eagle's medium (DMEM) containing 10% newborn calf serum, 10 mM HEPES, 100 IU/mL of penicillin, 0.25 μg/mL of amphotericin B, 50 μg/mL of gentamicin, and 100 μg/mL streptomycin [223]. Cells were plated into gelatin-coated 24-well plates. Cells, when reaching 50-70% confluency, were co-transfected with 0.25 μg/μL hMC3R or hMC4R with or without MRAP1 or MRAP2 plasmids using calcium phosphate precipitation method [224]. The total DNA was normalized using empty vector pcDNA3.1 in each well.

2.2.3 Flow cytometry assay

The influence of hMRAP1s or hMRAP2s on the total and cell surface expression of hMC3R and hMC4R was performed using flow cytometry (Accuri Cytometers, Ann Arbor, MI, USA) as described previously [118, 225]. Cells (6-well plates) were transfected with hMC3R or hMC4R (N-terminal c-myc tag) and hMRAP1a, hMRAP1b, hMRAP2a, hMRAP2b or hMRAP2c plasmids at a ratio of 1:5. Fluorescence of cells transfected with empty vector (pcDNA3.1) was used for background staining. The expression of the hMC3R or hMC4R was calculated as the percentage of the cell transfected with hMC3R or hMC4R but without MRAPs set as 100% [225].

2.2.4 Radioligand binding assays

Binding assay was described previously [57, 223]. To explore the regulation of hMRAP1s or hMRAP2s on the binding property of hMC3R or hMC4R, hMC3R or hMC4R (0.25 μg/μL) with hMRAP1 or hMRAP2 plasmids at a ratio of 1:5 was co-transfected into cells (24-well plate or 6-well plate). Two ligands, α-MSH (from 10^{-12} to 10^{-5} M) and ACTH (1-24) (from 10^{-12} to 10^{-6} M), were used in this study.

2.2.5 Ligand-stimulated cAMP assays

cAMP signaling assay was performed by radioimmunoassay (RIA) as described previously [74, 221, 223]. Cells (24-well plate) were transfected with hMC3R or hMC4R (0.25 μg/μL) and hMRAP21s or hMRAP2s plasmids at a ratio of 1:5, and two ligands, α-MSH and ACTH (1-24), were used.

2.2.6 Statistical analysis

All data were represented as mean ± S.E.M. The parameters and significance of differences were calculated by GraphPad Prism 8.3 software (GraphPad, San Diego, CA, USA). The

significance of differences in ligand binding, cAMP signaling, and flow cytometry parameters were all determined by One-way ANOVA, with $P < 0.05$ set as significant.

2.3 Results

2.3.1 Nucleotide and deduced amino acid sequences of hMRAP2s

Human *MRAP2* (NG_051944.1) is composed of 11 exons. Three *MRAP2* splice variants were identified: *MRAP2a* (XM_017010220.1) derived from 4 exons (1, 3, 4, and 6) that had 618 bp open reading frame (ORF), encoding a protein of 205 amino acids; *MRAP2b* (XM_017010221.2) derived from 6 exons (2, 3, 4, 7, 8, and 9) that had a 465 bp ORF, encoding a protein of 154 amino acids; and *MRAP2c* (XM_024446318.1) derived from 4 exons (2, 3, 4, and 5) that had a 381 bp ORF, encoding a protein of 126 amin acids (**Figure 2.1A**). Human MRAP2b and hMRAP2c had the same sequences in the N- termini, a putative LKAHKYS motif, and a single conserved TMD but different C-termini from hMRAP2a (**Figure 2.1B**). Two potential *N*-linked glycosylation site (Asn^3 and Asn^6) in N-termini of hMRAP1a and hMRAP1b, and one potential *N*-linked glycosylation site (Asn^9) in N-termini of hMRAP2a, hMRAP2b, and hMRAP2b (**Figure 2.1B**). In addition, a conserved motif (YEYY) was observed in all hMRAP1s and hMRAP2s (**Figure 2.1B**). LDYL motif was only present in hMRAP1s but not in hMRAP2s (**Figure 2.1B**). MRAP2a shared 60% amino acid identity to MRAP2b, and 97% identity to MRAP2c (**Figure 2.1C**). MRAP2b had 99% identity to MRAP2c (**Figure 2.1C).**

2.3.2 Regulation of hMC3R pharmacology by hMRAP1s and hMRAP2s

Flow cytometry was used to determine MRAP regulation of hMC3R expression (Figure 2.2). The results showed that hMRAP1a and hMRAP2c significantly increased the cell surface expression, and hMRAP1b decreased the cell surface expression of hMC3R (**Figure 2.2A**).

Human MRAP2a and hMRAP2b had no effect on the cell surface expression of hMC3R (**Figure 2.2A**). Only hMRAP1b decreased the total expression of hMC3R, and the other four MRAPs did not affect the total expression of hMC3R (**Figure 2.2B**).

Competitive ligand binding assays were performed to explore MRAP regulation of hMC3R binding properties. Different concentrations of unlabeled α-MSH or ACTH (1-24) were used to compete with a fixed amount of ^{125}I-NDP-MSH. Results showed that only hMRAP1b significantly decreased the maximal binding value (B_{max}), and hMRAP1a, hMRAP2a, hMRAP2b, and hMRAP2c had no significant effect on B_{max}s of hMC3R (**Figure 2.3** and **Table 2.1**). All MRAPs did not affect α-MSH affinities at hMC3R (**Figure 2.3A** and **Table 2.1**). Only hMRAP1a increased ACTH affinity of hMC3R, and the other MRAPs had no effect on affinities of hMC3R to ACTH (**Figure 2.3B** and **Table 2.1**).

The signaling properties of hMC3R modulated by MRAPs were determined using cAMP RIA. Results showed that all hMRAPs had no significant effect on potencies of hMC3R to α-MSH and ACTH (**Figures 2.4A & B** and **Table 2.2**). Four hMRAPs (hMRAP1a, hMRAP1b, hMRAP2a, and hMRAP2c) markedly decreased maximal responses (R_{max}) in response to α-MSH and ACTH, and hMRAP2b deceased R_{max} to ACTH but not α-MSH (**Figures 2.4A & B** and **Table 2.2**). In addition, all MRAPs significantly decreased the basal activities of hMC3R (**Table 2.2**).

2.3.3 Regulation of hMC4R pharmacology by hMRAP1s and hMRAP2s

Results of flow cytometry showed that hMRAP1a, hMRAP2a, and hMRAP2c significantly increased, while hMRAP1b and hMRAP2b had no significant effect on the cell surface and total expression of hMC4R (**Figures 2. 5A, B**).

Ligand binding assays indicated that at hMC4R, hMRAP1a and hMRAP1b significantly decreased B_{max}s, while hMRAP2a increased B_{max}s (**Figure 2.6 and Table 2.3**). No significant effect was observed for hMRAP1a, hMRAP1b, hMRAP2a, hMRAP2b, and hMRAP2c on α-MSH affinities at the hMC4R (**Figure 2.6A and Table 2.3**). Additionally, hMRAP1b increased affinity, whereas hMRAP2a decreased affinity of hMC4R to ACTH (**Figure 2.6B and Table 2.3**). MRAP1a, MRAP2b, and MRAP2c had no effect on affinities of hMC4R to ACTH (**Figure 2.6B and Table 2.3**).

Modulation of hMC4R signaling by MRAP1s and MRAP2s was also studied. Data showed that all MRAPs had no effect on α-MSH potencies of hMC4R (**Figure 2.7A and Table 2.4**). Only hMRAP1a significantly increased ACTH potency, and the other MRAPs did not affect ACTH potency at hMC4R (**Figure 2.7B and Table 2.4**). Both hMRAP1a and hMRAP1b significantly increased the basal cAMP levels, whereas all three MRAP2s decreased the basal activities of hMC4R (**Figure 2.7A**). Additionally, all MRAPs decreased R_{max}s of hMC4R when α-MSH was used (**Figure 2.7B**). Only hMRAP1b decreased ACTH-stimulated cAMP generation, and the other MRAPs had no effect on R_{max}s of hMC4R in response to ACTH (**Figure 2.7B**).

2.4. Discussion

Alternative splicing is prevalent in eukaryotes, resulting in greatly increased diversity of proteins encoded by the genome [226]. Tissue-specific and developmentally regulated alternative splicing is also modulated by divergent stimulation. Approximately 95% of multi-exon genes are alternatively spliced in humans [227, 228]. Isoforms produced by alternative splicing might have different functions. For example, two splice variants of receptor expression-enhancing protein 6

gene have distinct functions in the retina [229]. However, in the majority of cases, isoforms from alternative splicing have not been well investigated. In this study, we identified two human *MRAP2* splice variants, *MRAP2b* and *MRAP2c*. Additional studies are needed to confirm which tissues express these alternative splicing variants. Human MRAP1 also have two isoforms: MRAP1a and MRAP1b. The potential effects of the two MRAP1 and three MRAP2 isoforms on hMC3R and hMC4R pharmacology were investigated herein.

Human MRAP1s and hMRAP2s have several similar structural features as MRAP1 and MRAP2 of other species. The conserved motif, LKAHKHS in hMRAP1 or LKAHKYS in hMRAP2, is required for reverse topology (**Figure 2.1B**) [46, 177, 230], and the corresponding reverse topology motif is also observed in MRAP1 and MRAP2 orthologs of other species [199]. In addition, YEYY motif is apparent in both MRAP1 and MRAP2 of nearly every vertebrate examined [181], and play an important role for MC2R activation [182]. However, the activation motif (LDYL) was only found in the hMRAP1 paralogs but not in hMRAP2s (**Figure 2.1B**), which is a critical difference between MRAP1 and MRAP2 [199]. MRAP1 paralogs facilitate the activation of hMC2R, but MRAP2 paralogs (without this activation motif) cannot promote MC2R activation in teleosts and tetrapods [199, 230-232].

Detailed pharmacological studies were performed on potential MRAP regulation of hMC3R. There was no report on the regulation of hMC3R by hMRAP1b, hMRAP2b, and hMRAP2c. Both hMRAP1a and hMRAP2a were reported to decrease the cell surface expression of hMC3R [47, 189]. Our data showed that hMRAP1a and hMRAP2c increased, hMRAP1b decreased, and hMRAP2a and hMRAP2b had no effect on the cell surface expression of hMC3R (**Figure 2.2A**). Previously, it has been reported that both hMRAP1a and hMRAP2a decrease NDP-MSH-stimulated [47] or increase α-MSH-induced [49, 189] cAMP production of hMC3R.

The current study is the first to explore potential MRAP modulation of MC3R using ACTH. In this study, four MRAPs (hMRAP1a, hMRAP1b, hMRAP2a, and hMRAP2c) showed similar effects on MC3R signaling, resulting in decreased α-MSH- and ACTH-stimulated cAMP levels of hMC3R (MRAP2b only decreased ACTH-stimulated signaling of hMC3R) (**Figure 2.4 and Table 2.2**). Our findings indicated that hMRAP1b, hMRAP2b, and hMRAP2c might also be involved in regulating hMC3R in distinct ways compared with hMRAP1a and hMRAP2a. In addition, MRAP1 or MRAP2 has been reported to increase ACTH potency at chicken and frog MC3R [56, 190]. However, MRAP2s have no effect on ACTH potency of fish (topmouth culter) MC3R [60]. Our current results showed that all MRAPs had no effect on ACTH potency at hMC3R (**Table 2.2).** Further studies in MC3Rs from other species are needed to address whether MRAPs change MC3R to an ACTH-preferring receptor.

The regulation of MRAP1s and MRAP2s on hMC4R was also studied. It was reported that hMRAP1a and hMRAP2a decrease the cell surface expression of hMC4R [47, 189]. Our current results showed that hMRAP1a, hMRAP2a, and hMRAP2c increased the cell surface expression of hMC4R whereas hMRAP1b and hMRAP2b had no effect (**Figure 2.5A**). For signaling, conflicting results were reported previously: hMRAP1a was reported to either decrease NDP-MSH-stimulated [47] or increases [189, 191] or does not affect α-MSH-stimulated [49] signaling of hMC4R. Our data showed that MRAP1b decreased α-MSH- and ACTH-induced cAMP generation, while MRAP1a only decreased α-MSH-stimulated cAMP signaling of hMC4R (**Figure 2.7 and Table 2.4**). Inconsistent results were also reported on hMRAP2-regulated hMC4R signaling: MRAP2a has no effect [206] or increases [189, 191] α-MSH-stimulated signaling of hMC4R. MRAP2a does not affect ACTH-induced [206] or decreases NDP-MSH-stimulated [47] cAMP levels of hMC4R. Our study demonstrated that all

MRAP2s decreased α-MSH-stimulated cAMP signaling but had no effect on ACTH-induced signaling of hMC4R (**Figure 2.7 and Table 2.4**). Similar results were also observed in chicken MC4R, in which MRAP1 and MRAP2 do not affect ACTH-stimulated signaling, but inhibit α-MSH-induced signaling [56]. Our findings suggested that the new isoforms studied herein, hMRAP1b, hMRAP2b, and hMRAP2c, could modulate MC4R signaling.

An interesting observation reported previously is that MRAPs might change MC4R preference to different endogenous ligands. Previous results showed that hMRAP1a or hMRAP2a increase [191, 206] or do not affect α-MSH potency at hMC4R [49]. Two endogenous hormones, α-MSH and ACTH, are used in this study to investigate whether MRAPs change ligand potencies of hMC4R. Our results showed that MRAP1s and MRAP2s could not change α-MSH potencies of hMC4R (**Table 2.4**). For ACTH, there is no report on whether MRAP1 affects ACTH potency at hMC4R, and hMRAP2a was reported to increase ACTH potency at hMC4R [206]. MRAP2 increase of ACTH potency of MC4R has also been observed in several other species, including pig, chicken, frog, and zebrafish [56, 58, 190, 206, 207]. However, this phenomenon was not observed in several other species, such as orange-spotted grouper [117], Nile tilapia [209], topmouth culter [59], and snakehead [61]. Our results showed that only hMRAP1a significantly increased ACTH potency, and the other MRAPs had no effect on ACTH potency at hMC4R (**Table 2.4**). We conclude that the MRAP effect on ACTH potency at MC4R might be species dependent.

Human MC4R has modest basal cAMP signaling [74]. The loss of constitutive activity in *MC4R* mutations is considered as one cause of obesity [9, 146]. The higher constitutive activity of hMC4R is pivotal in regulating energy homeostasis [147], and increased basal activity of MC4R might protect against obesity. Human MRAP1a was shown to increase [49, 191] or have

no significant effects on the constitutive activity of hMC4R [47, 48]. The ratios between hMC4R and hMRAP1a have an important effect on the basal activity of hMC4R [49, 191], which might result in the inconsistent results. Our finding showed that both hMRAP1a and hMRAP1b significantly increased hMC4R basal activity (**Table 2.4**).

At hMC4R, MRAP2 was reported to have no significant effect on the basal activity [47, 48, 191, 233]. However, MRAP2(s) has been shown to decrease MC4R basal activity in other species, including zebrafish [55], orange-spotted grouper [117], Nile tilapia [209], topmouth culter [59], and snakehead [61]. In addition, hMRAP2a also inhibits the basal activity of ghrelin receptor [203]. Our study found that all three MRAP2s decreased hMC4R basal cAMP signaling (**Table 2.4**). MRAP2 regulates GPCR signaling in a dose-dependent manner [55, 59, 60, 117, 190, 203, 205]. Thus, different ratios between hMC4R and hMRAP2 in previous studies might lead to the inconsistent results. The potential regulation of constitutive activity in MC4R by MRAPs needs further study.

Splicing variants with different specific domains provide a nature-made opportunity to study functions of specific domain. Lab-generated truncated MRAPs indicate that N-terminus, but not C-terminus, of hMRAP1 has crucial roles in regulating hMC2R trafficking and signaling [184], and similar phenomena have been observed in the cells heterologously expressing truncated mouse MRAP1 and hMC2R [46, 177]. The present study found that hMRAP1a and hMRAP1b with different C-termini played different roles in regulating hMC3R or hMC4R pharmacology (**Tables 2.2 and 2.4**), indicating that C-termini of MRAP1 is important for modulation of MC3R and MC4R signaling. Results of MRAP2 deletion mutants and chimeras indicate that the C-terminus of MRAP2a is important for trafficking and signaling of GPCRs, such as ghrelin receptor, orexin receptor, and prokineticin receptor [203, 204]. Similar to

MRAP1s, hMRAP2a, hMRAP2b, and hMRAP2c are also different in C-termini. However, our study suggested that C-termini of hMRAP2s played distinct roles in regulating MC3R/MC4R trafficking with similar effects on signaling (**Figures 2.2 and 2.5, Tables 2.2 and 2.4**). Collectively, these results suggest that distinct regions of MRAP1s or MRAP2s might have different roles in regulating diverse GPCRs, resulting in increased complexity of MRAPs in modulating GPCRs.

In summary, MRAP1b and two newly identified MRAP2 splicing variants, hMRAP2b and hMRAP2c, had potential roles in regulating MC3R and MC4R pharmacology. All MRAPs except MRAP2b decreased α-MSH- and ACTH-stimulated cAMP generation of hMC3R. MRAP1s and MRAP2s showed opposite effects on the basal activity of hMC4R, with MRAP1s increasing and MRAP2s decreasing the basal activities of hMC4R. MRAP1a conferred increased potency for ACTH at the hMC4R whereas the other MRAPs had no effect on ACTH potency. These findings suggest complexity of MRAPs in modulating MC3R/MC4R and provide a new opportunity for regulating MC3R and MC4R signaling.

Table 2.1 The ligand binding properties of hMC3R regulated by hMRAP1s and hMRAP2s

	B_{max} (%)	α-MSH binding IC_{50} (nM)	ACTH binding IC_{50} (nM)
hMC3R	100	667.50 ± 152.87	85.81 ± 14.16
hMC3R+MRAP1a	85.69 ± 7.43	360.20 ± 47.09	17.49 ± 3.42[a]
hMC3R+MRAP1b	63.26 ± 6.19[a]	490.84 ± 179.41	42.75 ± 13.05
hMC3R+MRAP2a	91.42 ± 8.31	820.24 ± 177.02	80.64 ± 13.63
hMC3R+MRAP2b	102.49 ± 7.93	895.85 ± 131.95	65.03 ± 10.47
hMC3R+MRAP2c	87.77 ± 6.35	479.51 ± 71.39	80.94 ± 14.78

Values are expressed as the mean ± SEM of at least three independent experiments.
[a] Significant difference from the parameter of hMC3R, $P < 0.05$.

Table 2.2 The signaling properties of hMC3R regulated by hMRAP1s and hMRAP2s

		α-MSH		ACTH (1-24)	
	Basal (%)	EC_{50} (nM)	R_{max} (%)	EC_{50} (nM)	R_{max} (%)
hMC3R	100	1.39 ± 0.16	100	4.63 ± 0.81	100
hMC3R+MRAP1a	77.06 ± 5.95[b]	1.31 ± 0.28	58.22 ± 9.55[a]	1.81 ± 0.65	58.54 ± 8.98[b]
hMC3R+MRAP1b	58.25 ± 5.35[c]	5.46 ± 1.99	52.41 ± 11.58[a]	8.39 ± 2.58	34.26 ± 3.95[c]
hMC3R+MRAP2a	74.18 ± 10.50[a]	3.82 ± 1.14	39.07 ± 8.66[b]	4.91 ± 2.15	46.85 ± 17.28[a]
hMC3R+MRAP2b	67.39 ± 7.43[b]	1.25 ± 0.36	86.61 ± 10.49	2.07 ± 0.85	66.85 ± 16.92[a]
hMC3R+MRAP2c	64.36 ± 11.57[a]	1.79 ± 0.32	59.07 ± 6.60[b]	3.39 ± 1.19	52.10 ± 16.25[a]

Values are expressed as the mean ± SEM of at least three independent experiments.
[a] Significant difference from the parameter of hMC3R, $P < 0.05$.
[b] Significant difference from the parameter of hMC3R, $P < 0.01$.
[c] Significant difference from the parameter of hMC3R, $P < 0.001$.

Table 2.3 The ligand binding properties of hMC4R regulated by hMRAP1s and hMRAP2s

	B_{max} (%)	α-MSH IC_{50} (nM)	ACTH (1-24) IC_{50} (nM)
hMC4R	100	335.51 ± 32.19	53.62 ± 13.46
hMC4R+MRAP1a	48.96 ± 7.57[a]	234.73 ± 79.01	26.16 ± 13.77
hMC4R+MRAP1b	48.01 ± 8.94[a]	289.67 ± 77.10	19.08 ± 2.52[a]
hMC4R+MRAP2a	143.32 ± 11.76[a]	355.93 ± 39.71	123.18 ± 22.12[a]
hMC4R+MRAP2b	133.72 ± 14.64	330.42 ± 70.97	55.78 ± 18.24
hMC4R+MRAP2c	132.51 ± 9.31	380.19 ± 87.45	69.64 ± 10.53

Values are expressed as the mean ± SEM of at least three independent experiments.
[a] Significant difference from the parameter of hMC4R, $P < 0.05$.

Table 2.4 The signaling properties of hMC4R regulated by hMRAP1s and hMRAP2s

		α-MSH		ACTH (1-24)	
	Basal (%)	EC_{50} (nM)	R_{max} (%)	EC_{50} (nM)	R_{max} (%)
hMC4R	100	5.10 ± 0.80	100	1.81 ± 0.34	
hMC4R+MRAP1a	659.91 ± 97.58[c]	4.79 ± 2.31	47.81 ± 6.97[a]	0.33 ± 0.05a	93.28 ± 23.57
hMC4R+MRAP1b	152.41 ± 12.81[b]	4.27 ± 1.33	49.20 ± 7.90[a]	0.89 ± 0.19	66.29 ± 12.29[a]
hMC4R+MRAP2a	55.88 ± 8.92[b]	3.10 ± 0.14	56.90 ± 18.75[a]	3.20 ± 0.41	102.73 ± 22.28
hMC4R+MRAP2b	66.34 ± 7.52[b]	3.26 ± 0.63	45.96 ± 13.34[b]	1.89 ± 0.28	121.35 ± 22.98
hMC4R+MRAP2c	65.37 ± 7.55[b]	3.43 ± 0.96	33.04 ± 7.10[b]	3.27 ± 0.86	81.54 ± 14.07

Values are expressed as the mean ± SEM of at least three independent experiments.
[a] Significant difference from the parameter of hMC4R, $P < 0.05$.

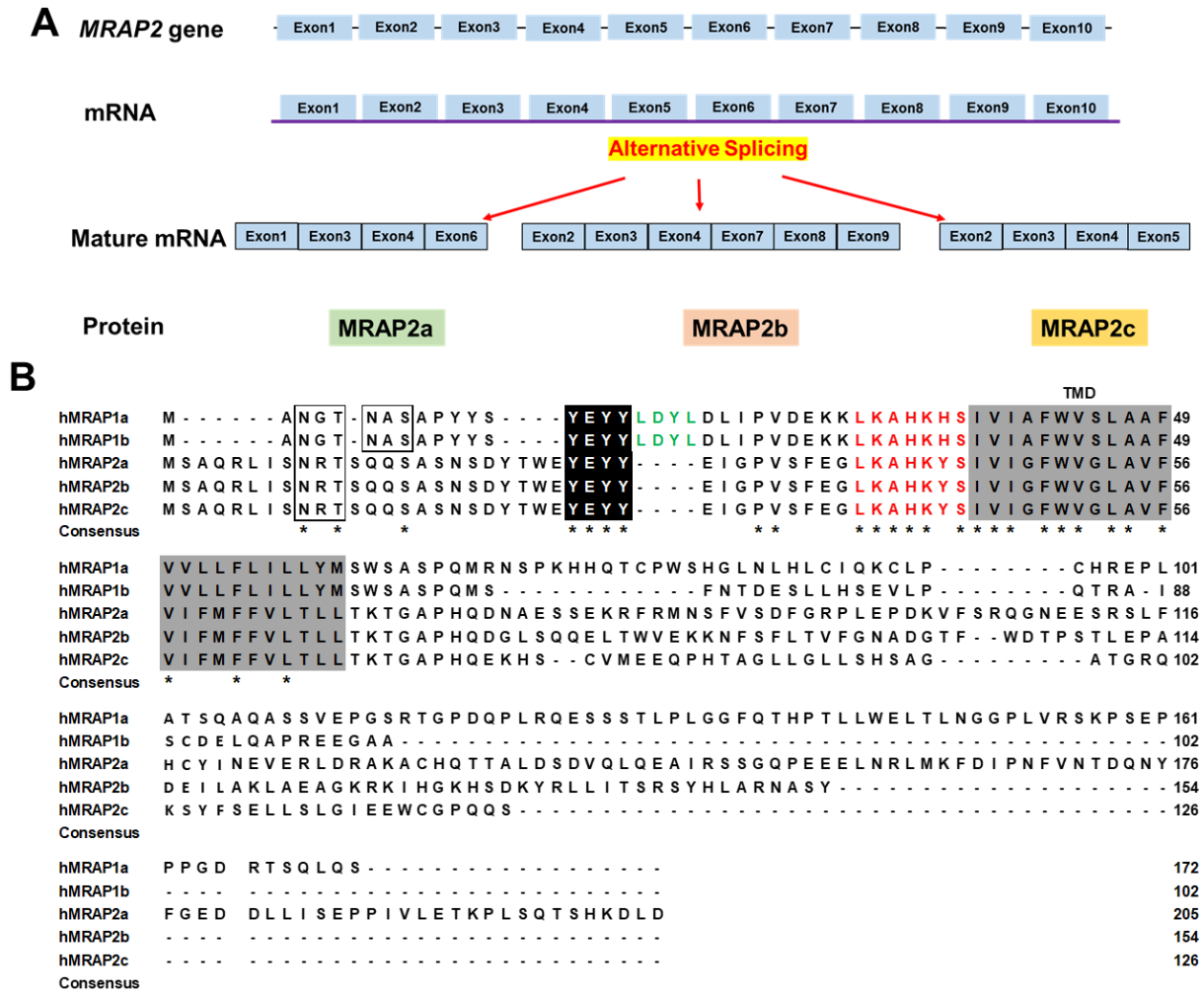

C

	MRAP1a	MRAP1b	MRAP2a	MRAP2b	MRAP2c
MRAP1a	100	80	43	44	44
MRAP1b		100	44	44	45
MRAP2a			100	60	97
MRAP2b				100	99
MRAP2c					100

Figure 2.1 Schematic diagram of the human *MRAP2* splice variants (A), comparison of amino acid sequences of human MRAP1s and MRAP2s (B), and amino acid sequence identities of MRAP1s and MRAP2s (C). Open boxes indicate potential *N*-linked glycosylation sites. Dark shadows show conserved motifs (YEYY) in both MRAP1 and MRAP2. Green color

indicates the activation motif (LDYL). LKAHKHS (red color) in MRAP1s and LKAHKYS (red color) in MRAP2s are required for dual topology. Transmembrane domains are shown in shaded boxes. Asterisk (*) denotes the same amino acids.

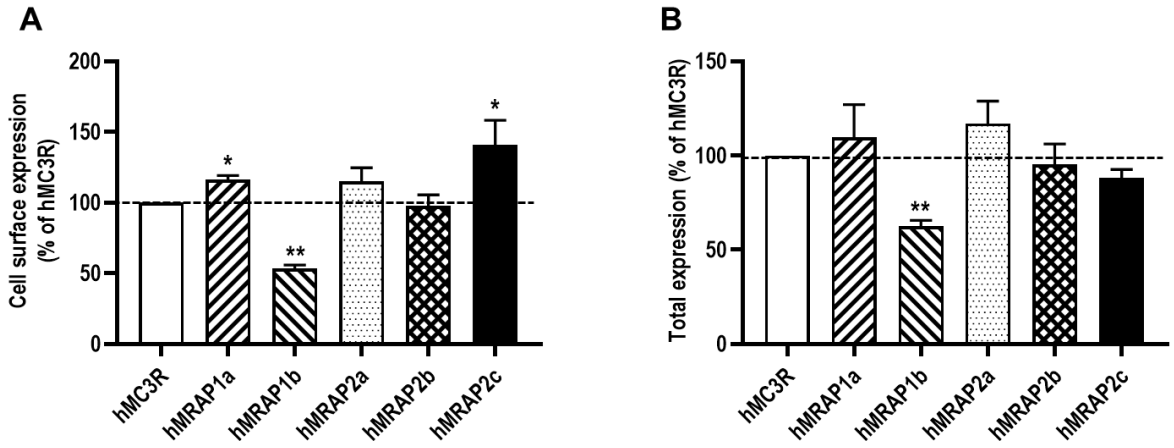

Figure 2.2 Regulation of hMC3R expression by hMRAP1s or hMRAP2s. Cell surface (A) and total (B) expression of hMC3R were measured by flow cytometry. HEK293T cells were co-transfected with hMC3R and hMRAP1s or hMRAP2s. Fluorescence in cells transfected with empty vector pcDNA3.1 was used for background staining. The results are calculated as % of 1:0 group. Each data point represented the mean ± SEM (n = 3). * indicates significant difference (*$P < 0.05$ and **$P < 0.01$) (One-way ANOVA followed by Tukey test).

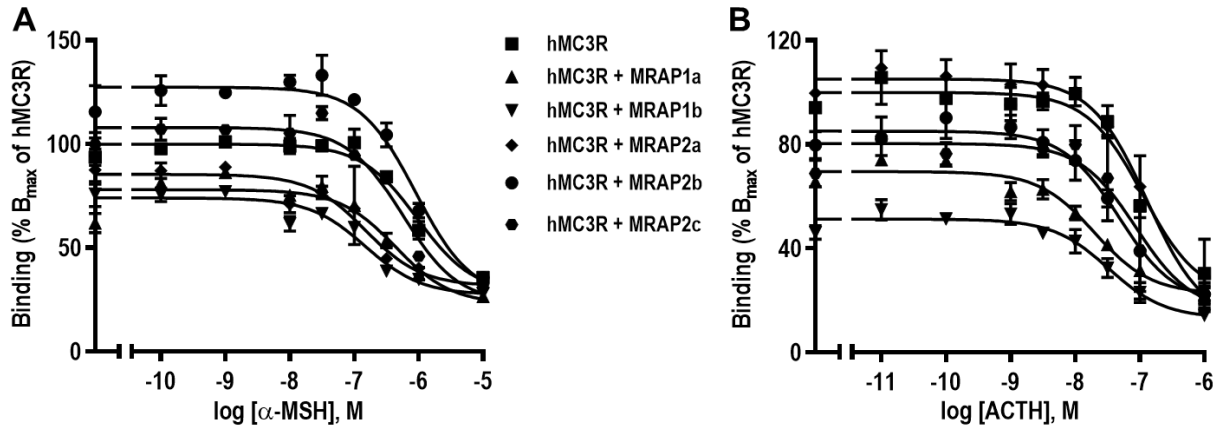

Figure 2.3 The ligand binding properties of hMC3R regulated by hMRAP1s or hMRAP2s to α-MSH (A) and ACTH (B). HEK293T cells were transiently transfected with hMC3R with or without hMRAP1a, hMRAP1b, hMRAP2a, hMRAP2b or hMRAP2c plasmids (1:5), and the binding properties were measured 48 h later by displacing the binding of ^{125}I-NDP-MSH using different concentrations of unlabeled α-MSH and ACTH (1-24). Data are expressed as % of hMC3R binding ± range from duplicate measurements within one experiment. The curves are representative of at least three independent experiments.

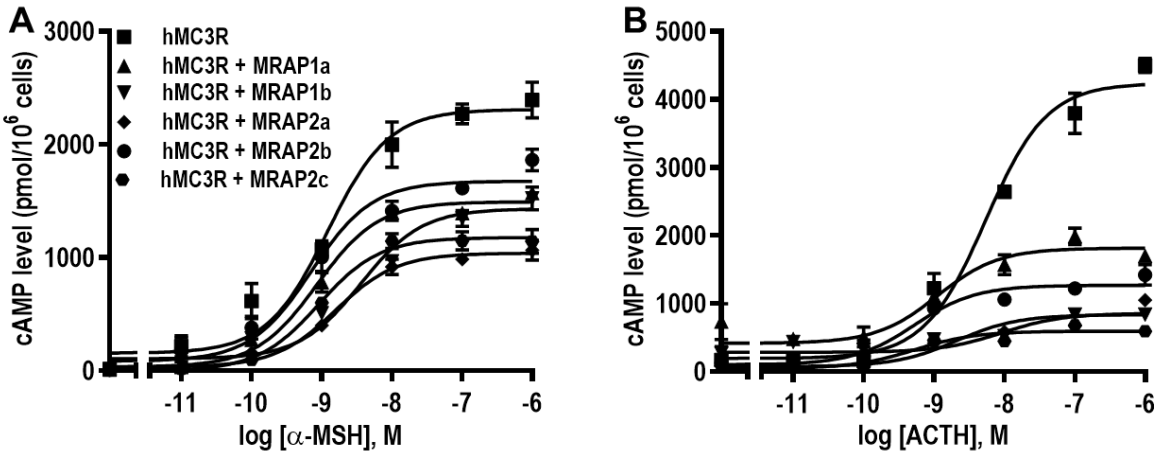

Figure 2.4 The signaling properties of hMC3R regulated by hMRAP1s or hMRAP2s in response to α-MSH (A) and ACTH (B). HEK293T cells were transiently transfected with hMC3R with or without hMRAP1a, hMRAP1b, hMRAP2a, hMRAP2b or hMRAP2c plasmids (1:5). Intracellular cAMP levels were measured by RIA after stimulation with different concentrations of α-MSH and ACTH (1-24). The curves are representative of at least three independent experiments. All experiments were performed at least three times independently.

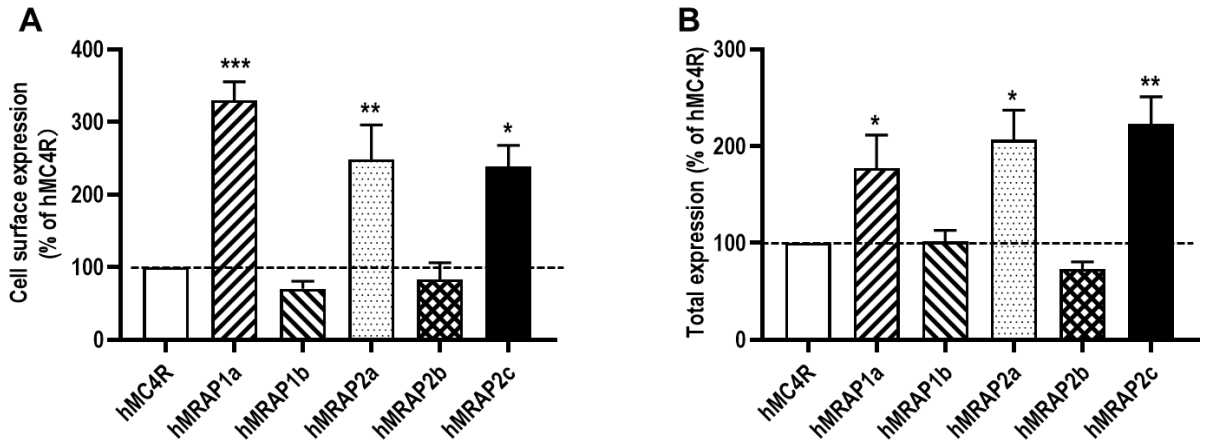

Figure 2.5 Regulation of hMC4R expression by hMRAP1s or hMRAP2s. Cell surface (A) and total (B) expression of hMC3R were measured by flow cytometry. HEK293T cells were co-transfected with hMC3R and hMRAP1s or hMRAP2s. Fluorescence in cells transfected with empty vector pcDNA3.1 was used for background staining. The results are calculated as % of 1:0 group. Each data point represented the mean ± SEM (n = 3). * indicates significant difference (*$P < 0.05$, **$P < 0.01$, and ***$P < 0.001$) (One-way ANOVA followed by Tukey test).

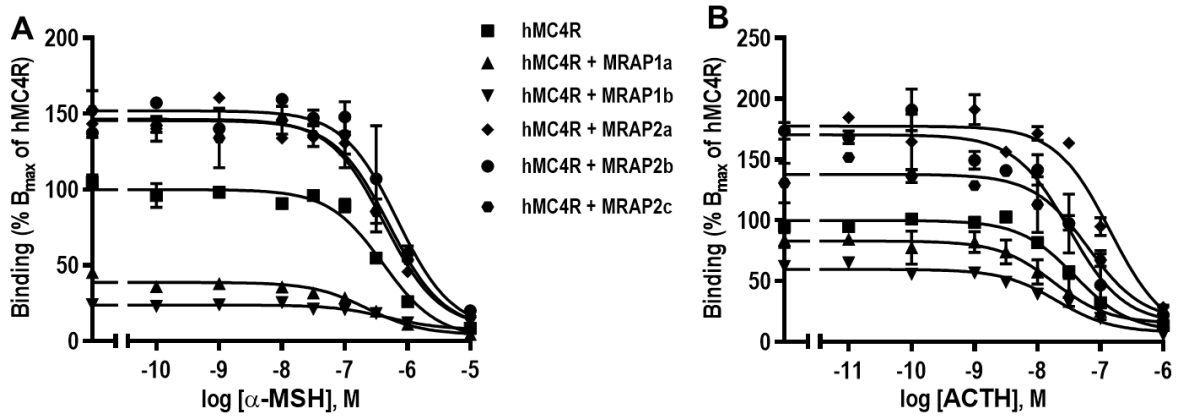

Figure 2.6 The ligand binding properties of hMC4R regulated by hMRAP1s or hMRAP2s to α-MSH (A) and ACTH (B). HEK293T cells were transiently transfected with hMC4R with or without MRAP1a, MRAP1b, MRAP2a, MRAP2b or MRAP2c plasmids (1:5), and the binding properties were measured 48 h later by displacing the binding of ^{125}I-NDP-MSH using different concentrations of unlabeled α-MSH and ACTH (1-24). Data are expressed as % of hMC4R binding ± range from duplicate measurements within one experiment. All experiments were performed at least three times independently.

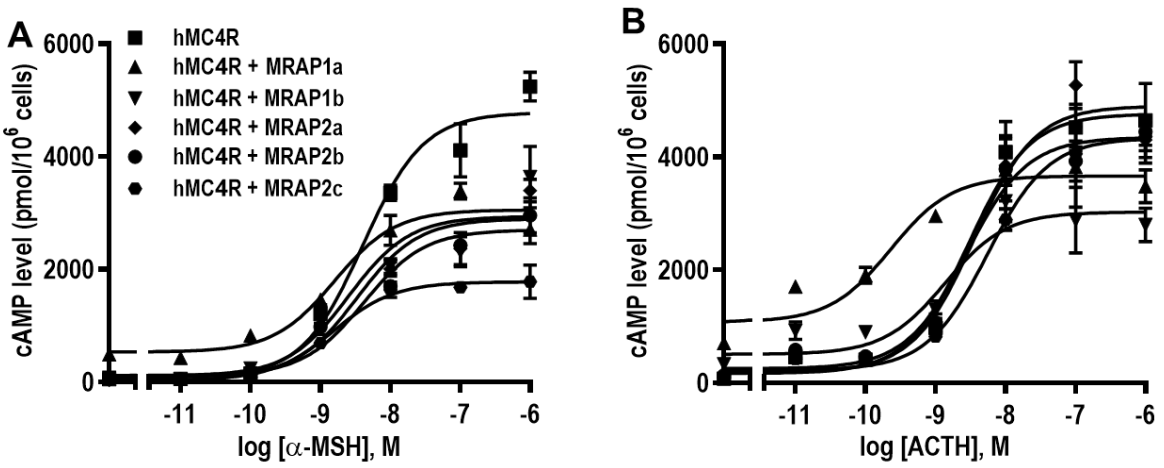

Figure 2. 7. The signaling properties of hMC4R regulated by hMRAP1s or hMRAP2s in response to α-MSH (A) and ACTH (B). HEK293T cells were transiently transfected hMC4R with or without MRAP1a, MRAP1b, MRAP2a, MRAP2b or MRAP2c plasmids (1:5), and intracellular cAMP levels were measured by RIA after stimulation with different concentrations of α-MSH or ACTH (1-24). Data are mean ± SEM from triplicate measurements within one experiment. All experiments were performed at least three times independently.

Chapter 3: Regulation of canine melanocortin-3 and -4 receptors by melanocortin-2 receptor accessory protein 1 and 2

3.1 Introduction

Melanocortin-3 and -4 receptors (MC3R and MC4R, neural MCRs), two of the five subtypes of melanocortin receptors (MCRs), have high expression in the central nervous system [19-22], and are essential for regulating energy homeostasis [13, 23, 24]. Mice lacking *Mc3r* have moderate obesity phenotype with normal food intake and metabolism, decreased lean and increased fat mass [27-29]. *Mc4r* knockout mice with morbid obesity have increased food intake and decreased energy expenditure [25, 26]. These findings suggest distinct non-redundant mechanisms of MC3R and MC4R in modulation of energy balance. Additionally, mutations in *MC3R* and *MC4R* show close association with monogenic obesity [13, 30-33]. MC3R was shown to be involved in other potential physiological functions in modulation of natriuresis [41], cardiovascular function [34, 35], immune response [36-40], and timing of sexual maturation [42]. MC4R also has crucial roles in sexual function and reproduction [13, 32].

MC3R and MC4R are activated by the endogenous agonists, including α-, β-, γ-melanocyte-stimulating hormones (MSHs) and adrenocorticotropin (ACTH) [17, 18]. As members of Family A G protein-coupled receptors (GPCRs), the neural MCRs primarily couple to the stimulatory G protein (Gs) to stimulate adenylyl cyclase activity, resulting in increased generation of the intracellular second messenger cyclic adenosine monophosphate (cAMP) to trigger downstream signaling.

MCRs have been shown to interact with small single transmembrane proteins-melanocortin-2 receptor accessory proteins (MRAPs, including MRAP1 and MRAP2) [44, 46, 47, 55] (reviewed in [3, 234]. MRAP1 was the first MC2R accessory protein identified, as the specific molecular chaperone for MC2R in modulation of receptor trafficking, ligand binding, and signaling [3, 44-46]. Human (h) *MRAP1* mutations account for ~20% of familial glucocorticoid deficiency cases [44, 176]. Sequent studies suggest that MRAP1 might possess multiple functions beyond regulating MC2R. Indeed, hMRAP1 has been shown to modulate five human MCRs in distinct ways [47-49]. Additionally, MRAP1 is involved in regulating MC3R and MC4R in chicken and frog [42, 56, 190]. The *mrap* gene is observed in rainbow trout and zebrafish, and absent in the most teleosts [198, 199]. So far, only a few publications focus on MRAP1-regulated neural MCRs [42, 47, 49, 56, 190-192, 235, 236].

MRAP2 is a paralog of MRAP1 and has distinct roles from MRAP1. MRAP2 with high expression in brain has essential roles in regulating energy homeostasis. Mice lacking *Mrap2* show early-onset severe obesity [50, 51]. Human *MRAP2* mutations are also associated with severe obesity [50, 52-54]. MRAP2 has been shown to modulate MC3R/MC4R trafficking and signaling in vertebrates [47, 50, 55-61, 192]. Human *MRAP2* has three alternatively spliced variants with different C-terminus in protein sequences, in which these three variants show different effects on MC3R/MC4R pharmacology [192].

Although many findings on the regulation of MC3R and MC4R by MRAPs, MRAPs have been shown to modulate neural MCRs in the receptor- and species-dependent manner. The effect of MRAP1 and MRAP2 on canine (c) MC3R and cMC4R has not been studied. In this study, canine (*Canis lupus familiaris*) was used as an animal model to explore pharmacology of cMC3R and cMC4R regulated by MRAP1 and MRAP2. Similar to human *MRAP2*, dog *MRAP2*

also has two alternatively spliced variants, *MRAP2a* and *MRAP2b*. In this study, we investigated pharmacology of cMC3R as well as pharmacological modulation of cMC3R and cMC4R by cMRAP1, cMRAP2a, and cMRAP2b.

3.2 Materials and Methods

3.2.1 Ligands and plasmids

NDP-MSH and D-Trp^{8}-γ-MSH were obtained from Vivitide (Louisville, KY, USA). Human α-MSH and β-MSH were purchased from Pi Proteomics (Huntsville, AL, USA). Human ACTH (1-24) was supplied by Phoenix Pharmaceuticals (Burlingame, CA, USA). Canine α-MSH, β-MSH, and ACTH share same sequences with the corresponding human counterparts (**Figure 3.1**). [^{125}I]-cAMP and [^{125}I]-NDP-MSH were iodinated using chloramine T method [221, 222]. N-terminal myc-tagged receptors (human MC3R (hMC3R), cMC3R, and cMC4R) and N-terminal Flag-tagged MRAPs (cMRAP1, cMRAP2a, and cMRAP2b) were commercially synthesized and subcloned into pcDNA3.1 by GenScript (Piscataway, NJ, USA).

3.2.2 Cell culture and transfection

Human embryonic kidney (HEK) 293T cells (ATCC, Manassas, VA, USA) were cultured at 37 °C in a 5% CO_2-humidified incubator [223]. Cells were plated into gelatin-coated 6-well or 24-well plates. Cells were co-transfected with 0.25 μg/μL MC3R or MC4R with or without MRAP plasmids using calcium phosphate precipitation method [224].

3.2.3 Flow cytometry assay

The regulation of cMRAP1 or cMRAP2s on the expression of cMC3R and cMC4R was carried out using flow cytometry (Accuri Cytometers, Ann Arbor, MI, USA) as described

previously [118, 225]. Cells were co-transfected with cMC3R or cMC4R and cMRAP1, cMRAP2a, or cMRAP2b plasmids (1:5). Fluorescence of cells transfected with pcDNA3.1 was used for background staining. The expression of receptors was calculated as the percentage of the cell transfected with receptors in absence of MRAPs (set as 100%) [225].

3.2.4 Ligand binding assays

Binding assay was performed as described previously [57, 223]. The ligands and their final concentrations used in this study were NDP-MSH (from 10^{-12} to 10^{-6} M), α-MSH (from 10^{-11} to 10^{-5} M), β-MSH (from 10^{-11} to 10^{-5} M), ACTH (1-24) (from 10^{-12} to 10^{-6} M), and D-Trp^{8}-γ-MSH (from 10^{-12} to 10^{-6} M). To investigate the regulation of MRAPs on the binding properties of cMC3R and cMC4R, cMC3R or cMC4R (0.25 μg/μL) and cMRAP1, cMRAP2a or cMRAP2b plasmids in two ratios (1:0 and 1:5) were co-transfected into cells (6-well plate), and two ligands, α-MSH and ACTH (1-24), were used.

3.2.5 Ligand-stimulated cAMP assays

Radioimmunoassay (RIA) was used to determine intracellular cAMP levels as described previously [221, 223]. Five ligands were used, including NDP-MSH, α-MSH, β-MSH, ACTH (1-24), and D-Trp^{8}-γ-MSH. To investigate effects of MRAPs on cMC3R or cMC4R signaling, cells were co-transfected with cMC3R or cMC4R (0.25 μg/μL) and cMRAP1, cMRAP2a or cMRAP2b plasmids (1:5), and two ligands, α-MSH and ACTH (1-24) were used.

3.2.6 Statistical analysis

All data were represented as mean ± S.E.M. GraphPad Prism 8.3 software (GraphPad, San Diego, CA, USA) was used to calculate the parameters of ligand binding, cAMP signaling, and

flow cytometry assay. The significant differences in ligand binding, and cAMP signaling parameters between cMC3R and hMC3R, as well as vehicle and ligand-treated groups, were all determined by Student's t-test. One-way ANOVA was used to analyze the significant differences in binding, cAMP, and flow cytometry among multiple groups.

3.3 Results

3.3.1 Nucleotide and deduced amino acid sequences of cMC3R, cMRAP1, and cMRAP2s

The cloned canine *MC3R* (GenBank: NM_001135124.1) had 972 bp open reading frame (ORF), encoding a putative protein of 323 amino acids with 35.79 kDa molecular mass (**Figure 3.2A**). Canine MC3R had seven hydrophobic transmembrane domains (TMDs). Several conserved motifs, including PMY, DRY, and DPxxY, and three potential *N*-linked glycosylation sites (Asn^2, Asn^{16}, and Asn^{28}) in N-terminus, were present at homologous positions with MC3Rs of other species (**Figures 3.2A and B**). Canine MC3R shared high identities with other MC3R orthologs, 96% to giant panda, 92% to human, 90% to cat, 89% to pig, 87% to mouse, 76% to chicken, 76% to turtle, 75% to frog, and 72% to zebrafish (**Figure 3.2B**). Phylogenetic tree showed that cMC3R nested with mammalian MC3Rs (**Figure 3.3C**).

The canine *MRAP1* had 336 bp ORF that encoded a putative protein of 111 amino acids with 12.90 kDa molecular mass (**Figure 3.3A**). Canine MRAP1 had the classical characteristic of other MRAP orthologs, including two potential *N*-linked glycosylation sites (Asn^3 and Asn^6), YEYY motif, LDYL motif, LKANKYL motif, and a single TMD (**Figures 3.3A,B**). Canine MRAP1 shared high identities with cat MRAP1(90%), and lower identities with other MRAP1 (44%-79%) (**Figure 3.3B**). Phylogenetic tree showed that were clustered with mammalian MRAP1s and evolutionarily closer to red fox MRAP1 (**Figure 3.3C**).

The canine *MRAP2* consists of 11 exons (**Figure 3.4A**). Two *MRAP2* splice variants were identified: *MRAP2a* (XM_038682814.1) derived from 4 exons (2, 6, 7, and 11) that had 621 bp ORF, encoding a putative protein of 206 amino acids with 23.62 kDa molecular mass (**Figures 3.4A and B**); *MRAP2b* (XM_038682813.1) derived from 5 exons (3, 4, 6, 7, and 11) that had 684 bp ORF encoding a putative protein of 232 amino acids with 26.71 kDa molecular mass (**Figures 3.4A and C**). Canine MRAP2b had an extended N-terminus (26 amino acids) compared with cMRAP2a, and they shared the common structure with other MRAP2s, such as one potential *N*-linked glycosylation sites (Asn^{9} in MRAP2a and Asn^{35} in MRAP2b), YEYY motif, LKAHKYS motif, and a single TMD (**Figures 3.4B, C, and D**). Multiple sequence alignment analysis showed that dog MRAP2a and MRAP2b shared high identities with mammalian MRAP2s (>81%) and lower identities with MRAP2s from other species (<78%) (**Figure 3.4D**). The two isoforms of cMRAP2s were clustered with different MRAP2s, in which MRAP2a was evolutionarily closer to cat MRAP2, and MRAP2b was nested with Nile tilapia MRAP2 (**Figure 3.4E**).

3.3.2 Ligand binding properties of cMC3R

Binding assay was performed using multiple MC3R ligands, including NDP-MSH, α-MSH, β-MSH, ACTH, and D-Trp^{8}-γ-MSH. We included hMC3R for comparison in the same experiments to explore whether cMC3R shows any unique pharmacological characterizations. The maximal binding value (B_{max}) of cMC3R was 247.97 ± 13.44% of that of hMC3R (**Figure 3.5 and Table 3.1**). Canine MC3R had significantly lower affinities to NDP-MSH and D-Trp^{8}-γ-MSH than that of hMC3R (**Figure 3.5 and Table 3.1**). The two MC3Rs showed similar IC_{50}s when α-MSH, β-MSH, and ACTH were used (**Figure 3.5 and Table 3.1**).

3.3.3 cAMP signaling properties of cMC3R

Intracellular cAMP levels were determined to explore whether cMC3R could respond to these agonists. All agonists could dose-dependently stimulate cMC3R and increase cAMP production (**Figure 3.6** and **Table 3.2**). Canine MC3R showed higher maximal responses (R_{max}) in response to four agonists (NDP-MSH, β-MSH, ACTH, and D-Trp^8-γ-MSH) than those of hMC3R (**Figure 3.6** and **Table 3.2**). Similar EC_{50}s between two MC3Rs were observed to response to five agonists (**Figure 3.6** and **Table 3.2**). Additionally, cMC3R showed similar basal activity with that of hMC3R **(Table 3.2**).

3.3.4 Modulation of cMC3R and cMC4R expression by MRAPs

Canine MC3R expression regulated by MRAPs was measured using flow cytometry. Results showed that cMRAP1, cMRAP2a, and cMRAP2b had no effect on cell membrane and total expression of cMC3R (**Figures 3.7A and B**). At cMC4R, cMRAP1 and cMRAP2a increased cell surface and total expression, and cMMRAP2b only increased total expression of cMC4R (**Figures 3.7C and D**).

3.3.5 Modulation of cMC3R pharmacology by MRAPs

Ligand binding assays with α-MSH and ACTH showed that cMRAP1 decreased the B_{max}, whereas cMRAP2a and cMRAP2b increased B_{max}s of cMC3R (**Figures 3.8A, B** and **Table 3.3**). All MRAPs had no significant effect on IC_{50}s of cMC3R to α-MSH and ACTH (**Figures 3.8A, B** and **Table 3.3**).

Modulation of cMRAPs on cMC3R signaling was also studied. Results showed that all MRAPs did not alter α-MSH and ACTH potencies of cMC3R (**Table 3.4**). Both MRAP1 and

MRAP2a decreased R_{max}s in response to α-MSH and ACTH; MRAP2b significantly decreased a-MSH-stimulated cAMP generation but showed similar ACTH-induced cAMP production of cMC3R (**Figures 3.8C, D** and **Table 3.4**). Only MRAP2b decreased the basal activity, and other MRAPs had no effect on the basal cAMP levels of cMC3R (**Table 3.4**).

3.3.6 Modulation of cMC4R pharmacology by MRAPs

Ligand binding assays showed that MRAP1 and MRAP2a increased B_{max}s of cMC4R and MRAP2b did not affect the B_{max} (**Figures 3.9A, B** and **Table 3.5**). All MRAPs increased affinities of cMC4R to α-MSH and ACTH (**Figures 3.9A, B** and **Table 3.5**).

Signaling results showed that all MRAPs did not affect EC_{50}s of cMC4R in response to α-MSH and ACTH (**Table 3.6**). MRAP1 had no effect on α-MSH- and ACTH-stimulated cAMP level of cMC4R (**Figures 3.9C, D** and **Table 3.6**). MRAP2a decreased α-MSH- and ACTH-induced cAMP signaling, whereas MRAP2b increased ACTH-stimulated and did not affect α-MSH-stimulated cAMP signaling (**Figures 3.9C, D** and **Table 3.6**). Canine MC4R showed higher basal cAMP production than that of hMC4R (2.38 times than that of hMC4R), indicating that cMC4R might be constitutively active. In this study, all MRAPs decreased the basal cAMP levels of cMC4R (**Table 3.6**).

3.4 Discussion

In this study, we cloned canine *MC3R* and investigated the pharmacological properties of cMC3R. We also identified a *MRAP2* variant, *MRAP2b*. The potential regulation of canine MRAP1 and two MRAP2 isoforms on cMC3R/cMC4R pharmacology were further studied.

To investigate the pharmacology of canine MC3R, ligand binding and signaling assays were performed. Canine MC3Rs showed higher binding capacity than that of hMC3R (**Figure 3.5 and Table 3.1**), consistent with results of other MC3Rs, including channel catfish [57], topmouth culter [60], and giant panda MC3Rs [237]. For signaling, different from results on giant panda and pig MC3Rs [237, 238], cMC3R had high ligand-induced cAMP levels than that of hMC3R (**Figure 3.6 and Table 3.2**). In two fishes, topmouth culter Mc3r has high agonist-stimulated cAMP production [60], whereas channel catfish Mc3r shows lower R_{max}s than that of hMC3R [57]. In addition, our current result was consistent with mammalian MC3Rs that MC3R has little or no basal cAMP signaling [74, 98, 237, 238]. Of interest, the high constitutive activities are present in several MC3Rs, including zebrafish [150], channel catfish [57], topmouth culter [60], chicken [56, 239], and Mexican axolotl [211].

The potential roles of MRAPs on cMC3R/cMC4R trafficking were studied. Human MRAP1a decreases [47, 189] or increases [192], and MRAP2a decreases [47, 189] or has no effect [192] on cell surface expression of hMC3R. The current studies showed that all MRAPs do not affect the cell surface expression of cMC3R (**Figures 3.7A, B**). In other species, frog MRAP1 increases and chicken MRAP1 does not alter the surface expression of MC3Rs [56, 190]. For MRAP2, MRAP2 decreases surface expression of clawed frog MC3R [190], increases surface expression of topmouth culter Mc3r [60], and has no effect on the surface expression of Mexican axolotl and chicken MC3Rs [56, 211]. At MC4R, hMRAP1a and hMRAP2a decrease [47, 189] or increase [192] the cell surface expression of hMC4R. In this study, MRAP1 and MRAP2a increased cell surface expression of cMC4R (**Figures 3.7C, D**). MRAP1 was shown to has no effect on surface expression of chicken MC4R [56] and increases frog MC4R expression [236]. MRAP2 has been reported to decrease surface expression of tilapia and Mexican axolotl

MC4Rs [209, 211], increases membrane expression of zebrafish (Mrap2b) [55], topmouth culter (Mrap2a and Mrap2b) [59], and Xenopus MC4Rs [190], or has no effect surface expression of chicken and snakehead MC4Rs [56, 61]. Collectively, MRAP1 and MRAP2 modulate the MC3R/MC4R trafficking to the plasma membrane in species- and receptor-specific manner.

Pharmacological studies were further performed on potential MRAP modulation of cMC3R. Human MRAP1 and MRAP2 decrease α-MSH and ACTH-induced [192] or increase α-MSH-stimulated [49, 189] cAMP production of hMC3R. Our results showed that MRAP1 and MRAP2a decreased α-MSH and ACTH-induced cAMP levels, and MRAP2b only decreased α-MSH-stimulated signaling of cMC3R (**Figure 3.8 and Table 3.4**). Xenopus MRAP1 increases α-MSH and ACTH-induced cAMP signaling, and chicken MRAP1 does not modulate agonist-induced signaling of MC3Rs [56, 190]. For MRAP2, MRAP2-decreased MC3R signaling is also reported in channel catfish, topmouth culter (Mrap2a) [59], and Mexican axolotl MC3Rs [211], whereas MRAP2-increased MC3R signaling is observed in chicken and Xenopus MC3Rs [190]. Zebrafish Mrap2s do not affect agonist-induced signaling of Mc3r [55].

The potential modulation of MRAPs on cMC4R pharmacology was also studied. Conflicting results were reported previously on hMRAP1a- and hMRAP2a-regulated signaling of hMC4R, where hMRAP1a decreases α-MSH-induced or does not affect α-MSH- and ACTH-stimulated hMC4R signaling [49, 192]; MRAP2a has no effect [206], decreases [192] or increases [189, 191] α-MSH-stimulated and does not affect ACTH-induced [192, 206] signaling of hMC4R. Our results indicated that MRAP1 had no effect on efficacies of cMC4R in response to α-MSH and ACTH and MRAP2a increased ACTH-stimulated and had no effect on α-MSH-induced cMC4R signaling (**Figure 3.9 and Table 3.6**). Chicken MRAP1 was shown to decrease α-MSH-

stimulated and has no effect on ACTH-induced signaling of MC4R [56]. MRAP1 increases α-MSH- and ACTH-stimulated signaling of Xenopus MC4R [190]. Mrap2-suppressed α-MSH- and/or ACTH-stimulated signaling of Mc4rs are present in several teleosts, including zebrafish [55], grouper [117], tilapia [209], topmouth culter [59], and snakehead [61].

Human MC4R shows modest basal cAMP signaling [74]. The defect in basal activities of *MC4R* mutations can cause obesity [9, 146]. Mrap2- and AgRP-suppressed the basal activity of Mc4r play important role in promoting growth of zebrafish and culter [55, 60, 141]. These indicate that the basal activity of MC4R play pivotal role in modulation of energy homeostasis [147]. Human MRAP1s increase [49, 191, 192] or do not affect the basal activities of hMC4R [47, 48], and MRAP2s decrease [192] or have no significant effect on the basal activities of hMC4R [47, 48, 191, 233]. Our studies showed that MRAP1 and MRAP2s decreased the basal cAMP signaling (**Table 3.6**). Mrap2(s) decreased Mc4r basal activities were reported in other species, including zebrafish [55], Nile tilapia [209], orange-spotted grouper [117], topmouth culter [59], and snakehead [61].

Alternative splicing is prevalent in eukaryotes and might have different functions [226-229]. Splicing variants provide a nature-made chance to investigate roles of specific domain. Human *MRAP* and *MRAP2* have two and three alternative splicing, respectively, and they show different effect on hMC3R/hMC4R pharmacology [44, 192]. Canine MRAP2 also has two alternatively spliced variants, *MRAP2a* and *MRAP2b* (MRAP2b with extension at N-terminus compared with MRAP2a). These extension sequences at N-terminus of MRAP2 are not found in other MRAP2s (**Figure 3.4D**). Our results showed that MRAP2a and MRAP2b have different effect on cMC3R/cMC4R pharmacology (**Figure 3.7 and Tables 3.3, 4, 5, and 6**). N-terminus of MRAP1 and MRAP2, with several conserved motifs, has important role in modulating GPCR

pharmacology [184, 192, 203, 204]. We speculate that extension sequences at N-terminus of MRAP2 might have important role in MC3R/MC4R pharmacology.

In summary, we cloned canine *MC3R* and investigated its pharmacology. MRAP1 did not affect the MC3R trafficking and decreased α-MSH and ACTH-induced signaling, whereas MRAP1 increased the cell surface expression of cMC4R and decreased the basal activity. Two MRAP2 isoforms showed different effect on cMC3R or MC4R pharmacology. MRAP2a decreased α-MSH and ACTH-induced signaling, while MRAP2b only decreased α-MSH-stimulated signaling of cMC3R. At cMC4R, MRAP2a increased cell surface expression and ACTH-induced signaling, decreased the basal activity of cMC4R, whereas MRAP2b had no effect on cMC4R trafficking, and decreased basal and α-MSH and ACTH-induced signaling. These findings indicate the complexity of MRAPs in regulating neural MCRs and contribute to further physiological studies of canine MC3R/MC4R.

Table 3.1 The ligand binding properties of cMC3R

MC3R		cMC3R	hMC3R
B_{max} (%)		247.97 ± 13.44[b]	100
NDP-MSH	IC_{50} (nM)	4.37 ± 0.72[a]	1.98 ± 0.43
α-MSH	IC_{50} (nM)	240.42 ± 37.34	221.57 ± 30.23
β-MSH	IC_{50} (nM)	140.18 ± 31.37	161.56 ± 31.45
ACTH	IC_{50} (nM)	58.52 ± 8.67	45.71 ± 5.23
D-Trp^8-γ-MSH	IC_{50} (nM)	39.30 ± 0.30[b]	24.62 ± 1.25

Results are presented as the mean ± SEM (n = 3 - 4).

[a] significant difference from the parameter of hMC3R, $P < 0.05$.

[b] significant difference from the parameter of hMC3R, $P < 0.001$.

Table 3.2 The signaling properties of cMC3R

MC3R		cMC3R	hMC3R
Basal (%)		100.72 ± 7.69	100
NDP-MSH	EC_{50} (nM)	0.40 ± 0.16	0.24 ± 0.11
	R_{max} (%)	199.38 ± 28.06[a]	100
α-MSH	EC_{50} (nM)	0.97 ± 0.35	1.49 ± 0.22
	R_{max} (%)	145.69 ± 14.30	100
β-MSH	EC_{50} (nM)	1.04 ± 0.23	1.46 ± 0.55
	R_{max} (%)	229.77 ± 46.45[a]	100
ACTH	EC_{50} (nM)	1.46 ± 0.30	2.12 ± 0.69
	R_{max} (%)	182.83 ± 25.21[a]	100
D-Trp^{8}-γ-MSH	EC_{50} (nM)	1.08 ± 0.15	0.71 ± 0.19
	R_{max} (%)	188.25 ± 19.56[a]	100

Results are presented as the mean ± SEM (n = 3 - 4).

[a] significant difference from the parameter of hMC3R, $P < 0.05$.

Table 3.3 The effect of MRAPs on ligand binding properties of cMC3R

cMC3R/cMRAPs	B_{max} (%)	α-MSH	ACTH
		IC_{50} (nM)	IC_{50} (nM)
cMC3R	100	106.68 ± 13.80	55.56 ± 11.64
cMC3R/cMRAP1	81.81 ± 5.01[a]	127.76 ± 30.47	68.59 ± 9.31
cMC3R/cMRAP2a	148.43 ± 14.94[a]	118.61 ± 22.25	57.58 ± 4.09
cMC3R/cMRAP2b	128.42 ± 9.06[a]	148.03 ± 30.16	49.59 ± 6.77

Results are expressed as the mean ± SEM (n = 3 - 4).

[a] Significant difference from the parameter of 1:0, $P < 0.05$.

Table 3.4 The effect of MRAPs on cAMP signaling of cMC3R

cMC3R/cMRAPs	Basal (%)	α-MSH		ACTH	
		EC_{50} (nM)	R_{max} (%)	EC_{50} (nM)	R_{max} (%)
cMC3R	100	3.08 ± 1.26	100	2.02 ± 0.39	100
cMC3R/cMRAP1	100.91 ± 16.74	0.88 ± 0.18	46.67 ± 8.88[b]	2.11 ± 0.56	46.61 ± 12.37[a]
cMC3R/cMRAP2a	84.71 ± 19.03	1.37 ± 0.26	73.02 ± 5.81[a]	2.18 ± 0.39	73.79 ± 4.94[a]
cMC3R/cMRAP2b	68.88 ± 9.35[a]	3.64 ± 1.11	66.93 ± 9.64[a]	3.41 ± 0.99	85.02 ± 11.04

Results are expressed as the mean ± SEM (n = 3 - 5).

[a] Significant difference from the parameter of 1:0, $P < 0.05$.

[b] Significant difference from the parameter of 1:0, $P < 0.001$.

Table 3.5 The effect of MRAPs on ligand binding properties of cMC4R

cMC4R/cMRAPs	B_{max} (%)	α-MSH	ACTH
		IC_{50} (nM)	IC_{50} (nM)
cMC4R	100	504.66 ± 124.33	348.29 ± 94.51
cMC4R/cMRAP1	151.36 ± 10.67[a]	186.62 ± 13.60[a]	37.63 ± 6.84[b]
cMC4R/cMRAP2a	167.03 ± 11.83[c]	228.40 ± 40.74[a]	35.63 ± 8.10[b]
cMC4R/cMRAP2b	121.60 ± 10.06	120.19 ± 22.41[b]	16.93 ± 5.69[c]

Results are expressed as the mean ± SEM (n = 4).

[a] Significant difference from the parameter of 1:0, $P < 0.05$.

[b] Significant difference from the parameter of 1:0, $P < 0.01$.

[c] Significant difference from the parameter of 1:0, $P < 0.001$.

Table 3. 6 The effect of MRAPs on cAMP signaling of cMC4R

	Basal (%)	α-MSH		ACTH	
		EC_{50} (nM)	R_{max} (%)	EC_{50} (nM)	R_{max} (%)
cMC4R	100	1.18 ± 0.21	100	0.92 ± 0.41	100
cMC4R/cMRAP1	53.89 ± 4.06[b]	1.37 ± 0.24	99.80 ± 3.80	1.92 ± 0.40	76.21 ± 13.29
cMC4R/cMRAP2a	74.70 ± 4.28[b]	0.90 ± 0.10	87.00 ± 10.28	3.82 ± 1.25	144.41 ± 13.36[a]
cMC4R/cMRAP2b	55.82 ± 3.43[b]	0.63 ± 0.10	52.62 ± 7.93[b]	1.20 ± 0.44	55.87 ± 9.82[a]

Results are expressed as the mean ± SEM (n = 3 - 4).

[a] Significant difference from the parameter of 1:0, $P < 0.05$.

[b] Significant difference from the parameter of 1:0, $P < 0.001$.

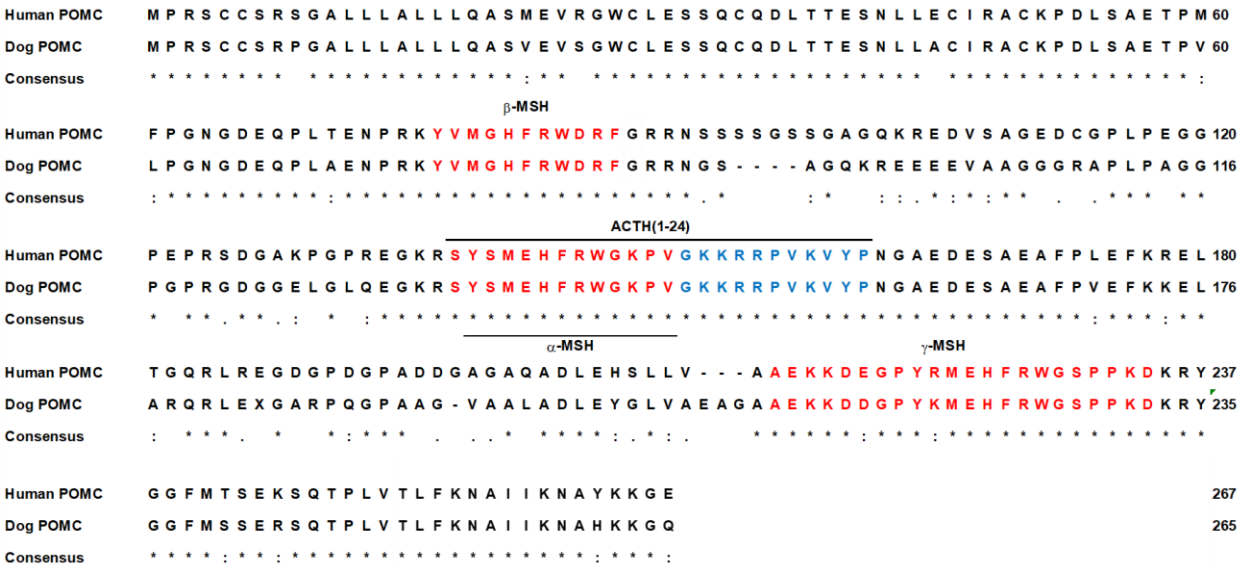

Figure 3.1 Comparison of amino acid sequences of POMCs between human and canine

A

```
1   ATG AAC GCT TCG TGC TGC CTA CTG TCT GCT CAG CCG ACG CTG CCC AAC AGC TCG GAG CAC 60
1   M   N   A   S   C   C   L   L   S   A   Q   P   T   L   P   N   S   S   E   H   20
61  CTC GCA GCC GCG TCC TTC GGC AAC CAG AGC GGC AGC GGC TTC TGC GAG CAG GTC TTC ATC 120
21  L   A   A   A   S   F   G   N   Q   S   G   S   G   F   C   E   Q   V   F   I   40
121 AAG CCC GAA GTC TTC CTG GCG CTG GGC ATC GTC AGC CTG CTG GAA AAC ATC CTG GTC ATC 180
40  K   P   E   V   F   L   A   L   G   I   V   S   L   L   E   N   I   L   V   I   60
181 CTG GCC GTG GCC AGG AAC GGC AAC CTG CAC TCC CCC ATG TAC TTC TTC CTC TGC AGC CTG 240
61  L   A   V   A   R   N   G   N   L   H   S   P   M   Y   F   F   L   C   S   L   80
241 GCG GTG GCC GAC ATG CTG GTG AGC GTG TCC AAC GCC CTG GAG ACC GTC ATG ATC GCC ATC 300
81  A   V   A   D   M   L   V   S   V   S   N   A   L   E   T   V   M   I   A   I   100
301 GTC AAC AGC AAC TAC CTG ACC TTC GAG GAC CGG TTC GTC CAG CAC ATG GAC AAC GTC TTC 360
101 V   N   S   N   Y   L   T   F   E   D   R   F   V   Q   H   M   D   N   V   F   120
361 GAC TCC ATG ATC TGC ATC TCC CTG GTG GCC TCC ATC TGC AAC CTC CTG GCC ATC GCC GTG 420
121 D   S   M   I   C   I   S   L   V   A   S   I   C   N   L   L   A   I   A   V   140
421 GAC AGG TAC GTC ACC ATC TTC TAC GCG CTG CGC TAC CAC AGC ATC ATG ACC GTG CGC AAG 480
141 D   R   Y   V   T   I   F   Y   A   L   R   Y   H   S   I   M   T   V   R   K   160
481 GCC CTG GCC TGG ATC GTG GCC ATC TGG GTG TGC TGC GGC GTG TGC GGC GTG GTG TTC ATC 540
161 A   L   A   W   I   V   A   I   W   V   C   C   G   V   C   G   V   V   F   I   180
541 GTC TAC TCC GAG AGC AAG ATG GTC ATC GTG TGC CTC ATC ACC ATG TTC TTC GCC ATG CTG 600
181 V   Y   S   E   S   K   M   V   I   V   C   L   I   T   M   F   F   A   M   L   200
601 CTC CTC ATG GGC ACC CTC TAC GTG CAC ATG TTC CTC TTC GCC CGG CTG CAC GTC CAG CGC 660
201 L   L   M   G   T   L   Y   V   H   M   F   L   F   A   R   L   H   V   Q   R   220
661 ATC GCG GCG CTG CCA CCT GCC GAC GGG GTG GCC CCG CAG CAG CAC TCG TGC ATG AAG GGG 720
221 I   A   A   L   P   P   A   D   G   V   A   P   Q   Q   H   S   C   M   K   G   240
721 GCT GTC ACC ATC ACC ATC CTG CTG GGG GTA TTC ATC TTC TGC TGG GCC CCC TTC TTC CTG 780
241 A   V   T   I   T   I   L   L   G   V   F   I   F   C   W   A   P   F   F   L   260
781 CAC CTC GTC CTC ATC ATA ACC TGC CCC ACC AAC CCC TAC TGC GTC TGC TAC ACG GCC CAC 840
261 H   L   V   L   I   I   T   C   P   T   N   P   Y   C   V   C   Y   T   A   H   280
841 TTC AAC ACC TAC CTG GTC CTC ATC ATG TGC AAC TCC ATC ATC GAC CCC CTC ATC TAC GCC 900
281 F   N   T   Y   L   V   L   I   M   C   N   S   I   I   D   P   L   I   Y   A   300
901 TTC CGG AGC CTA GAG CTA CGT AAC ACC TTC AAG GAG ATC CTC TGC AGC TGC AAC GGC ATG 960
301 F   R   S   L   E   L   R   N   T   F   K   E   I   L   C   S   C   N   G   M   320
961 AAC CTG GGG TAG
321 N   L   G   *
```

B

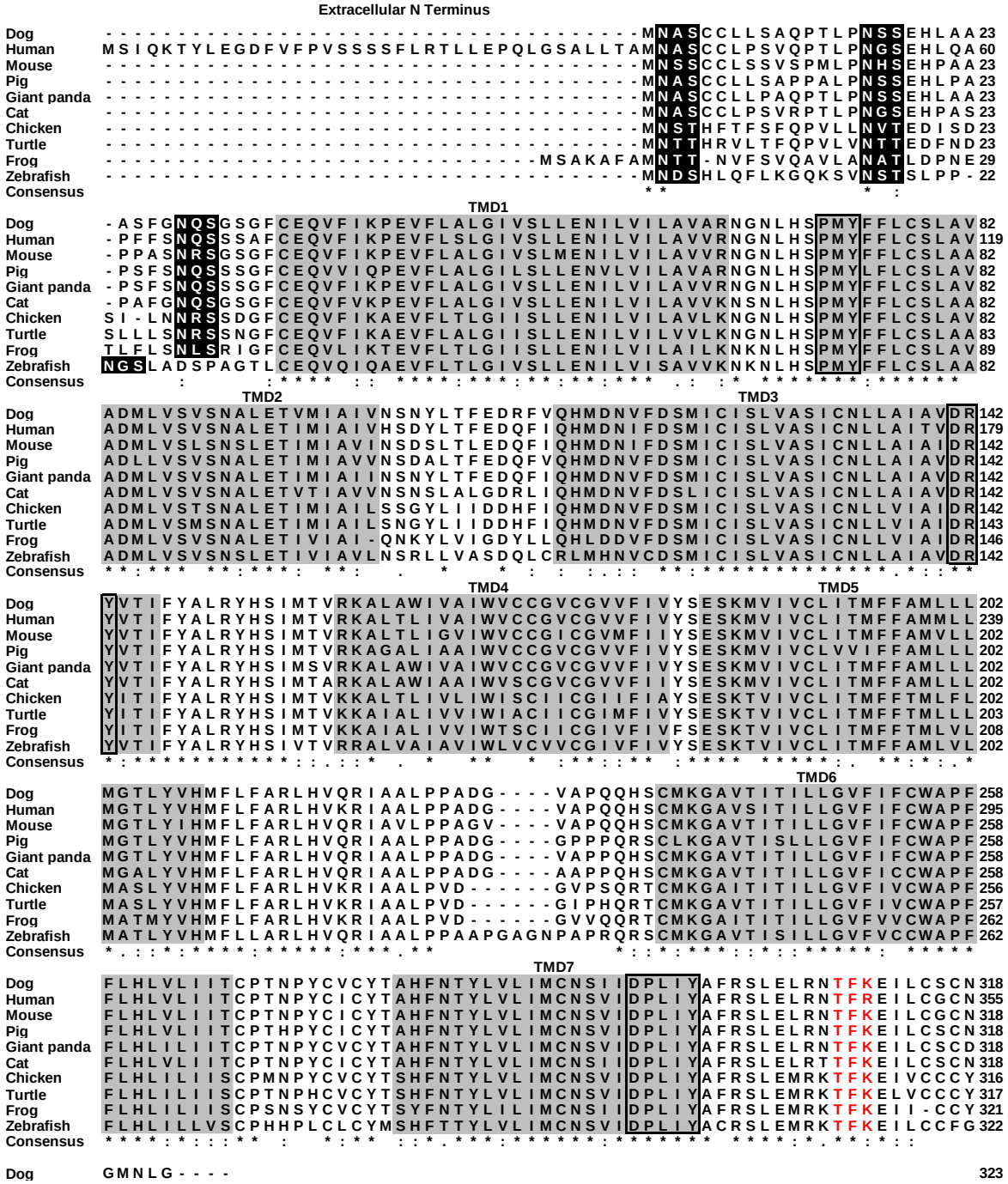
Extracellular N Terminus
TMD1
TMD2
TMD3
TMD4
TMD5
TMD6
TMD7
Dog
Human
Mouse
Pig
Giant panda
Cat
Chicken
Turtle
Frog
Zebrafish
Consensus

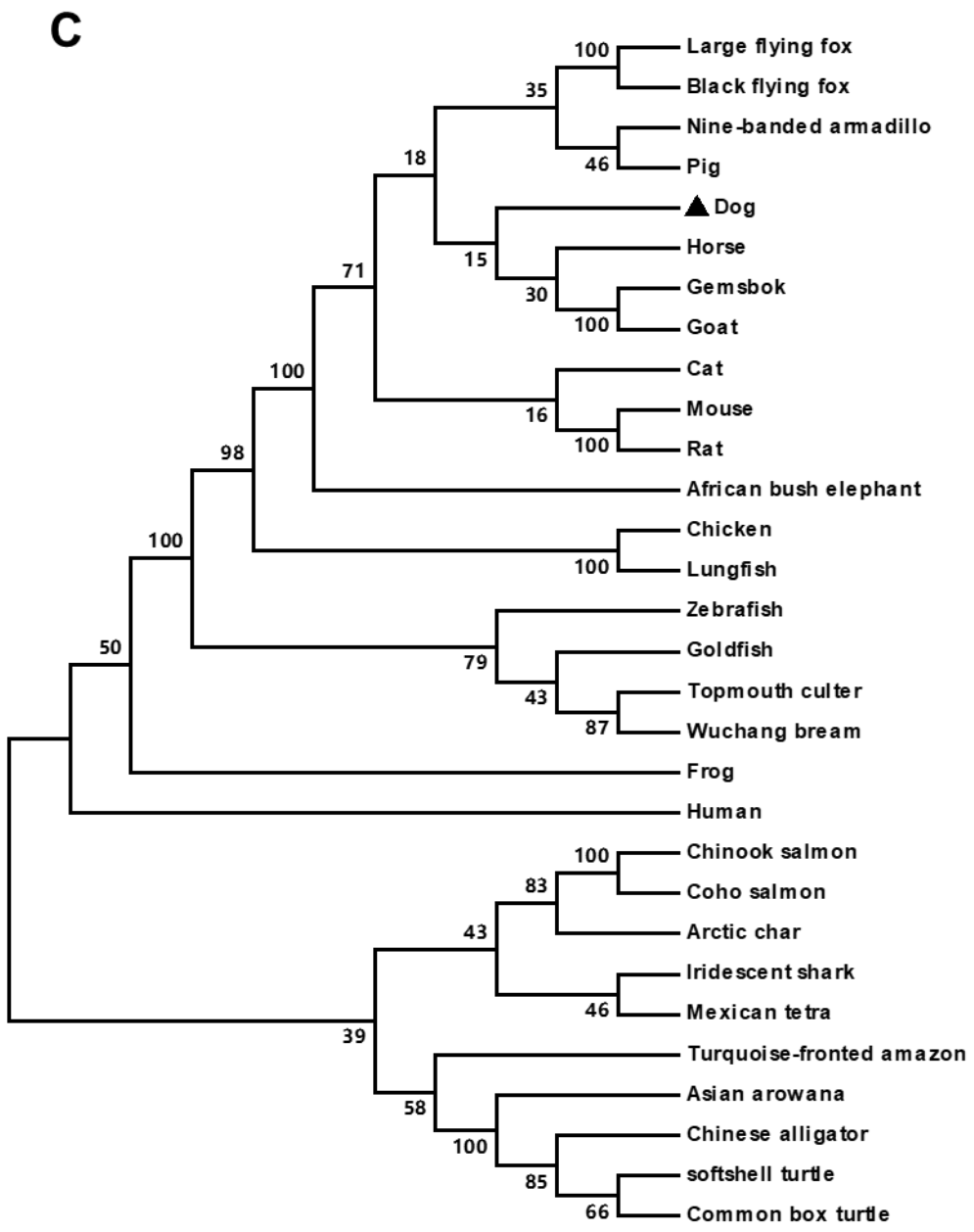

Figure 3.2 Nucleotide and deduced amino acid sequences (A), comparison of amino acid sequences (B), and phylogenetic tree (3) of canine MC3R. Positions of nucleotide and amino acid sequences are indicated on both sides. *N*-linked glycosylation sites are present in open boxes. Shaded boxes show putative TMD1-7. The conserved motifs (PMY, DRY and DPxxY) are underlined. Asterisk (*) shows stop codon. The tree was constructed by the Neighbor-joining

(NJ) method. Numbers at nodes indicate the bootstrap value, as percentages, obtained for 1000 replicates. Black dot denotes canine MC3R. MC3Rs: *Canis lupus familiaris* (dog, NM_001135124.1), *Capra hircus* (goat, XP_005688382.1), *Xenopus tropicalis* (frog, XP_002935436.1), *Protopterus annectens* (Lungfish, XP_043945978.1), *Megalobrama amblycephala* (Wuchang bream, AWA81517.1), *Culter alburnus* (topmouth culter, MT419813), *Carassius auratus* (goldfish, BAJ83473.1), *Oncorhynchus kisutch* (coho salmon, XP_020360426.1), *Danio rerio* (zebrafish, AAO24744.1), *Homo sapiens* (human, NP_063941.3), *Sus scrofa* (pig, AFK25142.1), *Mus musculus* (mouse, AAI03670.1), *Gallus gallus* (chicken, XP_004947293.1), *Rattus norvegicus* (rat, NP_001020441.3), *Pangasianodon hypophthalmus* (iridescent shark, XP_026770221.1), *Equus caballus* (horse, NP_001243901.1), *Astyanax mexicanus* (Mexican tetra, XP_007231215.1), *Pteropus vampyrus* (large flying fox, XP_011368476.1), *Oryx gazella* (gemsbok, AFH58734.1), *Pteropus alecto* (black flying fox, XP_006921991.1), *Felis catus* (cat, XP_023106851.1), *Dasypus novemcinctus* (nine-banded armadillo, XP_004447768.1), *Loxodonta africana* (African bush elephant, XP_003419952.1), *Salvelinus alpinus* (Arctic char, XP_023994975.1), *Oncorhynchus tshawytscha* (chinook salmon, XP_024229914.1), *Scleropages formosus* (Asian arowana, XP_018615783.1), *Amazona aestiva* (turquoise-fronted amazon, KQL61336.1), *Terrapene carolina triunguis* (common box turtle, XP_024059166.1), *Pelodiscus sinensis* (Chinese softshell turtle, XP_006129463.1), and *Alligator sinensis* (Chinese alligator, XP_006018246.1).

A

```
  1 ATG GCC AAC GAG ACC AAC GCC TCC ACC CTG TAT GAC AGC TAC GAG TAC TAC CTG GAC TAC  60
  1 M   A   N   E   T   N   A   S   T   L   Y   D   S   Y   E   Y   Y   L   D   Y    20
 61 TTG GAC CTC ATT CCC GTG GAT GAG AGG AAG CTG AAA GCC AAC AAA TAT CTG ATT GTC ATC 120
 21 L   D   L   I   P   V   D   E   R   K   L   K   A   N   K   Y   L   I   V   I    40
121 GCC TTC TGG GTG AGC CTG GCA CTT TTC GTC ATG CTT CTC TTC CTC ATC CTG CTC TAC ATG 180
 40 A   F   W   V   S   L   A   L   F   V   M   L   L   F   L   I   L   L   Y   M    60
181 TCC TGG TCA GGC TCC TCA CAG GTG AGG AAC AAC GCC CAG CAC CAC CCA ATA TGC CCC TGG 240
 61 S   W   S   G   S   S   Q   V   R   N   N   A   Q   H   H   P   I   C   P   W    80
241 AGT CAC AGC CTC CAC CTC CCG CTC TGC ATC CGG AGA CAC CCC CCA GGA TCC ATG GAG CTC 300
 81 S   H   S   L   H   L   P   L   C   I   R   R   H   P   P   G   S   M   E   L   100
301 GGG CGA GGA ACC AGG GAG CAG AGT ATC CAG CCC TGA                                 360
101 G   R   G   T   R   E   Q   S   I   Q   P   *                                    111
```

B

```
Dog MRAP1         -------------------------MANETNASTLYDSYEYYLDYLDLIPVDERKLKANK 35
Human MRAP1a      -------------------------MANGTNASAPYYSYEYYLDYLDLIPVDEKKLKAHK 35
Human MRAP1b      -------------------------MANGTNASAPYYSYEYYLDYLDLIPVDEKKLKAHK 35
Mouse MRAP1       -------------------------MANGTDASVPLTSYEYYLDYIDLIPVDEKKLKANK 35
Cat MRAP1         -------------------------MANQTNASTLYDSYEYYLDYVDLIPVDERKLKANK 35
Chicken MRAP1     -------------------------MANRTNSSEYFWSYEYYWDYIDPIPVDGRKLKVNK 35
Turtle MRAP1      -------------------------MAIRTNTSEYYWSYEYYWDYLDPVPVDERKLKANK 35
Frog MRAP1        MIGAAKPSLILTCTQLVISGTSSAHNAMMADTGNVSYTYEDYYDYEDFASFDESEPRANK 60
Lungfish MRAP1    -------------------------MTNTTNLSGYILAYEYYDDYIDFPAVDERTLIVHK 35
Zebrafish MRAP1   ---------------------------MKNSSEYVWGYEYYYDYVDPVLVNASTLKYSR 32
Consensus                                                 ** * ** *            .

                                  TMD
Dog MRAP1         YLIVIAFWVSLALFVMLLFLILLYMSWSGSSQVRNNAQHHPICP---WSHSLHLPLCIRR 92
Human MRAP1a      HSIVIAFWVSLAAFVVLLFLILLYMSWSASPQMRNSPKHHQTCP---WSHGLNLHLCIQK 92
Human MRAP1b      HSIVIAFWVSLAAFVVLLFLILLYMSWSASPQM---------------SFNTDESLLHSE 80
Mouse MRAP1       HSIVIALWLSLATFVVLLFLILLYMSWSGSPQMRHSPQPQPICS---WTHSFNLPLCLR- 91
Cat MRAP1         YLIVIAFWVSLALFVMLLFLILLYMSWSGSSQVRNNAQHHPTRP---WSRGLNLPLCVRR 92
Chicken MRAP1     YSIVIAFWVGLAAFVMFLFLILLYMSRSGSNPVKQVVVRNRVEE---SSSNSEQPHGDNV 92
Turtle MRAP1      YSIVIAFWVGIAAFVVFLFLILLYMSRSGSTPVKQVLAGNRIEHLEGSSSNVERLHCVDL 120
Frog MRAP1        YSIVIALWVGLAMFVVFLFLILLYMSRTVARSKNTARRK---------RKQMFLKGSTER 86
Lungfish MRAP1    YSIAIALWSGLAVFVILLFLMLLYVSRSESPLEQSLLK----------IDSLRNANCQWI 85
Zebrafish MRAP1   YSIVLIFWMILAAFIGFFFLILSLISHSGQLPRGPRVK----------KSGLPLMKG-YA 81
Consensus           * .  *  .* *.   **.*  .* .

Dog MRAP1         HP-PGSMELGRGTR-----EQSIQP----------------------------------- 111
Human MRAP1a      CLPCHREPLATSQAQASSVEPGSRTGPDQPLRQESSSTLPLGGFQTHPTLLWELTLNGGP 152
Human MRAP1b      VLPQTRA-ISCDELQAPREEGAA------------------------------------- 102
Mouse MRAP1       -----RASLQTTE------EPGRRAGTDQWLTQQSPSASAPGPLALP------------- 127
Cat MRAP1         X--PHRLPRARARS-----QAAEHPALSGGCGREPLRPAPPAPQTHP-ALFWEPGLDGDP 144
Chicken MRAP1     SS-PFPDPVAPGTPSCLPDHSGIHGSISA------------------------------- 120
Turtle MRAP1      SS-PDSDLIATEPCNSLSDEIGIHGSISA------------------------------- 123
Frog MRAP1        PKGREHGESSRDPE---------------------------------------------- 152
Lungfish MRAP1    CQRCHMDIMSCLRKHDSHTSSAVHLPLPMNRRDDCVDANQDHQGQNSTSDWSAANRCLPC 145
Zebrafish MRAP1   SSQ--------------------------------------------------------- 84
Consensus

Dog MRAP1         -------------------------------------------------            111
Human MRAP1a      LVRSKPSEPPPGDRTSQLQS-----------------------------            172
Human MRAP1b      -------------------------------------------------            102
Mouse MRAP1       -------------------------------------------------            127
Cat MRAP1         PQQQLTTGTRRGDPSRETEPLNCSLDASKRLVNSNQPGYTSAFEKPAYV            193
Chicken MRAP1     -------------------------------------------------            120
Turtle MRAP1      -------------------------------------------------            123
Frog MRAP1        -------------------------------------------------            125
Lungfish MRAP1    EDETKCV------------------------------------------            152
Zebrafish MRAP1   -------------------------------------------------            84
Consensus
```

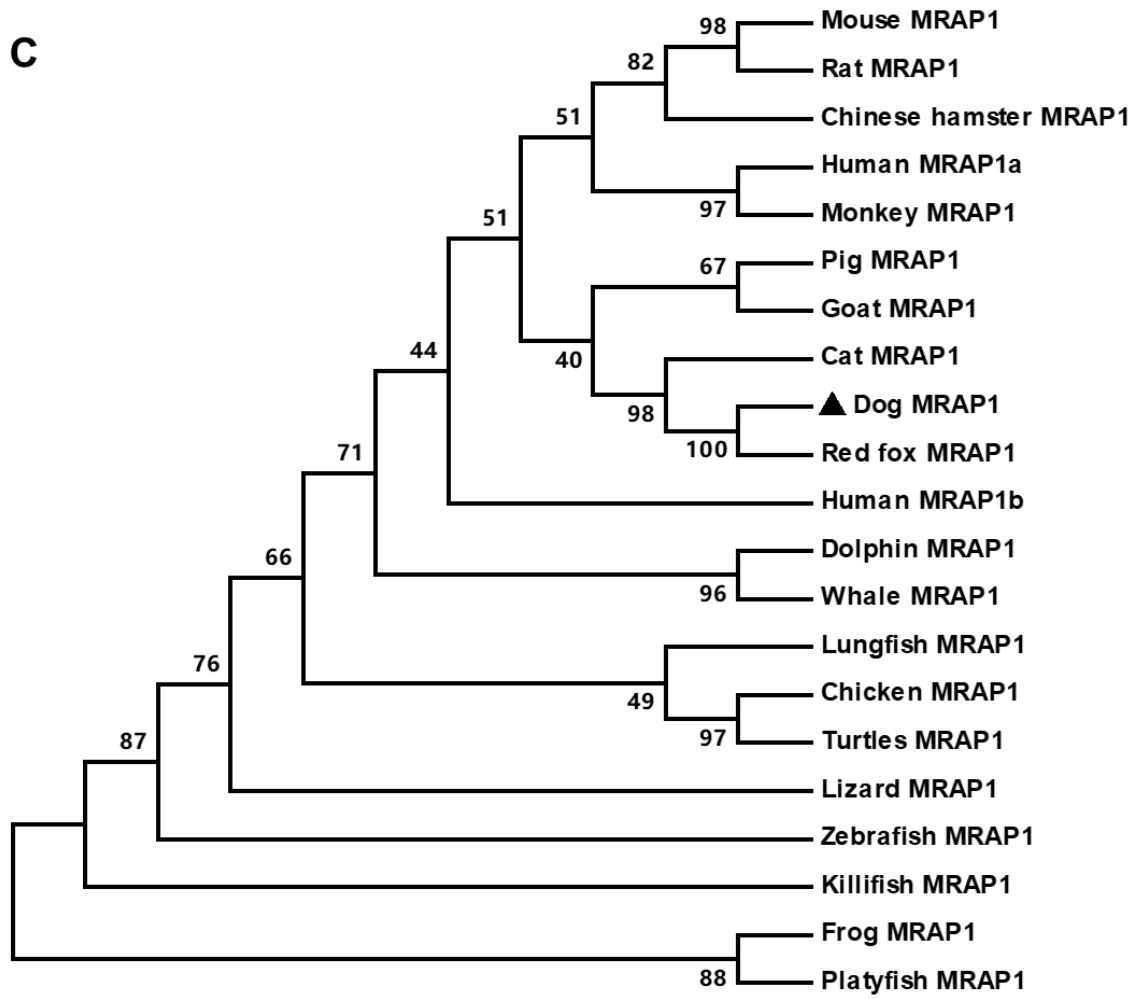

Figure 3.3 Nucleotide and deduced amino acid sequences (A), comparison of amino acid sequences (B), and phylogenetic tree (3) of cMRAP1. Positions of nucleotide and amino acid sequences are indicated on both sides. *N*-linked glycosylation sites are present in open boxes. Red box denotes YEYY motif. Light blue box indicates LDYL motif. Black box is LKANKYL motif. Shaded box shows putative TMD. Asterisk (*) shows stop codon. The tree was constructed by the Neighbor-joining (NJ) method. Numbers at nodes indicate the bootstrap value, as percentages, obtained for 1000 replicates. Black dot denotes canine MRAP1. MRAP1s: *Canis lupus familiaris* (dog, XP_005638887.1), *Homo sapiens* (human MRAP1a, AAH62721.1; human MRAP1b, NP_996781.1), *Mus musculus* (mouse, NP_084120.1); *Macaca mulatta*

(monkey, XP_001096328.3), *Gallus gallus* (chicken, XR_001470382.2), *Chrysemys picta bellii* (turtle, XP_005283970.1), *Xenopus tropicalis* (frog, XP_002938489.2), *Danio rerio* (zebrafish, ENSDART00000148193.3), *Sus scrofa* (pig, XP_020926573.1), *Cricetulus griseus* (chinese hamster, XP_003495626.1), *Protopterus annectens* (West African lungfish, XP_043927724.1), *Xiphophorus couchianus* (platyfish, XP_027854831.1*), Fundulus heteroclitus* (killifish, XP_012735037.2), *Rattus norvegicus* (rat, NP_001129306.1), *Lagenorhynchus obliquidens* (dolphin, XP_026957114.1), *Vulpes vulpes* (red fox, XP_025840964.1), *Delphinapterus leucas* (whale, XP_022408665.2), *Capra hircus* (goat, XP_005674803.2), and *Podarcis muralis* (Lizard, XP_028582856.1).

A

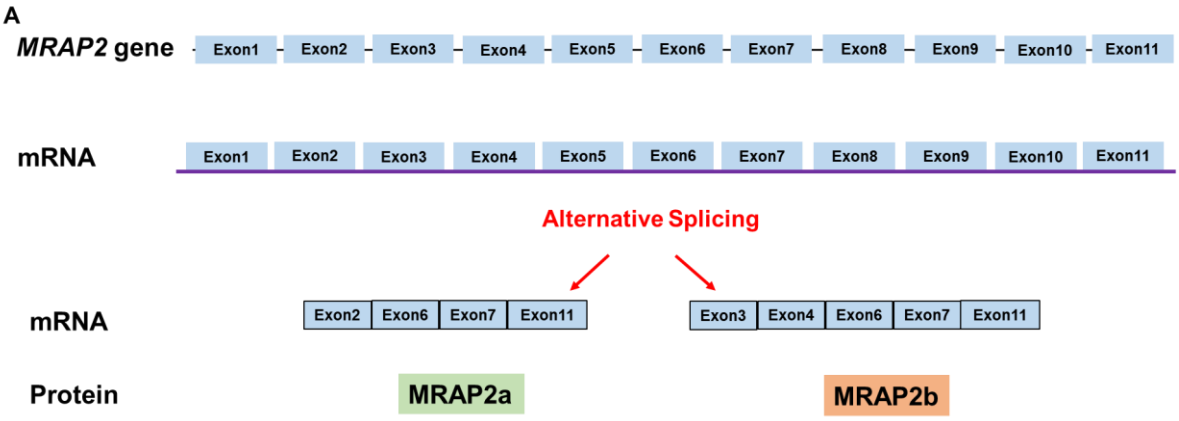

B

```
  1 ATG TCT GCC CAG AGA TTA ATT TCT AAC AGA ACA TCC CAG CCA TCT GCA CCT AAT TCT GAT  60
  1 M   S   A   Q   R   L   I   S   N   R   T   S   Q   P   S   A   P   N   S   D   20
 61 TAC ACC TGG GAA TAT GAA TAT TAT GAA ATT GGA CCA GTG TCC TTT GAA GGA CTG AAG GCT 120
 21 Y   T   W   E   Y   E   Y   Y   E   I   G   P   V   S   F   E   G   L   K   A   40
121 CAT AAA TAT TCC ATT GTG ATT GGA TTT TGG GTT GGT CTC GCT GTC TTT GTG ATT TTC ATG 180
 40 H   K   Y   S   I   V   I   G   F   W   V   G   L   A   V   F   V   I   F   M   60
181 TTT TTT GTG CTG ACT TTG CTG ACC AAG ACG GGA GCT CCA CAC CAA GAC AAT GCA GAA TCT 240
 61 F   F   V   L   T   L   L   T   K   T   G   A   P   H   Q   D   N   A   E   S   80
241 TCA GAG AAG AGA TTT AGA ATG AAT AGC TTT GTG TCA GAC TTT GGA AGA CCA CTG GAG CCA 300
 81 S   E   K   R   F   R   M   N   S   F   V   S   D   F   G   R   P   L   E   P  100
301 GAT AAG GTG TTT TCT CGA CAG GGC AAT GAT GAA TCC AGG TCT CTC TTT CAT TGC TAC ATC 360
101 D   K   V   F   S   R   Q   G   N   D   E   S   R   S   L   F   H   C   Y   I  120
361 AAT GAA GTG GAA CAC TTG GAT AGG GCT AAA GTT TGT CAT CAG ACC ACG GTC CTT GAC AGC 420
121 N   E   V   E   H   L   D   R   A   K   V   C   H   Q   T   T   V   L   D   S  140
421 AGT GTT CGA CTC CAG GAA GCC ATT AGA AGC AAT GGG CGT CCA GAG GAG GAG CTG AAT AGG 480
141 S   V   R   L   Q   E   A   I   R   S   N   G   R   P   E   E   E   L   N   R  160
481 CTT ATG AAG TTT GAT ATC CCT AAC TTT GTG AAT ACA GAC CAG AAC TCC TCC TTT GGG GAG 540
161 L   M   K   F   D   I   P   N   F   V   N   T   D   Q   N   S   S   F   G   E  180
541 GAT GAT CTT CTA ATT TCA GAA CCA CCT ATT GTT CTA GAA AAT AAG CCA GTT TCC CAG ACC 600
181 D   D   L   L   I   S   E   P   P   I   V   L   E   N   K   P   V   S   Q   T  200
601 TCA CAC AAA GAC CTG GAT TGA                                                   660
201 S   H   K   D   L   D   *                                                      206
```

C

```
   1 ATG ATT AAC CCA CAT TTC TGG GAT GCT GAA GCA GAG GCC AGG GCA ACC AGA ACC AAG GTG  60
   1 M   I   N   P   H   F   W   D   A   E   A   E   A   R   A   T   R   T   K   V   20
  61 GAG ATG TCT GCC CAG AGA TTA ATT TCT AAC AGA ACA TCC CAG CCA TCT GCA CCT AAT TCT 120
  21 E   M   S   A   Q   R   L   I   S   N   R   T   S   Q   P   S   A   P   N   S   40
 121 GAT TAC ACC TGG GAA TAT GAA TAT TAT GAA ATT GGA CCA GTG TCC TTT GAA GGA CTG AAG 180
  40 D   Y   T   W   E   Y   E   Y   Y   E   I   G   P   V   S   F   E   G   L   K   60
 181 GCT CAT AAA TAT TCC ATT GTG ATT GGA TTT TGG GTT GGT CTC GCT GTC TTT GTG ATT TTC 240
  61 A   H   K   Y   S   I   V   I   G   F   W   V   G   L   A   V   F   V   I   F   80
 241 ATG TTT TTT GTG CTG ACT TTG CTG ACC AAG ACG GGA GCT CCA CAC CAA GAC AAT GCA GAA 300
  81 M   F   F   V   L   T   L   L   T   K   T   G   A   P   H   Q   D   N   A   E  100
 301 TCT TCA GAG AAG AGA TTT AGA ATG AAT AGC TTT GTG TCA GAC TTT GGA AGA CCA CTG GAG 360
 101 S   S   E   K   R   F   R   M   N   S   F   V   S   D   F   G   R   P   L   E  120
 361 CCA GAT AAG GTG TTT TCT CGA CAG GGC AAT GAT GAA TCC AGG TCT CTC TTT CAT TGC TAC 420
 121 P   D   K   V   F   S   R   Q   G   N   D   E   S   R   S   L   F   H   C   Y  140
 421 ATC AAT GAA GTG GAA CAC TTG GAT AGG GCT AAA GTT TGT CAT CAG ACC ACG GTC CTT GAC 480
 141 I   N   E   V   E   H   L   D   R   A   K   V   C   H   Q   T   T   V   L   D  160
 481 AGC AGT GTT CGA CTC CAG GAA GCC ATT AGA AGC AAT GGG CGT CCA GAG GAG GAG CTG AAT 540
 161 S   S   V   R   L   Q   E   A   I   R   S   N   G   R   P   E   E   E   L   N  180
 541 AGG CTT ATG AAG TTT GAT ATC CCT AAC TTT GTG AAT ACA GAC CAG AAC TCC TCC TTT GGG 600
 181 R   L   M   K   F   D   I   P   N   F   V   N   T   D   Q   N   S   S   F   G  200
 601 GAG GAT GAT CTT CTA ATT TCA GAA CCA CCT ATT GTT CTA GAA AAT AAG CCA GTT TCC CAG 660
 201 E   D   D   L   L   I   S   E   P   P   I   V   L   E   N   K   P   V   S   Q  220
 661 ACC TCA CAC AAA GAC CTG GAT TGA                                               720
 221 T   S   H   K   D   L   D   *                                                 227
```

D

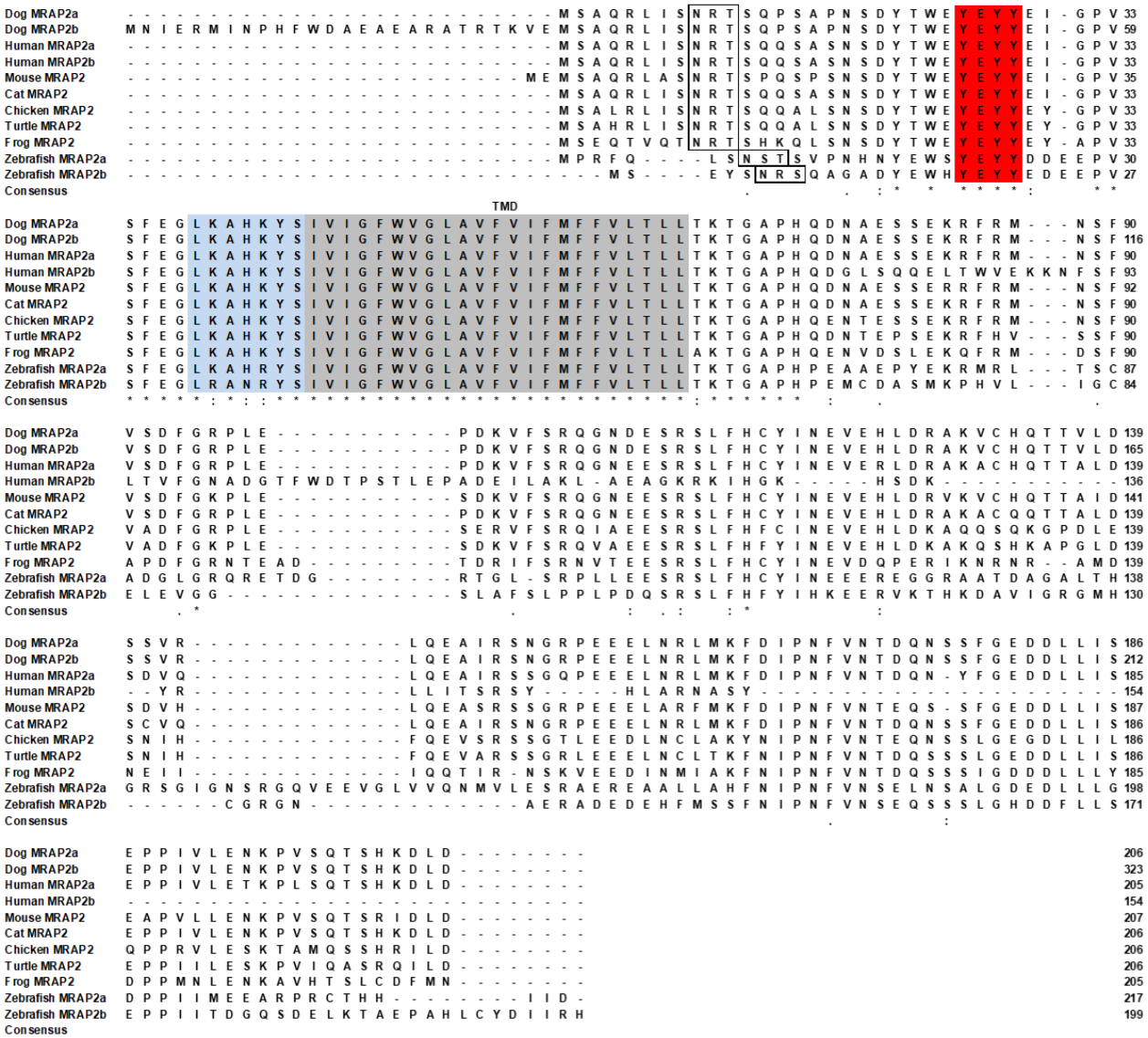
Dog MRAP2a
Dog MRAP2b
Human MRAP2a
Human MRAP2b
Mouse MRAP2
Cat MRAP2
Chicken MRAP2
Turtle MRAP2
Frog MRAP2
Zebrafish MRAP2a
Zebrafish MRAP2b
Consensus
TMD

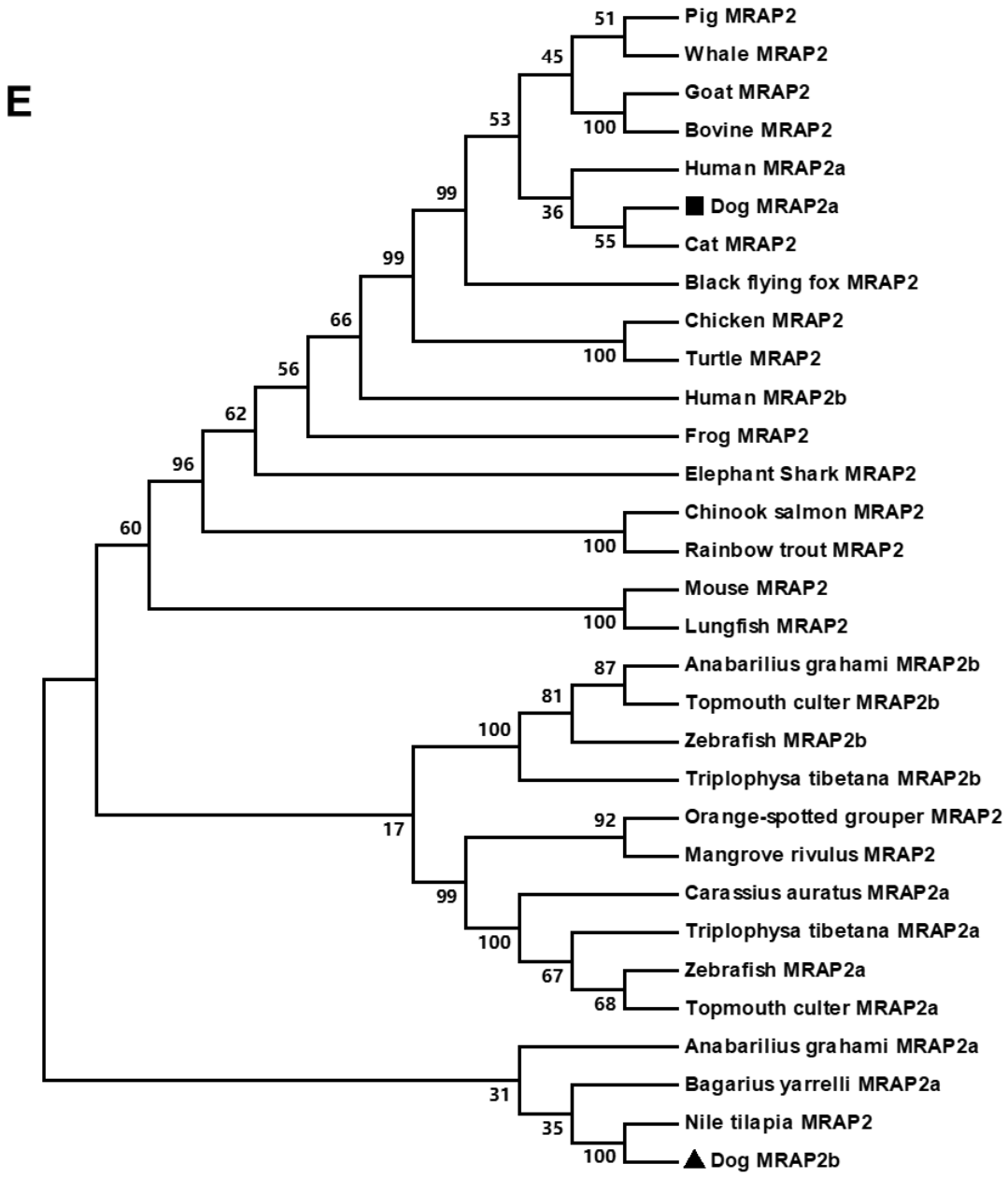

Figure 3.4 Schematic diagram of the canine MRAP2 splice variants (A), cMRAP2a amino acid sequences (B), cMRAP2b amino acid sequences, comparison of amino acid sequences, and phylogenetic tree (3) of cMRAP2s. Positions of nucleotide and amino acid sequences are indicated on both sides. *N*-linked glycosylation sites are present in open boxes. Red box denotes YEYY motif. Light blue box indicates LDYL motif. Black box is LKANKYL motif. Shaded box

shows putative TMD. Asterisk (*) shows stop codon. The tree was constructed by the Neighbor-joining (NJ) method. Numbers at nodes indicate the bootstrap value, as percentages, obtained for 1000 replicates. Black dot denotes canine MRAP1. MRAP1s: MRAP2s: *Canis lupus familiaris* (dog MRAP2a, XM_038682814.1; MRAP2b, XM_038682813.1), *Mus musculus* (mouse NP_001171202.1), *Sus scrofa* (pig, XP_003353296.2), *Capra hircus* (goat, XP_017908670.1), *Callorhinchus milii* (elelphant shark, XP_007906624.1), *Balaenoptera musculus* (whale, XP_036727732.1), *Bos taurus* (bovine, NP_001092863.1), *Protopterus annectens* (lungfish, XP_043922081.1), *Culter alburnus* (topmouth culter, MRAP2a: MT163516, and MRAP2b: MT163517), *Epinephelus coioides* (orange-spotted grouper, QED39647.1), *Danio rerio* (zebrafish, MRAP2a: F8W4H9.1 and MRAP2b: F8W4H9.1), *Oryzias latipes* (Japanese medaka, XP_023809099.1), *Maylandia zebra* (zebra mbuna, XP_004568825.1), *Kryptolebias marmoratus* (mangrove rivulus, XP_017267334.1), *Amphiprion ocellaris* (anemonefish, XP_023122806.1), *Oncorhynchus mykiss* (rainbow trout, XP_021467183.1), *Gallus gallus* (chicken, ALO81626.1), *Oreochromis niloticus* (Nile tilapia, XP_003458293.2), *Oncorhynchus tshawytscha* (Chinook salmon, XP_024278413.1), *Ictidomys tridecemlineatus* (thirteen-lined ground squirrel, XP_021581743.1), *Pteropus alecto* (black flying fox, XP_006926405.1), *Mus caroli* (Ryukyu mouse, XP_021029091.1), *Puma concolor* (puma, XP_025781535.1), *Bubalus bubalis* (water buffalo, XP_006054803.2), *Homo sapiens* (human, AAH10003.2), *Macaca nemestrina* (pig-tailed macaque, XP_011764298.1), *Anabarilius grahami* (Kanglang fish, MRAP2b ROJ29330.1), *Triplophysa tibetana* (MRAP2a: KAA0703529.1 and MRAP2b: KAA0720858.1), and *Carassius auratus* (goldfish, MRAP2a: XP_026139519).

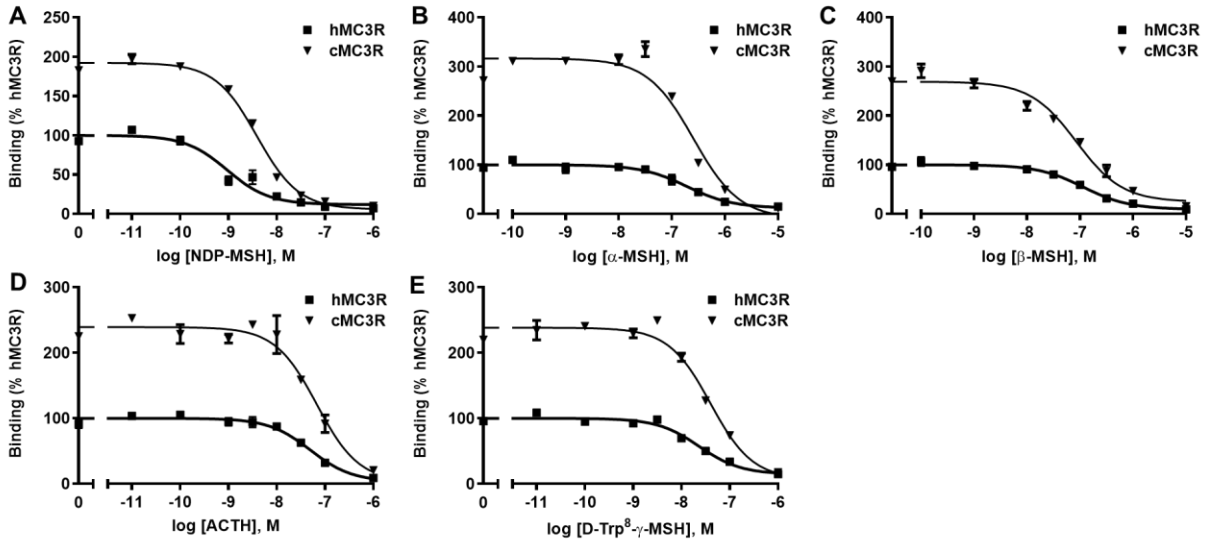

Figure 3.5 Ligand binding properties of cMC3R. Different concentrations of unlabeled NDP-MSH (A), α-MSH (B), β-MSH (C), ACTH (1-24) (D), and D-Trp^8-γ-MSH (E) were used to displace the binding of ^{125}I-NDP-MSH. Results are expressed as % of hMC3R binding ± range from duplicate determinations within one experiment. All experiments were repeated at least three independent times.

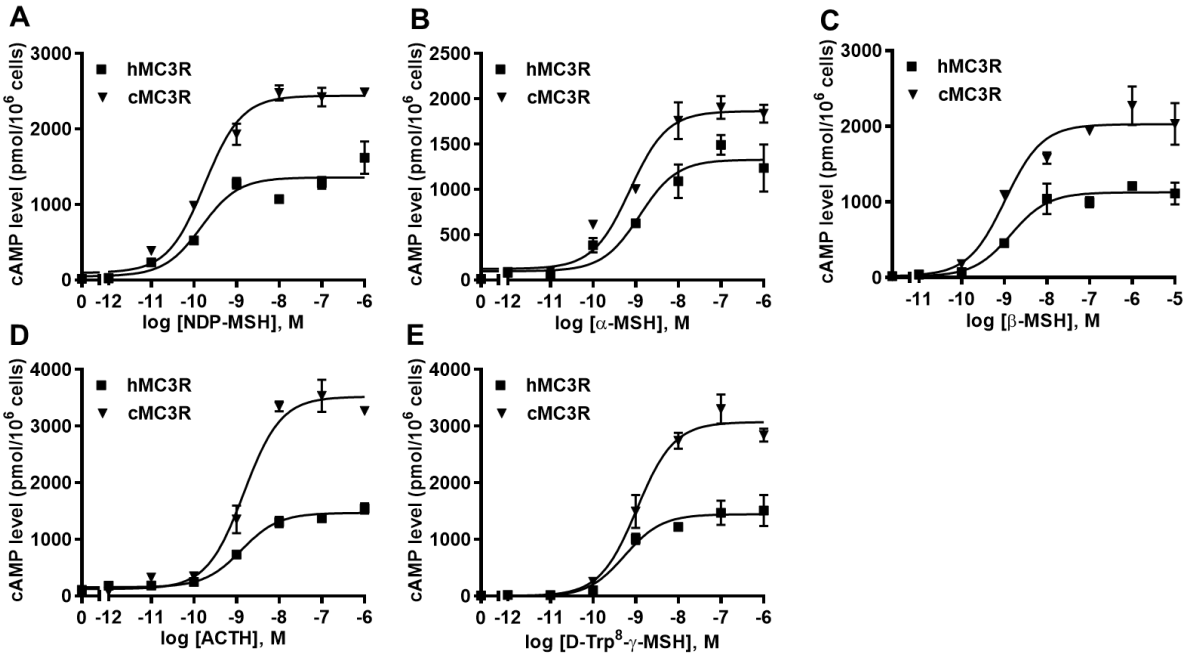

Figure 3.6 Signaling properties of cMC3R. HEK293T cells were transiently transfected with hMC3R or cMC3R plasmids. Different concentrations of NDP-MSH (A), α-MSH (B), β-MSH (C), ACTH (1-24) (D), and D-Trp^8-γ-MSH (E) were used to stimulate the cells. Data are mean ± SEM from triplicate measurements within one experiment. All experiments were performed at least three times independently.

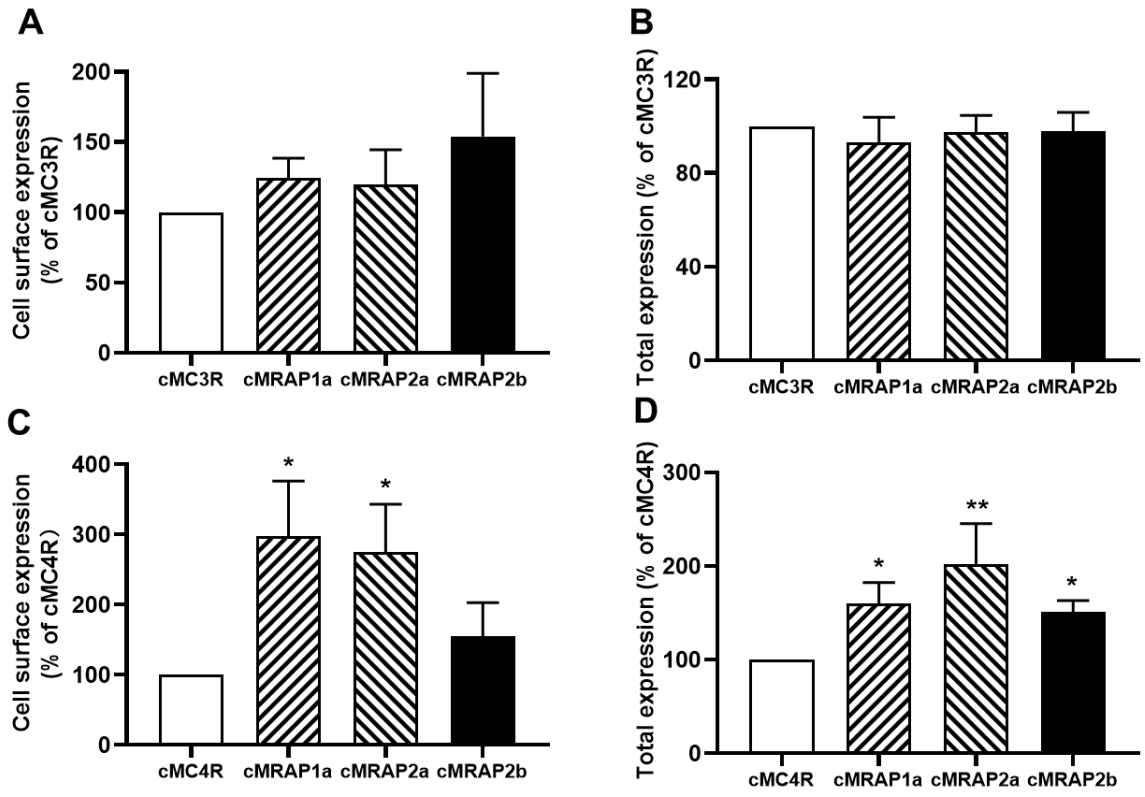

Figure 3.7 Regulation of cMC3R (A, B) and cMC4R (C, D) expression by MRAPs. Cell surface expression and total expression of cMC3R and MC4R were measured by flow cytometry. HEK293T cells were co-transfected with cMC3R or cMC4R and cMRAPs (1:5). The empty vector pcDNA3.1 fluorescence was used for background staining. The results are calculated as % of 1:0 group. Each data point represented as the mean ± SEM (n = 3-4). Different letters indicate significant difference ($P < 0.05$) (One-way ANOVA followed by Tukey test).

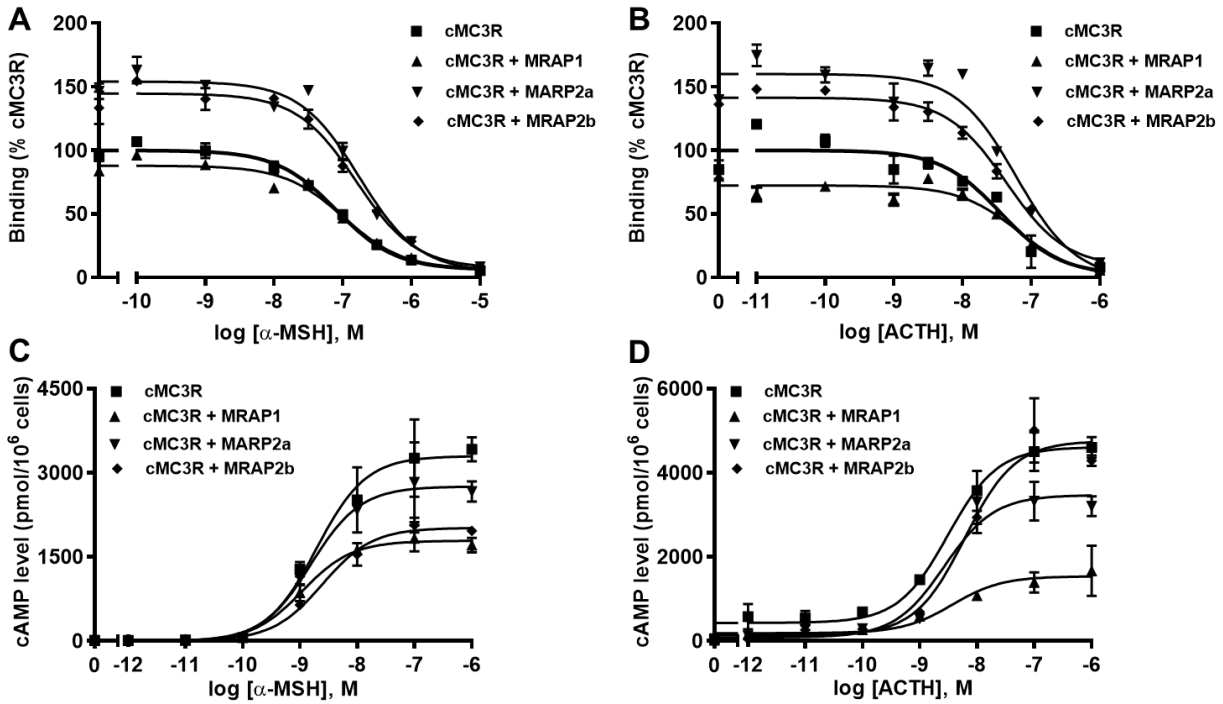

Figure 3.8 Modulation of cMC3R pharmacology by MRAPs. Ligand binding (A, B) and signaling (C, D) properties of cMC3R to α-MSH or ACTH (1-24) upon co-expression of cMC3R with cMRAP2, cMRAP2a or cMRAP2b were measured. Results of binding properties were calculated as % of cMC3R without MRAPs binding ± range from duplicate determinations within one experiment. All experiments were measured at least three independent experiments.

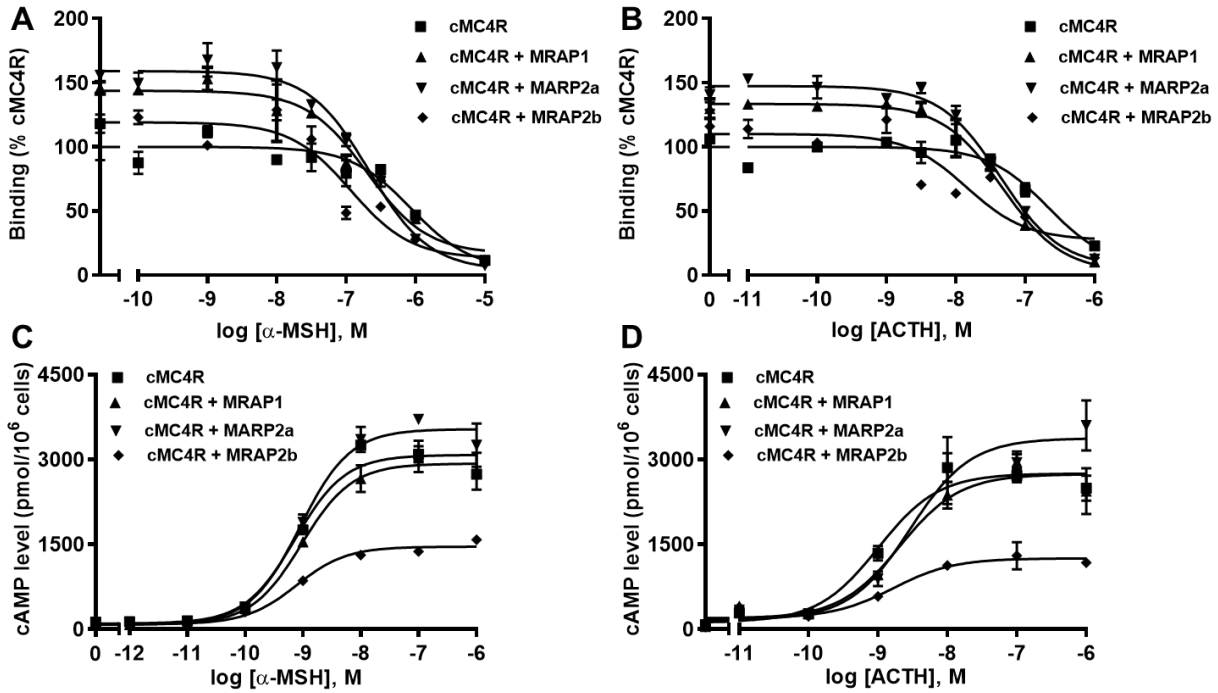

Figure 3.9 Modulation of cMC4R pharmacology by MRAPs. Ligand binding (A, B) and signaling (C, D) properties of cMC4R to α-MSH or ACTH (1-24) upon co-expression of cMC4R with cMRAP2, cMRAP2a or cMRAP2b were measured. Results of binding properties were calculated as % of cMC4R without MRAPs binding ± range from duplicate determinations within one experiment. All experiments were measured at least three independent experiments.

Chapter 4: Topmouth culter melanocortin-3 receptor: regulation by two isoforms of melanocortin receptor accessory protein 2

4.1 Introduction

Melanocortin receptors (MCRs) belong to rhodopsin-like Family A G-protein-coupled receptors (GPCRs). Five MCRs (named MC1R to MC5R), with diverse ligand affinities (including α-, β-, γ-melanocyte-stimulating hormones (MSHs) and adrenocorticotropic hormone (ACTH)) and multiple physiological roles, have been extensively studied in mammals [17, 240-242]. MC3R and MC4R are known as neural MCRs with high expression in the central nervous system [19-22]. These two MCRs play vital roles in modulation of energy homeostasis. Mutations in *MC3R* and *MC4R* are associated with obesity [30, 31, 33]. *Mc4r* knockout mice show obesity phenotype with increased food intake and decreased energy expenditure [25, 26]. Targeted deletion of *Mc3r* in mice show a moderate obesity phenotype with decreased lean mass, increased fat mass, normal food intake and metabolism, suggesting that MC3R could regulate feed efficiency and alterations in nutrient partitioning [27-29]. In addition, studies found that MC3R plays a key role in anomalous metabolic adaption to restricted feeding [83, 84]. A recent study showed that MC3R is a critical regulator of boundary controls on melanocortin signaling, providing rheostatic control on energy storage [82].

In addition to the central nervous system expression, MC3R is also expressed in several peripheral tissues, including the intestine, placenta, heart, gut, kidney, and macrophages [20, 38, 39, 78, 243]. Owing to its wide expression, MC3R has been shown to have other potential physiological functions in the periphery, including involvement in immune response and

inflammation [36-40], regulating cardiovascular function [34, 35] and natriuresis [41]. The MC3R primarily couples to the stimulatory G protein (Gs) to stimulate adenylyl cyclase activity, leading to increased production of the intracellular second messenger cyclic adenosine monophosphate (cAMP) to trigger downstream signaling.

MCRs have been shown to interact with small single transmembrane proteins: melanocortin-2 receptor accessory proteins (MRAPs, including MRAP1 and MRAP2) [44, 46, 47, 55] (reviewed in [3, 234]. MRAP2 has high expression in central nervous system and plays crucial role in regulating energy homeostasis. Targeted deletion of *Mrap2* in mice show severe obesity [50, 51]. MRAP2 interacts with and modulates MC4R signaling in mammals and other species [55, 56, 59, 61, 117, 236]. Additionally, the function of MRAP2 in regulating energy homeostasis through MC3R has also been reported [47, 56, 57].

Considering the crucial importance of energy metabolism, understanding the endocrine modulation of energy homeostasis is important for economically important fishes, and may potentially lead to novel approaches to manipulate fish growth, feed efficiency and final product quality in cultured fish. Hence it is not surprising that Mc3r has also attracted some attention in fish. Our mining of NCBI database and literature search revealed that the *mc3r* gene is found in some fish, including Holocephali (elephant shark *Callorhinchus milii*), Elasmobranchii (spiny dogfish *Squalus acanthias*, thorny skate *Amblyraja radiata*, red stingray *Hemitrygon akajei*, velvet belly lantern shark *Etmopterus spinax*), Polypteriformes (reedfish *Erpetoichthys calabaricus*, gray bichir *Polypterus senegalus*), Lepisosteiforme (spotted gar *Lepisosteus oculatus)*, Coelacanths (coelacanth *Latimeria chalumnae*), and teleosts including zebrafish *Danio rerio*, common carp *Cyprinus carpio*, Mexican tetra *Astyanax mexicanus*, red-bellied piranha *Pygocentrus nattereri*, yellow catfish *Tachysurus fulvidraco*, channel catfish *Ictalurus*

punctatus, striped catfish *Pangasianodon hypophthalmus*, electric eel *Electrophorus electricus*, Chinook salmon *Oncorhynchus tshawytscha*, coho salmon *Oncorhynchus kisutch*, river trout *Salmo trutta*, rainbow trout *Oncorhynchus mykiss*, Arctic char *Salvelinus alpinus*, northern pike *Esox lucius*, denticle herring *Denticeps clupeoides*, and Asian bonytongue *Scleropages formosus*, although it is absent in other species including lungfish *Dipnomorpha*, Acipenseriformes (Yangtze sturgeon *Acipenser dabryanus* and American paddlefish *Polyodon spathula*), cichlid *Simochromis diagramma*, medaka *Oryzias latipes*, fugu *Takifugu rubripes*, stickleback *Gasterosteus aculeatus*, ricefield eel *Monopterus albus*, and orange-spotted grouper *Epinephelus coioides* [113, 117, 148, 244, 245]. Since MC3R is considered a specific receptor for γ-MSH in higher vertebrates [20, 21] and γ-Msh is absent in teleosts [246], the absence of Mc3r in some fish might be considered as one example of co-evolution of ligand and receptor.

Only three studies have investigated the pharmacological properties of fish Mc3rs so far [57, 113, 150]. Of interest, two studies reported high constitutive activities in zebrafish and channel catfish Mc3rs [57, 150], similar to the results in teleost Mc4rs [59, 61, 115-118, 148, 247] and Mc1r [213]. In this study, topmouth culter (*Culter alburnus*) was used as an animal model to explore physiology and pharmacology of culter Mc3r. Topmouth culter is an important species of freshwater fish with wide distribution in reservoirs, rivers, and lakes in China [248, 249]. We cloned culter *mc3r* and investigated pharmacology of caMc3r and modulation by Mrap2 and Mrap2b.

4.2 Materials and Methods

4.2.1 Ligands and plasmids

NDP-MSH was purchased from Peptides International (Louisville, KY, USA). Human α-MSH was obtained from Pi Proteomics (Huntsville, AL, USA). Human ACTH (1-24) was purchased from Phoenix Pharmaceuticals (Burlingame, CA, USA). Human des-acetyl-α-MSH was obtained from GenScript (Piscataway, NJ, USA). Culter α-Msh and Acth are 100 and 87.5% identical with the corresponding human counterparts, respectively (**Figure 4.1**). [^{125}I]-cAMP and [^{125}I]-NDP-MSH were iodinated using chloramine T method [221, 222]. The human MC3R (hMC3R) subcloned into pcDNA3.1 vector (pcDNA3.1-hMC3R) was generated as previously described [96]. N-terminal Flag-tagged caMrap2a and N-terminal Flag-tagged caMrap2b were reported before [59]. N-terminal myc-tagged caMc3r was commercially synthesized and subcloned into pcDNA3.1 by GenScript (Piscataway, NJ, USA) to generate the plasmid used for transfection.

4.2.2 Gene cloning and sequence alignment

Gene sequences were provided by our collaborator: Dr. Min Tao from Hunan Normal University, Hunan, China.

4.2.3 Cell culture and transfection

Human embryonic kidney (HEK) 293T cells (ATCC, Manassas, VA, USA) were cultured at an incubator (37 °C in a 5% CO_2-humidified atmosphere) [223]. Briefly, the medium contained Dulbecco's Modified Eagle's medium (DMEM) (Invitrogen), 10% newborn calf serum, 0.25 μg/mL of amphotericin B, 100 IU/mL of penicillin, 100 μg/mL streptomycin, 50 μg/mL of gentamicin, and 10 mM HEPES. Cells were plated into 6-well or 24-well plates pre-coated with 0.1% gelatin. At approximately 70% confluency, cells were transfected with 0.25 μg/μL MC3R

with or without MRAP2s plasmids using calcium phosphate precipitation method [224]. Empty vector pcDNA3.1 was used to normalize the total DNA in each well.

4.2.4 Flow cytometry assay

The expression of the caMc3r was quantified with flow cytometry as described earlier [118, 225], carried out by the C6 Accuri Cytometer (Accuri Cytometers, Ann Arbor, MI, USA). Four ratios (1:0, 1:1, 1:3, and 1:5) of caMC3R and caMRAP2a/caMRAP2b plasmids were co-transfected into cells in 6-well plates. Fluorescence of cells transfected with empty vector (pcDNA3.1) was used for background staining. The expression of the caMc3r was calculated as the percentage of 1:0 group was set as 100% expression. The expression levels of other groups were calculated as % of the 1:0 group [225].

4.2.5 Ligand binding assays

Binding assay was described previously [57, 223]. The ligands and their final concentrations used in this study were NDP-MSH (from 10^{-12} to 10^{-6} M), α-MSH (from 10^{-12} to 10^{-6} M), des-acetyl-α-MSH (from 10^{-12} to 10^{-6} M), or ACTH (1-24) (from 10^{-12} to 10^{-6} M). To investigate the modulation of caMrap2a or caMrap2b on the binding property of caMc3r, caMC3R (0.25 μg/μL) and caMRAP2a or caMRAP2b plasmids in two ratios (1:0 and 1:5) were applied to co-transfect cells (6-well plate), and ACTH (1-24) (from 10^{-11} to 10^{-6} M) and α-MSH (from 10^{-10} to 10^{-5} M) were used.

4.2.6 cAMP assays

cAMP signaling assay was performed as described previously [221, 223]. The final concentration of ligands used were 10^{-12} to 10^{-6} M. To explore effects of caMrap2a and

caMrap2b on caMc3r signaling, cells (24-well plate) were transfected with caMC3R (0.25 μg/μL) and caMRAP2a or caMRAP2b plasmids in two ratios (1:0 and 1:5), and two ligands, α-MSH (from 10^{-13} to 10^{-7} M) and ACTH (1-24) (from 10^{-13} to 10^{-7} M) were used. To investigate the dose-dependent modulation of caMrap2a or caMrap2b on maximal response (R_{max}) of cAMP signaling of caMc3r to α-MSH stimulation (10^{-6} M), four ratios (1:0, 1:1, 1:3 and 1:5) of caMC3R (0.25 μg/μL) and caMRAP2a or caMRAP2b were co-transfected into cells (24-well plate). To study the constitutive activity of cAMP signaling, caMC3R plasmid in increasing concentrations (0, 0.007, 0.015, 0.030, 0.060, 0.125, and 0.250 μg/μL) were transfected into cells (6-well plate).

4.2.7 Statistical analysis

All data were shown as mean ± S.E.M. GraphPad Prism 8.3 software (GraphPad, San Diego, CA, USA) was used to calculate the parameters of ligand binding and cAMP signaling assays. The significance of differences in expression levels, ligand binding, and cAMP signaling parameters between caMc3r and hMC3R, as well as vehicle and ligand-treated groups, were all determined by Student's t-test. F test was first analyzed to compare variances for each study. If *P* value for F test is less than 0.05, unpaired t test with Welch's correction would be performed. If *P* value for F test is more than 0.05, normal unpaired t test would be performed. One-way ANOVA was used to analyze the significance of differences in binding, cAMP, flow cytometry and gene expression between multiple groups. For One-way ANOVA (more than two groups), if *P* value for F test is less than 0.05, transformation would be performed to meet the *P* value for F test. Statistical significance was set at $P < 0.05$.

4.3 Results

4.3.1 Nucleotide and deduced amino acid sequences of caMc3r, MRAP2a, and MRAP2b

The cloned culter *mc3r* (GenBank: MT419813) had 984 bp open reading frame (ORF), encoding a protein of 327 amino acids with an estimated molecular mass of 36.01 kDa (**Figure 4.2A**). Multiple alignment of MC3Rs revealed that the predicated caMc3r had the classical characteristic of Family A GPCRs, with seven hydrophobic transmembrane domains (TMDs) and several conserved motifs (PMY, DRY, and DPxxY) at homologous positions with MC3Rs of other species (**Figure 4.2B**). Three potential *N*-linked glycosylation site (Asn^{2}, Asn^{16} and Asn^{23}) in N-terminus, and consensus sequence for protein kinase C phosphorylation ($Thr^{313}Phe^{314}Lys^{315}$) in the C-terminus were found in caMc3r (**Figure 4.2A**). The identities between caMc3r and other piscine MC3R orthologs were 99% to Wuchang bream, 98% to goldfish, 97% to common carp, 95% to zebrafish, 81% to coho salmon, as well as high homology to mammalian MC3Rs (with 83% to pig and mouse, and 82% to human) (**Figure 4.2B**). Phylogenetic tree showed that caMc3r nested with Wuchang bream, goldfish, and zebrafish Mc3rs (**Figure 4.2C**).

The cloned culter *mrap2a* had 654 bp ORF, encoding a protein of 217 amino acids with an estimated molecular mass of 24.37 kDa (**Figure 4.3A**). The cloned culter *mrap2b* had 594 bp ORF, encoding a protein of 197 amino acids with an estimated molecular mass of 22.20 kDa (**Figure 4.3B**). Similar to other MRAP2s, the caMrap2a or caMrap2b contained several features including a single TMD, a potential *N*-linked glycosylation site (Asn^{8} of caMrap2a and Asn^{6} of caMrap2b) within N-terminus, a putative motif (LKAHKYS) crucial for the formation of antiparallel homodimers [180], and a long C-terminal tail with many conserved residues (**Figure 4.3C**). Multiple sequence alignment showed that caMrap2a shared high identities with zebrafish Mrap2a with 94%, and low identities (61%) with caMrap2b and other piscine MRAP2, with 64%

to rainbow trout Mrap2, 61% to tilapia Mrap2, as well as to mammalian MRAP2s with 62% to human MRAP2, 62% to mouse MRAP2 and 60% to goat MRAP2. Similar to caMrap2a, caMrap2b shared high identities with zebrafish Mrap2b with 81%, and low identities with other piscine MRAP2s, with 61% to rainbow trout Mrap2, 59% to tilapia Mrap2, as well as to mammalian MRAP2s with 58% to human MRAP2, 60% to mouse MRAP2 and 58% to goat MRAP2 **(Figure 4.3C)**. Phylogenetic analysis revealed that caMrap2a clustered with teleost Mrap2a, nested with zebrafish Mrap2a, and caMrap2b clustered with teleost Mrap2b, nested with kanglang fish Mrap2b (**Figure 4.3D**).

4.3.3 Ligand binding properties of caMc3r

Binding assay was performed using multiple MC3R ligands, including NDP-MSH, α-MSH, des-α-MSH, and ACTH (1-24). hMC3R was used for comparison in the same experiments. The maximal binding values (B_{max}) of caMc3r was 627.02 ± 68.52% of that of the hMC3R (set as 100%) ($P < 0.001$) (**Figure 4.4 and Table 4.1**). caMc3r had significantly higher affinity to ACTH (1-24) ($P < 0.05$) (**Figure 4.4 and Table 4.1**). IC_{50}s were similar between the two MC3Rs when NDP-MSH, α-MSH, or des-α-MSH, was used (**Figure 4.4 and Table 4.1**).

4.3.4 cAMP signaling properties of caMc3r

cAMP signaling properties were measured to investigate whether caMc3r could respond to NDP-MSH, α-MSH, des-α-MSH, or ACTH (1-24) stimulation. The results indicated that all agonists could stimulate caMc3r and dose-dependently increase intracellular cAMP generation (**Figure 4.5** and **Table 4.2**). caMc3r had higher maximal responses (R_{max}) to all agonists than those of hMC3R (**Figure 4.5** and **Table 4.2**). EC_{50}s were remarkably decreased when caMc3r was stimulated by ACTH (1-24) and des-α-MSH (**Figure 4.5** and **Table 4.2**).

The present study also showed that caMc3r had 4-times higher basal cAMP levels than that of hMC3R (**Table 4.2**). To further study whether caMc3r could be constitutively active, increasing concentrations (from 0 to 0.25 μg/μL) of caMc3r plasmid were transfected into cells. The data indicated that a low amount of caMc3r plasmid transfection could increase basal cAMP signaling, starting at 0.03 μg/μL (**Figure 4.5E**).

4.3.5 Regulation of caMc3r expression and pharmacology by caMrap2s

The study showed that the mRNA of culter *mc3r*, *mrap2a*, and *mrap2b*, were detected in the same tissues (data not shown), indicating that Mrap2s might affect Mc3r pharmacology. Therefore, we further investigated the potential modulation of caMrap2s on Mc3r expression and pharmacology.

Flow cytometry was used to measure caMc3r expression. We found that caMrap2a significantly decreased the cell surface expression in 1:5 group but had no effect on total expression of caMc3r (**Figures 4.6A and B**). However, caMrap2b did not significantly affect the cell surface and total expression of caMc3r (**Figures 4.6A and B**).

Ligand binding assays with α-MSH and ACTH indicated that only caMrap2a significantly decreased the B_{max} of caMc3r in 1:5 group, but caMrap2b did not (**Figures 4.7A, B** and **Table 4.3**). caMrap2a and caMrap2b had no significant effect on affinities of caMc3r to α-MSH and ACTH (1-24) (**Figures 4.7A, B** and **Table 4.3**).

Modulation of caMrap2a or caMrap2b on caMc3r signaling was also studied. Results showed that both caMrap2a and caMrap2b did not markedly affect EC_{50}s in response to α-MSH and ACTH; caMrap2a significantly decreased R_{max}, but caMrap2b did not (**Figures 4.7C, D** and **Table 4.4**). Additionally, increasing ratios of caMC3R/caMRAP2a or caMRAP2b (1:0, 1:1, 1:3,

and 1:5) were co-transfected into cells. Results showed that both caMrap2a and caMrap2b dose-dependently decreased basal cAMP generation (**Figure 4.6C**). The cAMP generation of caMc3r stimulated by 10^{-6} M α-MSH was dose-dependently decreased by Mrap2a but not Mrap2b (**Figure 4.6D**).

4.4 Discussion

In this study, we cloned culter *mc3r*, *mrap2a*, and *mrap2b,* and explored the pharmacological properties of caMc3r and its modulation by Mrap2a and Mrap2b.

Culter *mc3r* had the similar primary structure as MC3Rs of other species with 7 TMDs and several highly conserved motifs (**Figure 4.2B**). Phylogenetic tree analysis found that caMc3r was clustered with teleost MC3Rs (**Figure 4.2C**). Culter Mrap2a and Mrap2b were similar to MRAP2s of other species that had a potential *N*-linked glycosylation site in the N-terminal domain and single highly conserved TMD (**Figure 4.3**). Based on culter genomic data, we did not identify *mrap1* in topmouth culter [249], consistent with the hypothesis that *mrap1* gene is lost in lobe-finned fish, amphibians and reptiles [3, 197].

Detailed pharmacological studies were performed on culter Mc3r. Results showed that all agonists could bind and activate caMc3r (**Figures 4.4 and 4.5**). We found that caMc3r had high affinity and potency to ACTH (**Table 1 and Table 2**), similar to dogfish [113] and channel catfish [57] Mc3rs. Fish Mc4rs also show high affinities and potencies to ACTH [59, 115, 116, 148, 250, 251]. These indicated that ACTH may be the original ligand for the MC3R and MC4R [252]. In addition, caMc3r showed decreased EC_{50}s than hMC3R in response to α-MSH, des-α-MSH, and ACTH (**Figure 4.5 and Table 4.2**). These results were similar to those of channel catfish Mc3r (ipMc3r) where ipMc3r shows significant decrease of EC_{50}s in response to α-MSH

and ACTH [57]. In addition, caMc3r had higher R_{max}s than that of hMC3R to all agonist (**Figure 4.5 and Table 4.2**). In channel catfish, Mc3r shows lower R_{max}s than that of hMC3R to NDP-MSH, α-MSH, β-MSH, and ACTH [57].

We further explored the potential modulation of the trafficking, ligand binding and signaling on caMc3r by caMrap2s. Culter Mrap2a decreased cell surface expression but had no effect on total expression of caMc3r, and Mrap2b did not affect cell surface and total expression of caMc3r (**Figures 4.6A and B**). Both human MRAP1a and MRAP2 do not significantly affect hMC3R cell surface expression [47, 49]. Zhang et al. showed that MRAP1 and MRAP2 have no effect on the cell surface expression of chicken MC3R [56]. Collectively, the potential roles of MRAPs on MC3R cell surface expression varies in different species.

In this study, we also showed that Mrap2a and Mrap2b did not affect affinities of caMc3r to α-MSH and ACTH (**Figure 4.7A, B and Table 4.3**). Mrap2a decreased the B_{max} of caMc3r, probably due to decreased cell surface expression. As for signaling, both Mrap2a and Mrap2b significantly decreased caMc3r basal activity (**Figure 4.6C**), and only Mrap2a markedly decreased the R_{max} (**Table 4.4**). Similar results were observed in channel catfish Mc3r that Mrap2 decreases basal and ligand-stimulated cAMP signaling [57]. In zebrafish, Mrap2a and Mrap2b do not modulate Mc3r signaling [55]. In hMC3R, MRAP2 significantly decreases NDP-MSH-induced cAMP generation, and MRAP1a increases agonist-stimulated cAMP signaling [47, 49]. In chicken, MRAP2 increases agonist-induced cAMP production and reduces constitutive activity of MC3R, while MRAP1 has no effect on basal and agonist-induced cAMP generation [56]. Furthermore, MRAP1 and MRAP2 increase sensitivity to ACTH of chicken MC3R [56]. Mrap2a increases the sensitivity of zebrafish Mc4r to ACTH [206, 207]. MRAP2 also increases ACTH potency and makes hMC4R act as the ACTH-preferring receptor [206]. However, this

study and our previous reports on grouper Mc4r do not find that MRAP2s could make MC3R or MC4R act as ACTH-preferring receptor [59, 117].

Results of the present study demonstrated that caMc3r had high constitutive activity in cAMP signaling (**Figure 4.5E** and **Table 4.2**), consistent with zebrafish, channel catfish, and chicken Mc3rs [56, 57, 150]. The high basal activity of MC3R were decreased by MRAP2s in culter, channel catfish, and chicken [56, 57]. AgRP, as the antagonist, decreases constitutive activity of MC3R in channel catfish, and chicken [56, 57]. However, hMC3R has little or no basal activity in cAMP pathway [74, 98]. hMC4R shows modest constitutive activity, and the defect in basal activity of *MC4R* mutations is considered as one cause of obesity [9, 146]. Mrap2- and AgRP-suppressed the basal activity of MC4R is essential for promoting zebrafish growth [55, 141]. Thus, high basal activity of Mc3r might provide new strategies to reduce Mc3r signaling by antagonist or Mrap2 for growth promotion in aquaculture. The potential relevance and physiological functions of constitutive activity in teleost Mc3rs need further study.

In summary, we cloned culter *mc3r*. Culter Mc3r had high constitutive activity in cAMP pathway. Only caMrap2a markedly decreased cell surface expression and R_{max} of caMc3r. Both caMrap2a and caMrap2b decreased basal cAMP production. These findings laid the foundation for further physiological studies of culter Mc3r that might provide new strategies for promoting growth and culture of culter.

Table 4.1 The ligand binding properties of caMc3r

MC3R		caMc3r	hMC3R
B_{max} %		627.02 ± 68.52[b]	100
NDP-MSH	IC_{50} (nM)	2.78 ± 0.71	1.78 ± 0.15
α-MSH	IC_{50} (nM)	20.81 ± 3.88	30.73 ± 1.31
des-α-MSH	IC_{50} (nM)	123.97 ± 11.48	117.95 ± 14.72
ACTH (1-24)	IC_{50} (nM)	19.66 ± 5.58[a]	43.61 ± 3.44

Results are presented as the mean ± SEM (n = 3 - 4).

[a] significant difference from the parameter of hMC3R, $P < 0.05$.

[b] significant difference from the parameter of hMC3R, $P < 0.001$.

Table 4.2 The signaling properties of caMc3r

MC3R		caMc3r	hMC3R
Basal (%)		406.89 ± 50.49[c]	100
NDP-MSH	EC_{50} (nM)	0.42 ± 0.13	0.28 ± 0.08
	R_{max} (%)	208.87 ± 15.15[a]	100
α-MSH	EC_{50} (nM)	0.22 ± 0.04	1.70 ± 0.42
	R_{max} (%)	171.91 ± 15.40[a]	100
des-α-MSH	EC_{50} (nM)	0.29 ± 0.05[a]	3.14 ± 0.38
	R_{max} (%)	168.17 ± 11.07[a]	100
ACTH (1-24)	EC_{50} (nM)	0.44 ± 0.12[b]	4.82 ± 0.79
	R_{max} (%)	140.92 ± 7.05[a]	100

Results are presented as the mean ± SEM (n = 3 - 4).

[a] significant difference from the parameter of hMC3R, $P < 0.05$.

[b] significant difference from the parameter of hMC3R, $P < 0.01$.

[c] significant difference from the parameter of hMC3R, $P < 0.001$.

Table 4.3 The effect of caMrap2s on ligand binding properties of caMc3r

caMc3r/caMrap2s	B_{max}	α-MSH	ACTH
		IC_{50} (nM)	IC_{50} (nM)
caMc3r	100	40.97 ± 8.63	83.73 ± 13.89
caMc3r/caMrap2a	48.71 ± 5.03[a]	33.97 ± 7.18	57.43 ± 12.43
caMc3r/caMrap2b	86.57 ± 6.61	49.20 ± 2.97	107.13 ± 27.48

Results are expressed as the mean ± SEM (n = 3 - 4).

[a] Significant difference from the parameter of 1:0, $P < 0.001$.

Table 4.4 The effect of caMrap2s on cAMP signaling of caMc3r

caMc3r/caMrap2s	α-MSH		ACTH	
	EC_{50} (nM)	R_{max}	EC_{50} (nM)	R_{max}
caMc3r	0.41 ± 0.02	100	2.09 ± 0.17	100
caMc3r/caMrap2a	0.29 ± 0.04	50.86 ± 7.13[b]	1.91 ± 0.57	42.49 ± 9.45[a]
caMc3r/caMrap2b	0.57 ± 0.15	111.62 ± 6.28	1.87 ± 0.38	99.36 ± 13.22

Results are expressed as the mean ± SEM (n = 3 - 4).

[a] Significant difference from the parameter of 1:0, $P < 0.05$.

[b] Significant difference from the parameter of 1:0, $P < 0.001$.

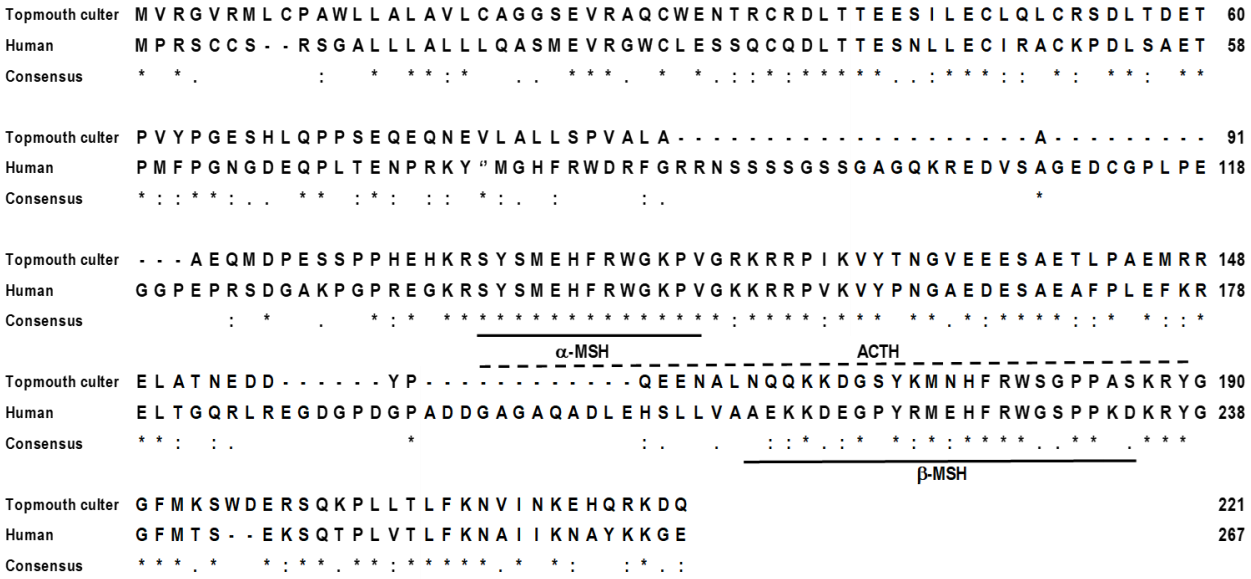

Figure 4.1 Comparison of amino acid sequences of POMCs between human and culter

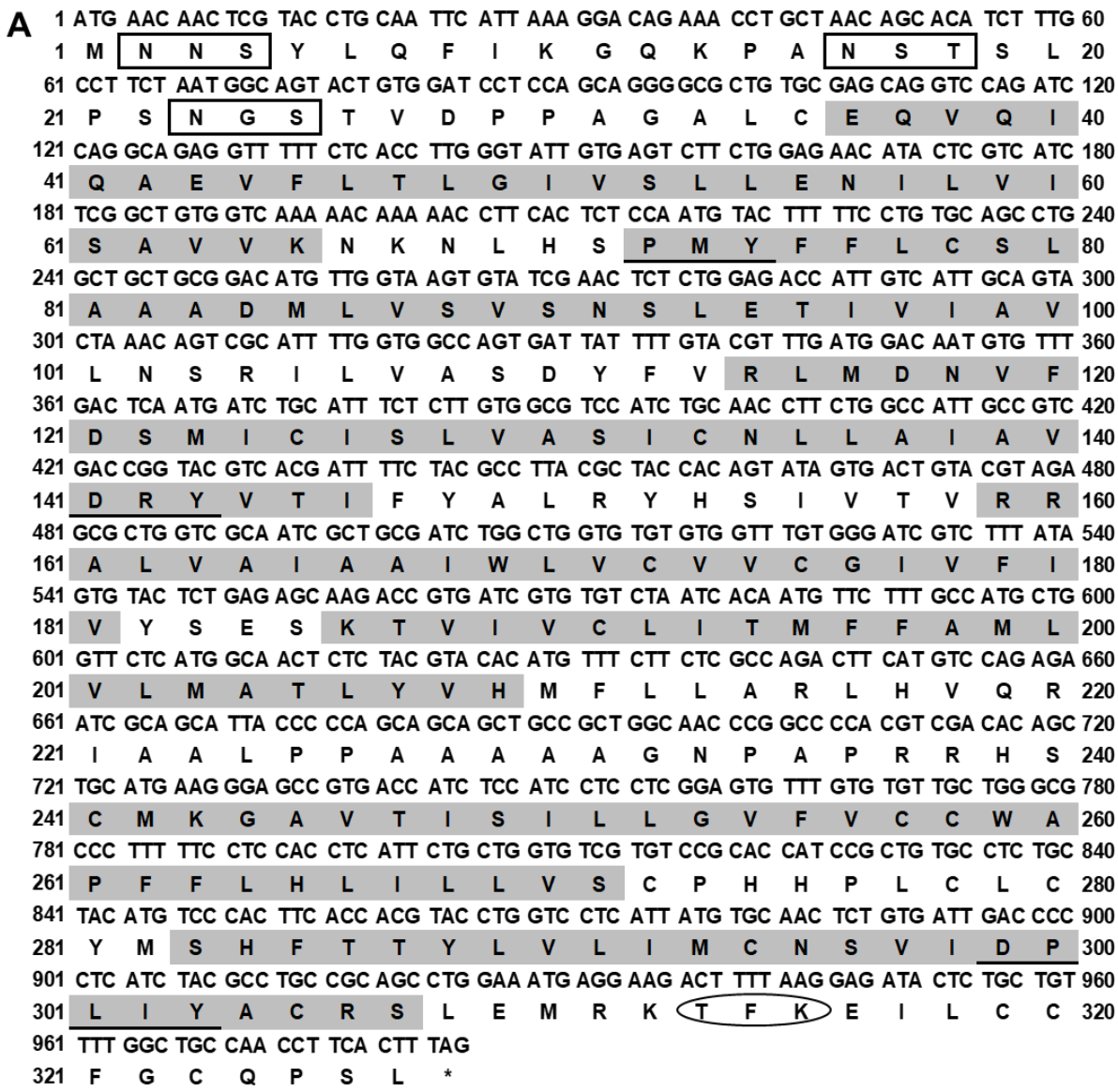
A
1 ATG AAC AAC TCG TAC CTG CAA TTC ATT AAA GGA CAG AAA CCT GCT AAC AGC ACA TCT TTG 60
1 M N N S Y L Q F I K G Q K P A N S T S L 20
61 CCT TCT AAT GGC AGT ACT GTG GAT CCT CCA GCA GGG GCG CTG TGC GAG CAG GTC CAG ATC 120
21 P S N G S T V D P P A G A L C E Q V Q I 40
121 CAG GCA GAG GTT TTT CTC ACC TTG GGT ATT GTG AGT CTT CTG GAG AAC ATA CTC GTC ATC 180
41 Q A E V F L T L G I V S L L E N I L V I 60
181 TCG GCT GTG GTC AAA AAC AAA AAC CTT CAC TCT CCA ATG TAC TTT TTC CTG TGC AGC CTG 240
61 S A V V K N K N L H S P M Y F F L C S L 80
241 GCT GCT GCG GAC ATG TTG GTA AGT GTA TCG AAC TCT CTG GAG ACC ATT GTC ATT GCA GTA 300
81 A A A D M L V S V S N S L E T I V I A V 100
301 CTA AAC AGT CGC ATT TTG GTG GCC AGT GAT TAT TTT GTA CGT TTG ATG GAC AAT GTG TTT 360
101 L N S R I L V A S D Y F V R L M D N V F 120
361 GAC TCA ATG ATC TGC ATT TCT CTT GTG GCG TCC ATC TGC AAC CTT CTG GCC ATT GCC GTC 420
121 D S M I C I S L V A S I C N L L A I A V 140
421 GAC CGG TAC GTC ACG ATT TTC TAC GCC TTA CGC TAC CAC AGT ATA GTG ACT GTA CGT AGA 480
141 D R Y V T I F Y A L R Y H S I V T V R R 160
481 GCG CTG GTC GCA ATC GCT GCG ATC TGG CTG GTG TGT GTG GTT TGT GGG ATC GTC TTT ATA 540
161 A L V A I A A I W L V C V V C G I V F I 180
541 GTG TAC TCT GAG AGC AAG ACC GTG ATC GTG TGT CTA ATC ACA ATG TTC TTT GCC ATG CTG 600
181 V Y S E S K T V I V C L I T M F F A M L 200
601 GTT CTC ATG GCA ACT CTC TAC GTA CAC ATG TTT CTT CTC GCC AGA CTT CAT GTC CAG AGA 660
201 V L M A T L Y V H M F L L A R L H V Q R 220
661 ATC GCA GCA TTA CCC CCA GCA GCA GCT GCC GCT GGC AAC CCG GCC CCA CGT CGA CAC AGC 720
221 I A A L P P A A A A A G N P A P R R H S 240
721 TGC ATG AAG GGA GCC GTG ACC ATC TCC ATC CTC CTC GGA GTG TTT GTG TGT TGC TGG GCG 780
241 C M K G A V T I S I L L G V F V C C W A 260
781 CCC TTT TTC CTC CAC CTC ATT CTG CTG GTG TCG TGT CCG CAC CAT CCG CTG TGC CTC TGC 840
261 P F F L H L I L L V S C P H H P L C L C 280
841 TAC ATG TCC CAC TTC ACC ACG TAC CTG GTC CTC ATT ATG TGC AAC TCT GTG ATT GAC CCC 900
281 Y M S H F T T Y L V L I M C N S V I D P 300
901 CTC ATC TAC GCC TGC CGC AGC CTG GAA ATG AGG AAG ACT TTT AAG GAG ATA CTC TGC TGT 960
301 L I Y A C R S L E M R K T F K E I L C C 320
961 TTT GGC TGC CAA CCT TCA CTT TAG
321 F G C Q P S L *

B

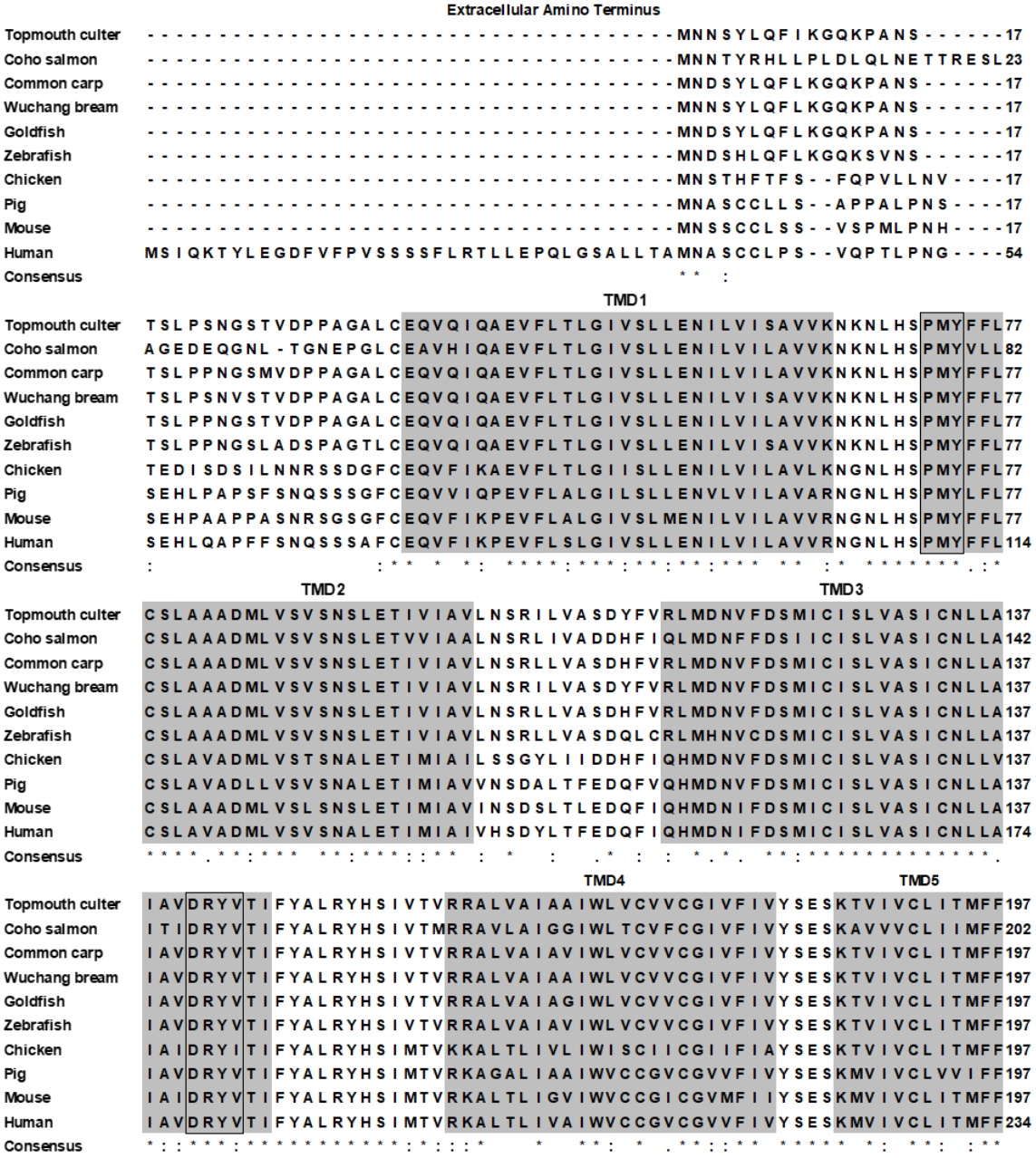
Extracellular Amino Terminus
TMD1
TMD2
TMD3
TMD4
TMD5
Topmouth culter
Coho salmon
Common carp
Wuchang bream
Goldfish
Zebrafish
Chicken
Pig
Mouse
Human
Consensus

B continued

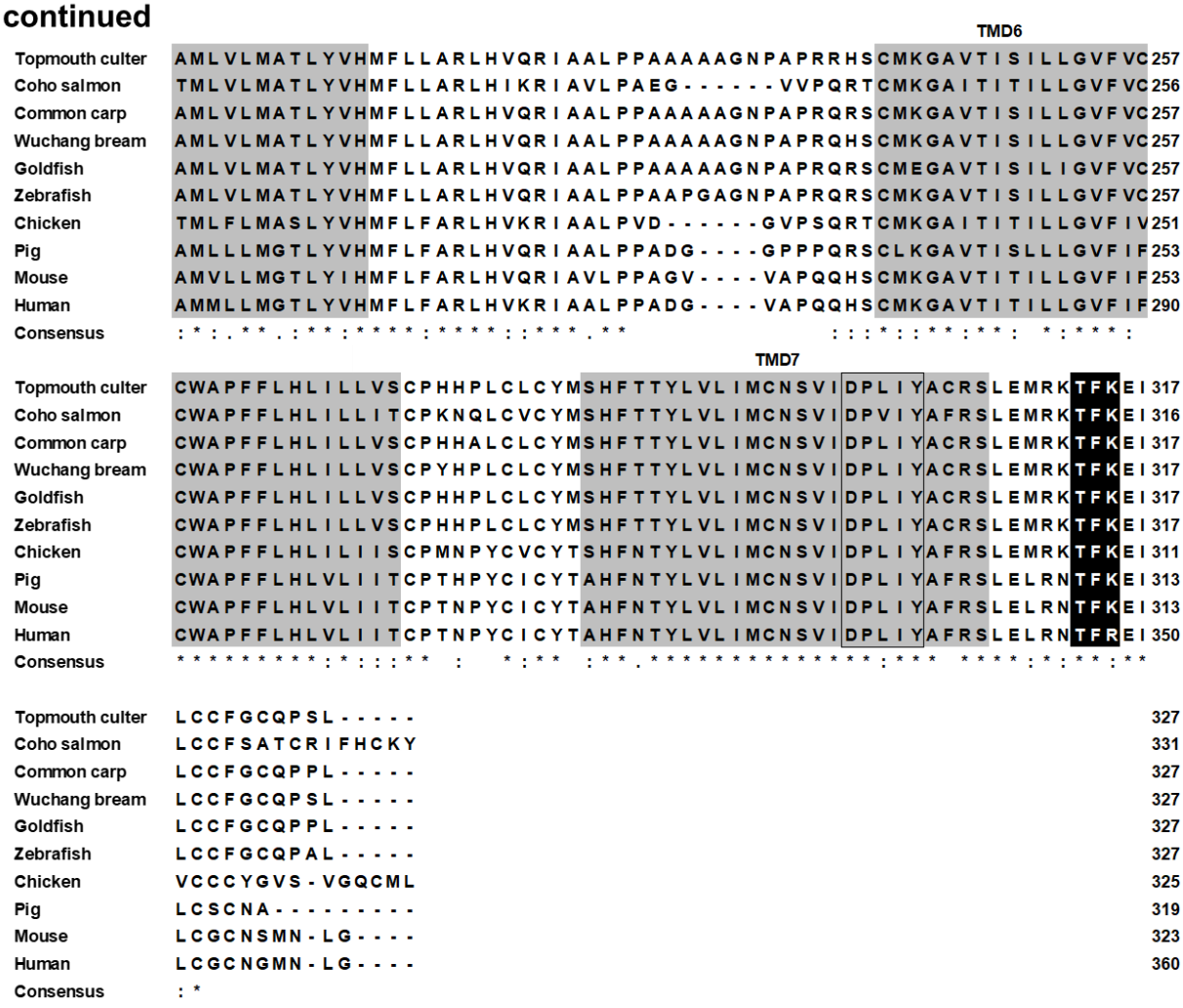
TMD6
TMD7
Topmouth culter AMLVLMATLYVHMFLLARLHVQRIAALPPAAAAAAGNPAPRRHSCMKGAVTISILLGVFVC 257
Coho salmon TMLVLMATLYVHMFLLARLHIKRIAVLPAEG------VVPQRTCMKGAITITILLGVFVC 256
Common carp AMLVLMATLYVHMFLLARLHVQRIAALPPAAAAAAGNPAPRQRSCMKGAVTISILLGVFVC 257
Wuchang bream AMLVLMATLYVHMFLLARLHVQRIAALPPAAAAAAGNPAPRQHSCMKGAVTISILLGVFVC 257
Goldfish AMLVLMATLYVHMFLLARLHVQRIAALPPAAAAAAGNPAPRQRSCMEGAVTISILIGVFVC 257
Zebrafish AMLVLMATLYVHMFLLARLHVQRIAALPPAAPGAGNPAPRQRSCMKGAVTISILLGVFVC 257
Chicken TMLFLMASLYVHMFLFARLHVKRIAALPVD------GVPSQRTCMKGAITITILLGVFIV 251
Pig AMLLLMGTLYVHMFLFARLHVQRIAALPPADG----GPPPQRSCLKGAVTISLLLGVFIF 253
Mouse AMVLLMGTLYIHMFLFARLHVQRIAVLPPAGV----VAPQQHSCMKGAVTITILLGVFIF 253
Human AMMLLMGTLYVHMFLFARLHVKRIAALPPADG----VAPQQHSCMKGAVTITILLGVFIF 290
Consensus :*:.**.:**:****:****::***.** :::*::**:**: *:***:
Topmouth culter CWAPFFLHLILLVSCPHHPLCLCYMSHFTTYLVLIMCNSVIDPLIYACRSLEMRKTFKEI 317
Coho salmon CWAPFFLHLILLITCPKNQLCVCYMSHFTTYLVLIMCNSVIDPVIYAFRSLEMRKTFKEI 316
Common carp CWAPFFLHLILLVSCPHHALCLCYMSHFTTYLVLIMCNSVIDPLIYACRSLEMRKTFKEI 317
Wuchang bream CWAPFFLHLILLVSCPYHPLCLCYMSHFTTYLVLIMCNSVIDPLIYACRSLEMRKTFKEI 317
Goldfish CWAPFFLHLILLVSCPHHPLCLCYMSHFTTYLVLIMCNSVIDPLIYACRSLEMRKTFKEI 317
Zebrafish CWAPFFLHLILLVSCPHHPLCLCYMSHFTTYLVLIMCNSVIDPLIYACRSLEMRKTFKEI 317
Chicken CWAPFFLHLILIISCPMNPYCVCYTSHFNTYLVLIMCNSVIDPLIYAFRSLEMRKTFKEI 311
Pig CWAPFFLHLVLIITCPTHPYCICYTAHFNTYLVLIMCNSVIDPLIYAFRSLELRNTFKEI 313
Mouse CWAPFFLHLVLIITCPTNPYCICYTAHFNTYLVLIMCNSVIDPLIYAFRSLELRNTFKEI 313
Human CWAPFFLHLVLIITCPTNPYCICYTAHFNTYLVLIMCNSVIDPLIYAFRSLELRNTFREI 350
Consensus *********:*:::** : *:** :**.**************:*** ****:*:**:**
Topmouth culter LCCFGCQPSL----- 327
Coho salmon LCCFSATCRIFHCKY 331
Common carp LCCFGCQPPL----- 327
Wuchang bream LCCFGCQPSL----- 327
Goldfish LCCFGCQPPL----- 327
Zebrafish LCCFGCQPAL----- 327
Chicken VCCCYGVS-VGQCML 325
Pig LCSCNA--------- 319
Mouse LCGCNSMN-LG---- 323
Human LCGCNGMN-LG---- 360
Consensus :*

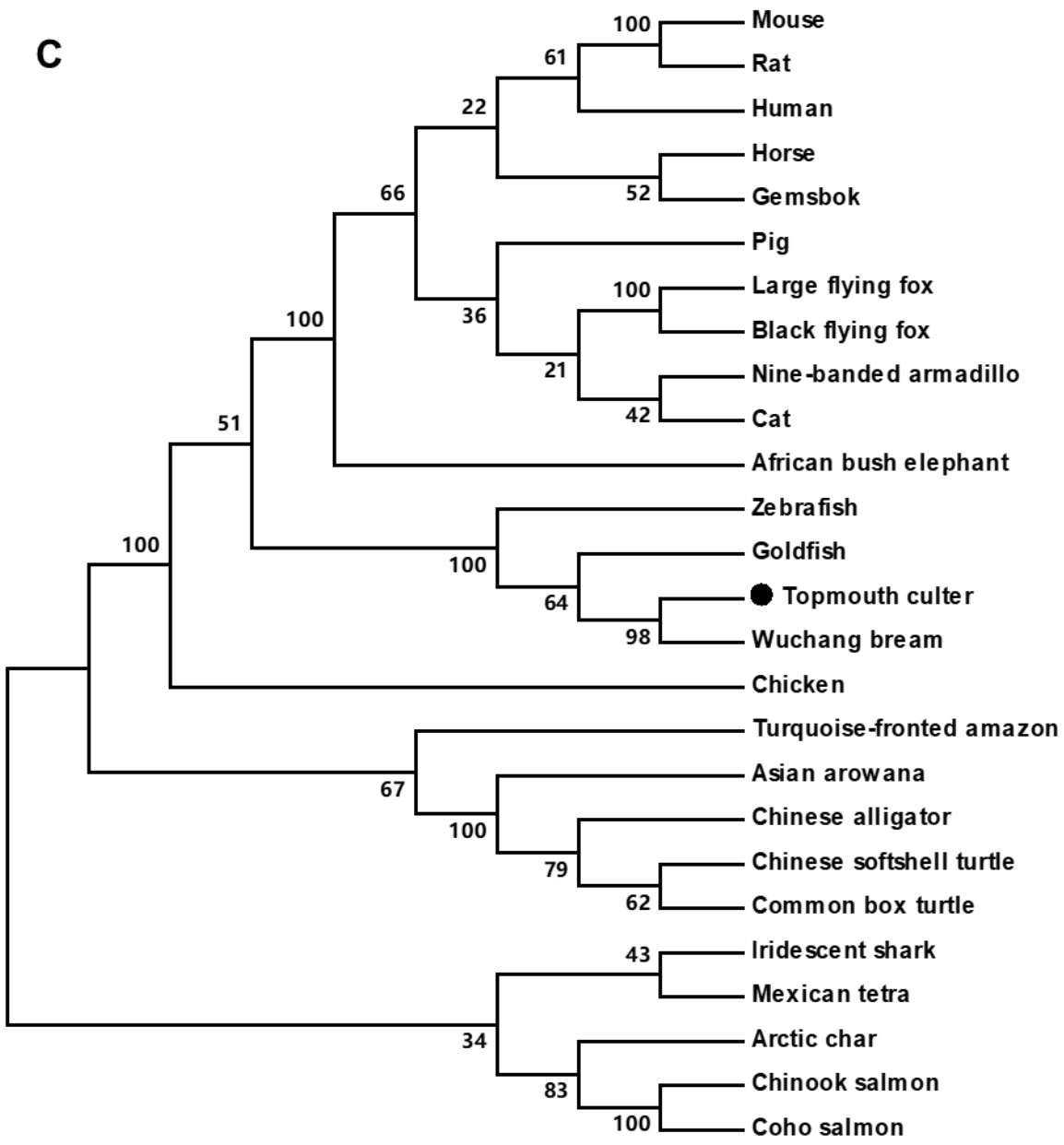

Figure 4.2 Nucleotide and deduced amino acid sequences (A), comparison of amino acid sequences (B), and phylogenetic tree (3) of caMc3r. Positions of nucleotide and amino acid sequences are indicated on both sides. *N*-linked glycosylation sites are present in open boxes. Shaded boxes show putative TMD1-7. Oval frame denotes potential phosphorylation site. The conserved motifs (PMY, DRY and DPxxY) are underlined. Asterisk (*) shows stop codon. The

tree was constructed by the Neighbor-joining (NJ) method. Numbers at nodes indicate the bootstrap value, as percentages, obtained for 1000 replicates. Black dot denote culter Mc3r. MC3Rs: *Culter alburnus* (topmouth culter, MT419813), *Megalobrama amblycephala* (Wuchang bream, AWA81517.1), *Carassius auratus* (goldfish, BAJ83473.1), *Danio rerio* (zebrafish, AAO24744.1), *Oncorhynchus kisutch* (coho salmon, XP_020360426.1), *Homo sapiens* (human, NP_063941.3), *Mus musculus* (mouse, AAI03670.1), *Gallus gallus* (chicken, XP_004947293.1), *Sus scrofa* (pig, AFK25142.1), *Rattus norvegicus* (rat, NP_001020441.3), *Equus caballus* (horse, NP_001243901.1), *Pangasianodon hypophthalmus* (iridescent shark, XP_026770221.1), *Astyanax mexicanus* (Mexican tetra, XP_007231215.1), *Oryx gazella* (gemsbok, AFH58734.1), *Pteropus vampyrus* (large flying fox, XP_011368476.1), *Pteropus alecto* (black flying fox, XP_006921991.1), *Dasypus novemcinctus* (nine-banded armadillo, XP_004447768.1), *Felis catus* (cat, XP_023106851.1), *Loxodonta africana* (African bush elephant, XP_003419952.1), *Oncorhynchus tshawytscha* (chinook salmon, XP_024229914.1), *Salvelinus alpinus* (Arctic char, XP_023994975.1), *Amazona aestiva* (turquoise-fronted amazon, KQL61336.1), *Scleropages formosus* (Asian arowana, XP_018615783.1), *Pelodiscus sinensis* (Chinese softshell turtle, XP_006129463.1), *Terrapene carolina triunguis* (common box turtle, XP_024059166.1), and *Alligator sinensis* (Chinese alligator, XP_006018246.1).

A

```
1   ATG CCG AGG TTC CAG TTT TTA AAC AGT ACT AGT ATG CCA AAT CAT AAT TAT GAA TGG AGC  60
1     M   P   R   F   Q   F   L   N   S   T   S   M   P   N   H   N   Y   E   W   S  20
61  TAC GAA TAC TAC GAC GAC GAA GAG CCC GTG TCT TTT GAA GGA CTC AAA GCA CAT CGA TAT 120
21    Y   E   Y   Y   D   D   E   E   P   V   S   F   E   G   L   K   A   H   R   Y  40
121 TCC ATT GTG ATT GGC TTC TGG GTG GGT CTT GCA GTT TTT GTC ATA TTT ATG TTT TTT GTT 180
41    S   I   V   I   G   F   W   V   G   L   A   V   F   V   I   F   M   F   F   V  60
181 CTG ACT CTT CTG ACC AAA ACA GGA GCC CCA CAC CCA GAG GCC GCG GAG CCT TAC GAG AAA 240
61    L   T   L   L   T   K   T   G   A   P   H   P   E   A   A   E   P   Y   E   K  80
241 CGG ATG CGT CTC ACC AGC TGC GCC GAG GGT CTG GGG CGC CAA CGT GAG GCG GAC ACC CGA 300
81    R   M   R   L   T   S   C   A   E   G   L   G   R   Q   R   E   A   D   T   R 100
301 ACG GGT CTC TCC CGC CCA TTG CTG GAG GAG TCC CGG TCT CTT TTT CAC TGT TAT ATT AAT 360
101   T   G   L   S   R   P   L   L   E   E   S   R   S   L   F   H   C   Y   I   N 120
361 GAA GAA GAG CGA GAT GGA GGC CGG GTA ACG AGC AAC GCT GGC GGT GCC GCC CAC GGA CGT 420
121   E   E   E   R   D   G   G   R   V   T   S   N   A   G   G   A   A   H   G   R 140
421 ACG GGC AGC GGC AAC TCA AGA GAA CAG GTG GAA GCG GTC GGC CTT GTC GTC CAA AGC ATG 480
141   T   G   S   G   N   S   R   E   Q   V   E   A   V   G   L   V   V   Q   S   M 160
481 GGT ATG GAG ACC AGG GAG GAA CGA GAG GCG GCG CTC CTG GTG CAT TTC AAT ATC CCC AAC 540
161   G   M   E   T   R   E   E   R   E   A   A   L   L   V   H   F   N   I   P   N 180
541 TTT GTG AAC TCA GAA TTG AGC TCC GCA CTT GGA GAC GAA GAT TTA CTA TTG GGC GAT CCA 600
181   F   V   N   S   E   L   S   S   A   L   G   D   E   D   L   L   L   G   D   P 200
601 CCG ATC ATA ATG GAG GAG GCC CGT CCG CGC TGC ACC CAT CAC ATC ATT GAC TAA         654
201   P   I   I   M   E   E   A   R   P   R   C   T   H   H   I   I   D   *       217
```

B

```
1   ATG ACT GAA TAT TCA AAC CAC AGT CAG TCC GCT GGA GAT TAT GAG TGG CAT TAT GAA TAC  60
1     M   T   E   Y   S   N   H   S   Q   S   A   G   D   Y   E   W   H   Y   E   Y  20
61  TAT GAT GAC GAG GAG CCC GTG TCC TTC GAG GGA CTG AGA GCA AAC AGA TAC TCT ATC GTG 120
21    Y   D   D   E   E   P   V   S   F   E   G   L   R   A   N   R   Y   S   I   V  40
121 ATT GGT TTC TGG GTC GGA CTG GCT GTG TTC GTC ATC TTT ATG TTC TTT GTT TTG ACC CTG 180
41    I   G   F   W   V   G   L   A   V   F   V   I   F   M   F   F   V   L   T   L  60
181 ATT ACT AAA ACT GGA GCT CCA CAT CCA GAG ATC CCT GAC CCG AGA GAA AAG CAT CAT GGT 240
61    I   T   K   T   G   A   P   H   P   E   I   P   D   P   R   E   K   H   H   G  80
241 CTA GGT GAC TGT GTG CTG GAG GTC GGC GGC TCT CAG GCC TTT TCT CTC CCG CCG CTG CCG 300
81    L   G   D   C   V   L   E   V   G   G   S   Q   A   F   S   L   P   P   L   P 100
301 GAT GAA TCA CGT TCC CTC TTT CAC TTC TAC ATC CAC GAG GAG GAA CAA GCC AAA GCC GAC 360
101   D   E   S   R   S   L   F   H   F   Y   I   H   E   E   E   Q   A   K   A   D 120
361 AGA GAT GCT GTG ATT GGC AGA GGG AGG CGT TGT GGG CGG GCC TCT GCT GGA CTC CGC CTC 420
121   R   D   A   V   I   G   R   G   R   R   C   G   R   A   S   A   G   L   R   L 140
421 CAG GGG ACG ACA GAC GAA GAC GAG CAC TTC CTG TCC AAC TTC AAC ATT CCA AAC TTT GTG 480
141   Q   G   T   T   D   E   D   E   H   F   L   S   N   F   N   I   P   N   F   V 160
481 AAC TCT GAG CAG AGC TCC AGC GTC GAC GAC TTA CTG CTG TGT GAG CCG CCA ATC ATC ACA 540
161   N   S   E   Q   S   S   S   V   D   D   L   L   L   C   E   P   P   I   I   T 180
541 GGC AGC CAA TCA CCT GTG CCG AAG AGC TTA GAG CCC GCC CAC CCT TCT TAT GAT GTC ATC 600
181   G   S   Q   S   P   V   P   K   S   L   E   P   A   H   P   S   Y   D   V   I 200
601 CAG TAT TAA                                                                   609
201   Q   Y   *                                                                   202
```

C

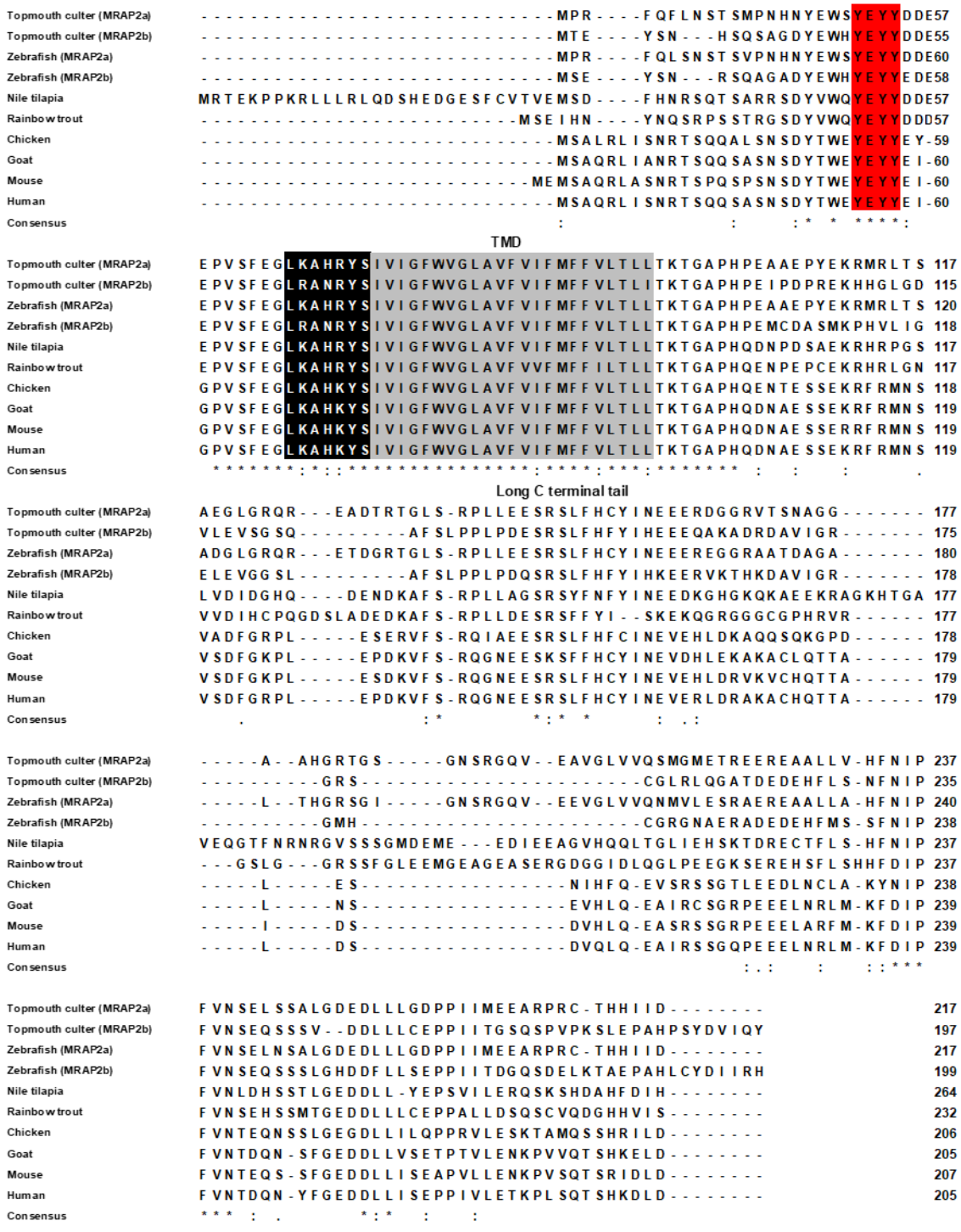
Topmouth culter (MRAP2a)
Topmouth culter (MRAP2b)
Zebrafish (MRAP2a)
Zebrafish (MRAP2b)
Nile tilapia
Rainbow trout
Chicken
Goat
Mouse
Human
Consensus
TMD
Long C terminal tail

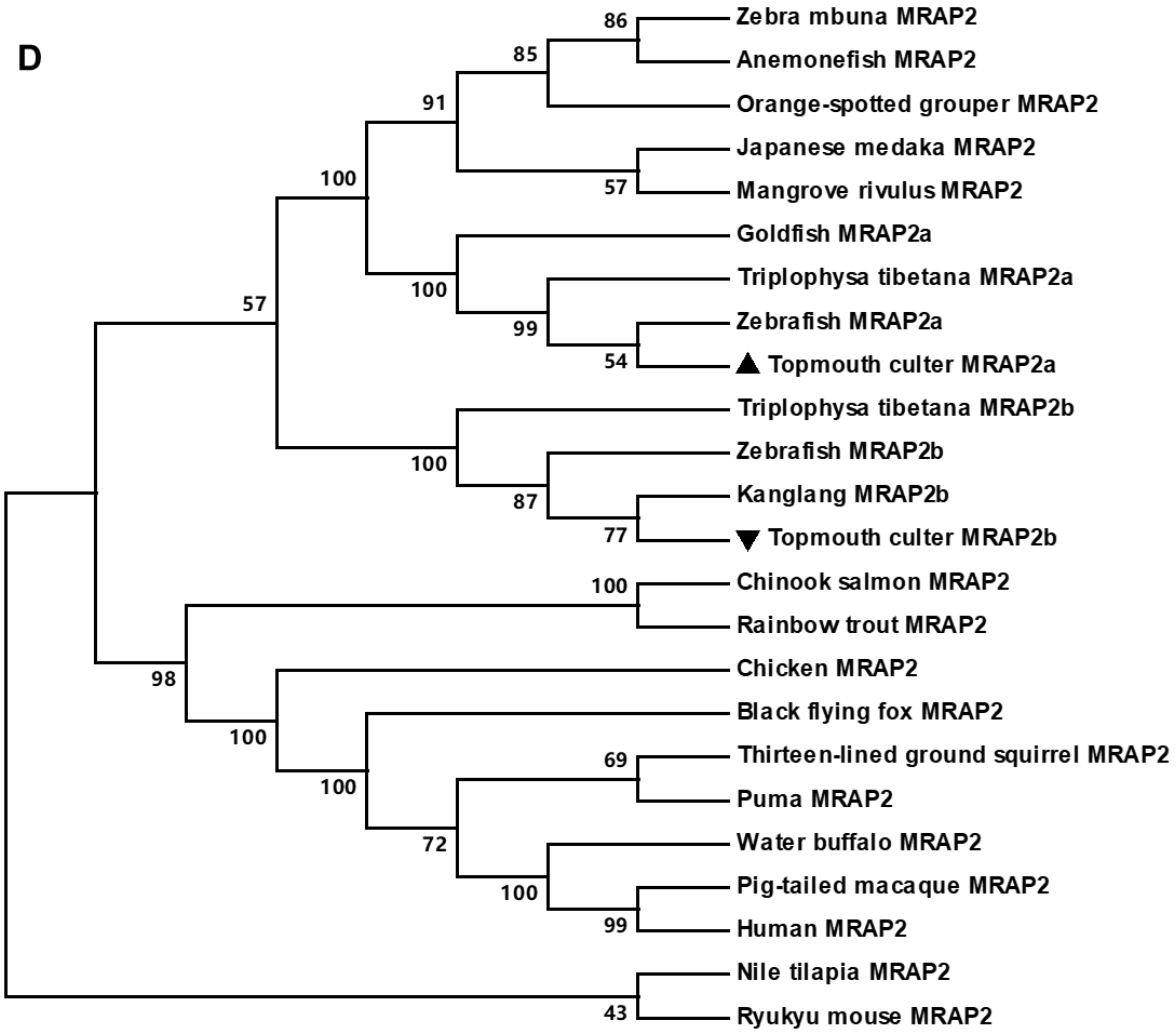

Figure 4.3 Nucleotide and deduced amino acid sequences of Mrap2a (A) and Mrap2b (B), and comparison of amino acid sequences (C) and phylogenetic tree (D) of MRAP2. Positions of nucleotide and amino acid sequences are indicated on both sides. *N*-linked glycosylation sites are present in open boxes. Red box denotes YEYY motif. Black box is LKANKYL motif. Shaded box shows putative TMD. Asterisk (*) shows stop codon. Nucleotide and deduced amino acid sequences and phylogenetic tree of caMrap2a and caMrap2b. A. Nucleotide and deduced amino acid sequences of caMrap2a. B. Nucleotide and deduced amino acid sequences of caMrap2b. Positions of nucleotide and amino acid sequences are indicated on both sides. Amino acids in shaded box indicate putative transmembrane domain. Open box

shows putative N-linked glycosylation sites. Initiation and stop codons are underlined. Asterisk (*) denotes stop codon. C. Phylogenetic tree of MRAP2. The tree was constructed using the neighbor-joining (NJ) method. Numbers at nodes indicate the bootstrap value, as percentages, obtained for 1000 replicates. Black dot and open boxes show caMrap2a and caMrap2b and outgroup, respectively. MRAP2s: *Culter alburnus* (topmouth culter, MRAP2a: MT163516, and MRAP2b: MT163517), *Epinephelus coioides* (orange-spotted grouper, QED39647.1), *Danio rerio* (zebrafish, MRAP2a: F8W4H9.1 and MRAP2b: F8W4H9.1), *Oreochromis niloticus* (Nile tilapia, XP_003458293.2), *Oryzias latipes* (Japanese medaka, XP_023809099.1), *Kryptolebias marmoratus* (mangrove rivulus, XP_017267334.1), *Maylandia zebra* (zebra mbuna, XP_004568825.1), *Oncorhynchus tshawytscha* (Chinook salmon, XP_024278413.1), *Amphiprion ocellaris* (anemonefish, XP_023122806.1), *Oncorhynchus mykiss* (rainbow trout, XP_021467183.1), *Gallus gallus* (chicken, ALO81626.1), *Ictidomys tridecemlineatus* (thirteen-lined ground squirrel, XP_021581743.1), *Mus caroli* (Ryukyu mouse, XP_021029091.1), *Puma concolor* (puma, XP_025781535.1), *Homo sapiens* (human, AAH10003.2), *Bubalus bubalis* (water buffalo, XP_006054803.2), *Pteropus alecto* (black flying fox, XP_006926405.1), *Macaca nemestrina* (pig-tailed macaque, XP_011764298.1), *Triplophysa tibetana* (MRAP2a: KAA0703529.1 and MRAP2b: KAA0720858.1), *Anabarilius grahami* (Kanglang fish, MRAP2b ROJ29330.1), *Carassius auratus* (goldfish, MRAP2a: XP_026139519).

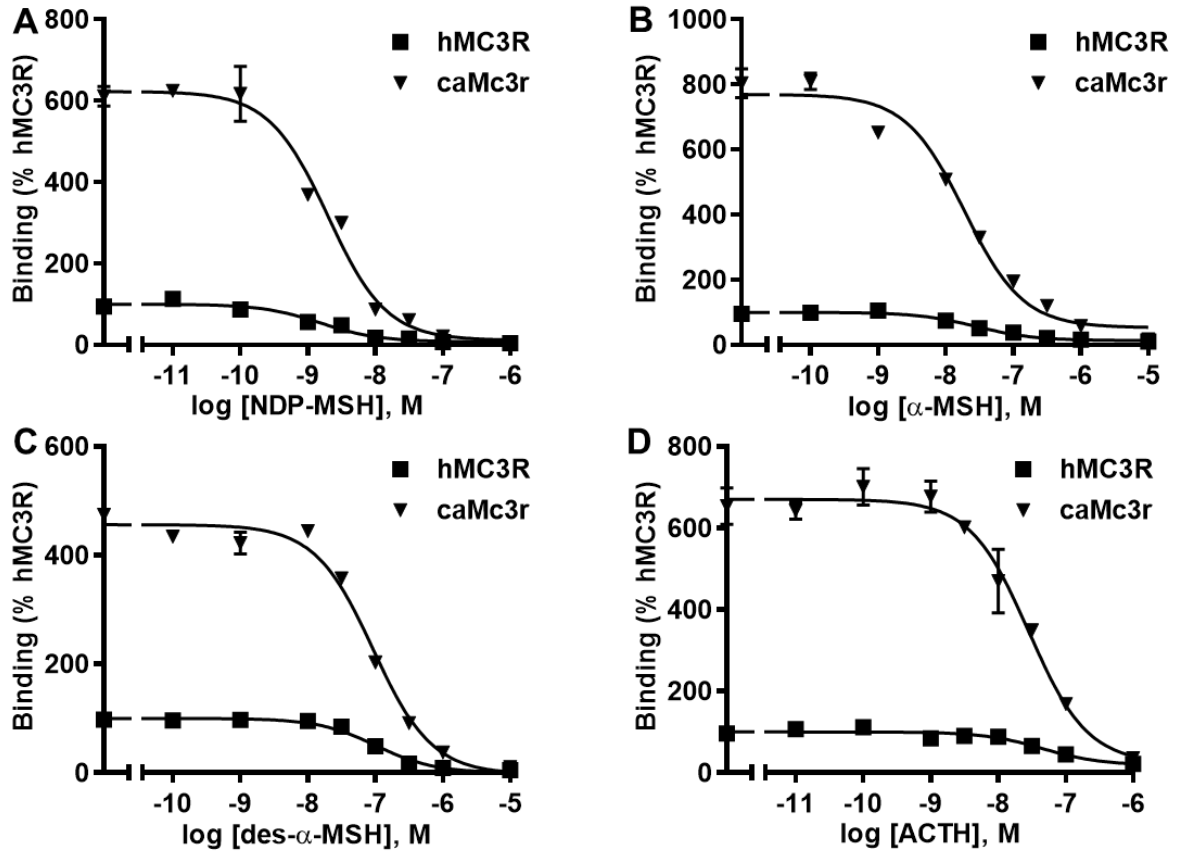

Figure 4.4 Ligand binding properties of caMc3r. Different concentrations of unlabeled NDP-MSH (A), α-MSH (B), des-α-MSH (C), and ACTH (1-24) (D) were used to displace the binding of ^{125}I-NDP-MSH. Results are expressed as % of hMC3R binding ± range from duplicate determinations within one experiment. All experiments were repeated at least three independent times.

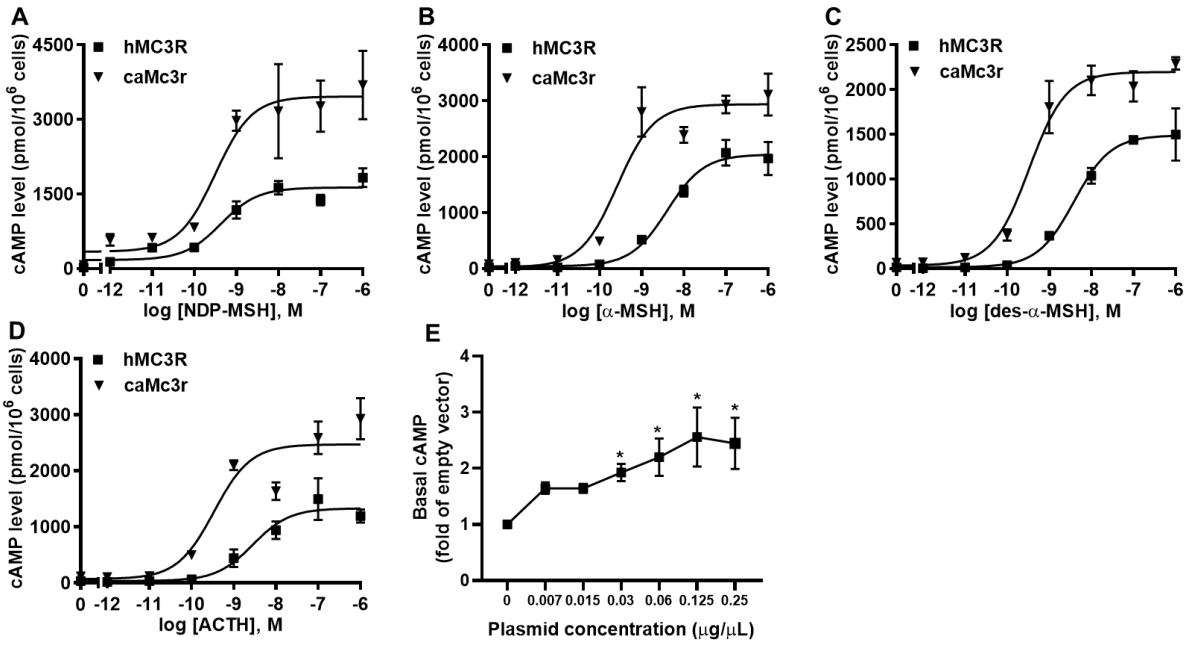

Figure 4.5. Signaling properties of caMc3r. HEK293T cells were transiently transfected with hMC3R or caMc3r plasmids. Different concentrations of NDP-MSH (A), α-MSH (B), des-α-MSH (C), and ACTH (1-24) (D) were used to stimulate the cells. (E) Constitutive activities of caMc3r in cAMP pathway. Increasing concentrations of caMc3r plasmid were transfected into HEK293T cells. Cells transfected with empty pcDNA3.1 vector were used as the control group. Data are mean ± SEM from triplicate measurements within one experiment. All experiments were performed at least three times independently.

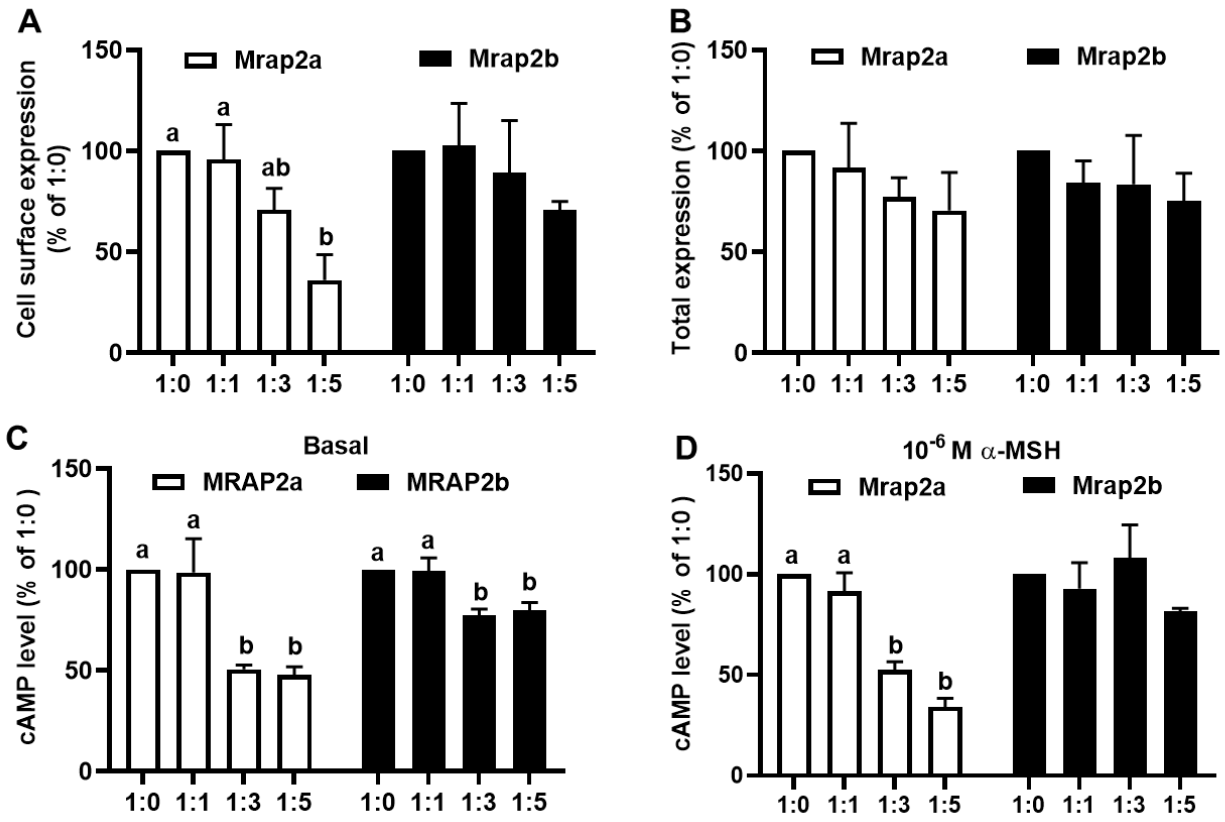

Figure 4.6 Regulation of caMc3r expression and signaling by caMrap2s. Cell surface expression (A) and total expression (B) of caMc3r modulated by caMrap2a or caMrap2b were measured by flow cytometry. Basal (C) and maximal signaling (D) of caMc3r regulated by MRAP2a or MRAP2b were determined by RIA. HEK293T cells were co-transfected with different ratios of caMc3r/caMrap2a or caMc3r/caMrap2b (1:0, 1:1, 1:3, and 1:5). The empty vector pcDNA3.1 fluorescence is used for background staining. The results are calculated as % of 1:0 group. Each data point represented as the mean ± SEM (n = 3 - 4). Different letters indicate significant difference ($P < 0.05$) (One-way ANOVA followed by Tukey test).

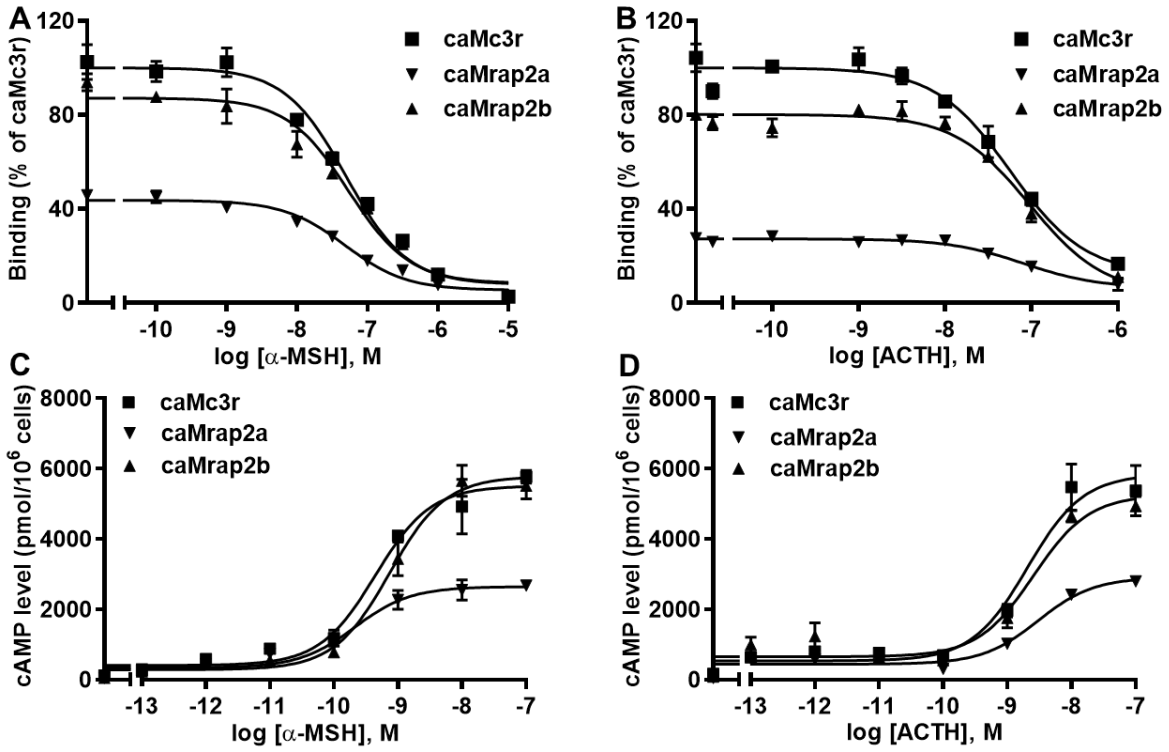

Figure 4.7 Modulation of caMc3r pharmacology by caMrap2s. Ligand binding (A, B) and signaling (C, D) properties of caMc3r to α-MSH or ACTH (1-24) upon co-expression of caMc3r with caMrap2a or caMrap2b were measured. HEK293T cells were co-transfected with caMc3r/caMrap2a or caMc3r/caMrap2b in two different ratios (1:0 and 1:5). Results of binding properties were calculated as % of hMC3R binding ± range from duplicate determinations within one experiment. All experiments were measured at least three independent experiments.

Chapter 5: Regulation of melanocortin-4 receptor pharmacology by two isoforms of melanocortin receptor accessory protein 2 in topmouth culter (*Culter alburnus*)

5.1 Introduction

The melanocortins are derived from tissue-specific post-translational processing of proopiomelanocortin (POMC), including α-, β-, γ-melanocyte-stimulating hormones (α-, β-, γ-MSH) and adrenocorticotropic hormone (ACTH) [17, 18]. The physiological functions of these peptides are exerted by five melanocortin receptors (MC1R-MC5R), members of rhodopsin-like Family A G-protein-coupled receptors (GPCRs), including regulation of pigmentation, adrenal steroidogenesis, energy homeostasis, lipolysis, stress, cardiovascular and sexual function [240-242]. MC4R is highly expressed in the central nervous system and involved in regulating energy homeostasis via modulating both food intake and energy expenditure; it is also involved in regulating sexual function and reproduction by affecting the secretion of reproductive hormones (reviewed in [24, 32]). Targeted deletion of *Mc4r* increases food intake and decreases energy expenditure, resulting in obesity in mice [25, 26]. *MC4R* mutation is the leading cause of human monogenic obesity [127] (reviewed in [30, 131]).

The MC4R is primarily coupled to the stimulatory heterotrimeric G protein (Gs). MC4R activation leads to stimulation of adenylyl cyclase activity, which will increase the level of the second messenger cyclic adenosine monophosphate (cAMP) to trigger downstream signaling [20]. MC4R also phosphorylates extracellular signal-regulated kinase 1 and 2 (ERK1/2) [157, 158, 222, 253].

Melanocortin receptor accessory proteins (MRAPs, including MRAP1 and MRAP2), small single transmembrane domain proteins, are identified as receptor-specific molecular chaperones, regulating MC2R trafficking, ligand binding and cAMP generation [44, 46, 47, 55]. MRAP2 is involved in modulating energy homeostasis due to its high expression in central nervous system. MRAP2 deceases agonist-stimulated signaling but does not affect basal signaling of human (h) MC4R [47], while MRAP2 in mice decreases the basal activity and increases maximal response (R_{max}) [50]. *MRAP2* mutations were shown to be potentially pathogenic for early-onset obesity [50, 254]. Mice with whole body and brain-specific deletion of *Mrap2* also have early-onset severe obesity [50]. These results suggest that MRAP2 is involved in regulating MC4R signaling and body weight in mammals.

Mc4r has also been characterized in teleosts [55, 114-118, 132, 148, 209, 255], and shown to act as a regulator in energy balance, sexual behavior, and reproduction [137, 139, 140, 143, 144]. Non-mammalian MRAPs are different from those of mammals. Some fishes only have *mrap2*, lacking *mrap1* [197, 256], and some have two *mrap2* genes (*mrap2a* and *mrap2b*) [55, 207]. In zebrafish, two Mrap2s have different expression patterns at different stages, with Mrap2a expressed from embryos to adults, stimulating growth by blocking Mc4r action in larvae, and Mrap2b mainly expressed in adults, enhancing Mc4r response [55]. In vitro, Mrap2a decreases the Mc4r affinity for α-MSH, but Mrap2b increases ligand sensitivity of zebrafish Mc4r [55]. Hence, a better understanding of the vital functions of MC4R in modulating energy homeostasis and reproductive function and the interaction between Mrap2 and Mc4r is important for feeding and artificial breeding of economical species.

The topmouth culter (*Culter alburnus*), which belongs to Cyprinidae, Cultrinae, Erythroculter, is an economically important freshwater fish widely distributed in large rivers, reservoirs, and lakes in China [248, 249, 257, 258]. With excellent taste, rapid growth, and strong performance in culture, this fish has been extensively cultured over the past few decades due to high market demand [259]. In this study, we cloned culter *mc4r*. We then studied the pharmacological properties of caMc4r and the effects of Mrap2a and Mrap2b on caMc4r.

5.2 Materials and methods

5.2.1 Ligands and plasmids

NDP-MSH was purchased from Peptides International (Louisville, KY, USA), human α- and β-MSHs from Pi Proteomics (Huntsville, AL, USA), and ACTH (1-24) from Phoenix Pharmaceuticals (Burlingame, CA, USA), and THIQ (N-[(3R)-1,2,3,4-Tetrahydroisoquinolinium-3-ylcarbonyl]-(1R)-1-(4-chlorobenzyl)-2-[4-cyclohexyl-4-(1H-1,2,4-triazol-1-ylmethyl)piperidin-1-yl]-2-oxoethylamine) [260] from Tocris Bioscience (Ellisville, MO, USA). We analyzed culter Pomc from culter genome, found that culter α-Msh, Acth (1-24) and β-Msh were conserved with human α-MSH (100%), ACTH (1-24) (87.5%) and β-MSH (57.1%), respectively. [^{125}I]-NDP-MSH and [^{125}I]-cAMP were iodinated using chloramine T method [221, 222]. The N-terminal c-myc-tagged wild-type hMC4R was subcloned into pcDNA3.1 vector as previously described [223]. N-terminal c-myc-tagged caMC4R, N-terminal flag-tagged caMRAP2a, and N-terminal flag-tagged caMRAP2b were synthesized and subcloned into pcDNA3.1 vector by GenScript (Piscataway, NJ, USA) to obtain the plasmids.

5.2.2Gene cloning and sequence alignment

Gene sequences were provided by our collaborator: Dr. Min Tao from Hunan Normal University, Hunan, China.

5.2.3 Cell culture and transfection

Human Embryonic Kidney (HEK) 293 T cells (ATCC, Manassas, VA, USA) were cultured at an incubator (37 °C in a 5% CO_2-humidified atmosphere). The medium contained Dulbecco's Modified Eagle's medium (DMEM) (Invitrogen, Carlsbad, CA, USA) 10% newborn calf serum, 10 mM HEPES, 50 μg/mL of gentamicin, 0.25 μg/mL of amphotericin B, 100 μg/mL of streptomycin and 100 IU/mL of penicillin. Cells were plated into 24-wells or 6-wells plates (Corning, NY, USA) pre-coated with 0.1% gelatin. At approximately 60-70% confluence, cells were transfected with plasmids by calcium phosphate precipitation method [224]. The total DNA was normalize using empty vector pcDNA3.1 in each well.

5.2.4 Flow cytometry assay

The influence of caMrap2a or caMrap2b on the cell surface and total expression levels of caMc4r was studied using flow cytometry as described earlier [118]. Cells were plated into 6-well plates and transfected with caMC4R (N-terminal c-myc tag) and caMRAP2a or caMRAP2b plasmids in four ratios (1:0, 1:1, 1:3, and 1:5). The C6 Accuri Cytometer (Accuri Cytometers, Ann Arbor, MI, USA) was used for analysis. The empty vector (pcDNA3.1) fluorescence was used for background staining. The expression of the caMc4r was calculated as the percentage of

1:0 (caMc4r/caMrap2a or caMc4r/caMrap2b) group was set as 100%. The other groups were calculated as % of the 1:0 group [225].

5.2.5 Ligand binding assays

Binding assay was used to study the binding properties of caMc4r to different ligands as described previously [57, 223]. Culter MC4R or hMC4R plasmid (0.25 μg/μL) were transfected into cells (6-well plate). The ligands and final concentration were: NDP-MSH (from 10^{-11} to 10^{-6} M), α-MSH (from 10^{-10} to 10^{-5} M), β-MSH (from 10^{-10} to 10^{-5} M), ACTH (1-24) (from 10^{-10} to 10^{-5} M) or THIQ (from 10^{-11} to 10^{-6} M). To study the effect of caMrap2a or caMrap2b on the binding property of caMc4r, caMC4R (0.25 μg/μL) with caMRAP2a or caMRAP2b in two ratios (1:0 and 1:5) were transfected into cells (6-well plate), and two ligands, α-MSH (from 10^{-10} to 10^{-5} M) and ACTH (1-24) (from 10^{-10} to 10^{-5} M) were used.

5.2.6 cAMP assays

Intracellular cAMP was tested as described previously [221, 223]. The final concentration of ligands used were NDP-MSH (from 10^{-11} to 10^{-6} M), α-MSH (from 10^{-10} to 10^{-5} M), β-MSH (from 10^{-10} to 10^{-5} M), ACTH (1-24) (from 10^{-10} to 10^{-5} M), or THIQ (from 10^{-10} to 10^{-5} M).

To study the potential effect of caMrap2a and caMrap2b on caMc4r signaling, caMC4R (0.25 μg/μL) and caMRAP2a or caMRAP2b plasmids in two ratios (1:0 and 1:5) were co-transfected into cells (24-well plate), and two ligands, α-MSH (from 10^{-10} to 10^{-5} M) and ACTH (1-24) (from 10^{-10} to 10^{-5} M) were used.

To study the dose-dependent effect of caMrap2a or caMrap2b on the R_{max} of cAMP levels of caMc4r to α-MSH stimulation, caMC4R (0.25 μg/μL) and caMRAP2a or caMRAP2b plasmids in four ratios (1:0, 1:1, 1:3 and 1:5) were co-transfected into cells (24-well plate).

To explore the constitutive activity of Gs-cAMP, cells were transfected with caMC4R plasmid in different concentrations (0, 0.007, 0.015, 0.030, 0.060, 0.125, and 0.250 μg/μL) (6-well plate).

5.2.7 Erk1/2 phosphorylation assay

To explore the constitutive pErk1/2 level, cells were transfected with caMC4R plasmid in different concentrations (0, 0.007, 0.015, 0.030, 0.060, 0.125, and 0.250 μg/μL). The phosphorylated Erk1/2 levels were detected as described previously [222, 253]. Rabbit anti-pErk1/2 antibody (Cell Signaling, Beverly, MA) and mouse anti-β-tubulin antibody (Developmental Studies Hybridoma Bank, University of Iowa, Iowa City, IA) were used in this study. ImageJ 1.44 software (National Institute of Health, Bethesda, MD) were used to quantify the films. The pErk1/2 levels were normalized as a ratio of pErk1/2 over β-tubulin in the same gel.

5.2.8 Statistical analysis

All data were shown as mean ± SEM. GraphPad Prism 8.3 software (San Diego, CA, USA) was used to calculate parameters including maximal binding (B_{max}), IC_{50}, maximal response (R_{max}), basal activity and EC_{50}. The significance of differences in ligand binding and signaling between caMc4r and hMC4R were determined by Student's *t-test*. Ligand binding, cAMP, flow

cytometry parameters of caMc4r regulated by Mrap2s and ERK1/2 signaling were analyzed the significance of differences by one-way ANOVA. Statistical significance was analyzed using GraphPad Prism 8.3 software.

5.3 Results

5.3.1 Nucleotide and deduced amino acid sequences of caMc4r

The cloned topmouth culter *mc4r* had 981 bp open reading frame (ORF) that encoded a pupative protein of 326 amino acids and 36.57 kDa molecular mass (**Figure 5.1A**). The culter Mc4r had seven putative hydrophobic transmembrane domains (TMDs) with an extracellular amino terminus, extracellular loops (ECLs), intracellular loops (ICLs), and an intracellular carboxyl terminus (**Figures 5.1A** and **B**). The deduced amino acid sequence in the TMDs of caMc4r was significantly conserved with these of other species. The PMY, DRY, and DPxxY motifs were predicted at homologous positions with MC4Rs of other species (**Figure 5.1B**). Two potential *N*-linked glycosylation site (Asn^{2} and Asn^{15}) in N-terminus, 15 cysteine residues and consensus sequence for protein kinase C phosphorylation ($Thr^{310}Phe^{311}Lys^{312}$) in C-terminus were observed in the caMc4r amino acid sequence (**Figure 5.1B**). By multiple sequence alignment analysis, we found that caMc4r shared high identities with other piscine MC4Rs, with 99% homology to grass carp, 99% to zebrafish, 87% to flounder, 88% to fugu, and 88% to sea bass, as well as to mammalian MC4Rs with 81% to human, 81% to mouse, and 82% to pig. Phylogenetic tree between caMc4r and other MC4Rs revealed that caMc4r was localized in a clade of grass carp and zebrafish (**Figure 5.1C**).

5.3.2 Ligand binding properties of caMc4r

A comparative ligand binding assay was performed to investigate the binding properties of caMc4r using hMC4R for comparison. Different concentrations of five unlabeled agonists (NDP-MSH, α-MSH, β-MSH, ACTH (1-24), and THIQ) were used as competitors with a fixed amount of ^{125}I-NDP-MSH. The maximal binding values (B_{max}) of caMc4r was 34.49 ± 3.43% of that of the hMC4R (**Figure 5.2** and **Table 5.1**). Similar as the binding affinity order of hMC4R, caMc4r bound to superpotent agonist NDP-MSH with the highest affinity (IC_{50}, 4.87 ± 1.80 nM), followed by ACTH (1-24) (123.03 ± 31.15 nM), α-MSH (126.33 ± 8.95 nM), and β-MSH (442.00 ± 65.43 nM) (**Table 5.1**). Culter Mc4r had a significantly higher affinity to β-MSH than hMC4R. THIQ was able to displace the ^{125}I-NDP-MSH bound with caMc4r, although it had a lower affinity (1260.33 ± 272.61 nM) compared with that for hMC4R (**Figure 5.2** and **Table 5.1**).

5.3.3 Signaling properties of caMc4r

All agonists (NDP-MSH, α-MSH, β-MSH, ACTH (1-24) and THIQ) were able to stimulate caMc4r and dose-dependently increased the level of intracellular cAMP (**Figure 5.3** and **Table 5.2**). Similar maximal responses (R_{max}) and EC_{50}s to NDP-MSH, α-MSH, β-MSH, and ACTH (1-24) stimulation were observed between caMc4r and hMC4R. However, EC_{50} was significantly increased and R_{max} was significantly decreased when stimulated by THIQ (**Figure 5.3** and **Table 5.2**).

In this study, we found that the basal signaling of caMc4r was 4.08 times that of hMC4R (**Table 5.2**), indicating that caMc4r might be constitutively active. Different concentrations of caMC4R plasmid were transfected into cells and basal intracellular cAMP levels measured. We

found that a low amount of caMC4R plasmid (0.007 μg/μL) transfected resulted in high-level cAMP production (**Figure 5.4A**). Similar results were found in basal Erk1/2 phosphorylation, starting with a transfection of 0.015 μg/μL caMC4R that significantly increased basal pErk1/2 level (**Figures 5.4A** and **B**). Therefore, our data indicated that caMc4r could be constitutively active in both cAMP and Erk1/2 pathways.

5.3.4 Modulation of caMc4r expression and pharmacology by caMrap2s

The influence of caMrap2a and caMrap2b on the cell surface and total expression levels of caMc4r was performed by flow cytometry (**Figure 5.5**). The results demonstrated that caMrap2a increased the cell surface and total expression of caMc4r, and there were no significant differences among groups (**Figures 5.5A** and **B**). Cuter Mrap2b significantly increased the cell surface and total expression of caMc4r in 1:3 group than that in the 1:0 group (**Figures 5.5C** and **D**).

Competitive ligand binding assays with ACTH (1-24) and α-MSH showed that c caMrap2a significantly increased the B_{max} of caMc4r in the 1:5 group, while caMrap2b did not affect the B_{max} (**Figures 5.6A, B and Table 5.3**). Culter Mrap2a and Mrap2b significantly increased affinity of caMc4r to ACTH (1-24) but did not affect the IC_{50}s of caMc4r to α-MSH (**Table 5.3**).

To study the effect of caMrap2a or caMrap2b on the cAMP signaling of caMc4r, cells were co-transfected with caMC4R/caMRAP2a or caMC4R/caMRAP2b in two different ratios (1:0 and 1:5) and ACTH (1-24) and α-MSH were used as agonists. The results showed that caMrap2a or caMrap2b had no effect on EC_{50}s; caMrap2a significantly decreased the R_{max}, but caMrap2b did not affect the R_{max} (**Figures 5.6C, D and Table 5.4**).

We further investigated the dose-dependent effects of caMrap2a or caMrap2b on basal and maximal signaling to α-MSH stimulation (**Figure 5.7**). Cells were co-transfected with four ratios of caMC4R/caMRAP2a or caMC4R/caMRAP2b (1:0, 1:1, 1:3, and 1:5). We found that the basal cAMP production of caMc4r were dose-dependently decreased by both caMrap2a or caMrap2b (**Figures 5.7A** and **B**). In addition, maximal cAMP levels of caMc4r activated by 10^{-6} M α-MSH were also dose-dependently decreased by caMrap2a in 1:3 and 1:5 groups but not caMrap2b (**Figures 5.7 C** and **D**).

5.4 Discussion

In the present study, we demonstrated that cloned culter *mc4r* was predicted to encode a protein of 326 amino acids with similar structural characteristics as MC4Rs of other species **(Figure 5.1B**), including other teleost Mc4rs [115-118, 148]. Phylogenetic analysis revealed that caMc4r clustered with teleost Mc4rs (**Figure 5.1C**). The tissue expression data showed that *mrap2a*/*mrap2b* and *mc4r* are co-expressed in the central nervous system and in the periphery (data not shown), indicating that caMrap2a or caMrap2b might modulate Mc4r signaling in the central nervous system and in the periphery.

We also explored the pharmacology of the cloned caMc4r with binding and signaling assays. Our results showed that NDP-MSH bound to caMc4r with the highest affinity (IC_{50} of 4.87 nM) and activated caMc4r with the highest potency (EC_{50} was 0.44 nM) (**Tables 5.1 and 2**). Lower binding capacity was observed in caMc4r (about 35% of that of hMC4R) (**Table 5.1**), consistent with previous studies in spotted scat [115], grass carp [116], swamp eel [148], sea bass [118], and orange-spotted grouper [117]. In culter, ACTH had higher affinity and was more efficacious

than α-MSH for caMc4r, consistent with the suggestion that ACTH may be the original ligand for the MCRs [252].

In cAMP signaling assay, α-MSH, β-MSH, and ACTH (1-24) stimulated caMc4r and hMC4R with similar potencies (**Figure 5.3** and **Table 5.2**). THIQ, a small molecule agonist, bound to caMc4r and displaced the ^{125}I-NDP-MSH with a lower affinity (**Table 5.1**), activated caMc4r and initiated cAMP accumulation with an EC_{50} of 75.71 nM (~15-fold higher than that of hMC4R) (**Table 5.2**). These data suggested that THIQ was not an allosteric agonist at caMc4r, different from our previous studies in grass carp and swamp eel [116, 148].

The hMC4R has been shown to have constitutive activity in Gs-cAMP signaling [147], and N-terminus is an important modulator in regulating constitutive activities in hMC4R [146]. Mutations in *MC4R* leading to decreased constitutive activity are associated with obesity pathogenesis [9, 24, 146]. Compared to hMC4R, teleost Mc4rs showed much higher constitutive activity in cAMP signaling [115-118, 148]. Our present study also showed that caMc4r significantly increased basal activities in Gs-cAMP and Erk1/2 signaling (**Figure 5.4**). The potential relevance of constitutive activity in teleost Mc4rs remains to be studied more extensively.

We further investigated whether Mrap2a and Mrap2b could modulate the trafficking, ligand binding and signaling of caMc4r. Culter Mrap2a and Mrap2b both increased the cell surface expression of caMc4r (**Figure 5.5**). In zebrafish, Mrap2b dose-dependently increases the cell surface expression of Mc4r, while Mrap2a has no effect on the cell surface expression of Mc4r [55]. Human MRAP1 and MRAP2 decrease the cell surface expression of MC4R [47]. In

chicken, MRAP1 and MRAP2 have no significant effect the cell surface expression of MC4R [56]. In tilapia, Mrap2 dose-dependently decreases the cell surface expression of Mc4r [209]. Mrap2 also decreases the cell surface expression of Mcra and Mcrb in sea lamprey, which has only two Mcrs [208]. Therefore, the effect of MRAP2 on cell surface and total expression of the MC4R varies in different species. Culter Mrap2a increased the B_{max} of c caMc4r but caMrap2b did not affect the B_{max} (**Table 5.3**). caMrap2a and caMrap2b significantly increased affinity of caMc4r to ACTH (1-24) but did not affect the IC_{50} of caMc4r to α-MSH (**Table 5.3**).

Remarkably, culter Mrap2a and Mrap2b also inhibited the constitutive activity of caMc4r (**Figure 5.7**). Furthermore, caMrap2a significantly decreased the R_{max} (**Table 5.4**), and caMrap2b had no effect on the R_{max}. Mrap2 decreases the constitutive activity and the R_{max} of Mc4r in tilapia and grouper [117, 209]. In zebrafish, Mrap2a suppresses the constitutive activity of Mc4r, reduces the R_{max}, while increases α-MSH potency; Mrap2b suppresses the constitutive activity of Mc4r and increases the R_{max} [55]. In sea lamprey, Mrap2 increases agonist-stimulated signaling of Mcra and Mcrb [208]. In chicken, MRAP1 and MRAP2 decrease the basal activity and increases sensitivity to ACTH [56]. Human MRAP1 and MRAP2 decreases agonist-stimulated cAMP production [47]. Therefore, different effects of MRAPs on MC4R basal and agonist-stimulated signaling are observed in different species.

One shortcoming of this study is that we used human ACTH and β-MSH for the experiments. α-MSH has been shown to be fully conserved in all species with POMC gene studied so far, including culter investigated here. For ACTH (1-24), there were 3 amino acids different between human and culter sequences, but two of these changes were very conservative [60]. Therefore, we deduce that culter Acth (1-24) would likely behave similarly as human

ACTH (1-24) that we used in the experiments. There was only 57% homology between human and culter β-MSHs [60]. Therefore, we need to interpret the data obtained for β-MSH with caution. In future studies, we need to identify the molecular forms of the endogenous MSHs produced and the modifications (for example, acetylated or des-acetylated) and synthesize these peptides for functional characterization experiments.

In summary, we cloned *mc4r* and investigated its pharmacology and regulation by Mrap2a/Mrap2b. Culter Mc4r had high constitutive activities, and similar potencies to several agonists as hMC4R. Culter Mrap2a significantly increased the B_{max} and decreased agonist-stimulated cAMP, whereas caMrap2b increased the cell surface and total expression but did not affect B_{max} and agonist-stimulated cAMP. Therefore, these data suggested that Mrap2a/Mrap2b had differential effects on the expression, binding, and signaling of caMc4r. These findings lay the foundation for future physiological studies on the functions of culter Mc4r that might provide new strategies to improve growth and reproduction in culter culture.

Table 5.1 Ligand binding properties of caMc4r

MC4R	B_{max} %	NDP-MSH	α-MSH	β-MSH	ACTH	THIQ
		IC_{50} (nM)	IC_{50} (nM)	IC_{50} (nM)	IC_{50} (nM)	IC_{50} (nM)
hMC4R	100	14.27 ± 2.98	280.47 ± 95.49	825.87 ± 66.17	61.96 ± 17.57	164.63 ± 30.15
caMc4r	34.49 ± 3.43[b]	4.87 ± 1.80	126.33 ± 8.95	442.00 ± 65.43[a]	123.03 ± 31.15	1260.33 ± 272.61

Results are expressed as the mean ± SEM of at least three independent experiments. Human MC4R was used for comparison.

a: Significantly different from the parameter of hMC4R, $P < 0.05$.

b: Significantly different from the parameter of hMC4R, $P < 0.001$.

Table 5.2 The signaling properties of hMC4R and caMc4r

MC4R		caMc4r	hMC4R
Basal (%)		408.65 ± 103.30[a]	100
NDP-MSH	**EC_{50} (nM)**	0.44 ± 0.24	0.30 ± 0.05
	R_{max} (%)	84.48 ± 8.28	100
α-MSH	**EC_{50} (nM)**	1.23 ± 0.32	1.16 ± 0.32
	R_{max} (%)	166.21 ± 47.26	100
β-MSH	**EC_{50} (nM)**	5.76 ± 1.62	3.91 ± 1.09
	R_{max} (%)	167.74 ± 27.91	100
ACTH	**EC_{50} (nM)**	1.60 ± 0.76	1.16 ± 0.27
	R_{max} (%)	149.21 ± 26.94	100
THIQ	**EC_{50} (nM)**	75.71 ± 10.57[a]	5.70 ± 1.74
	R_{max} (%)	39.73 ± 1.37[b]	100

Results are expressed as the mean ± SEM of at least three independent experiments.

a: Significantly different from the parameter of hMC4R, $P < 0.01$.

b: Significantly different from the parameter of hMC4R, $P < 0.001$.

Table 5.3 The effect of Mrap2s on ligand binding properties of caMc4r

caMc4r/caMrap2s	B_{max}	α-MSH IC_{50} (nM)	ACTH IC_{50} (nM)
caMc4r	100	229.00 ± 79.70	235.13 ± 16.70
caMc4r/caMrap2a	170.74 ± 13.08[a]	233.07 ± 44.80	6.34 ± 1.07[a]
caMc4r/caMrap2b	123.58 ± 9.86	153.47 ± 33.83	10.43 ± 1.12[a]

Results are expressed as the mean ± SEM of at least three independent experiments.

a: Significantly different from the parameter of 1:0, $P < 0.001$.

Table 5.4 The effect of Mrap2s on cAMP signaling properties of caMc4r

caMc4r/caMrap2s	α-MSH		ACTH	
	EC_{50} (nM)	**R_{max}**	**EC_{50} (nM)**	**R_{max}**
caMc4r	1.53 ± 0.15	100	3.63 ± 1.21	100
caMc4r/caMrap2a	5.93 ± 1.73	47.60 ± 7.94[a]	1.29 ± 0.34	60.18 ± 3.62[a]
caMc4r/caMrap2b	4.76 ± 1.13	85.21 ± 5.27	1.75 ± 0.15	98.86 ± 4.02

Results are expressed as the mean ± SEM of at least three independent experiments.

a: Significantly different from the parameter of 1:0, $P < 0.001$.

A

```
1   ATG AAC ACC TCA CAT CAT CAT GGA CTG CAT CAT TTG TAC CGG AAT CAC AGC CAG GGA GCT 60
1   M   N   T   S   H   H   H   G   L   H   H   L   Y   R   N   H   S   Q   G   A   20
61  CTG CCG GTG GGA AAG CCT GAT CAG GTT GAG AGA GGA TCA GCC TCT GGA TGC TAT GAG CAG 120
21  L   P   V   G   K   P   D   Q   V   E   R   G   S   A   S   G   C   Y   E   Q   40
121 CTG CTC ATC TCC ACA GAG GTC TTC CTC ACG CTC GGG CTT GTC AGT CTC CTG GAG AAC ATT 180
41  L   L   I   S   T   E   V   F   L   T   L   G   L   V   S   L   L   E   N   I   60
181 CTG GTG ATT GCT GCT ATT GTC AAG AAC AAG AAC CTT CAT TCT CCC ATG TAT TTC TTT ATC 240
61  L   V   I   A   A   I   V   K   N   K   N   L   H   S   P   M   Y   F   F   I   80
241 TGC AGT TTA GCC GTA GCA GAC TTG TTG GTC AGT GTC TCC AAT GCT TCA GAA ACG GTC GTG 300
81  C   S   L   A   V   A   D   L   L   V   S   V   S   N   A   S   E   T   V   V   100
301 ATG GCG CTC ATC ACG GGG GGC AAC CTG ACC AAC CGC GAG AGC ATC ATC AAG AAC ATG GAC 360
101 M   A   L   I   T   G   G   N   L   T   N   R   E   S   I   I   K   N   M   D   120
361 AAC GTT TTT GAC TCG ATG ATC TGC AGC TCG CTT TTA GCC TCC ATT TGG AGT TTG TTG GCC 420
121 N   V   F   D   S   M   I   C   S   S   L   L   A   S   I   W   S   L   L   A   140
421 ATC GCG GTG GAC CGG TAC ATC ACA ATA TTC TAC GCC TTG CGC TAC CAC AAC ATC ATG ACC 480
141 I   A   V   D   R   Y   I   T   I   F   Y   A   L   R   Y   H   N   I   M   T   160
481 CAG CGG AGG GCA GGA ACC ATC ATA ACC TGC ATC TGG ACC TTC TGC ACG GTC TCC GGT GTG 540
161 Q   R   R   A   G   T   I   I   T   C   I   W   T   F   C   T   V   S   G   V   180
541 CTC TTT ATT GTG TAC TCG GAG AGC ACC ACC GTT CTC ATC TGC CTT ATT AGC ATG TTC TTC 600
181 L   F   I   V   Y   S   E   S   T   T   V   L   I   C   L   I   S   M   F   F   200
601 ACC ATG TTG GCT CTC ATG GCC TCG CTC TAT GTC CAC ATG TTT CTT CTA GCC CGG CTG CAC 660
201 T   M   L   A   L   M   A   S   L   Y   V   H   M   F   L   L   A   R   L   H   220
661 ATG AAG CGC ATT GCT GCC CTC CCT GGC AAT GGC CCT ATC TGG CAG GCA GCA AAT ATG AAG 720
221 M   K   R   I   A   A   L   P   G   N   G   P   I   W   Q   A   A   N   M   K   240
721 GGG GCC ATC ACC ATC ACT ATC CTG CTG GGG GTA TTT GTA GTG TGC TGG GCT CCC TTT TTC 780
241 G   A   I   T   I   T   I   L   L   G   V   F   V   V   C   W   A   P   F   F   260
781 TTG CAC CTC ATC CTC ATG ATC TCC TGC CCC CGG AAC CCC TAC TGC ATC TGC TTT ATG TCT 840
261 L   H   L   I   L   M   I   S   C   P   R   N   P   Y   C   I   C   F   M   S   280
841 CAT TTC AAC ATG TAT CTG ATA CTC ATT ATG TGC AAC TCA GTC ATA GAC CCT CTC ATC TAT 900
281 H   F   N   M   Y   L   I   L   I   M   C   N   S   V   I   D   P   L   I   Y   300
901 GCC TTC AGG AGC CAA GAG ATG AGG AAG ACC TTC AAG GAG ATC TGC TGC TGC TGG TAT GGA 960
301 A   F   R   S   Q   E   M   R   K   T   F   K   E   I   C   C   C   W   Y   G   320
961 CTG ACC TCT CTA TGT GTA TAA                                                     981
321 L   T   S   L   C   V   *                                                       326
```

B

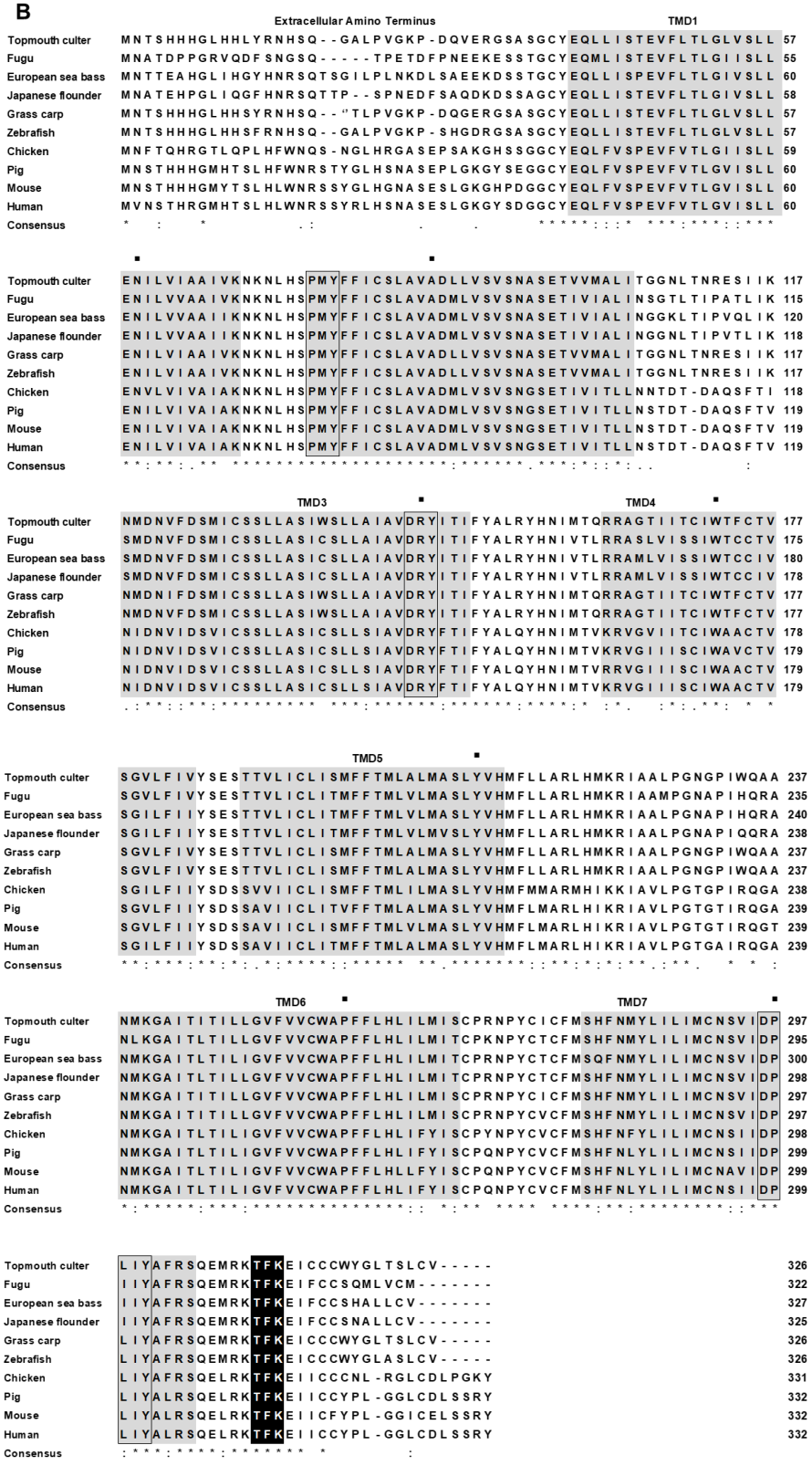
Extracellular Amino Terminus
TMD1
Topmouth culter
Fugu
European sea bass
Japanese flounder
Grass carp
Zebrafish
Chicken
Pig
Mouse
Human
Consensus
TMD3
TMD4
TMD5
TMD6
TMD7

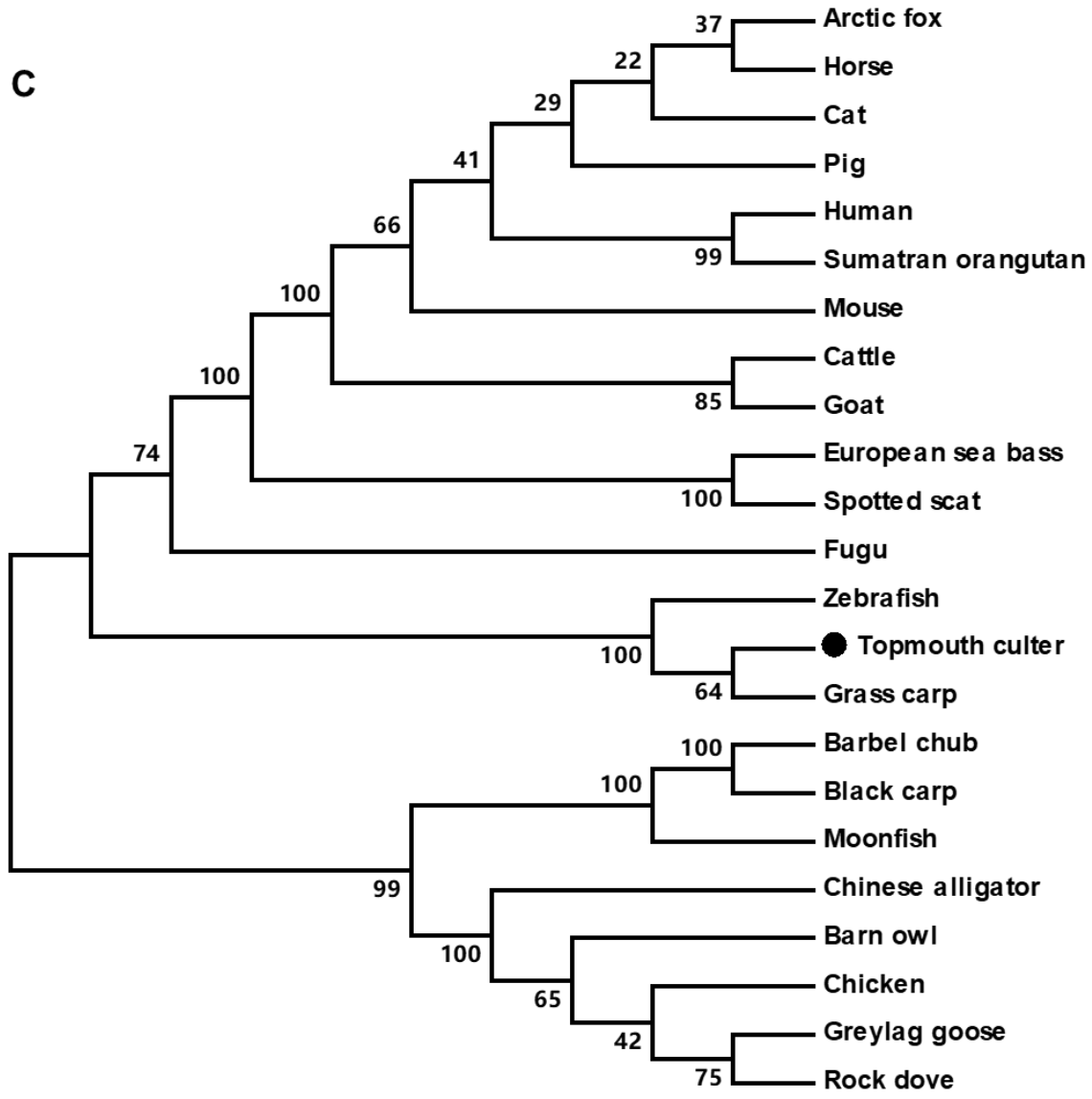

Figure 5.1 Nucleotide and deduced amino acid sequences (A), comparison of amino acid sequences (B), and phylogenetic tree (3) of caMc4r. Nucleotide and deduced amino acid sequences of caMc4r. Positions of nucleotide and amino acid sequences are indicated on both sides. Shaded boxes denote putative TMD1-7. Potential phosphorylation sites are present in oval frame. Underline show PMY, DRY, DPxxY motifs. Open boxes denote the consensus sequence for *N*-linked glycosylation sites. Asterisk (*) indicates stop codon. The tree was constructed by

the neighbor-joining (NJ) method. Numbers at nodes indicate the bootstrap value, as percentages, obtained for 1000 replicates. Black dot shows caMC4R. MC4Rs: *Culter alburnus* (topmouth culter, MT163518), *Scatophagus argus* (spotted scat, KU760724.1), *Dicentrarchus labrax* (european sea bass, CBN82190.1), *Lepisosteus oculatus* (spotted gar, XP_006634516.1), *Danio rerio* (zebrafish, NP_775385.1), *Vulpes lagopus* (arctic fox, ACN55093.1), *Ctenopharyngodon idella* (grass carp, AOZ60534.1), *Paralichthys olivaceus* (Japanese flounder, ADP09415.1), *Squaliobarbus curriculus* (barbel chub, ADV40875.1), *Takifugu rubripes* (fugu, NP_001027732.1), *Mylopharyngodon piceus* (black carp, ADV40871.1), *Tyto alba* (barn owl, ATN96237.1), *Columba livia* (rock dove, XP_021153678.1), *Bos taurus* (cattle, NP_776535.1), *Alligator sinensis* (chinese alligator, XP_006025279.1), *Anser anser* (greylag goose, ABF19809.1), *Pongo abelii* (sumatran orangutan, XP_002828309.1), *Equus caballus* (horse, XP_001489706.1), *Felis catus* (cat, XP_019670932.2), *Gallus gallus* (chicken, AEP17334.10), *Sus scrofa* (pig, ABD28176.1), *Mus musculus* (mouse, NP_058673.2), *Capra hircus* (goat, NP_001272520.1), and *Homo sapiens* (human, NP_005903.2).

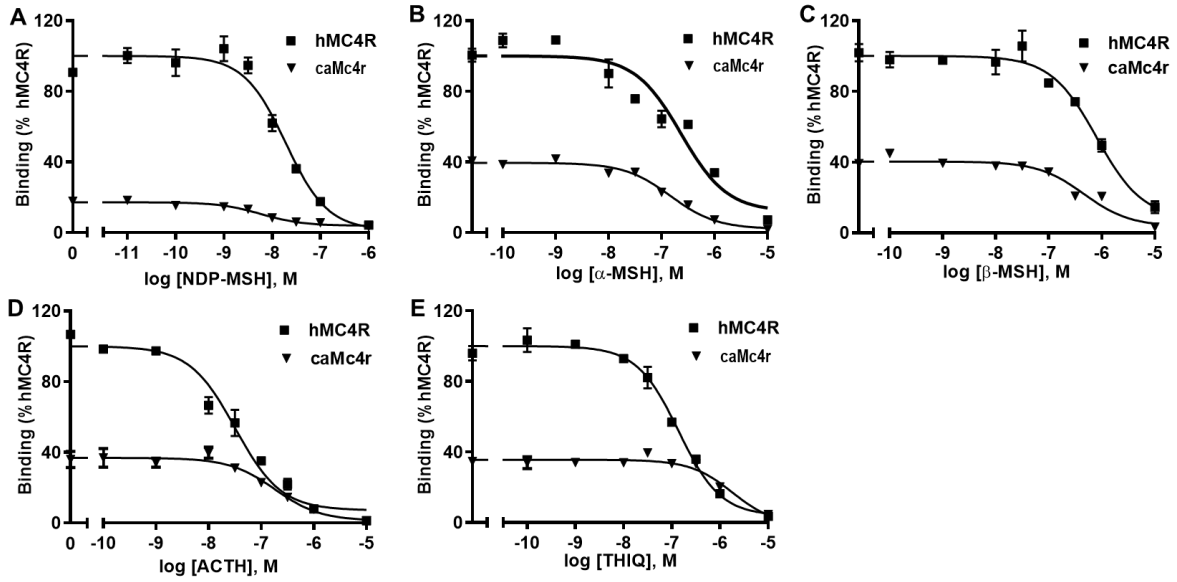

Figure 5.2 Ligand binding properties of caMc4r. HEK293T cells were transiently transfected with caMC4R plasmids (hMC4R was used as a control). Different concentrations of unlabeled NDP-MSH (A), α-MSH (B), β-MSH (C), ACTH (1-24) (D), and THIQ (E) was used to displace the binding of ^{125}I-NDP-MSH. Results are expressed as % of hMC4R binding ± range from duplicate determinations within one experiment. All experiments were measured at least three independent experiments.

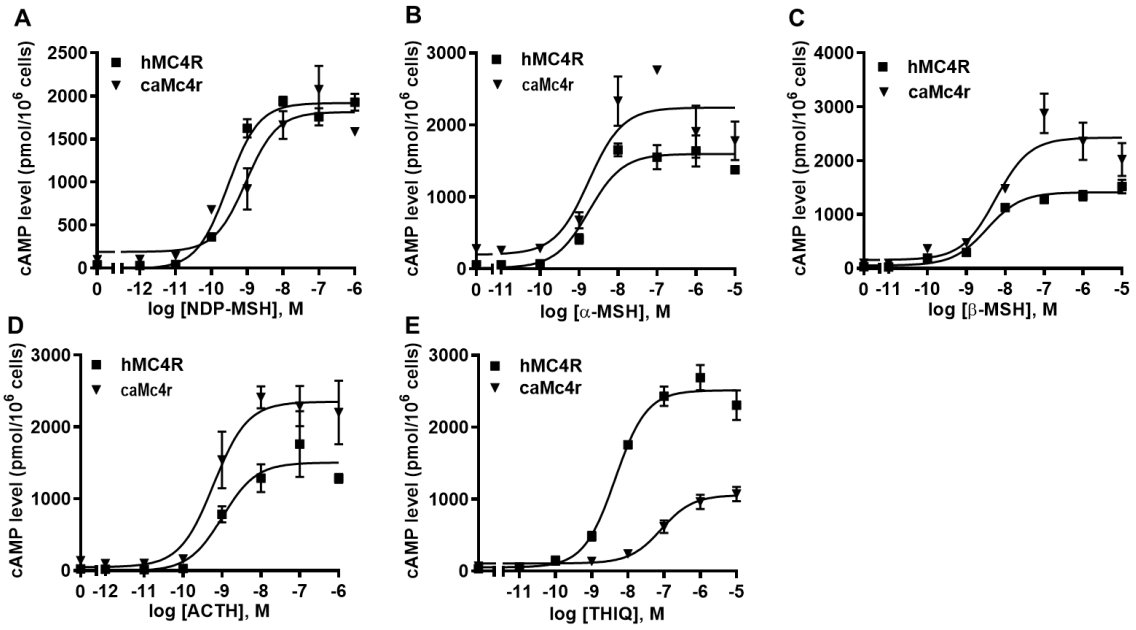

Figure 5.3 Signaling properties of caMc4r. HEK293T cells were transiently transfected with hMC4R or caMC4R plasmids. Forty-eight hours after transfection, cells were stimulated with different concentrations of NDP-MSH (A), α-MSH (B), β-MSH (C), ACTH (1-24) (D), and THIQ (E). Data are mean ± SEM from triplicate measurements within one experiment. All experiments were performed at least three times independently.

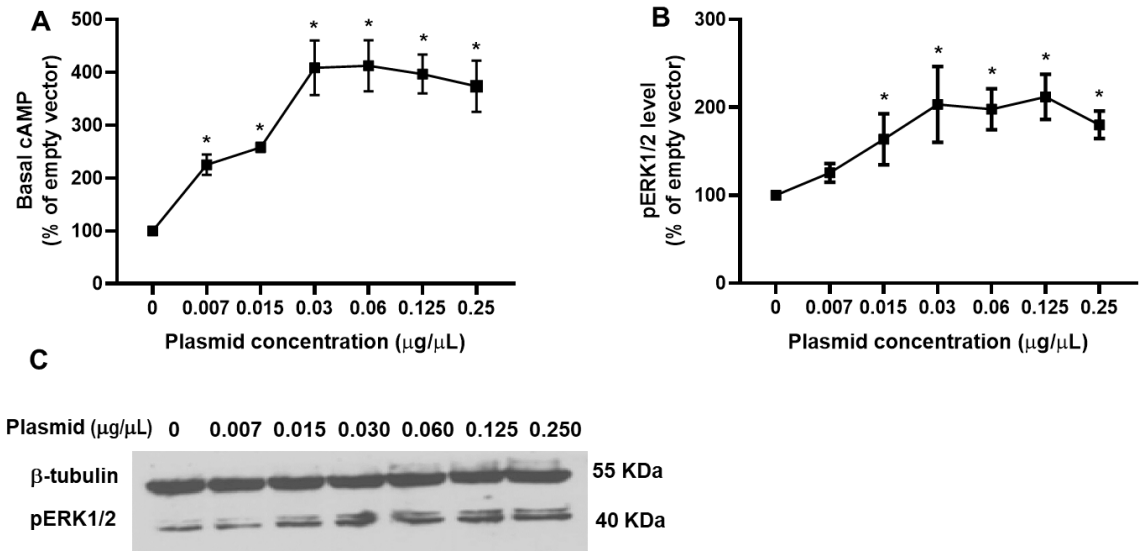

Figure 5.4 Constitutive activities of caMc4r. HEK293T cells transfected with increasing concentrations of caMC4R plasmids. Cells transfected with empty pcDNA3.1 vector was considered as control group. (A) cAMP levels were measured by RIA. The curve is made with three independent experiments. (B, C) The Erk1/2 phosphorylation levels were detected by western blot. Values are expressed as mean ± SEM (n = 3). Asterisk (*) showed significant difference of cAMP and pErk1/2 levels compared with control group ($P < 0.05$) (One-way ANOVA followed by Tukey test).

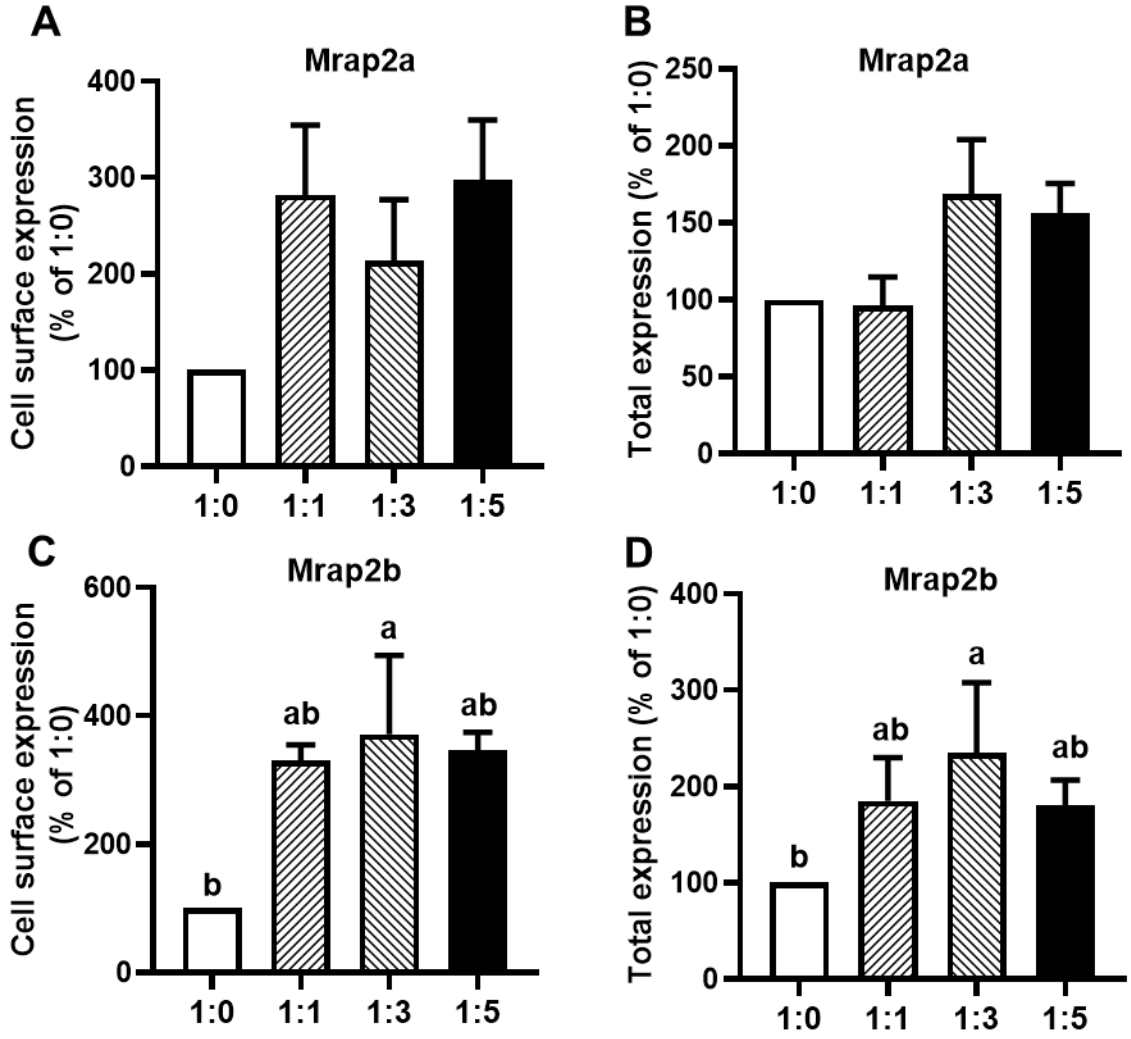

Figure 5.5 Modulation of caMc4r expression by caMrap2s. Cell surface (A, C) and total expression (B, D) of caMc4r was measured by flow cytometry. HEK293T cells were cotransfected with different ratios of caMC4R/caMRAP2a or caMC4R/caMRAP2b (1:0, 1:1, 1:3, and 1:5). The empty vector (pcDNA3.1) fluorescence was used for background staining. The results were calculated as % of 1:0 group after correction of the background staining. Each data point repressented as the mean ± SEM (n = 3-4). Different letters indicated significant difference ($P < 0.05$) (One-way ANOVA followed by Tukey test).

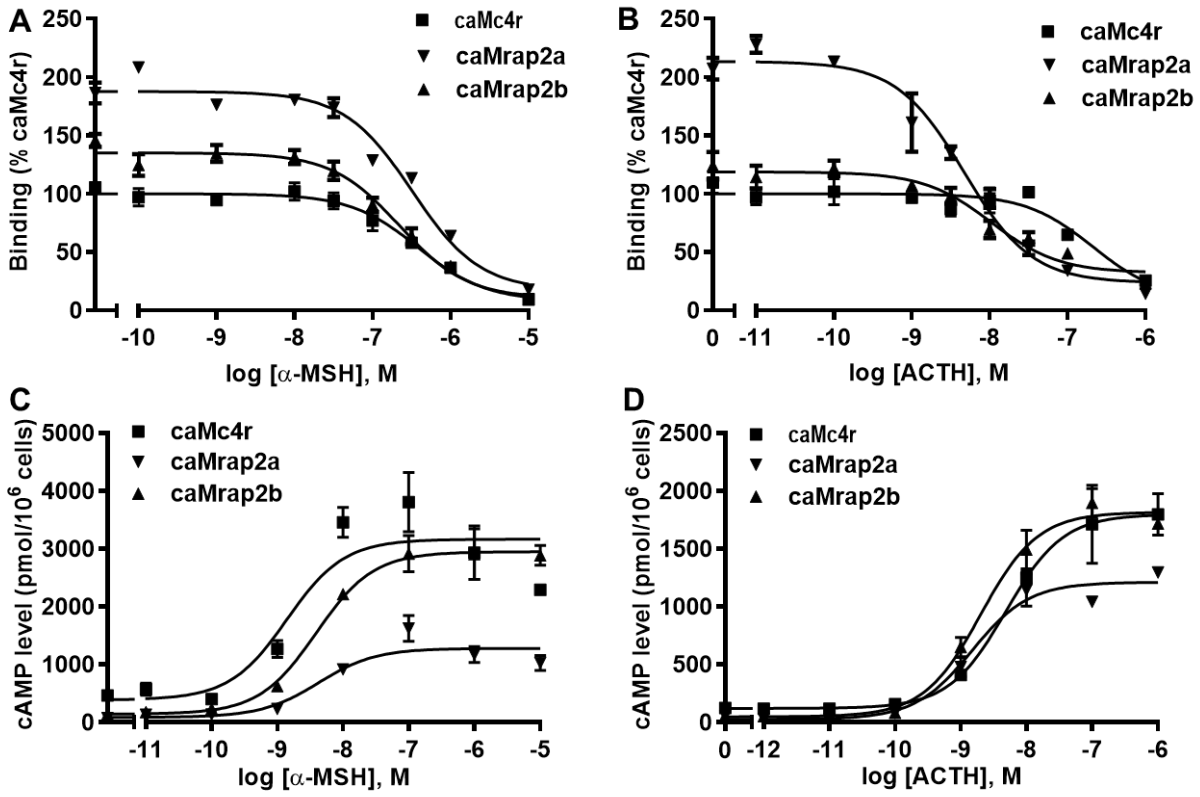

Figure 5.6 Modulation of caMc4r pharmacology by Mrap2s. Ligand binding properties (A, B) and signaling properties (C, D) of caMc4r to α-MSH or ACTH (1-24) upon co-expression of caMrap2a or caMrap2b. HEK293T cells were co-transfected with caMC4R/caMRAP2a or caMC4R/caMRAP2b in two different ratios (1:0, and 1:5). Results of binding properties were calculated as % of hMC4R binding ± range from duplicate determinations within one experiment. All experiments were measured at least three independent experiments.

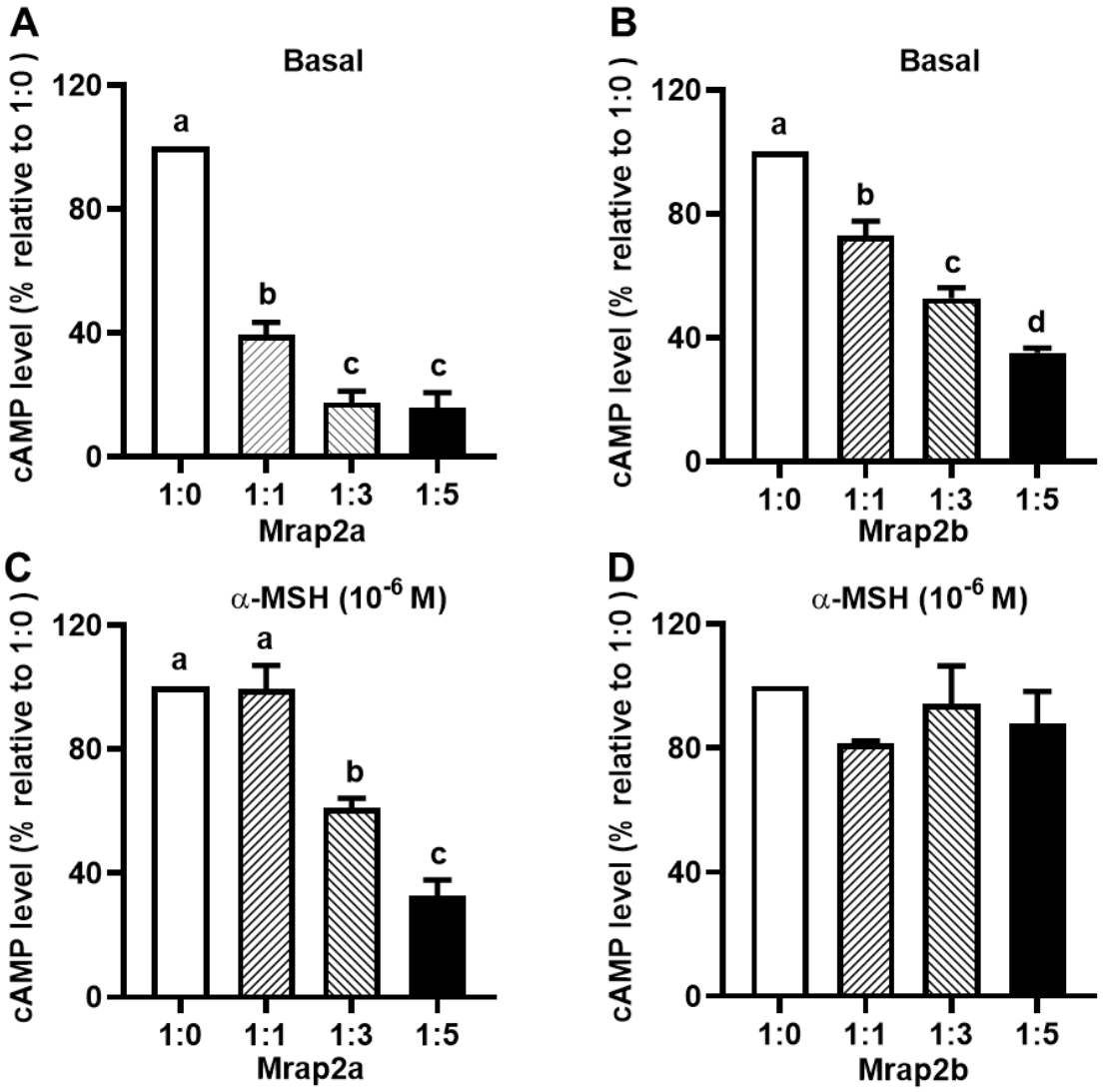

Figure 5.7 The effect of Mrap2s on caMc4r signaling. HEK293T cells were co-transfected with different ratios of caMC4R/caMRAP2a or caMC4R/caMRAP2b (1:0, 1:1, 1:3, and 1:5) and cAMP levels under basal (A, B) or stimulated (with 10^{-6} M α-MSH, C, D) conditions were measured. Data are analysed as % of 1:0 group. Values are expressed as mean ± SEM (n = 3). Different letters indicate significant difference (one-way ANOVA followed by Tukey test).

Conclusions

In conclusion, firstly, we identified two human *MRAP2* splice variants, *MRAP2b* and *MRAP2c*. We investigated effects of five isoforms of MRAPs, hMRAP1a, hMRAP1b, hMRAP2a, hMRAP2b, and hMRAP2c, on MC3R and MC4R pharmacology. MRAP1b, MRAP2b, and MRAP2c were involved in regulating hMC3R and hMC4R pharmacology. At MC3R, MRAP1a and MRAP2c increased, and MRAP1b decreased cell surface expression of hMC3R; Four MRAPs decreased α-MSH- and ACTH-stimulated cAMP signaling of hMC3R. For MC4R, MRAP1a, MRAP2a, and MRAP2c, increased cell surface and total expression of hMC4R; Four MRAPs decreased α-MSH-induced and did not affect ACTH-induced cAMP of hMC4R; MRAP1s and MRAP2s have opposite effects on the basal activities of hMC4R. These findings suggest the complexity of MRAPs in modulating MC3R/MC4R and provide a new opportunity for regulating MC3R and MC4R signaling.

Secondly, we also identified one canine *MRAP2* splice variant, *MRAP2b*. We further investigated modulation of cMRAP1, cMRAP2a, and cMRAP2b, on cMC3R and cMC4R pharmacology. All MRAPs increased cMC4R cell surface expression but did not affect cMC3R trafficking; All MRAPs increased cMC4R affinities to α-MSH and ACTH, whereas had no effect on cMC3R affinities; MRAP1 deceased ligand-stimulated signaling of cMC3R; MRAP2a/MRAP2b had the different effects on agonist-induced signaling of cMC3R/cMC4R. cMC4R had high basal activity in cAMP signaling, and all MRAPs decreased the basal activity of cMC4R. These findings indicate the complexity of MRAPs in regulating neural MCRs and contribute to further physiological studies of canine MC3R/MC4R.

Finally, we functionally investigated Mc3r and Mc4r and its regulation by two isoforms of Mrap2 in topmouth culter. Culter Mc3r and Mc4r were both functional receptors. At Mc3r, Mc3r had high constitutive activity in cAMP pathway, and similar potencies to several agonists as hMC3R. Only caMrap2a markedly decreased cell surface expression and R_{max} of caMc3r. Both caMrap2a and caMrap2b decreased basal cAMP production. For Mc4r, Mc4r had high constitutive activities, and similar potencies to several agonists as hMC4R. Mrap2a significantly increased the B_{max} and decreased agonist-stimulated cAMP, whereas Mrap2b increased the cell surface and total expression but did not affect B_{max} and agonist-stimulated cAMP. Therefore, these data suggested that Mrap2a/Mrap2b had differential effects on the expression, binding, and signaling of Mc3r and Mc4r. These findings lay the foundation for future physiological studies on the functions of Mc3r and Mc4r that might provide new strategies to improve growth and reproduction in culter culture.

References

[1] R. Fredriksson, M.C. Lagerstrom, L.G. Lundin, H.B. Schioth, The G-protein-coupled receptors in the human genome form five main families. Phylogenetic analysis, paralogon groups, and fingerprints, Mol Pharmacol 63(6) (2003) 1256-1272.

[2] R.J. Lefkowitz, A brief history of G-protein coupled receptors (Nobel Lecture), Angew Chem Int Ed Engl 52(25) (2013) 6366-6378.

[3] Y.X. Tao, Molecular chaperones and G protein-coupled receptor maturation and pharmacology, Mol Cell Endocrinol 511 (2020) 110862.

[4] J. Bockaert, J.P. Pin, Molecular tinkering of G protein-coupled receptors: an evolutionary success, EMBO Journal 18(7) (1999) 1723-1729.

[5] A.M. Spiegel, L.S. Weinstein, A. Shenker, Abnormalities in G protein-coupled signal transduction pathways in human disease, J Clin Invest 92(3) (1993) 1119-1125.

[6] A.M. Spiegel, L.S. Weinstein, Inherited diseases involving G proteins and G protein-coupled receptors, Annual Review of Medicine 55 (2004) 27-39.

[7] T. Schoneberg, A. Schulz, H. Biebermann, T. Hermsdorf, H. Rompler, K. Sangkuhl, Mutant G-protein-coupled receptors as a cause of human diseases, Pharmacol Ther 104(3) (2004) 173-206.

[8] Y.X. Tao, Inactivating mutations of G protein-coupled receptors and diseases: Structure-function insights and therapeutic implications, Pharmacol Ther 111(3) (2006) 949-973.

[9] Y.X. Tao, Constitutive activation of G protein-coupled receptors and diseases: Insights into mechanism of activation and therapeutics, Pharmacol Ther 120 (2008) 129-148.

[10] G. Vassart, S. Costagliola, G protein-coupled receptors: mutations and endocrine diseases, Nat Rev Endocrinol 7(6) (2011) 362-372.

[11] T. Schoneberg, I. Liebscher, Mutations in G protein-coupled receptors: Mechanisms, pathophysiology and potential therapeutic approaches, Pharmacol Rev 73(1) (2021) 89-119.

[12] L.K. Yang, Z.S. Hou, Y.X. Tao, Biased signaling in naturally occurring mutations of G protein-coupled receptors associated with diverse human diseases, Biochim Biophys Acta Mol Basis Dis 1867(1) (2021) 165973.

[13] T. Liu, R.L. Ji, Y.X. Tao, Naturally occurring mutations in G protein-coupled receptors associated with obesity and type 2 diabetes mellitus, Pharmacol Ther (2022) 108044.

[14] R. Zhang, X. Xie, Tools for GPCR drug discovery, Acta Pharmacol Sin 33(3) (2012) 372-384.

[15] D.B. Goswami, L.M. Ogawa, J.M. Ward, G.M. Miller, E.J. Vallender, Large-scale polymorphism discovery in macaque G-protein coupled receptors, BMC Genom 14(1) (2013) 703.

[16] K. Sriram, P.A. Insel, G protein-coupled receptors as targets for approved drugs: How many targets and how many drugs?, Mol Pharmacol 93(4) (2018) 251-258.

[17] A.I. Smith, J.W. Funder, Proopiomelanocortin processing in the pituitary, central nervous system, and peripheral tissues, Endocr Rev 9(1) (1988) 159-179.

[18] R.M. Dores, S. Lecaude, Trends in the evolution of the proopiomelanocortin gene, Gen Comp Endocrinol 142(1-2) (2005) 81-93.

[19] I. Gantz, H. Miwa, Y. Konda, Y. Shimoto, T. Tashiro, S.J. Watson, J. DelValle, T. Yamada, Molecular cloning, expression, and gene localization of a fourth melanocortin receptor, J Biol Chem 268(20) (1993) 15174-15179.

[20] I. Gantz, Y. Konda, T. Tashiro, Y. Shimoto, H. Miwa, G. Munzert, S.J. Watson, J. DelValle, T. Yamada, Molecular cloning of a novel melanocortin receptor, J Biol Chem 268(11) (1993) 8246-8250.

[21] L. Roselli-Rehfuss, K.G. Mountjoy, L.S. Robbins, M.T. Mortrud, M.J. Low, J.B. Tatro, M.L. Entwistle, R.B. Simerly, R.D. Cone, Identification of a receptor for γ melanotropin and other proopiomelanocortin peptides in the hypothalamus and limbic system, Proc Natl Acad Sci U S A 90(19) (1993) 8856-8860.

[22] K.G. Mountjoy, M.T. Mortrud, M.J. Low, R.B. Simerly, R.D. Cone, Localization of the melanocortin-4 receptor (MC4-R) in neuroendocrine and autonomic control circuits in the brain, Mol Endocrinol 8(10) (1994) 1298-1308.

[23] R.D. Cone, Anatomy and regulation of the central melanocortin system, Nat Neurosci 8(5) (2005) 571-578.

[24] Y.X. Tao, Molecular mechanisms of the neural melanocortin receptor dysfunction in severe early onset obesity, Mol Cell Endocrinol 239(1-2) (2005) 1-14.

[25] D. Huszar, C.A. Lynch, V. Fairchild-Huntress, J.H. Dunmore, Q. Fang, L.R. Berkemeier, W. Gu, R.A. Kesterson, B.A. Boston, R.D. Cone, F.J. Smith, L.A. Campfield, P. Burn, F. Lee, Targeted disruption of the melanocortin-4 receptor results in obesity in mice, Cell 88(1) (1997) 131-141.

[26] N. Balthasar, L.T. Dalgaard, C.E. Lee, J. Yu, H. Funahashi, T. Williams, M. Ferreira, V. Tang, R.A. McGovern, C.D. Kenny, L.M. Christiansen, E. Edelstein, B. Choi, O. Boss, C. Aschkenasi, C.Y. Zhang, K. Mountjoy, T. Kishi, J.K. Elmquist, B.B. Lowell, Divergence of melanocortin pathways in the control of food intake and energy expenditure, Cell 123(3) (2005) 493-505.

[27] A.S. Chen, D.J. Marsh, M.E. Trumbauer, E.G. Frazier, X.M. Guan, H. Yu, C.I. Rosenblum, A. Vongs, Y. Feng, L. Cao, J.M. Metzger, A.M. Strack, R.E. Camacho, T.N. Mellin, C.N. Nunes, W. Min, J. Fisher, S. Gopal-Truter, D.E. MacIntyre, H.Y. Chen, L.H. Van der Ploeg, Inactivation of the mouse melanocortin-3 receptor results in increased fat mass and reduced lean body mass, Nat Genet 26(1) (2000) 97-102.

[28] A.A. Butler, R.A. Kesterson, K. Khong, M.J. Cullen, M.A. Pelleymounter, J. Dekoning, M. Baetscher, R.D. Cone, A unique metabolic syndrome causes obesity in the melanocortin-3 receptor-deficient mouse, Endocrinology 141(9) (2000) 3518-3521.

[29] Y. Zhang, G.E. Kilroy, T.M. Henagan, V. Prpic-Uhing, W.G. Richards, A.W. Bannon, R.L. Mynatt, T.W. Gettys, Targeted deletion of melanocortin receptor subtypes 3 and 4, but not CART, alters nutrient partitioning and compromises behavioral and metabolic responses to leptin, FASEB J 19(11) (2005) 1482-1491.

[30] Y.X. Tao, Mutations in melanocortin-4 receptor and human obesity, Prog Mol Biol Transl Sci 88 (2009) 173-204.

[31] Y.X. Tao, Mutations in the melanocortin-3 receptor (MC3R) gene: Impact on human obesity or adiposity, Curr Opin Investig Drugs 11(10) (2010) 1092-1096.

[32] Y.X. Tao, The melanocortin-4 receptor: physiology, pharmacology, and pathophysiology, Endocr Rev 31(4) (2010) 506-543.

[33] Z. Yang, Y.X. Tao, Mutations in melanocortin-3 receptor gene and human obesity, Prog Mol Biol Transl Sci 140 (2016) 97-129.

[34] D.H. Versteeg, P. Van Bergen, R.A. Adan, D.J. De Wildt, Melanocortins and cardiovascular regulation, Eur J Pharmacol 360(1) (1998) 1-14.

[35] C. Mioni, D. Giuliani, M.M. Cainazzo, S. Leone, C. Bazzani, P. Grieco, E. Novellino, A. Tomasi, A. Bertolini, S. Guarini, Further evidence that melanocortins prevent myocardial reperfusion injury by activating melanocortin MC3 receptors, Eur J Pharmacol 477(3) (2003) 227-234.

[36] S.J. Getting, H.C. Christian, C.W. Lam, F.N. Gavins, R.J. Flower, H.B. Schioth, M. Perretti, Redundancy of a functional melanocortin 1 receptor in the anti-inflammatory actions of melanocortin peptides: studies in the recessive yellow (e/e) mouse suggest an important role for melanocortin 3 receptor, J Immunol 170(6) (2003) 3323-3330.

[37] A. Catania, S. Gatti, G. Colombo, J.M. Lipton, Targeting melanocortin receptors as a novel strategy to control inflammation, Pharmacol Rev 56(1) (2004) 1-29.

[38] S.J. Getting, Y. Riffo-Vasquez, S. Pitchford, M. Kaneva, P. Grieco, C.P. Page, M. Perretti, D. Spina, A role for MC3R in modulating lung inflammation, Pulm Pharmacol Ther 21(6) (2008) 866-873.

[39] H.B. Patel, T. Montero-Melendez, K.V. Greco, M. Perretti, Melanocortin receptors as novel effectors of macrophage responses in inflammation, Front Immunol 2 (2011) 41.

[40] W. Wang, D.Y. Guo, Y.J. Lin, Y.X. Tao, Melanocortin regulation of inflammation, Front Endocrinol (Lausanne) 10 (2019) 683.

[41] G. Chandramohan, N. Durham, S. Sinha, K. Norris, N.D. Vaziri, Role of γ melanocyte-stimulating hormone-renal melanocortin 3 receptor system in blood pressure regulation in salt-resistant and salt-sensitive rats, Metabolism 58(10) (2009) 1424-1429.

[42] B.Y.H. Lam, A. Williamson, S. Finer, F.R. Day, J.A. Tadross, A. Goncalves Soares, K. Wade, P. Sweeney, M.N. Bedenbaugh, D.T. Porter, A. Melvin, K.L.J. Ellacott, R.N. Lippert, S. Buller, J. Rosmaninho-Salgado, G.K.C. Dowsett, K.E. Ridley, Z. Xu, I. Cimino, D. Rimmington,

K. Rainbow, K. Duckett, S. Holmqvist, A. Khan, X. Dai, E.G. Bochukova, Genes, T. Health Research, R.C. Trembath, H.C. Martin, A.P. Coll, D.H. Rowitch, N.J. Wareham, D.A. van Heel, N. Timpson, R.B. Simerly, K.K. Ong, R.D. Cone, C. Langenberg, J.R.B. Perry, G.S. Yeo, S. O'Rahilly, MC3R links nutritional state to childhood growth and the timing of puberty, Nature 599 (2021) 436-441.

[43] A. Xu, K.L. Choi, Y. Wang, P.A. Permana, L.Y. Xu, C. Bogardus, G.J. Cooper, Identification of novel putative membrane proteins selectively expressed during adipose conversion of 3T3-L1 cells, Biochem Biophys Res Commun 293(4) (2002) 1161-1167.

[44] L.A. Metherell, J.P. Chapple, S. Cooray, A. David, C. Becker, F. Ruschendorf, D. Naville, M. Begeot, B. Khoo, P. Nurnberg, A. Huebner, M.E. Cheetham, A.J.L. Clark, Mutations in *MRAP*, encoding a new interacting partner of the ACTH receptor, cause familial glucocorticoid deficiency type 2, Nat Genet 37(2) (2005) 166-170.

[45] S. Roy, M. Rached, N. Gallo-Payet, Differential regulation of the human adrenocorticotropin receptor [melanocortin-2 receptor (MC2R)] by human MC2R accessory protein isoforms alpha and beta in isogenic human embryonic kidney 293 cells, Mol Endocrinol 21(7) (2007) 1656-1669.

[46] J.A. Sebag, P.M. Hinkle, Melanocortin-2 receptor accessory protein MRAP forms antiparallel homodimers, Proc Natl Acad Sci U S A 104(51) (2007) 20244-20249.

[47] L.F. Chan, T.R. Webb, T.T. Chung, E. Meimaridou, S.N. Cooray, L. Guasti, J.P. Chapple, M. Egertova, M.R. Elphick, M.E. Cheetham, L.A. Metherell, A.J. Clark, MRAP and MRAP2 are bidirectional regulators of the melanocortin receptor family, Proc Natl Acad Sci U S A 106(15) (2009) 6146-6151.

[48] P.M. Hinkle, M.N. Serasinghe, A. Jakabowski, J.A. Sebag, K.R. Wilson, C. Haskell-Luevano, Use of chimeric melanocortin-2 and -4 receptors to identify regions responsible for ligand specificity and dependence on melanocortin 2 receptor accessory protein, Eur J Pharmacol 660(1) (2011) 94-102.

[49] E.I. Kay, R. Botha, J.M. Montgomery, K.G. Mountjoy, hMRAPa increases αMSH-induced hMC1R and hMC3R functional coupling and hMC4R constitutive activity, J Mol Endocrinol 50(2) (2013) 203-215.

[50] M. Asai, S. Ramachandrappa, M. Joachim, Y. Shen, R. Zhang, N. Nuthalapati, V. Ramanathan, D.E. Strochlic, P. Ferket, K. Linhart, C. Ho, T.V. Novoselova, S. Garg, M. Ridderstrale, C. Marcus, J.N. Hirschhorn, J.M. Keogh, S. O'Rahilly, L.F. Chan, A.J. Clark, I.S. Farooqi, J.A. Majzoub, Loss of function of the melanocortin 2 receptor accessory protein 2 is associated with mammalian obesity, Science 341(6143) (2013) 275-278.

[51] T.V. Novoselova, R. Larder, D. Rimmington, C. Lelliott, E.H. Wynn, R.J. Gorrigan, P.H. Tate, L. Guasti, S. O'Rahilly, A.J.L. Clark, Loss of Mrap2 is associated with Sim1 deficiency and increased circulating cholesterol, J Endocrinol 230(1) (2016) 13-26.

[52] E. Geets, D. Zegers, S. Beckers, A. Verrijken, G. Massa, K. Van Hoorenbeeck, S. Verhulst, L. Van Gaal, W. Van Hul, Copy number variation (CNV) analysis and mutation analysis of the 6q14.1-6q16.3 genes SIM1 and MRAP2 in Prader Willi like patients, Mol Genet Metab 117(3) (2016) 383-8.

[53] M. Baron, J. Maillet, M. Huyvaert, A. Dechaume, R. Boutry, H. Loiselle, E. Durand, B. Toussaint, E. Vaillant, J. Philippe, J. Thomas, A. Ghulam, S. Franc, G. Charpentier, J.M. Borys, C. Levy-Marchal, M. Tauber, R. Scharfmann, J. Weill, C. Aubert, J. Kerr-Conte, F. Pattou, R. Roussel, B. Balkau, M. Marre, M. Boissel, M. Derhourhi, S. Gaget, M. Canouil, P. Froguel, A.

Bonnefond, Loss-of-function mutations in MRAP2 are pathogenic in hyperphagic obesity with hyperglycemia and hypertension, Nat Med 25(11) (2019) 1733-1738.

[54] A.C.P. da Fonseca, G.M. Abreu, V.M. Zembrzuski, M. Campos Junior, J.R.I. Carneiro, J.F. Nogueira Neto, F. Magno, E.L. Rosado, P.T. Bozza, G.M.K. de Cabello, P.H. Cabello, Study of LEP, MRAP2 and POMC genes as potential causes of severe obesity in Brazilian patients, Eat Weight Disord 26(5) (2021) 1399-1408.

[55] J.A. Sebag, C. Zhang, P.M. Hinkle, A.M. Bradshaw, R.D. Cone, Developmental control of the melanocortin-4 receptor by MRAP2 proteins in zebrafish, Science 341(6143) (2013) 278-281.

[56] J. Zhang, X. Li, Y. Zhou, L. Cui, J. Li, C. Wu, Y. Wan, J. Li, Y. Wang, The interaction of MC3R and MC4R with MRAP2, ACTH, α-MSH and AgRP in chickens, J Endocrinol 234 (2017) 155-174.

[57] L.K. Yang, Z.R. Zhang, H.S. Wen, Y.X. Tao, Characterization of channel catfish (*Ictalurus punctatus*) melanocortin-3 receptor reveals a potential network in regulation of energy homeostasis, Gen Comp Endocrinol 277 (2019) 90-103.

[58] J. Zhang, J. Li, C. Wu, Z. Hu, L. An, Y. Wan, C. Fang, X. Zhang, J. Li, Y. Wang, The Asp298Asn polymorphism of melanocortin-4 receptor (MC4R) in pigs: evidence for its potential effects on MC4R constitutive activity and cell surface expression, Anim Genet 51(5) (2020) 694-706.

[59] M. Tao, R.L. Ji, L. Huang, S.Y. Fan, T. Liu, S.J. Liu, Y.X. Tao, Regulation of melanocortin-4 receptor pharmacology by two isoforms of melanocortin receptor accessory protein 2 in topmouth culter (*Culter alburnus*), Front Endocrinol (Lausanne) 11 (2020) 538.

[60] R.L. Ji, L. Huang, Y. Wang, T. Liu, S.Y. Fan, M. Tao, Y.X. Tao, Topmouth culter melanocortin-3 receptor: regulation by two isoforms of melanocortin-2 receptor accessory protein 2, Endocr Connect 10 (2021) 1489-1501.

[61] Z.Y. Wen, T. Liu, C.J. Qin, Y.C. Zou, J. Wang, R. Li, Y.X. Tao, MRAP2 interaction with melanocortin-4 receptor in snakehead (*Channa argus*), Biomolecules 11(3) (2021) 481.

[62] L.E. Pritchard, A.V. Turnbull, A. White, Pro-opiomelanocortin processing in the hypothalamus: impact on melanocortin signalling and obesity, J Endocrinol 172(3) (2002) 411-21.

[63] M.J. Krashes, B.B. Lowell, A.S. Garfield, Melanocortin-4 receptor-regulated energy homeostasis, Nat Neurosci 19(2) (2016) 206-19.

[64] Z.A. Abdel-Malek, M.C. Scott, M. Furumura, M.L. Lamoreux, M. Ollmann, G.S. Barsh, V.J. Hearing, The melanocortin 1 receptor is the principal mediator of the effects of agouti signaling protein on mammalian melanocytes, J Cell Sci 114(Pt 5) (2001) 1019-1024.

[65] D. Lu, D. Willard, I.R. Patel, S. Kadwell, L. Overton, T. Kost, M. Luther, W. Chen, R.P. Woychik, W.O. Wilkison, R.D. Cone, Agouti protein is an antagonist of the melanocyte-stimulating-hormone receptor, Nature 371(6500) (1994) 799-802.

[66] W. Fan, B.A. Boston, R.A. Kesterson, V.J. Hruby, R.D. Cone, Role of melanocortinergic neurons in feeding and the agouti obesity syndrome, Nature 385(6612) (1997) 165-168.

[67] T.M. Fong, C. Mao, T. MacNeil, R. Kalyani, T. Smith, D. Weinberg, M.R. Tota, L.H. Van der Ploeg, ART (protein product of agouti-related transcript) as an antagonist of MC-3 and MC-4 receptors, Biochem Biophys Res Commun 237(3) (1997) 629-631.

[68] M.M. Ollmann, B.D. Wilson, Y.K. Yang, J.A. Kerns, Y. Chen, I. Gantz, G.S. Barsh, Antagonism of central melanocortin receptors in vitro and in vivo by agouti-related protein, Science 278(5335) (1997) 135-138.

[69] M.M. Hagan, P.A. Rushing, L.M. Pritchard, M.W. Schwartz, A.M. Strack, L.H. Van Der Ploeg, S.C. Woods, R.J. Seeley, Long-term orexigenic effects of AgRP-(83---132) involve mechanisms other than melanocortin receptor blockade, Am J Physiol Regul Integr Comp Physiol 279(1) (2000) R47-R52.

[70] V. Tolle, M.J. Low, In vivo evidence for inverse agonism of Agouti-related peptide in the central nervous system of proopiomelanocortin-deficient mice, Diabetes 57(1) (2008) 86-94.

[71] Q. Wu, M.P. Howell, M.A. Cowley, R.D. Palmiter, Starvation after AgRP neuron ablation is independent of melanocortin signaling, Proc Natl Acad Sci U S A 105(7) (2008) 2687-2692.

[72] C. Haskell-Luevano, R.D. Cone, E.K. Monck, Y.P. Wan, Structure activity studies of the melanocortin-4 receptor by in vitro mutagenesis: identification of agouti-related protein (AGRP), melanocortin agonist and synthetic peptide antagonist interaction determinants, Biochemistry 40(20) (2001) 6164-6179.

[73] W.A. Nijenhuis, J. Oosterom, R.A. Adan, AgRP(83-132) acts as an inverse agonist on the human melanocortin-4 receptor, Mol Endocrinol 15(1) (2001) 164-171.

[74] Y.X. Tao, H. Huang, Z.Q. Wang, F. Yang, J.N. Williams, G.V. Nikiforovich, Constitutive activity of neural melanocortin receptors, Methods Enzymol 484 (2010) 267-279.

[75] P. Tarnow, A. Rediger, A. Schulz, A. Gruters, H. Biebermann, Identification of the translation start site of the human melanocortin 3 receptor, Obes Facts 5(1) (2012) 45-51.

[76] J. Park, N. Sharma, G.R. Cutting, Melanocortin 3 receptor has a 5' exon that directs translation of apically localized protein from the second in-frame ATG, Mol Endocrinol 28(9) (2014) 1547-1557.

[77] S. Jegou, I. Boutelet, H. Vaudry, Melanocortin-3 receptor mRNA expression in pro-opiomelanocortin neurones of the rat arcuate nucleus, J Neuroendocrinol 12(6) (2000) 501-505.

[78] V. Chhajlani, Distribution of cDNA for melanocortin receptor subtypes in human tissues, Biochem Mol Biol Intl 38(1) (1996) 73-80.

[79] S.J. Getting, Targeting melanocortin receptors as potential novel therapeutics, Pharmacol Ther 111(1) (2006) 1-15.

[80] C. Girardet, A.A. Butler, Neural melanocortin receptors in obesity and related metabolic disorders, Biochim Biophys Acta 1842(3) (2014) 482-494.

[81] B.J. Renquist, J.G. Murphy, E.A. Larson, D. Olsen, R.F. Klein, K.L. Ellacott, R.D. Cone, Melanocortin-3 receptor regulates the normal fasting response, Proc Natl Acad Sci U S A 109(23) (2012) E1489-E1498.

[82] M. Ghamari-Langroudi, I. Cakir, R.N. Lippert, P. Sweeney, M.J. Litt, K.L.J. Ellacott, R.D. Cone, Regulation of energy rheostasis by the melanocortin-3 receptor, Sci Adv 4 (2018) eaat0866.

[83] G.M. Sutton, D. Perez-Tilve, R. Nogueiras, J. Fang, J.K. Kim, R.D. Cone, J.M. Gimble, M.H. Tschop, A.A. Butler, The melanocortin-3 receptor is required for entrainment to meal intake, J Neurosci 28(48) (2008) 12946-12955.

[84] K. Begriche, O.J. Marston, J. Rossi, L.K. Burke, P. McDonald, L.K. Heisler, A.A. Butler, Melanocortin-3 receptors are involved in adaptation to restricted feeding, Genes Brain Behav 11(3) (2012) 291-302.

[85] M. Lee, A. Kim, I.M. Conwell, V. Hruby, A. Mayorov, M. Cai, S.L. Wardlaw, Effects of selective modulation of the central melanocortin-3-receptor on food intake and hypothalamic POMC expression, Peptides 29(3) (2008) 440-447.

[86] D.L. Marks, V. Hruby, G. Brookhart, R.D. Cone, The regulation of food intake by selective stimulation of the type 3 melanocortin receptor (MC3R), Peptides 27(2) (2006) 259-264.

[87] D.W. Bowden, M. Sale, T.D. Howard, A. Qadri, B.J. Spray, C.B. Rothschild, G. Akots, S.S. Rich, B.I. Freedman, Linkage of genetic markers on human chromosomes 20 and 12 to NIDDM in Caucasian sib pairs with a history of diabetic nephropathy, Diabetes 46(5) (1997) 882-886.

[88] S. Ghosh, R.M. Watanabe, E.R. Hauser, T. Valle, V.L. Magnuson, M.R. Erdos, C.D. Langefeld, J. Balow, Jr., D.S. Ally, K. Kohtamaki, P. Chines, G. Birznieks, H.S. Kaleta, A. Musick, C. Te, J. Tannenbaum, W. Eldridge, S. Shapiro, C. Martin, A. Witt, A. So, J. Chang, B. Shurtleff, R. Porter, K. Kudelko, A. Unni, L. Segal, R. Sharaf, J. Blaschak-Harvan, J. Eriksson, T. Tenkula, G. Vidgren, C. Ehnholm, E. Tuomilehto-Wolf, W. Hagopian, T.A. Buchanan, J. Tuomilehto, R.N. Bergman, F.S. Collins, M. Boehnke, Type 2 diabetes: evidence for linkage on chromosome 20 in 716 Finnish affected sib pairs, Proc Natl Acad Sci U S A 96(5) (1999) 2198-2203.

[89] L. Ji, M. Malecki, J.H. Warram, Y. Yang, S.S. Rich, A.S. Krolewski, New susceptibility locus for NIDDM is localized to human chromosome 20q, Diabetes 46(5) (1997) 876-881.

[90] A.V. Lembertas, L. Perusse, Y.C. Chagnon, J.S. Fisler, C.H. Warden, D.A. Purcell-Huynh, F.T. Dionne, J. Gagnon, A. Nadeau, A.J. Lusis, C. Bouchard, Identification of an obesity quantitative trait locus on mouse chromosome 2 and evidence of linkage to body fat and insulin on the human homologous region 20q, J Clin Invest 100(5) (1997) 1240-1247.

[91] H. Zouali, E.H. Hani, A. Philippi, N. Vionnet, J.S. Beckmann, F. Demenais, P. Froguel, A susceptibility locus for early-onset non-insulin dependent (type 2) diabetes mellitus maps to chromosome 20q, proximal to the phosphoenolpyruvate carboxykinase gene, Human Molecular Genetics 6(9) (1997) 1401-1408.

[92] W.D. Li, E.J. Joo, E.B. Furlong, M. Galvin, K. Abel, C.J. Bell, R.A. Price, Melanocortin 3 receptor (MC3R) gene variants in extremely obese women, Int J Obes Relat Metab Disord 24(2) (2000) 206-210.

[93] E.H. Hani, S. Dupont, E. Durand, C. Dina, S. Gallina, I. Gantz, P. Froguel, Naturally occurring mutations in the melanocortin receptor 3 gene are not associated with type 2 diabetes mellitus in French Caucasians, J Clin Endocrinol Metab 86(6) (2001) 2895-2898.

[94] A.P. Demidowich, J.Y. Jun, J.A. Yanovski, Polymorphisms and mutations in the melanocortin-3 receptor and their relation to human obesity, Biochim Biophys Acta 1863 (2017) 2468-2476.

[95] M. Rached, A. Buronfosse, M. Begeot, A. Penhoat, Inactivation and intracellular retention of the human I183N mutated melanocortin 3 receptor associated with obesity, Biochim Biophys Acta 1689(3) (2004) 229-234.

[96] Y.X. Tao, D.L. Segaloff, Functional characterization of melanocortin-3 receptor variants identify a loss-of-function mutation involving an amino acid critical for G protein-coupled receptor activation, J Clin Endocrinol Metab 89(8) (2004) 3936-3942.

[97] Y.S. Lee, L.K. Poh, B.L. Kek, K.Y. Loke, The role of melanocortin 3 receptor gene in childhood obesity, Diabetes 56(10) (2007) 2622-2630.

[98] Y.X. Tao, Functional characterization of novel melanocortin-3 receptor mutations identified from obese subjects, Biochim Biophys Acta 1772(10) (2007) 1167-1174.

[99] M. Mencarelli, G.E. Walker, S. Maestrini, L. Alberti, B. Verti, A. Brunani, M.L. Petroni, M. Tagliaferri, A. Liuzzi, A.M. Di Blasio, Sporadic mutations in melanocortin receptor 3 in morbid obese individuals, Eur J Hum Genet 16(5) (2008) 581-586.

[100] J. Cieslak, K.A. Majewska, A. Tomaszewska, B. Skowronska, P. Fichna, M. Switonski, Common polymorphism (81Val>Ile) and rare mutations (257Arg>Ser and 335Ile>Ser) of the MC3R gene in obese Polish children and adolescents, Mol Biol Rep 40(12) (2013) 6893-6898.

[101] Y.S. Lee, L.K. Poh, K.Y. Loke, A novel melanocortin 3 receptor gene (MC3R) mutation associated with severe obesity, J Clin Endocrinol Metab 87(3) (2002) 1423-1426.

[102] M. Mencarelli, B. Dubern, R. Alili, S. Maestrini, L. Benajiba, M. Tagliaferri, P. Galan, M. Rinaldi, C. Simon, P. Tounian, S. Hercberg, A. Liuzzi, A.M. Di Blasio, K. Clement, Rare melanocortin-3 receptor mutations with in vitro functional consequences are associated with human obesity, Human Molecular Genetics 20(2) (2011) 392-399.

[103] M. Lek, K.J. Karczewski, E.V. Minikel, K.E. Samocha, E. Banks, T. Fennell, A.H. O'Donnell-Luria, J.S. Ware, A.J. Hill, B.B. Cummings, T. Tukiainen, D.P. Birnbaum, J.A. Kosmicki, L.E. Duncan, K. Estrada, F. Zhao, J. Zou, E. Pierce-Hoffman, J. Berghout, D.N. Cooper, N. Deflaux, M. DePristo, R. Do, J. Flannick, M. Fromer, L. Gauthier, J. Goldstein, N. Gupta, D. Howrigan, A. Kiezun, M.I. Kurki, A.L. Moonshine, P. Natarajan, L. Orozco, G.M. Peloso, R. Poplin, M.A. Rivas, V. Ruano-Rubio, S.A. Rose, D.M. Ruderfer, K. Shakir, P.D. Stenson, C. Stevens, B.T. Thomas, G. Tiao, M.T. Tusie-Luna, B. Weisburd, H. Won, D. Yu, D.M. Altshuler, D. Ardissino, M. Boehnke, J. Danesh, S. Donnelly, R. Elosua, J.C. Florez, S.B. Gabriel, G. Getz, S.J. Glatt, C.M. Hultman, S. Kathiresan, M. Laakso, S. McCarroll, M.I. McCarthy, D. McGovern, R. McPherson, B.M. Neale, A. Palotie, S.M. Purcell, D. Saleheen, J.M. Scharf, P. Sklar, P.F. Sullivan, J. Tuomilehto, M.T. Tsuang, H.C. Watkins, J.G. Wilson, M.J.

Daly, D.G. MacArthur, E.A. Consortium, Analysis of protein-coding genetic variation in 60,706 humans, Nature 536(7616) (2016) 285-297.

[104] G. Leoni, H.B. Patel, A.L. Sampaio, F.N. Gavins, J.F. Murray, P. Grieco, S.J. Getting, M. Perretti, Inflamed phenotype of the mesenteric microcirculation of melanocortin type 3 receptor-null mice after ischemia-reperfusion, FASEB J 22(12) (2008) 4228-4238.

[105] S.C. Land, Inhibition of cellular and systemic inflammation cues in human bronchial epithelial cells by melanocortin-related peptides: mechanism of KPV action and a role for MC3R agonists, Int J Physiol Pathophysiol Pharmacol 4(2) (2012) 59-73.

[106] H.B. Patel, M. Bombardieri, A.L.F. Sampaio, F. D'Acquisto, M. Gray, P. Grieco, S.J. Getting, C. Pitzalis, M. Perretti, Anti-inflammatory and antiosteoclastogenesis properties of endogenous melanocortin receptor type 3 in experimental arthritis, FASEB J 24 (2010) 4835-4843.

[107] S.J. Getting, R.J. Flower, M. Perretti, Agonism at melanocortin receptor type 3 on macrophages inhibits neutrophil influx, Inflamm Res 48 Suppl 2 (1999) S140-1.

[108] S. Taherzadeh, S. Sharma, V. Chhajlani, I. Gantz, N. Rajora, M.T. Demitri, L. Kelly, H. Zhao, T. Ichiyama, A. Catania, J.M. Lipton, α-MSH and its receptors in regulation of tumor necrosis factor-α production by human monocyte/macrophages, Am J Physiol 276(5 Pt 2) (1999) R1289-R1294.

[109] S.J. Getting, C.W. Lam, G. Leoni, F.N. Gavins, P. Grieco, M. Perretti, [D-Trp^{8}]-γ-melanocyte-stimulating hormone exhibits anti-inflammatory efficacy in mice bearing a nonfunctional MC1R (recessive yellow e/e mouse), Mol Pharmacol 70(6) (2006) 1850-1855.

[110] S.J. Getting, M. Perretti, Arthritic diseases: melanocortin type 3 receptor agonists as potential therapeutics, Curr Opin Investig Drugs 2(8) (2001) 1064-9.

[111] S.J. Getting, H.B. Schioth, M. Perretti, Dissection of the anti-inflammatory effect of the core and C-terminal (KPV) alpha-melanocyte-stimulating hormone peptides, J Pharmacol Exp Ther 306(2) (2003) 631-637.

[112] K.G. Mountjoy, C.S. Jenny Wu, L.M. Dumont, J.M. Wild, Melanocortin-4 receptor messenger ribonucleic acid expression in rat cardiorespiratory, musculoskeletal, and integumentary systems, Endocrinology 144(12) (2003) 5488-5496.

[113] J. Klovins, T. Haitina, A. Ringholm, M. Lowgren, D. Fridmanis, M. Slaidina, S. Stier, H.B. Schioth, Cloning of two melanocortin (MC) receptors in spiny dogfish: MC3 receptor in cartilaginous fish shows high affinity to ACTH-derived peptides while it has lower preference to γ-MSH, Eur J Biochem 271(21) (2004) 4320-4331.

[114] R. Wei, D. Yuan, C. Zhou, T. Wang, F. Lin, H. Chen, H. Wu, Z. Xin, S. Yang, D. Chen, Y. Wang, J. Liu, Y. Gao, Z. Li, Cloning, distribution and effects of fasting status of melanocortin 4 receptor (MC4R) in *Schizothorax prenanti*, Gene 532(1) (2013) 100-107.

[115] J.T. Li, Z. Yang, H.P. Chen, C.H. Zhu, S.P. Deng, G.L. Li, Y.X. Tao, Molecular cloning, tissue distribution, and pharmacological characterization of melanocortin-4 receptor in spotted scat, *Scatophagus argus*, Gen Comp Endocrinol 230-231 (2016) 143 -152.

[116] L. Li, Z. Yang, Y.P. Zhang, S. He, X.F. Liang, Y.X. Tao, Molecular cloning, tissue distribution, and pharmacological characterization of melanocortin-4 receptor in grass carp (*Ctenopharyngodon idella*), Domest Anim Endocrinol 59 (2017) 140-151.

[117] Y.Z. Rao, R. Chen, Y. Zhang, Y.X. Tao, Orange-spotted grouper melanocortin-4 receptor: Modulation of signaling by MRAP2, Gen Comp Endocrinol 284 (2019) 113234.

[118] K.Q. Zhang, Z.S. Hou, H.S. Wen, Y. Li, X. Qi, W.J. Li, Y.X. Tao, Melanocortin-4 receptor in spotted sea bass, *Lateolabrax maculatus*: Cloning, tissue distribution, physiology, and pharmacology, Front Endocrinol (Lausanne) 10 (2019) 705.

[119] A. Kask, L. Rago, F. Mutulis, R. Pahkla, J.E. Wikberg, H.B. Schioth, Selective antagonist for the melanocortin 4 receptor (HS014) increases food intake in free-feeding rats, Biochem Biophys Res Commun 245(1) (1998) 90-93.

[120] A. Kask, F. Mutulis, R. Muceniece, R. Pahkla, I. Mutule, J.E. Wikberg, L. Rago, H.B. Schioth, Discovery of a novel superpotent and selective melanocortin-4 receptor antagonist (HS024): evaluation in vitro and in vivo, Endocrinology 139(12) (1998) 5006-5014.

[121] A.V. Vergoni, A. Bertolini, J.E. Wikberg, H.B. Schioth, Selective melanocortin MC4 receptor blockage reduces immobilization stress-induced anorexia in rats, Eur J Pharmacol 369(1) (1999) 11-15.

[122] S.C. Benoit, M.W. Schwartz, J.L. Lachey, M.M. Hagan, P.A. Rushing, K.A. Blake, K.A. Yagaloff, G. Kurylko, L. Franco, W. Danhoo, R.J. Seeley, A novel selective melanocortin-4 receptor agonist reduces food intake in rats and mice without producing aversive consequences, J Neurosci 20(9) (2000) 3442-3448.

[123] B.L. Palucki, M.K. Park, R.P. Nargund, Z. Ye, I.K. Sebhat, P.G. Pollard, R.N. Kalyani, R. Tang, T. Macneil, D.H. Weinberg, A. Vongs, C.I. Rosenblum, G.A. Doss, R.R. Miller, R.A. Stearns, Q. Peng, C. Tamvakopoulos, E. McGowan, W.J. Martin, J.M. Metzger, C.A. Shepherd, A.M. Strack, D.E. Macintyre, L.H. Van der Ploeg, A.A. Patchett, Discovery of (2S)-N-[(1R)-2-[4-cyclohexyl-4-[[(1,1-dimethylethyl)amino]carbonyl]-1-pipe ridinyl]-1-[(4-fluorophenyl)methyl]-2-oxoethyl]-4-methyl-2-piperazinecarbo xamide (MB243), a potent and selective melanocortin subtype-4 receptor agonist, Bioorg Med Chem Lett 15(1) (2005) 171-175.

[124] G.S. Yeo, I.S. Farooqi, S. Aminian, D.J. Halsall, R.G. Stanhope, S. O'Rahilly, A frameshift mutation in *MC4R* associated with dominantly inherited human obesity, Nat Genet 20(2) (1998) 111-112.

[125] C. Vaisse, K. Clement, B. Guy-Grand, P. Froguel, A frameshift mutation in human *MC4R* is associated with a dominant form of obesity, Nat Genet 20(2) (1998) 113-114.

[126] I.S. Farooqi, G.S. Yeo, J.M. Keogh, S. Aminian, S.A. Jebb, G. Butler, T. Cheetham, S. O'Rahilly, Dominant and recessive inheritance of morbid obesity associated with melanocortin 4 receptor deficiency, J Clin Invest 106(2) (2000) 271-279.

[127] I.S. Farooqi, J.M. Keogh, G.S. Yeo, E.J. Lank, T. Cheetham, S. O'Rahilly, Clinical spectrum of obesity and mutations in the melanocortin 4 receptor gene, N Engl J Med 348(12) (2003) 1085-1095.

[128] B. Dubern, S. Bisbis, H. Talbaoui, J. Le Beyec, P. Tounian, J.M. Lacorte, K. Clement, Homozygous null mutation of the melanocortin-4 receptor and severe early-onset obesity, J Pediatr 150(6) (2007) 613-617, 617 e1.

[129] H. Vollbach, S. Brandt, G. Lahr, C. Denzer, J. Von Schnurbein, K.M. Debatin, M. Wabitsch, Prevalence and phenotypic characterization of MC4R variants in a large pediatric cohort, Int J Obes 41(1) (2017) 13-22.

[130] E.W. Iepsen, J. Zhang, M. Hollensted, S. Madsbad, T. Hansen, J.J. Holst, N.R. Jørgensen, J.C. Holm, S.S. Torekov, Adults with pathogenic MC4R mutations have increased final height and thereby increased bone mass, J Bone Miner Metab 38(1) (2020) 117-125.

[131] A. Hinney, A.L. Volckmar, N. Knoll, Melanocortin-4 receptor in energy homeostasis and obesity pathogenesis, Prog Mol Biol Transl Sci 114 (2013) 147-191.

[132] J.M. Cerdá-Reverter, A. Ringholm, H.B. Schioth, R.E. Peter, Molecular cloning, pharmacological characterization, and brain mapping of the melanocortin 4 receptor in the goldfish: involvement in the control of food intake, Endocrinology 144(6) (2003) 2336-2349.

[133] J.M. Cerdá-Reverter, H.B. Schioth, R.E. Peter, The central melanocortin system regulates food intake in goldfish, Regul Pept 115(2) (2003) 101-113.

[134] J. Schjolden, H.B. Schioth, D. Larhammar, S. Winberg, E.T. Larson, Melanocortin peptides affect the motivation to feed in rainbow trout (*Oncorhynchus mykiss*), Gen Comp Endocrinol 160(2) (2009) 134-138.

[135] I. Gantz, Y. Shimoto, Y. Konda, H. Miwa, C.J. Dickinson, T. Yamada, Molecular cloning, expression, and characterization of a fifth melanocortin receptor, Biochem Biophys Res Commun 200(3) (1994) 1214-1220.

[136] T. Yada, S. Moriyama, Y. Suzuki, T. Azuma, A. Takahashi, S. Hirose, N. Naito, Relationships between obesity and metabolic hormones in the "cobalt" variant of rainbow trout, Gen Comp Endocrinol 128(1) (2002) 36-43.

[137] A.C. Aspiras, N. Rohner, B. Martineau, R.L. Borowsky, C.J. Tabin, Melanocortin 4 receptor mutations contribute to the adaptation of cavefish to nutrient-poor conditions, Proc Natl Acad Sci U S A 112(31) (2015) 9668-9673.

[138] J.M. Cerdá-Reverter, M.J. Agulleiro, R.G. R, E. Sanchez, R. Ceinos, J. Rotllant, Fish melanocortin system, Eur J Pharmacol 660(1) (2011) 53-60.

[139] Y. Zhang, H.S. Wen, Y. Li, L.K. Lyu, Z.X. Zhang, X.J. Wang, J.S. Li, Y.X. Tao, X. Qi, Melanocortin-4 receptor regulation of reproductive function in black rockfish (*Sebastes schlegelii*), Gene 741 (2020) 144541.

[140] K.P. Lampert, C. Schmidt, P. Fischer, J.N. Volff, C. Hoffmann, J. Muck, M.J. Lohse, M.J. Ryan, M. Schartl, Determination of onset of sexual maturation and mating behavior by melanocortin receptor 4 polymorphisms, Curr Biol 20(19) (2010) 1729-1734.

[141] C. Zhang, P.M. Forlano, R.D. Cone, AgRP and POMC neurons are hypophysiotropic and coordinately regulate multiple endocrine axes in a larval teleost, Cell Metab 15(2) (2012) 256-264.

[142] J.N. Volff, Y. Selz, C. Hoffmann, A. Froschauer, C. Schultheis, C. Schmidt, Q. Zhou, W. Bernhardt, R. Hanel, A. Bohne, F. Brunet, B. Segurens, A. Couloux, S. Bernard-Samain, V. Barbe, C. Ozouf-Costaz, D. Galiana, M.J. Lohse, M. Schartl, Gene amplification and functional diversification of melanocortin 4 receptor at an extremely polymorphic locus controlling sexual maturation in the platyfish, Genetics 195(4) (2013) 1337-52.

[143] C.C. Smith, R.M. Harris, K.P. Lampert, M. Schartl, H.A. Hofmann, M.J. Ryan, Copy number variation in the melanocortin 4 receptor gene and alternative reproductive tactics the swordtail *Xiphophorus multilineatus*, Environ Biol Fishes 98(1) (2015) 23-33.

[144] D.N. Jiang, J.T. Li, Y.X. Tao, H.P. Chen, S.P. Deng, C.H. Zhu, G.L. Li, Effects of melanocortin-4 receptor agonists and antagonists on expression of genes related to reproduction in spotted scat, *Scatophagus argus*, J Comp Physiol B 187 (2017) 603-612.

[145] R.Q. Liu, K. Du, J. Ormanns, M.C. Adolfi, M. Schartl, Melanocortin 4 receptor signaling and puberty onset regulation in *Xiphophorus* swordtails, Gen Comp Endocrinol 295 (2020) 113521.

[146] S. Srinivasan, C. Lubrano-Berthelier, C. Govaerts, F. Picard, P. Santiago, B.R. Conklin, C. Vaisse, Constitutive activity of the melanocortin-4 receptor is maintained by its N-terminal

domain and plays a role in energy homeostasis in humans, J Clin Invest 114(8) (2004) 1158-1164.

[147] Y.X. Tao, Constitutive activity in melanocortin-4 receptor: biased signaling of inverse agonists, Adv Pharmacol 70 (2014) 135-154.

[148] T.L. Yi, L.K. Yang, G.L. Ruan, D.Q. Yang, Y.X. Tao, Melanocortin-4 receptor in swamp eel (*Monopterus albus*): Cloning, tissue distribution, and pharmacology, Gene 678 (2018) 79-89.

[149] Z. Yang, X.F. Liang, G.L. Li, Y.X. Tao, Biased signaling in fish melanocortin-4 receptors (MC4Rs): Divergent pharmacology of four ligands on spotted scat (*Scatophagus argus*) and grass carp (*Ctenopharyngodon idella*) MC4Rs, Mol Cell Endocrinol 515 (2020) 110929.

[150] B.J. Renquist, C. Zhang, S.Y. Williams, R.D. Cone, Development of an assay for high-throughput energy expenditure monitoring in the zebrafish, Zebrafish 10(3) (2013) 343-352.

[151] E.A. Newman, B.X. Chai, W. Zhang, J.Y. Li, J.B. Ammori, M.W. Mulholland, Activation of the melanocortin-4 receptor mobilizes intracellular free calcium in immortalized hypothalamic neurons, J Surg Res 132(2) (2006) 201-207.

[152] S. Sharma, S. Thibodeau, J. Lytton, Signal pathway analysis of selected obesity-associated melanocortin-4 receptor class V mutants, Biochim Biophys Acta Mol Basis Dis 1866(8) (2020) 165835.

[153] T.R. Büch, D. Heling, E. Damm, T. Gudermann, A. Breit, Pertussis toxin-sensitive signaling of melanocortin-4 receptors in hypothalamic GT1-7 cells defines agouti-related protein as a biased agonist, J Biol Chem 284(39) (2009) 26411-26420.

[154] Y.Q. Li, Y. Shrestha, M. Pandey, M. Chen, A. Kablan, O. Gavrilova, S. Offermanns, L.S. Weinstein, $G_{q/11}\alpha$ and $G_s\alpha$ mediate distinct physiological responses to central melanocortins, J Clin Invest 126(1) (2016) 40-49.

[155] K. Clément, H. Biebermann, I.S. Farooqi, L. Van der Ploeg, B. Wolters, C. Poitou, L. Puder, F. Fiedorek, K. Gottesdiener, G. Kleinau, N. Heyder, P. Scheerer, U. Blume-Peytavi, I. Jahnke, S. Sharma, J. Mokrosinski, S. Wiegand, A. Müller, K. Weiß, K. Mai, J. Spranger, A. Grüters, O. Blankenstein, H. Krüde, P. Kühnen, MC4R agonism promotes durable weight loss in patients with leptin receptor deficiency, Nat Med 24(5) (2018) 551-555.

[156] A. Inoue, F. Raimondi, F.M.N. Kadji, G. Singh, T. Kishi, A. Uwamizu, Y. Ono, Y. Shinjo, S. Ishida, N. Arang, K. Kawakami, J.S. Gutkind, J. Aoki, R.B. Russell, Illuminating G-protein-coupling selectivity of GPCRs, Cell 177(7) (2019) 1933-1947 e25.

[157] D. Daniels, C.S. Patten, J.D. Roth, D.K. Yee, S.J. Fluharty, Melanocortin receptor signaling through mitogen-activated protein kinase in vitro and in rat hypothalamus, Brain Res 986(1-2) (2003) 1-11.

[158] A. Vongs, N.M. Lynn, C.I. Rosenblum, Activation of MAP kinase by MC4-R through PI3 kinase, Regul Pept 120(1-3) (2004) 113-118.

[159] G.M. Sutton, B. Duos, L.M. Patterson, H.R. Berthoud, Melanocortinergic modulation of cholecystokinin-induced suppression of feeding through extracellular signal-regulated kinase signaling in rat solitary nucleus, Endocrinology 146(9) (2005) 3739-47.

[160] B. Chai, J.Y. Li, W. Zhang, E. Newman, J. Ammori, M.W. Mulholland, Melanocortin-4 receptor-mediated inhibition of apoptosis in immortalized hypothalamic neurons via mitogen-activated protein kinase, Peptides 27(11) (2006) 2846-2857.

[161] E. Damm, T.R. Buech, T. Gudermann, A. Breit, Melanocortin-induced PKA activation inhibits AMPK activity via ERK-1/2 and LKB-1 in hypothalamic GT1-7 cells, Mol Endocrinol 26(4) (2012) 643-654.

[162] L.A. Lotta, J. Mokrosinski, E. Mendes de Oliveira, C. Li, S.J. Sharp, J. Luan, B. Brouwers, V. Ayinampudi, N. Bowker, N. Kerrison, V. Kaimakis, D. Hoult, I.D. Stewart, E. Wheeler, F.R. Day, J.R.B. Perry, C. Langenberg, N.J. Wareham, I.S. Farooqi, Human gain-of-function *MC4R* variants show signaling bias and protect against obesity, Cell 177(3) (2019) 597-607 e9.

[163] Y. Minokoshi, T. Alquier, N. Furukawa, Y.B. Kim, A. Lee, B. Xue, J. Mu, F. Foufelle, P. Ferre, M.J. Birnbaum, B.J. Stuck, B.B. Kahn, AMP-kinase regulates food intake by responding to hormonal and nutrient signals in the hypothalamus, Nature 428(6982) (2004) 569-74.

[164] B. Chai, J.Y. Li, W. Zhang, H. Wang, M.W. Mulholland, Melanocortin-4 receptor activation inhibits c-Jun N-terminal kinase activity and promotes insulin signaling, Peptides 30(6) (2009) 1098-1104.

[165] M. Ghamari-Langroudi, G.J. Digby, J.A. Sebag, G.L. Millhauser, R. Palomino, R. Matthews, T. Gillyard, B.L. Panaro, I.R. Tough, H.M. Cox, J.S. Denton, R.D. Cone, G-protein-independent coupling of MC4R to Kir7.1 in hypothalamic neurons, Nature 520 (2015) 94-98.

[166] Z. Yang, Y.X. Tao, Biased signaling initiated by agouti-related peptide through human melanocortin-3 and -4 receptors, Biochim Biophys Acta 1862(9) (2016) 1485-1494.

[167] E.J.P. Anderson, M. Ghamari-Langroudi, I. Cakir, M.J. Litt, V. Chen, R.E. Reggiardo, G.L. Millhauser, R.D. Cone, Late onset obesity in mice with targeted deletion of potassium inward rectifier Kir7.1 from cells expressing the melanocortin-4 receptor, J Neuroendocrinol 31(1) (2019) e12670.

[168] Y. Konda, I. Gantz, J. DelValle, Y. Shimoto, H. Miwa, T. Yamada, Interaction of dual intracellular signaling pathways activated by the melanocortin-3 receptor, J Biol Chem 269(18) (1994) 13162-13166.

[169] B. Chai, J.Y. Li, W. Zhang, J.B. Ammori, M.W. Mulholland, Melanocortin-3 receptor activates MAP kinase via PI3 kinase, Regul Pept 139(1-3) (2007) 115-121.

[170] D.C. Nyan, R. Anbazhagan, C.A. Hughes-Darden, S.J. Wachira, Endosomal colocalization of melanocortin-3 receptor and β-arrestins in CAD cells with altered modification of AKT/PKB, Neuropeptides 42(3) (2008) 355-366.

[171] K.G. Mountjoy, P.L. Kong, J.A. Taylor, D.H. Willard, W.O. Wilkison, Melanocortin receptor-mediated mobilization of intracellular free calcium in HEK293 cells, Physiol Genomics 5(1) (2001) 11-19.

[172] S.J. Wachira, C.A. Hughes-Darden, C.V. Taylor, R. Ochillo, T.J. Robinson, Evidence for the interaction of protein kinase C and melanocortin 3-receptor signaling pathways, Neuropeptides 37(4) (2003) 201-10.

[173] A.J. Clark, A. Weber, Adrenocorticotropin insensitivity syndromes, Endocr Rev 19(6) (1998) 828-843.

[174] A.J. Clark, L.A. Metherell, M.E. Cheetham, A. Huebner, Inherited ACTH insensitivity illuminates the mechanisms of ACTH action, Trends Endocrinol Metab 16(10) (2005) 451-457.

[175] L.A. Noon, J.M. Franklin, P.J. King, N.J. Goulding, L. Hunyady, A.J. Clark, Failed export of the adrenocorticotrophin receptor from the endoplasmic reticulum in non-adrenal cells: evidence in support of a requirement for a specific adrenal accessory factor, J Endocrinol 174(1) (2002) 17-25.

[176] T. Novoselova, P. King, L. Guasti, L.A. Metherell, A.J.L. Clark, L.F. Chan, ACTH signalling and adrenal development: lessons from mouse models, Endocr Connect 8 (2019) R122-R130.

[177] J.A. Sebag, P.M. Hinkle, Regions of melanocortin 2 (MC2) receptor accessory protein necessary for dual topology and MC2 receptor trafficking and signaling, J Biol Chem 284(1) (2009) 610-618.

[178] S.N. Cooray, I. Almiro Do Vale, K.Y. Leung, T.R. Webb, J.P. Chapple, M. Egertova, M.E. Cheetham, M.R. Elphick, A.J. Clark, The melanocortin 2 receptor accessory protein exists as a homodimer and is essential for the function of the melanocortin 2 receptor in the mouse Y1 cell line, Endocrinology 149(4) (2008) 1935-1941.

[179] S. Roy, S.J. Roy, S. Pinard, M.J. Agulleiro, J.M. Cerda-Reverter, J.L. Parent, N. Gallo-Payet, The C-terminal domains of melanocortin-2 receptor (MC2R) accessory proteins (MRAP1) influence their localization and ACTH-induced cAMP production, Gen Comp Endocrinol 176(2) (2012) 265-74.

[180] J.A. Sebag, P.M. Hinkle, Opposite effects of the melanocortin-2 (MC2) receptor accessory protein MRAP on MC2 and MC5 receptor dimerization and trafficking, J Biol Chem 284(34) (2009) 22641-22648.

[181] R.M. Dores, E. Chapa, Hypothesis and Theory: Evaluating the co-evolution of the melanocortin-2 receptor and the accessory protein MRAP1, Front Endocrinol (Lausanne) 12 (2021) 747843.

[182] S. Malik, T.M. Dolan, Z.J. Maben, P.M. Hinkle, Adrenocorticotropic hormone (ACTH) responses require actions of the melanocortin-2 receptor accessory protein on the extracellular surface of the plasma membrane, J Biol Chem 290(46) (2015) 27972-27985.

[183] J.A. Sebag, P.M. Hinkle, Regulation of G protein-coupled receptor signaling: specific dominant-negative effects of melanocortin 2 receptor accessory protein 2, Sci Signal 3(116) (2010) ra28.

[184] T.R. Webb, L. Chan, S.N. Cooray, M.E. Cheetham, J.P. Chapple, A.J. Clark, Distinct melanocortin 2 receptor accessory protein domains are required for melanocortin 2 receptor interaction and promotion of receptor trafficking, Endocrinology 150(2) (2009) 720-6.

[185] T.V. Novoselova, M. Hussain, P.J. King, L. Guasti, L.A. Metherell, M. Charalambous, A.J.L. Clark, L.F. Chan, MRAP deficiency impairs adrenal progenitor cell differentiation and gland zonation, FASEB J (2018) fj201701274RR.

[186] X. Zhang, A.M. Saarinen, L.E. Campbell, E.A. De Filippis, J. Liu, Regulation of Lipolytic Response and Energy Balance by Melanocortin 2 Receptor Accessory Protein (MRAP) in Adipocytes, Diabetes 67(2) (2018) 222-234.

[187] U.W. Khan, O. Overli, P.M. Hinkle, F.A. Pasha, I.B. Johansen, I. Berget, P.I. Silva, S. Kittilsen, E. Hoglund, S.W. Omholt, D.I. Vage, A novel role for pigment genes in the stress response in rainbow trout (Oncorhynchus mykiss), Sci Rep 6 (2016) 28969.

[188] X. Tai, Y. Zhang, X. Li, J. Yao, J. Liu, J. Lyu, G. Lin, C. Zhang, Pharmacological modulation of melanocortin 1 receptor signaling by Mrap proteins in Xenopus tropicalis, Front Endocrinol (Lausanne) (2022) 1023.

[189] J. Liang, L. Li, X. Jin, B. Xu, L. Pi, S. Liu, W. Zhu, C. Zhang, B. Luan, L. Gong, C. Zhang, Pharmacological effect of human melanocortin-2 receptor accessory protein 2 variants on hypothalamic melanocortin receptors, Endocrine 61(1) (2018) 94-104.

[190] X. Tai, S. Xue, C. Zhang, Y. Liu, J. Chen, Y. Han, G. Lin, C. Zhang, Pharmacological evaluation of MRAP proteins on Xenopus neural melanocortin signaling, J Cell Physiol 236(9) (2021) 6344-6361.

[191] E.I. Kay, R. Botha, J.M. Montgomery, K.G. Mountjoy, hMRAPα, but not hMRAP2, enhances hMC4R constitutive activity in HEK293 cells and this is not dependent on hMRAPα induced changes in hMC4R complex N-linked glycosylation, PloS One 10(10) (2015) e0140320.

[192] R.L. Ji, Y.X. Tao, Regulation of Melanocortin-3 and -4 Receptors by Isoforms of Melanocortin-2 Receptor Accessory Protein 1 and 2, Biomolecules 12(2) (2022).

[193] M. Wang, J. Xu, X.W. Lei, C. Zhang, S.Y. Liu, L.N. Jin, C. Zhang, Selective Interactions of Mouse Melanocortin Receptor Accessory Proteins with Somatostatin Receptors, Cells 11(2) (2022).

[194] L.M. McLatchie, N.J. Fraser, M.J. Main, A. Wise, J. Brown, N. Thompson, R. Solari, M.G. Lee, S.M. Foord, RAMPs regulate the transport and ligand specificity of the calcitonin-receptor-like receptor, Nature 393 (1998) 333-339.

[195] D.L. Hay, A.A. Pioszak, Receptor Activity-Modifying Proteins (RAMPs): New Insights and Roles, Annu Rev Pharmacol Toxicol 56 (2016) 469-87.

[196] E. Lorenzen, T. Dodig-Crnkovic, I.B. Kotliar, E. Pin, E. Ceraudo, R.D. Vaughan, M. Uhlen, T. Huber, J.M. Schwenk, T.P. Sakmar, Multiplexed analysis of the secretin-like GPCR-RAMP interactome, Sci Adv 5(9) (2019) eaaw2778.

[197] R. Valsalan, A. Krishnan, M.S. Almen, R. Fredriksson, H.B. Schioth, Early vertebrate origin of melanocortin 2 receptor accessory proteins (MRAPs), Gen Comp Endocrinol 188 (2013) 123-132.

[198] R.M. Dores, Y. Garcia, Views on the co-evolution of the melanocortin-2 receptor, MRAPs, and the hypothalamus/pituitary/adrenal-interrenal axis, Mol Cell Endocrinol 408 (2015) 12-22.

[199] R.M. Dores, Hypothesis and theory: Revisiting views on the co-evolution of the melanocortin receptors and the accessory proteins, MRAP1 and MRAP2, Front Endocrinol (Lausanne) 7 (2016) 79.

[200] R.J. Gorrigan, L. Guasti, P. King, A.J. Clark, L.F. Chan, Localisation of the melanocortin-2-receptor and its accessory proteins in the developing and adult adrenal gland, Journal of Molecular Endocrinolgoy 46(3) (2011) 227-232.

[201] G. Bruschetta, J.D. Kim, S. Diano, L.F. Chan, Overexpression of melanocortin 2 receptor accessory protein 2 (MRAP2) in adult paraventricular MC4R neurons regulates energy intake and expenditure, Mol Metab 18 (2018) 79-87.

[202] D. Srisai, T.C. Yin, A.A. Lee, A.A.J. Rouault, N.A. Pearson, J.L. Grobe, J.A. Sebag, MRAP2 regulates ghrelin receptor signaling and hunger sensing, Nat Commun 8(1) (2017) 713.

[203] A.A.J. Rouault, L.K. Rosselli-Murai, C.C. Hernandez, L.E. Gimenez, G.G. Tall, J.A. Sebag, The GPCR accessory protein MRAP2 regulates both biased signaling and constitutive activity of the ghrelin receptor GHSR1a, Sci Signal 13(613) (2020).

[204] A.A.J. Rouault, A.A. Lee, J.A. Sebag, Regions of MRAP2 required for the inhibition of orexin and prokineticin receptor signaling, Biochim Biophys Acta Mol Cell Res 1864(12) (2017) 2322-2329.

[205] A.L. Chaly, D. Srisai, E.E. Gardner, J.A. Sebag, The Melanocortin Receptor Accessory Protein 2 promotes food intake through inhibition of the Prokineticin Receptor-1, eLife 5 (2016) e12397.

[206] L. Soletto, S. Hernandez-Balfago, A. Rocha, P. Scheerer, G. Kleinau, J.M. Cerdá-Reverter, Melanocortin receptor accessory protein 2-induced adrenocorticotropic hormone response of human melanocortin 4 receptor, J Endocr Soc 3(2) (2019) 314-323.

[207] M. Josep Agulleiro, R. Cortes, B. Fernandez-Duran, S. Navarro, R. Guillot, E. Meimaridou, A.J. Clark, J.M. Cerdá-Reverter, Melanocortin 4 receptor becomes an ACTH receptor by coexpression of melanocortin receptor accessory protein 2, Mol Endocrinol 27(11) (2013) 1934-1945.

[208] M. Zhu, B. Xu, M. Wang, S. Liu, Y. Zhang, C. Zhang, Pharmacological modulation of MRAP2 protein on melanocortin receptors in the sea lamprey, Endocr Connect 8 (2019) 378-388.

[209] M. Wang, Y.J. Chen, M. Zhu, B.X. Xu, W.X. Guo, Y.S. Lyu, C. Zhang, Pharmacological modulation of melanocortin-4 receptor by melanocortin receptor accessory protein 2 in Nile tilapia, Gen Comp Endocrinol 282 (2019) 113219.

[210] M. Habara, N. Mori, Y. Okada, K. Kawasumi, N. Nakao, Y. Tanaka, T. Arai, I. Yamamoto, Molecular characterization of feline melanocortin 4 receptor and melanocortin 2 receptor accessory protein 2, Gen Comp Endocrinol 261 (2018) 31-39.

[211] X. Wang, S. Xue, X. Lei, W. Song, L. Li, X. Li, Y. Fu, C. Zhang, H. Zhang, Y. Luo, M. Wang, G. Lin, C. Zhang, J. Guo, Pharmacological Evaluation of Melanocortin 2 Receptor Accessory Protein 2 on Axolotl Neural Melanocortin Signaling, Front Endocrinol (Lausanne) 13 (2022) 820896.

[212] R. Cortés, M.J. Agulleiro, S. Navarro, R. Guillot, E. Sánchez, J.M. Cerdá-Reverter, Melanocortin receptor accessory protein 2 (MRAP2) interplays with the zebrafish melanocortin 1 receptor (MC1R) but has no effect on its pharmacological profile, Gen Comp Endocrinol 201 (2014) 30-36.

[213] L.Q. Ji, Y.Z. Rao, Y. Zhang, R. Chen, Y.X. Tao, Regulation of melanocortin-1 receptor pharmacology by melanocortin receptor accessory protein 2 in orange-spotted grouper (*Epinephelus coioides*), Gen Comp Endocrinol 285 (2020) 113291.

[214] T. Liu, T.L. Yi, D.Q. Yang, Y.X. Tao, Regulation of melanocortin-5 receptor pharmacology by two isoforms of MRAP2 in ricefield eel (Monopterus albus), Gen Comp Endocrinol 314 (2021) 113928.

[215] R.M. Dores, M. Scuba-Gray, B. McNally, P. Davis, A. Takahashi, Evaluating the interactions between red stingray (*Dasyatis akajei*) melanocortin receptors and elephant shark (*Callorhinchus milii*) MRAP1 and MRAP2 following stimulation with either stingray ACTH(1-24) or stingray Des-Acetyl-αMSH: A pharmacological study in Chinese Hamster Ovary cells, Gen Comp Endocrinol 265 (2018) 133-140.

[216] E. Barney, M.R. Dores, D. McAvoy, P. Davis, R.C. Racareanu, A. Iki, S. Hyodo, R.M. Dores, Elephant shark melanocortin receptors: Novel interactions with MRAP1 and implication for the HPI axis, Gen Comp Endocrinol 272 (2019) 42-51.

[217] A.A.J. Rouault, P. Buscaglia, J.A. Sebag, MRAP2 inhibits beta-arrestin recruitment to the ghrelin receptor by preventing GHSR1a phosphorylation, J Biol Chem (2022) 102057.

[218] M. Wang, J. Xu, X. Lei, C. Zhang, K. Zhe, H. Lan, Q. Li, Identification of GLP1R and MCHR1 signaling as novel GPCR targets of MRAP2 protein, (2022).

[219] M. Uhlen, L. Fagerberg, B.M. Hallstrom, C. Lindskog, P. Oksvold, A. Mardinoglu, A. Sivertsson, C. Kampf, E. Sjostedt, A. Asplund, I. Olsson, K. Edlund, E. Lundberg, S. Navani, C.A. Szigyarto, J. Odeberg, D. Djureinovic, J.O. Takanen, S. Hober, T. Alm, P.H. Edqvist, H. Berling, H. Tegel, J. Mulder, J. Rockberg, P. Nilsson, J.M. Schwenk, M. Hamsten, K. von Feilitzen, M. Forsberg, L. Persson, F. Johansson, M. Zwahlen, G. von Heijne, J. Nielsen, F. Ponten, Proteomics. Tissue-based map of the human proteome, Science 347(6220) (2015) 1260419.

[220] N.N.A. Berruien, C.L. Smith, Emerging roles of melanocortin receptor accessory proteins (MRAP and MRAP2) in physiology and pathophysiology, Gene 757 (2020) 144949.

[221] A.L. Steiner, D.M. Kipnis, R. Utiger, C. Parker, Radioimmunoassay for the measurement of adenosine 3',5'-cyclic phosphate, Proc Natl Acad Sci U S A 64(1) (1969) 367-373.

[222] X.L. Mo, R. Yang, Y.X. Tao, Functions of transmembrane domain 3 of human melanocortin-4 receptor, J Mol Endocrinol 49(3) (2012) 221-235.

[223] Y.X. Tao, D.L. Segaloff, Functional characterization of melanocortin-4 receptor mutations associated with childhood obesity, Endocrinology 144(10) (2003) 4544-4551.

[224] C. Chen, H. Okayama, High-efficiency transformation of mammalian cells by plasmid DNA, Mol Cell Biol 7(8) (1987) 2745-2752.

[225] S.X. Wang, Z.C. Fan, Y.X. Tao, Functions of acidic transmembrane residues in human melanocortin-3 receptor binding and activation, Biochem Pharmacol 76(4) (2008) 520-530.

[226] D.L. Black, Mechanisms of alternative pre-messenger RNA splicing, Annu Rev Biochem 72 (2003) 291-336.

[227] Q. Pan, O. Shai, L.J. Lee, B.J. Frey, B.J. Blencowe, Deep surveying of alternative splicing complexity in the human transcriptome by high-throughput sequencing, Nat Genet 40(12) (2008) 1413-5.

[228] M.C. Wahl, C.L. Will, R. Luhrmann, The spliceosome: design principles of a dynamic RNP machine, Cell 136(4) (2009) 701-18.

[229] Q. Liang, N. Wu, S. Zaneveld, H. Liu, S. Fu, K. Wang, R. Bertrand, J. Wang, Y. Li, R. Chen, Transcript isoforms of Reep6 have distinct functions in the retina, Hum Mol Genet 30(21) (2021) 1907-1918.

[230] P.M. Hinkle, J.A. Sebag, Structure and function of the melanocortin2 receptor accessory protein (MRAP), Mol Cell Endocrinol 300(1-2) (2009) 25-31.

[231] M.J. Agulleiro, S. Roy, E. Sanchez, S. Puchol, N. Gallo-Payet, J.M. Cerdá-Reverter, Role of melanocortin receptor accessory proteins in the function of zebrafish melanocortin receptor type 2, Mol Cell Endocrinol 320(1-2) (2010) 145-152.

[232] L. Liang, J.A. Sebag, L. Eagelston, M.N. Serasinghe, K. Veo, C. Reinick, J. Angleson, P.M. Hinkle, R.M. Dores, Functional expression of frog and rainbow trout melanocortin 2 receptors using heterologous MRAP1s, Gen Comp Endocrinol 174(1) (2011) 5-14.

[233] T. Gillyard, K. Fowler, S.Y. Williams, R.D. Cone, Obesity-associated mutant melanocortin-4 receptors with normal Gαs coupling frequently exhibit other discoverable pharmacological and biochemical defects, J Neuroendocrinol 31(10) (2019) e12795.

[234] A.A.J. Rouault, D.K. Srinivasan, T.C. Yin, A.A. Lee, J.A. Sebag, Melanocortin receptor accessory proteins (MRAPs): Functions in the melanocortin system and beyond, Biochim Biophys Acta 1864 (2017) 2322-2329.

[235] E.I. Kay, R. Botha, J.M. Montgomery, K.G. Mountjoy, hMRAPa specifically alters hMC4R molecular mass and N-linked complex glycosylation in HEK293 cells, J Mol Endocrinol 50(2) (2013) 217-227.

[236] L. Li, Y. Xu, J. Zheng, Z. Kuang, C. Zhang, N. Li, G. Lin, C. Zhang, Pharmacological modulation of dual melanocortin-4 receptor signaling by melanocortin receptor accessory proteins in the Xenopus laevis, J Cell Physiol 236(8) (2021) 5980-5993.

[237] H.J. Zhang, H.J. Xie, W. Wang, Z.Q. Wang, Y.X. Tao, Pharmacology of the giant panda (*Ailuropoda melanoleuca*) melanocortin-3 receptor, Gen Comp Endocrinol 277 (2019) 73-81.

[238] Z.C. Fan, J.L. Sartin, Y.X. Tao, Molecular cloning and pharmacological characterization of porcine melanocortin-3 receptor, J Endocrinol 196(1) (2008) 139-148.

[239] H.J. Zhang, Z.H. Cui, M. Liu, T.Q. Min, X. Xiao, Z.Q. Wang, Y.X. Tao, Pharmacological characterization of three chicken melanocortin-3 receptor mutants, Domest Anim Endocrinol 74 (2021) 106507.

[240] I. Gantz, T.M. Fong, The melanocortin system, Am J Physiol Endocrinol Metab 284(3) (2003) E468-E474.

[241] R.D. Cone, Studies on the physiological functions of the melanocortin system, Endocr Rev 27(7) (2006) 736-749.

[242] Y.X. Tao, Melanocortin receptors, Biochim Biophys Acta 1863(10 Pt A) (2017) 2411-2413.

[243] S.J. Getting, C.W. Lam, A.S. Chen, P. Grieco, M. Perretti, Melanocortin 3 receptors control crystal-induced inflammation, FASEB J 20(13) (2006) 2234-2241.

[244] D.W. Logan, R.J. Bryson-Richardson, M.S. Taylor, P. Currie, I.J. Jackson, Sequence characterization of teleost fish melanocortin receptors, Ann NY Acad Sci 994 (2003) 319-330.

[245] Y. Selz, I. Braasch, C. Hoffmann, C. Schmidt, C. Schultheis, M. Schartl, J.N. Volff, Evolution of melanocortin receptors in teleost fish: the melanocortin type 1 receptor, Gene 401(1) (2007) 114-122.

[246] A. Rocha, A. Godino-Gimeno, J.M. Cerda-Reverter, Evolution of proopiomelanocortin, Vitam Horm 111 (2019) 1-16.

[247] E. Sanchez, V.C. Rubio, D. Thompson, J. Metz, G. Flik, G.L. Millhauser, J.M. Cerdá-Reverter, Phosphodiesterase inhibitor-dependent inverse agonism of agouti-related protein on

melanocortin 4 receptor in sea bass (*Dicentrarchus labrax*), Am J Physiol Regul Integr Comp Physiol 296(5) (2009) R1293-R1306.

[248] Y.Y. Chen, Fauna Sinica Osteichthyes Cypriniformes II, Science Press, Beijing, 1998.

[249] L. Ren, W.H. Li, Q.B. Qin, H. Dai, F.M. Han, J. Xiao, X. Gao, J.L. Cui, C. Wu, X.J. Yan, G.L. Wang, G.M. Liu, J. Liu, J.M. Li, Z. Wan, C.H. Yang, C. Zhang, M. Tao, J. Wang, K.K. Luo, S. Wang, F.Z. Hu, R.R. Zhao, X.M. Li, M. Liu, H.K. Zheng, R. Zhou, Y.Q. Shu, Y.D. Wang, Q.F. Liu, C.C. Tang, W. Duan, S.J. Liu, The subgenomes show asymmetric expression of alleles in hybrid lineages of *Megalobrama amblycephala* x *Culter alburnus*, Genome Res 29(11) (2019) 1805-1815.

[250] T. Haitina, J. Klovins, J. Andersson, R. Fredriksson, M.C. Lagerstrom, D. Larhammar, E.T. Larson, H.B. Schioth, Cloning, tissue distribution, pharmacology and three-dimensional modelling of melanocortin receptors 4 and 5 in rainbow trout suggest close evolutionary relationship of these subtypes, Biochem J 380(Pt 2) (2004) 475-486.

[251] J. Klovins, T. Haitina, D. Fridmanis, Z. Kilianova, I. Kapa, R. Fredriksson, N. Gallo-Payet, H.B. Schioth, The melanocortin system in Fugu: determination of POMC/AGRP/MCR gene repertoire and synteny, as well as pharmacology and anatomical distribution of the MCRs, Mol Biol Evol 21(3) (2004) 563-579.

[252] J.R. Metz, J.J. Peters, G. Flik, Molecular biology and physiology of the melanocortin system in fish: a review, Gen Comp Endocrinol 148(2) (2006) 150-62.

[253] H. Huang, Y.X. Tao, Pleiotropic functions of the transmembrane domain 6 of human melanocortin-4 receptor, J Mol Endocrinol 49(3) (2012) 237-248.

[254] L. Schonnop, G. Kleinau, N. Herrfurth, A.L. Volckmar, C. Cetindag, A. Müller, T. Peters, S. Herpertz, J. Antel, J. Hebebrand, H. Biebermann, A. Hinney, Decreased melanocortin-4

receptor function conferred by an infrequent variant at the human melanocortin receptor accessory protein 2 gene, Obesity 24(9) (2016) 1976-1982.

[255] Y. Song, R.D. Cone, Creation of a genetic model of obesity in a teleost, FASEB J 21(9) (2007) 2042-2049.

[256] Å. Västermark, H.B. Schiöth, The early origin of melanocortin receptors, agouti-related peptide, agouti signalling peptide, and melanocortin receptor-accessory proteins, with emphasis on pufferfishes, elephant shark, lampreys, and amphioxus, Eur J Pharmacol 660(1) (2011) 61-69.

[257] X.J. Cao, W.M. Wang, Haematological and biochemical characteristics of two aquacultured carnivorous cyprinids, topmouth culter *Culter alburnus* (Basilewsky) and yellowcheek carp *Elopichthys bambusa* (Richardson), Aquaculture Res 41 (2010) 1331-1338.

[258] L. Ren, X.J. Tan, Y.F. Xiong, K. Xu, Y. Zhou, H. Zhong, Y. Liu, Y.H. Hong, S.J. Liu, Transcriptome analysis reveals positive selection on the divergent between topmouth culter and zebrafish, Gene 552(2) (2014) 265-71.

[259] W. Wang, L.Q. Chen, P. Yang, L. Hou, C.B. He, Z.M. Gu, Z.J. Liu, Assessing genetic diversity of populations of topmouth culter (*Culter alburnus*) in China using AFLP markers, Biochem System Ecol 35 (2007) 662-669.

[260] I.K. Sebhat, W.J. Martin, Z. Ye, K. Barakat, R.T. Mosley, D.B. Johnston, R. Bakshi, B. Palucki, D.H. Weinberg, T. MacNeil, R.N. Kalyani, R. Tang, R.A. Stearns, R.R. Miller, C. Tamvakopoulos, A.M. Strack, E. McGowan, D.E. Cashen, J.E. Drisko, G.J. Hom, A.D. Howard, D.E. MacIntyre, L.H. van der Ploeg, A.A. Patchett, R.P. Nargund, Design and pharmacology of N-[(3R)-1,2,3,4-tetrahydroisoquinolinium- 3-ylcarbonyl]-(1R)-1-(4-chlorobenzyl)- 2-[4-cyclohexyl-4-(1H-1,2,4-triazol- 1-ylmethyl)piperidin-1-yl]-2-oxoethylamine (1), a potent, selective, melanocortin subtype-4 receptor agonist, J Med Chem 45(21) (2002) 4589-4593.